Università degli Studi dell'Insubria

Dottorato di Ricerca in Scienze Chimiche e Ambientali

GUIDELINES FOR RISK ANALYSIS TO SUPPORT SAFETY REPORT ACCORDING TO THE SEVESO DIRECTIVE (D.LGS. 105/2015)

Tutor
Prof.ssa Sabrina Copelli

Author
Alessandra Melchiore

Reviewers
Prof. Andrea Cattaneo
Prof. Carlo Pirola
Ing. Tiago Do Monte Correa Novo

Academic Year 2022–2025
XXXVIII Cycle

To my family

Abstract

This PhD thesis presents the development of a comprehensive set of practical guidelines aimed at supporting both public authorities and risk analysts in the drafting and reviewing of Safety Report, as required by Direttiva Seveso III (D.Lgs. 105/2015). The main objective of the proposed guidelines is to clearly define the minimum technical information that must be always included in a Safety Report, thereby improving the overall quality of such reports while reducing the time required for their review and approval.

The guidelines are structured to follow the typical sequential steps of the risk analysis process and they dedicate a full chapter to each of them: characterization of Direttiva Seveso III "substances", frequency assessment, consequence analysis, and overall risk calculation.

Bringing all the phases that make up the risk analysis process into a single comprehensive document, this PhD thesis represents a significant innovation, as currently, in Italy, there are no existing works compiling all these information together. Typically, the available literature addresses these topics separately, with individual publications focusing on calorimetry, flammability, frequency assessment, or consequence modelling. In addition, to integrate all these topics into a unified framework, this thesis also provides numerous references and practical sources, including websites, databases, and technical standards, where further information can be retrieved, such as IDLH values, chemical compatibility data, failure rates, and physicochemical parameters.
Within this doctoral work, particular emphasis has been placed on the crucial importance of thoroughly characterizing hazardous substances falling under the scope of Direttiva Seveso III, especially in relation to their reactivity, flammability, explosiveness, and toxicity. The fundamental rationale behind this approach is that every time a hazard is not properly identified and characterized, it becomes an unassessed risk for which no preventive or mitigative measures can be designed or implemented. An unknown hazard is, by definition, an unmanaged risk, and this represents a critical gap in the context of major accident hazard assessment and control.

To address this, a dedicated chapter of the thesis was structured into four comprehensive sections, each focusing on one of the aforementioned hazardous properties. The first section was devoted to chemical reactivity, which represents one of the most critical aspects in preventing loss of thermal control (runaway) during industrial processes. In this part, several experimental techniques that are commonly employed to investigate the thermal behavior and reactivity of chemical substances were described in detail. These

techniques include Differential Thermal Analysis (DTA), Differential Scanning Calorimetry (DSC), Thermogravimetric Analysis (TGA), Accelerating Rate Calorimeter (ARC), Low Thermal Inertia Adiabatic Calorimetry (Phi-TEC, VSP), and Reaction Calorimetry (RC1). For each of these techniques, the operational procedures, experimental setup and instrumentation, main advantages and limitations, as well as the thermokinetic and thermodynamic parameters that can be directly obtained or indirectly derived through empirical correlations were presented and discussed. These parameters provide essential information for assessing the energetic behavior of chemical substances and for designing inherently safer processes capable of avoiding thermal runaway scenarios.

The following sections focused on flammability and explosiveness, which are key properties for assessing the potential for ignition, combustion, or explosion of hazardous substances under specific operating or accidental conditions. In the flammability section, the main safety-related parameters that are considered essential for evaluating the flammable behavior of a substance were reported and discussed. These include: Autoignition Temperature, Flash Point, Lower Flammable Limit (LFL) and Upper Flammable Limit (UFL), Minimum Ignition Energy (MIE), and Limiting Oxygen Concentration (LOC). In the explosiveness section, the focus was on those parameters that are required to evaluate both the explosive potential and the intensity of an explosion, such as Minimum Explosive Concentration (MEC), Minimum Ignition Temperature (MIT), Maximum Explosion Pressure ($P_{\max}$), Maximum rate of pressure rise ($(dP/dt)_{\max}$), Mean rate of pressure rise ($(dP/dt)_{\text{mean}}$), and Explosivity Index. For all these parameters, the experimental methodologies and measuring instruments, together with the main technical standards and guidelines used as reference in laboratory practice, were described in detail. The discussion highlighted how these data represent an essential input to risk assessment studies, being directly used for the evaluation of fire and explosion scenarios within major accident hazard analyses.

The last section of the chapter was dedicated to toxicity, which represents a different but equally important dimension of chemical hazard characterization. In this part, particular attention was given to the role of Safety Data Sheets (SDS) as a primary source of toxicological information, and to the regulatory frameworks governing the classification of hazardous substances and wastes. A specific focus was placed on illustrating the similarities and differences between CLP Regulation, Direttiva Seveso III, and legislation on hazardous waste classification. This comparison revealed that a substance or a waste classified as hazardous according to the CLP criteria is not necessarily considered hazardous under the Seveso Directive, and vice versa. This finding underscores the necessity of carefully assessing and interpreting the available toxicological and regulatory data, in order to avoid inconsistencies that could lead to an underestimation or misclassification of the actual hazards associated with a substance or waste stream.

The second part of this doctoral thesis focuses on both the estimation of accidental consequences and the software tools that are commonly used for this purpose in the context of major accident hazard assessment. Accurate consequence modelling represents a fundamental step in the overall risk analysis process, as it allows the prediction and quantification of the physical effects that may result from the accidental release of

hazardous substances. These effects, which may include thermal radiation, overpressure waves, and toxic dispersion, directly determine the severity of potential damage to people, environment, and surrounding installations.

In this work, three consequence modelling software tools have been selected and systematically compared: PHAST (version 9.1), developed by DNV; ALOHA (version 5.4.7), developed by the United States Environmental Protection Agency (EPA); and ADAM, developed by the Joint Research Centre (JRC) of the European Commission (EC). While PHAST and ALOHA are widely used in industrial and regulatory contexts for the evaluation of fire, explosion, and toxic release scenarios, ADAM has been specifically designed to support the activities of the Competent Authorities of Direttiva Seveso III within the European Union. More precisely, ADAM has been developed to serve as an operational decision-support tool for national authorities, governmental institutions, and research bodies across the EU Member States, Candidate and Accession Countries, and European Neighborhood Policy regions, all of which are involved in chemical accident prevention, emergency preparedness, and regulatory compliance under the Seveso framework.

ADAM has been conceived to implement a set of scientifically validated physical models that allow the estimation of the possible evolution of an industrial accident following the loss of containment of a hazardous substance. It is capable of simulating the sequence of phenomena that may occur after an accidental release, from the initial discharge to the subsequent atmospheric dispersion of the substance, and ultimately to the assessment of its consequences in terms of thermal radiation, overpressure waves, or toxic concentrations. These models are internally combined in an integrated framework, which allows users to both evaluate different release scenarios and quantify the potential impact areas associated with each scenario. Compared to general-purpose commercial software, ADAM offers a simplified but consistent approach that is fully aligned with the needs of public authorities responsible for implementing Seveso Directive, making it particularly suitable for regulatory inspections, land-use planning assessments, and the evaluation of safety reports submitted by industrial operators.

To explore the capabilities and differences of these software tools, a dedicated case study was developed. The study focused on three representative hazardous substances that are commonly stored and handled in Seveso establishments: ammonia and chlorine, and methanol. For each of these substances, multiple accidental release scenarios were defined to reflect different possible failure modes, including the rupture of a storage tank, the rupture of a process pipeline, and a catastrophic vessel failure. Each scenario was modelled using PHAST, ALOHA, and ADAM under consistent boundary conditions, in order to ensure the comparability of results.

The output data obtained from the three software tools were then systematically analyzed and compared. The main parameters considered in the comparison included the mass release rate and its time evolution, the outlet velocity of the released substance, the dispersion behavior of the resulting cloud in the atmosphere, and, in case of ignition, the thermal radiation produced by the ensuing fire or explosion. By comparing these key indicators across the different models and scenarios, it was possible to evaluate

strengths, limitations, and levels of conservatism of each software tool. This comparison also provided valuable insights into the influence of model assumptions on the predicted size of the hazard zones, which represents a critical aspect for the safety assessment of Seveso establishments and for the definition of emergency planning zones.

Contents

List of Abbreviation

ACGIH	American Conference of Governmental Industrial Hygienists
AEGL	Acute Exposure Guideline Levels
AIChE	American Institute of Chemical Engineers
AIHA	American Industrial Hygiene Association
AIT	Autoignition Temperature
ALARP	As Low As Reasonably Practicable
ARC	Accelerating Rate Calorimetry
ARPA	Agenzia Regionale per la Protezione dell'Ambiente (Regional Environmental Protection Agency
ARSST	Advanced Reactive System Screening Tool
ASTM	American Society for Testing and Materials
BLEVE	Boiling Liquid Expanding Vapor Explosion
CLP	Regulation (EC) No 1272/2008 on the Classification, Labelling and Packaging of substances and mixtures
CRW	Chemical Reactivity Worksheet
D.Lgs	Decreto Legislativo (Legislative Decree)
D.M	Decreto Ministeriale (Ministerial Decree)
DPCM	Decreto del Presidente del Consiglio dei Ministri (Decree of the President of the Council of Ministers)
DSC	Differential Scanning Calorimetry
DTA	Differential Thermal Analysis
EPA	U.S. Environmental Protection Agency
ERPG	Emergency Response Planning Guideline
ETA	Event Tree Analysis
FMEA	Failure Mode and Effects Analysis
FTA	Fault Tree Analysis
H&MBs	Heat and Material Balances
HAZOP	Hazard and Operability Study
HRA	Human Reliability Analysis
IDLH	Immediately Dangerous to Life or Health
INAIL	Istituto Nazionale per l'Assicurazione contro gli Infortuni sul Lavoro (Italian National Institute for Insurance against Accidents at Work)
ISPRA	Istituto Superiore per la Protezione e Ricerca Ambientale

LFL	Lower Flammability Limits
LIT	Layer Ignition Temperature
LOC	Limiting Oxygen Concentration
LTE	Lower-tier establishments
MAT	Maximum Allowable Temperature
MEC	Minimum Explosible Concentration
MIE	Minimum Ignition Energy
MIT	Minimum Ignition Temperature
MTSR	Maximum Temperature due to Synthesis Reaction
NAQQS	National Ambient Air Quality Standards
Natech	Natural Hazard Triggering Technological Disasters
NFPA	National Fire Protection Association
NOAA	National Oceanic and Atmospheric Administration
OELs	Occupational Exposure Limits
OSHA	Occupational Safety and Health Administration
P&ID	Piping and Instrumentation Diagrams
QRA	Quantitative Risk Analysis
RC	Reaction Calorimeters
ROA	Recursive Operability Analysis
SDS	Safety Data Sheets
SIT	Self-Ignition Temperature
TEs	Top Events
TGA	Thermogravimetric Analysis
TLV	Threshold Limiti Value
TMR	Time to Maximum Rate
UFL	Upper Flammability Limits
UTE	Upper-tier establishments
VSP	Vent Sizing Package

Chapter 1

Introduction

The discipline of industrial safety in Europe emerged following a series of major accidents that occurred in the 1970s. The most significant of these, which later gave its name to the Seveso Directive, was the accident occurred at the ICMESA chemical plant in Meda on 10 July 1976, which resulted in the release of a dioxin cloud over the town of Seveso. As a consequence, 447 people suffered skin lesions, and 179 children developed chloracne due to toxic exposure.

Even before this event, other serious accidents had highlighted the need for a harmonized regulatory framework. Among them there was the Flixborough accident in the United Kingdom occurred on 1 June 1974, where the release of liquid cyclohexane formed a flammable vapor cloud that ignited, causing an explosion which resulted in 28 fatalities and more than 100 injuries. Another significant event was the disaster occurred at the Dutch State Mines (DSM) in Beek on 7 November 1975, caused by a steam release and subsequent explosion, which led to 14 deaths and 107 injuries.

These events prompted the European Community to establish a common regulatory system, leading to the adoption of Directive 82/501/EEC, known as Seveso I, concerning the control of major-accident hazards involving certain industrial activities. This directive was primarily focused on plant-level control measures and the prevention of impacts on human health and the environment.

Regulatory evolution continued in response to further incidents, particularly the Bhopal disaster occurred in India on 3 December 1984, where the release of methyl isocyanate resulted in thousands of fatalities. This led to the adoption of Directive 96/82/EC, known as Seveso II, which placed greater emphasis on safety management systems, systematic risk prevention, and the principle of continuous improvement.

Each accident provides an opportunity to learn from past failures and prevent future occurrences, and this concept is at the core of the Seveso regulatory framework. Following additional accidents, such as the fireworks warehouse explosion in Enschede, the Netherlands, on 13 May 2000, and the AZF fertilizer plant explosion in Toulouse, France, on 21 September 2001, the European Union introduced Directive 2003/105/EC, commonly referred to as Seveso II-bis. This directive introduced new requirements, including mandatory external emergency plans and an expanded scope of application,

particularly for establishments handling ammonium nitrate and pyrotechnic materials.

Finally, the introduction of Regulation (EC) No. 1272/2008 (CLP) on the classification, labelling and packaging of substances and mixtures necessitated a revision of the Seveso legislation, resulting in Directive 2012/18/EU (Seveso III), which was implemented in Italy through Legislative Decree No. 105 of 26 June 2015.

Legislative Decree 105/2015 consists of six numerical annexes (1–6) and six lettered annexes (A–M). Annex C, in particular, establishes the criteria, data and information required for the preparation and assessment of the Safety Report.

This doctoral thesis has been developed as a technical and methodological support for the assessment of Safety Reports, with specific focus on risk analysis and the determination of hazard impact areas, which are key elements in industrial risk management and land-use planning.

1.1 Definitions

Within the framework of the Seveso legislation, the term "dangerous substances" is often interpreted as referring exclusively to those materials that determine the Seveso classification of the establishment. However, this narrow interpretation may lead to an underestimation of the actual risks present within an industrial site. A comprehensive assessment should instead include wastes, by-products, and all substances that may be generated during abnormal or accidental process conditions.

The current European reference for the prevention of major industrial accidents is the Directive 2012/18/EU (Seveso III Directive), which was implemented in Italy through the Legislative Decree no. 105 of 26 June 2015, hereafter referred to as D.Lgs. 105/2015.

The main definitions reported in Article 3, letters (l), (m) and (n) of the D.Lgs. 105/2015 are provided below:

> *dangerous substance* means a substance or mixture covered by Part 1 or listed in Part 2 of Annex I, including in the form of a raw material, product, by-product, residue or intermediate;
>
> *mixture* means a mixture or solution composed of two or more substances;
>
> *presence of dangerous substances* means the actual or anticipated presence of dangerous substances in the establishment, or of dangerous substances which it is reasonable to foresee may be generated during loss of control of the processes, including storage activities, in any installation within the establishment, in quantities equal to or exceeding the qualifying quantities set out in Part 1 or Part 2 of Annex I;

It is important to underline that the expression Seveso substance should not be interpreted as referring solely to the substance or mixture responsible for the establishment's Seveso classification. Instead, all substances listed in Annex I, Part 1 and Part 2 must be taken into consideration, and for each of them the potential accidental scenarios should be properly assessed.

In the case of mixtures classified under the Seveso framework, the entire amount of the mixture must be considered when determining whether the establishment falls within the scope of the Directive, not merely the percentage of the hazardous component. This aspect frequently causes confusion: during the review of Safety Reports, it is often observed that analysts consider only the proportion of the dangerous substance within the mixture, rather than the total mass of the mixture itself.

The D.Lgs. 105/2015 also provides the following definitions for Seveso establishments, distinguishing between upper-tier and lower-tier sites (Article 3):

> *establishment* means the whole location under the control of an operator where dangerous substances are present in one or more installations, including common or related infrastructures or activities; establishments are either lower-tier establishments or upper-tier establishments;
>
> *lower-tier establishment* means an establishment where dangerous substances are present in quantities equal to or in excess of the quantities listed in Column 2 of Part 1 or in Column 2 of Part 2 of Annex I, but less than the quantities listed in Column 3 of Part 1 or in Column 3 of Part 2 of Annex I, where applicable using the summation rule laid down in note 4 to Annex I;
>
> *upper-tier establishment* means an establishment where dangerous substances are present in quantities equal to or in excess of the quantities listed in Column 3 of Part 1 or in Column 3 of Part 2 of Annex I, where applicable using the summation rule laid down in note 4 to Annex I.

For a correct risk analysis, it is essential to consider not only the specific area where the Seveso substance is handled or stored, but the entire industrial site under the control of the operator. This broader approach ensures that all potential interactions among installations are accounted for, thereby supporting the proper development of both the Internal and External Emergency Plans.

Finally, Article 3 of the D.Lgs. 105/2015 defines the term operator as follows:

> *operator* means any natural or legal person who operates or controls an establishment or installation or, where provided for by national legislation, to whom the decisive economic or decision-making power over the technical functioning of the establishment or installation has been delegated.

1.1.1 Distinction between "Hazard" and "Risk"

It is important to clearly distinguish between the concepts of hazard and risk, which are often used interchangeably in non-specialist contexts but have distinct meanings within the Seveso framework.

According to Article 3 of the D.Lgs. 105/2015, the following definitions apply:

> *hazard* means the intrinsic property of a dangerous substance or physical situation, with a potential for creating damage to human health or the environment;

> *risk* means the likelihood of a specific effect occurring within a specified period or in specified circumstances.

Hazard is a qualitative property: it can be eliminated, but not reduced. Risk is a quantitative measure: it can be reduced, but not eliminated. While hazard represents an inherent characteristic of a substance or a situation, risk expresses the probability that this hazardous potential may actually lead to an adverse event.

1.2 Quantitative Risk Analysis

Quantitative Risk Analysis (QRA) represents a fundamental tool for risk management and for the continuous improvement of safety in the process industry.

Several authoritative definitions exist, including the following:

> The systematic development of numerical estimates of the expected frequency and consequence of potential accidents associated with a facility or operation, based on engineering evaluation and mathematical techniques [1].

> A Quantitative Risk Assessment (QRA) is a valuable tool for determining the risk of the use, handling, transport and storage of dangerous substances. QRAs are used to demonstrate the risk caused by the activity and to provide the competent authorities with relevant information to enable decisions on the acceptability of risk related to developments on site, or around the establishment or transport route [2].

The aim of a quantitative risk analysis is to provide a numerical measure of the risk associated with a specific industrial installation, by estimating the expected frequency and the severity of the potential accident consequences.

It is essential to identify hazards and reduce the associated risks before they can materialize into actual accidents. However, in many cases, hazards are not recognized until an incident related to them occurs.

Whenever a facility is analyzed, the following fundamental questions should be addressed:

- What are the existing hazards?
- How can these hazards develop into accidental events?
- How frequently could such events occur?
- What would be the expected consequences on the surrounding population and environment?

The first question concerns the identification of the hazards present in the plant; the second refers to the definition of the accidental scenarios, i.e., the events capable of initiating an accident and their logical chain of causality.

The last two questions belong to the risk evaluation phase, which involves estimating both the probability of occurrence of the identified accident scenarios and their associated consequences, in terms of potential harm to people, the environment, and infrastructure. The main steps that constitute the risk analysis process are eight, as illustrated in Figure 1.1.

The initial phase consists of the description of the process and the identification of hazards, aimed at determining all the accidental scenarios associated with them. This is followed by the study of the frequency and consequence of each identified scenario: these data allow the quantitative estimation and final evaluation of risk. If the resulting risk is acceptable (and all relevant scenarios have been analyzed), the study can be considered complete. Conversely, if the risk is unacceptable, mitigation measures must be introduced, i.e., the system must be modified, and the evaluation process must be repeated until a tolerable level of risk is achieved.

1.2.1 System Definition

The first phase of the risk analysis involves the collection of all the information required to initiate the assessment process.This activity can be summarized through the following operational steps:

- Identification of the type of industrial activity, that is, determining whether the facility is a chemical plant, a waste treatment plant, a storage installation, or another type of industrial site.
- Location of the establishment and verification of its potential exposure to NATECH risks (Natural Hazard Triggering Technological Accidents), such as floods, earthquakes, or landslides. When a potential exposure to NATECH events is identified, a systematic collection of available historical data should be carried out in order to evaluate the need for a dedicated risk assessment for such events.
- Collection of site-specific meteorological data, including wind speed and direction, temperature, and atmospheric stability. These data are particularly important in the subsequent consequence assessment phase, especially in the case of accidental scenarios involving the atmospheric dispersion of toxic or flammable substances.
- Compilation of the technical documentation of the plant, such as Process Flow Diagrams (PFDs), Piping and Instrumentation Diagrams (P&IDs), Operating and Maintenance Procedures, and Heat and Material Balances (H&MBs).

These documents are essential both for hazard identification and for the definition of credible accident scenarios. During this stage, it is also advisable to prepare a comprehensive inventory of all installed instrumentation and equipment, specifying operating conditions (e.g., temperature, pressure), the substance involved and its physical phase, and, where available, the failure rates associated with each component. This information will be used later in the estimation of the probability of occurrence of the identified accident events.

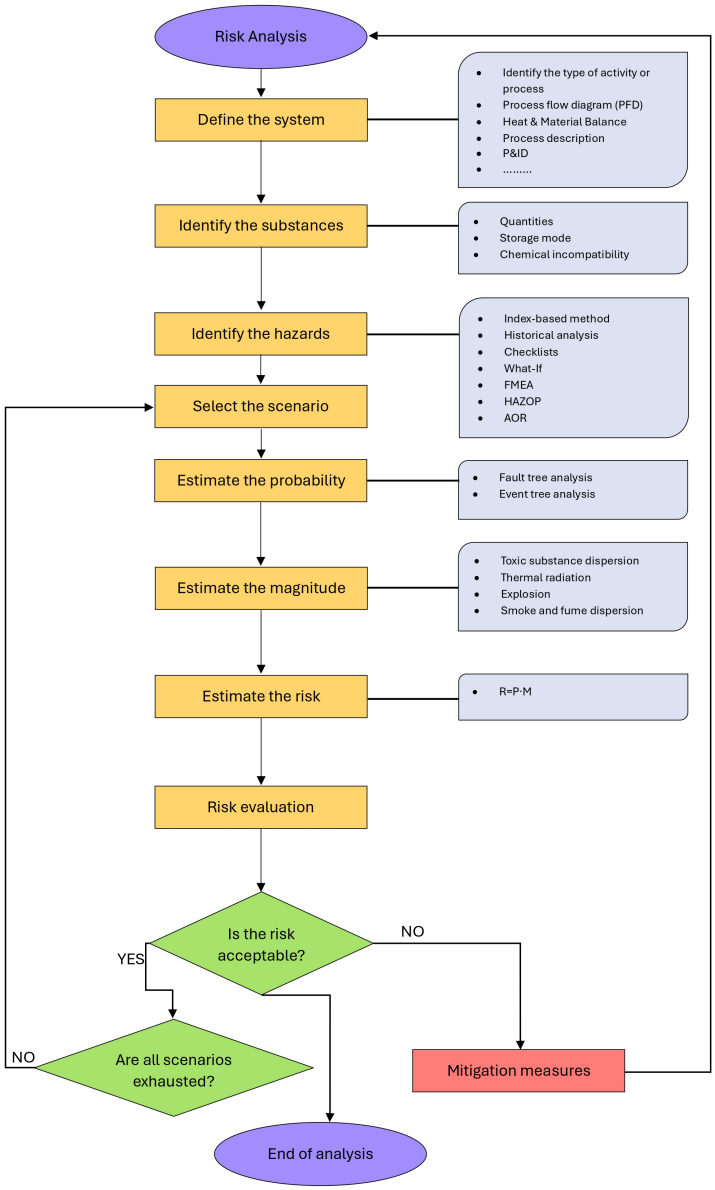

Figure 1.1: Main phases of risk analysis

The concepts introduced in this section are further developed in Chapter 2 , which provides a detailed description of the system definition, the classification of Seveso establishments in the Lombardy region, and the collection of technical and environmental information required for the risk analysis.

1.2.2 Identification of Substances for the Evaluation of Potential Accident Scenarios

In this phase, the substances and/or mixtures that will be considered as references for the development of potential accident scenarios are identified. This involves analyzing the storage conditions, evaluating any chemical incompatibilities, and collecting all relevant information concerning the physicochemical, toxicological, and thermal stability properties of the selected substances.

It is essential to clearly state the criteria adopted for the identification of the reference substances and/or mixtures that will be used in the subsequent stages of the risk assessment.

The detailed methodology and data requirements for this phase are further discussed in Chapter 3 .

1.2.3 Hazard and Accident Scenario Identification

The third phase consists of the identification of hazards and accident scenarios, commonly referred to in reliability engineering as Top Events (TEs), associated with handling, transport, and storage of the dangerous substances previously identified, in accordance with the methodology described in Chapter 4.

This represents one of the most critical stages of the analysis, since only a proper identification of hazards allows the reduction of the associated risk by preventing their escalation into accident events, for instance, through the implementation of appropriate mitigation or prevention measures.

Conversely, unidentified hazards become latent risks, not subject to mitigation and therefore potentially capable of leading to severe consequences.

The most commonly used methodologies for this phase include:

- Index-based Methods;
- Historical Analysis;
- Check-List Analysis;
- What-If Analysis;
- Bow-Tie Analysis;
- Hazard and Operability Study (HAZOP) and its derivatives;
- Recursive Operability Analysis (ROA) and related approaches.

The detailed description and practical application of these methodologies are discussed in Chapter 4.

1.2.4 Estimation of the Probability of Occurrence

The fourth phase is based on the use of probabilistic models to determine the frequency of occurrence of each accidental event associated with the substances and/or mixtures identified in the previous stage. The most commonly used techniques include:

- Fault Tree Analysis (FTA);
- Event Tree Analysis (ETA).

In addition to these methodologies, other supporting techniques may be adopted to assist in the quantitative estimation of the probability associated with the selected Top Event (TE), such as:

- Human Reliability Analysis (HRA): used to assess the likelihood of human errors (for instance, omissions in procedures or incorrect manual operations);
- External Events Analysis: used to consider the influence of natural phenomena such as strong winds, heavy rainfall, lightning strikes, or other environmental conditions that may cause equipment malfunction or mechanical failure, for example, tank rupture due to accidental impact. This analysis is particularly important for the assessment of NATECH (Natural Hazard Triggering Technological Accidents) scenarios.

The estimation of the probability of occurrence is generally referred to a one-year time frame (reference mission time). Any different time basis adopted for the analysis must be explicitly justified, depending on the actual presence or residence time of the identified reference substances and/or mixtures within the plant.

The detailed methodology for this phase is presented in Chapter 5.

1.2.5 Estimation of Consequence Magnitude

The fifth phase consists of the analysis of the identified accidental events consequences, that is, the release of substances and/or energy into the environment. The accidental scenarios that typically occur in major hazard establishments include:

- Dispersion of toxic and/or flammable substances or mixtures into the atmosphere (or within confined work environments).
- Thermal radiation resulting from open flames (fireball, jet fire, pool fire, etc.).
- Physical explosion of vessels and/or pipelines.
- Dispersion of toxic fumes as a result of a fire.

Through the use of mathematical models and simulation software, it is possible to estimate:

- the ground-level and/or waterborne concentration (surface and groundwater) of toxic substances;
- the thermal radiation intensity generated by fires;
- the overpressure and fragment trajectory resulting from explosions.

These results allow the determination of the extent of the so-called "damage zones", i.e., areas centered on the accidental release source within which specific levels of harm to people, environment, and structures are expected to occur. Defining the extent of these areas is a fundamental step for the preparation of both Internal and External Emergency Plans.

The detailed methodology and models applied in this phase are described in Chapter 6.

1.2.6 Risk Evaluation

The sixth phase consists of the calculation of the risk index (R), or simply risk, which, for events involving acute effects (such as those considered under the Seveso Directive), can be defined as the product of the probability (P) of occurrence and the magnitude (M) of the corresponding Top Event (TE):

$$R = P \cdot M \tag{1.1}$$

The calculated risk value shall then be compared with the acceptable risk threshold. Within the framework of the present Guidelines, and assuming a reference mission time of one calendar year, an acceptable individual risk level is considered to be below 10^{-6} per year, unless otherwise specified by the Competent Authority, particularly in cases involving highly toxic substances or specific territorial conditions.

If the calculated risk index exceeds the selected reference value, appropriate mitigation measures must be implemented. According to the adopted definition, such measures may consist of:

- Prevention systems, aimed at reducing the frequency of occurrence of the Top Event;
- Protection systems, aimed at reducing the magnitude (i.e., the consequences) of the event once it has occurred.

A summary representation of this relationship is shown in Figure 1.2. Further details regarding the risk calculation methodology are discussed in Chapter 7.

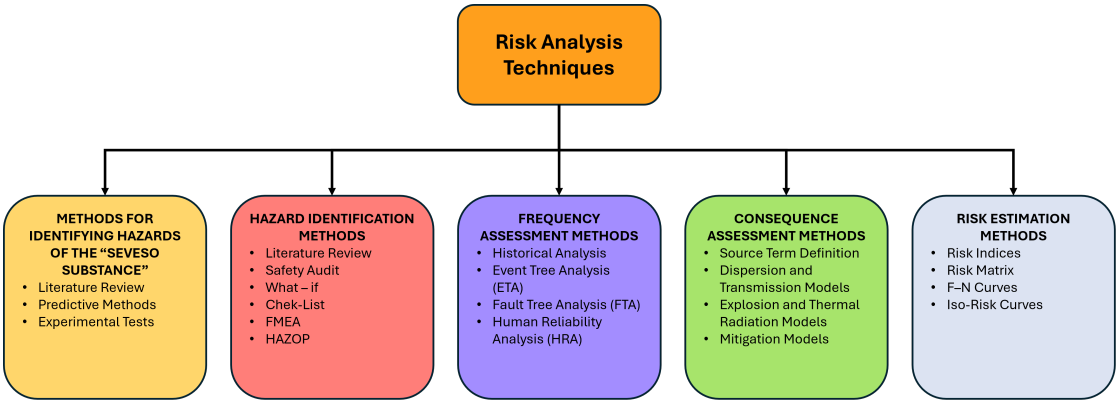

Figure 1.2: Summary diagram of the main methodologies applied in the different phases of risk analysis.

1.3 Structure of the Thesis

The present thesis is structured in 8 chapters, each addressing a specific aspect of the proposed methodology and its application to Seveso establishments.

Chapter 1 introduces the regulatory framework and presents the main phases of the Quantitative Risk Analysis (QRA) methodology, which form the basis for the development of the proposed Guidelines.

Chapter 2 describes the general characteristics of Seveso establishments located in Lombardy, illustrating their classification, and grouping according to activity type and hazard category. The chapter also presents the approach adopted for the systematic collection of technical and environmental information, including meteorological data, process flow diagrams (PFDs), and piping and instrumentation diagrams (P&ID), which are essential for the subsequent phases of risk analysis.

Chapter 3 describes the identification and classification criteria for Seveso substances and the minimum technical information required for their characterization.

Chapter 4 illustrates the main hazard identification techniques, outlining their principles, fields of application and limitations. The most commonly adopted industrial methods (such as HAZOP, What-if Analysis, FMEA and checklists) are examined, highlighting their role in the prevention of major accidents and within the overall risk analysis process.

Chapter 5 focuses on the assessment of failure frequencies and the probabilistic approach used for the estimation of event likelihood.

Chapter 6 provides the methodology and reference criteria for the consequence analysis of accidental scenarios.

Chapter 7 presents the different approaches used for quantitative risk evaluation, including the calculation of individual and societal risk, and their graphical representation through risk matrices, F–N curves, and iso-risk contours.

Chapter 8 includes a practical case study aimed at demonstrating the applicability of

the developed Guidelines through a comparison of different modelling tools (PHAST, ALOHA, and ADAM).

Chapter 9 presents the main conclusions of the thesis and discusses possible future developments of the proposed methodological framework.

Chapter 2

System Definition

In the Lombardy Region there are 244 Seveso establishments, of which 135 are classified as upper-tier establishments (UTE) and 109 as lower-tier establishments (LTE) (Table 2.1).

For an accurate system definition, it is essential to identify the type of industrial activity which each establishment belongs to. The classification currently available from the ISPRA database for the Lombardy Region includes a wide range of industrial sectors, which are reported in Table 2.1.

Such a large number of categories is not functional for providing concise and targeted indications on the types of risks involved. For this reason, and to simplify the subsequent stages of risk analysis, the establishments have been aggregated according to their predominant hazard typology.

As it can be expected, the risks associated with logistics and storage facilities (e.g. categories 10 or 20) are very different from those ones present in a pharmaceutical plant (19) or in a refinery (08). Likewise, there is no substantial difference between the risks encountered in a pharmaceutical plant (19), a chemical plant producing organic substances (38) or a generic chemical production facility (22).

Based on these considerations, seven macro-categories of industrial activities were identified, labelled from A to H (Table 2.2).

For example, all establishments involving chemical reactions, such as the production of pharmaceuticals (19), pesticides and biocides (17), basic organic chemicals (23), plastics and rubber (24), as well as waste treatment (20), were grouped into a single category, as they share similar process dynamics and risk characteristics. A separate category was defined for storage and logistics facilities (10), as well as for metal-processing plants (04, 05, 06, 07), pyrotechnic and explosive facilities (11, 12), and for hydrocarbon-related activities, such as refineries (08) and energy production and distribution plants (09).

Activities subject to specific sectoral regulations, such as mining operations (03) or LPG-related installations (13, 14, 15), were kept as independent categories.

Table 2.1: List of upper-tier and lower-tier Seveso establishments located in the Lombardy Region.

LIST OF ESTABLISHMENTS	UTE	LTE
(03) Mining activities (tailings and physico-chemical processes)	5	0
(04) Metal processing	1	1
(05) Ferrous metal processing (foundries, smelting, etc.)	3	3
(06) Non-ferrous metal processing (foundries, smelting, etc.)	5	0
(07) Metal treatment by electrolytic or chemical processes	3	22
(08) Oil and petrochemical refineries	1	0
(09) Energy production, supply and distribution	0	1
(10) Fuel storage (including heating, retail distribution, etc.)	6	2
(11) Production, destruction and storage of explosives	1	0
(12) Production and storage of pyrotechnic articles	1	0
(13) Production, bottling and wholesale distribution of liquefied petroleum gas (LPG)	1	0
(14) LPG storage	11	11
(16) Storage and wholesale/retail distribution (excluding LPG)	13	13
(17) Production and storage of pesticides, biocides and fungicide	9	1
(18) Production and storage of fertilisers	0	1
(19) Pharmaceutical production	4	16
(20) Waste storage, treatment and disposal	6	4
(22) Chemical plants	34	14
(23) Production of basic organic chemicals	4	4
(24) Manufacture of plastics and rubber	10	1
(29) General engineering, manufacturing and assembly	0	1
(38) Manufacture of chemicals (not otherwise specified)	6	6
(39) Other activities (not otherwise specified)	1	8
TOTAL	**135**	**109**

Source: Seveso Inventory (isprambiente.gov.it), accessed 15 April 2025.

Table 2.2: Grouping of industrial activities in the Lombardy Region by type, identified by the letters A to H.

Letter	Type of Facility	Activities
A	Chemical plants	(17), (18), (19), (20), (22), (23), (24), (38)
B	Storage facilities	(10), (16)
C	Metal processing	(04), (05), (06), (07)
D	Pyrotechnic and explosive plants	(11), (12)
E	LPG	(13), (14), (15)
F	Mining activities	(03)
G	Hydrocarbon processing	(08)
H	Energy production and distribution	(09)

2.1 Site location and NATECH risk assessment

According to the technical specification UNI/TS 11816-1:2021, the term NATECH refers to technological accidents triggered by natural events. These include accidents such as fires, explosions, or toxic releases that may occur within industrial facilities or along distribution networks as a result of natural hazards such as earthquakes, floods, lightning strikes, or extreme meteorological phenomena.

Although these events are generally rare and often difficult to predict, they can lead to significant consequences for both human health and environment, particularly in establishments subject to the Seveso Directive.

For this reason, NATECH events should be adequately considered within the Safety Management System (SMS) to ensure effective prevention, protection, and emergency response measures. It is therefore necessary to assess whether the establishment is potentially exposed to such natural hazards, referring to both the guidelines provided in UNI/TS 11816-1:2021 and the technical documentation published by INAIL, particularly for seismic risk, while also considering other extreme natural events such as floods, lightning, tornadoes, and hailstorms. For hydrogeological risk, data provided by the Lombardy Region can be consulted at: `https://www.geoportale.regione.lombardia.it/`.

2.2 Collection of Meteorological Data

Meteorological data represent a fundamental element for either the accurate execution of dispersion simulations or the evaluation of the consequences of major accidents.

The minimum information required by Annex C, Part I, point C.3 of Legislative Decree 105/2015 concerns wind speed and direction, atmospheric stability conditions, and, where available, historical data covering a period of at least five years. Such information is essential for performing simulations of the dispersion of toxic and/or

flammable substances, as well as for assessing the expected thermal radiation and the overpressure generated by shock waves.

For the collection and processing of meteorological data, reference should be made to the ARPA Lombardia Guidelines titled "Indicazioni relative all'utilizzo di tecniche modellistiche per la simulazione della dispersione di inquinanti negli studi di impatto sulla componente atmosfera" (Guidelines on the use of modelling techniques for pollutant dispersion simulations in atmospheric impact studies).

In particular, Section 4 of the above-mentioned document provides operational guidance for determining:

- the number of meteorological stations from which to collect data and their location in relation to the identified emission point;
- the temporal frequency of meteorological data to be used;
- the minimum temporal domain of the simulation;
- the meteorological processor employed.

Depending on the selected meteorological processor and on the spatial and temporal extension of the simulation domain, it is necessary to verify the availability and quality of all required meteorological data.

2.3 Collection of Process Flow Diagrams, Operating Schemes, and Operating and Maintenance Procedures

Along with meteorological data, process documentation represents a key element for the correct definition of the system.

Risk analysis requires that the analyst has access to a complete and up-to-date set of documentation, including:

- process flow Fiagrams (PFDs);
- operating schemes and control diagrams (e.g. P&ID);
- ordinary and emergency operating procedures;
- maintenance procedures and plans.

It is the responsibility of the establishment operator to both provide all the necessary documentation and to check that it is up to date at the time the risk analysis is performed, thereby ensuring the availability of consistent and reliable information. This phase is preparatory to the subsequent stages of the risk analysis, in particular to hazard identification (e.g. HAZOP) and frequency assessment (e.g. Event Tree and Fault Tree analysis). Accurate and updated documentation is essential to ensure the correct identification of deviations, failure modes, and safety barriers within the process.

Chapter 3

Characterization of Hazardous Substances and Reference Mixtures

The purpose of this chapter is to define the criteria to be applied for the selection of hazardous substances and/or reference mixtures to be used in the subsequent development of accident scenarios. This represents one of the most critical stages in the assessment of industrial risks.

It is essential that the risk analyst evaluates the physicochemical, toxicological, and ecotoxicological properties of the substances and/or mixtures, as well as their use conditions and quantities stored. Both the substances that may be generated as a result of accidental events and the residues from production processes must also be taken into account.

As mentioned in Section 1.2.2, the selection of the reference substance(s) and/or mixture(s) should reasonably focus on those leading to the largest damage areas and, for equivalent extensions, to the most severe consequences on people, the environment, and property. The analyst must justify and clearly explain the selection of the reference substance(s) and/or mixture(s) used for scenario development.

The logical approach that can be adopted for the identification and characterization of reference substances can be summarized as follows:

- compilation of an inventory of all possible substances, mixtures, residues, intermediates, and wastes present at the establishment, in accordance with Annex I (Parts 1 and 2) of Legislative Decree 105/2015. At this stage, it is advisable to conduct a historical analysis, that is, a detailed review of databases and company records of past accidents in similar industrial facilities involving the identified substances.

- In the absence of such data, the consulted databases should still be specified. Grouping of substances into "behavioral classes", when CLP harmonized classifications are unavailable or incomplete. The concept of a behavioral class, analogous to the QSAR (Quantitative Structure–Activity Relationship) approach, assumes that

substances containing the same functional groups (e.g. nitro group $-NO_2$ exhibit similar physicochemical, thermal stability/reactivity, flammability/explosivity, and toxicological properties.

- Identification, for each behavioral class, of one or more reference substances showing the worst properties in terms of reactivity, thermal stability, flammability, explosivity, and toxicity, or those that may generate the widest damage areas and/or the most severe consequences.

- Identification of the physicochemical properties, thermal stability and reactivity, as well as ecological and toxicological aspects of all substances. Reference may be made to Sections 9, 10, 11, and 12 of the Safety Data Sheets (SDS), critically evaluating the quality of the reported data. Where gaps are identified, a new experimental characterization shall be carried out.

3.1 Intrinsic Hazard of Reference Substances/Mixtures

To develop an accurate methodology for identifying the chemical hazards arising from the combined physicochemical, toxicological, and instability/reactivity properties of chemical compounds, it is essential to collect comprehensive and detailed information on the characteristics of the substances involved in the process (whether they are reagents, intermediates, products, by-products, or wastes). It is equally important to assess the intrinsic instability of a substance in its pure form, due to the safety implications associated with its storage and handling. Table 3.1 summarises the main physicochemical properties that characterize a substance.

It is often assumed that chemical reactivity hazards are limited to the synthesis phase; however, they can also occur during other operations such as:

- mixing and physical transformation, which may include operations as crushing, blending, sieving, drying, distillation, absorption, heating, or dilution;

- storage, transfer, and packaging.

According to an investigation conducted by the U.S. Chemical Safety Board (CSB) [3], among 167 incidents that occurred in the United States between January 1980 and June 2001, 67 % were caused by reactions occurring in process equipment such as tanks, pipelines, and storage vessels, while only 25 % involved chemical reactors (Figure 3.1). The main causes of these accidents were chemical incompatibility and runaway reactions. It is estimated that approximately 90 % of these incidents could have been prevented by conducting preliminary studies based on information already available in the literature (Figure 3.1).

Table 3.1: Main properties for the characterisation of substances.

Physicochemical Properties	
Empirical formula	Molecular structure
Physical state under standard conditions (25 °C and 1 atm)	Melting point
Boiling point	Latent heat of fusion
Latent heat of vaporisation	Vapour pressure
Density	Viscosity
Solubility	Specific heat capacity
Thermal conductivity	Electrical conductivity
Dielectric constant	
Flammability - Explosiveness	
Flash point	Fire point
Explosibility range	Ignition or auto-ignition temperature
Flammability range	Minimum ignition energy (MIE)**
Limiting oxygen concentration (LOC)*	Explosion limits
Lower and upper flammability limits (LFL, UFL)	Minimum explosible concentration (MEC)*
Minimum ignition temperature (MIT)*	Deflagration index K_{st}*
Maximum explosion pressure $P_{\max}$*	
Stability - Reactivity	
Thermal stability	Heat of formation
Heat of decomposition	Heat of combustion
Decomposition products	Incompatibility
Reactivity with water	Propensity to polymerise
Corrosivity	Impact sensitivity
Toxicity Indicators	
IDLH	AEGL
ERPG (1,2,3)	TLV (TWA, STEL, C)
Physicochemical Properties Relevant to Environmental Fates	
Henry's constant	Octanol–water partition coefficient K_{OW}
Organic carbon partition coefficient K_{OC}	Soil distribution coefficient K_d
Soil half-life t_{50}	

** These parameters apply exclusively to powders.*

*** This parameter describes the behaviour of flammable liquids, vapours, and powders.*

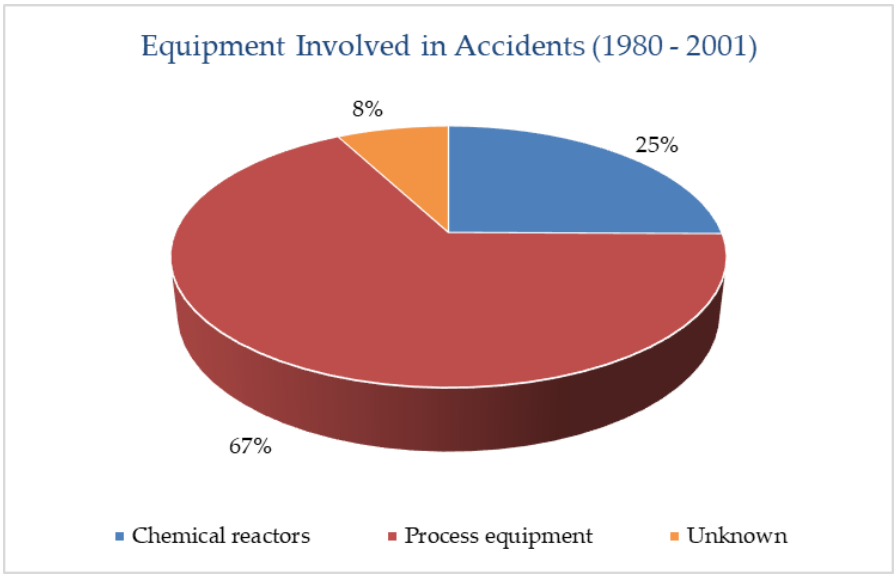

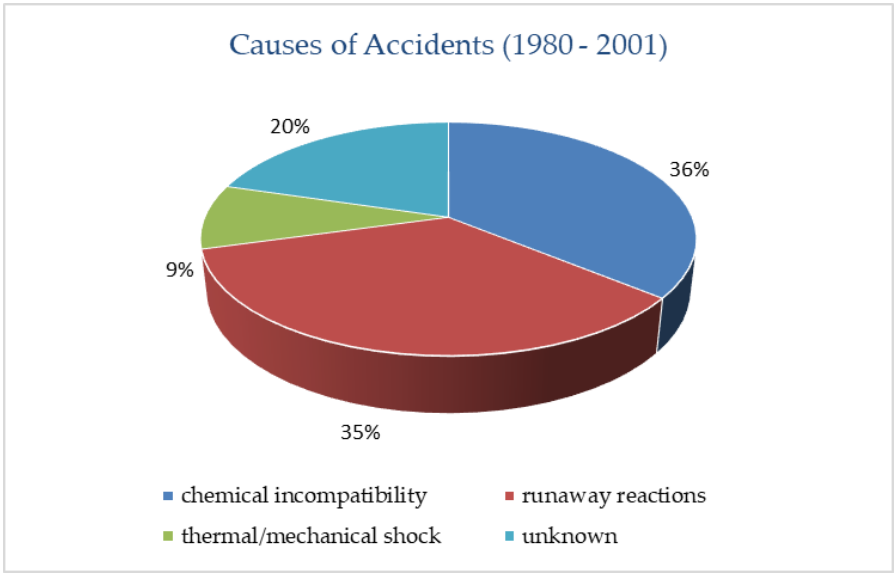

Figure 3.1: Equipment involved in industrial accidents in the United States (1980–2001) (top) and causes of industrial accidents in the United States (1980–2001) (bottom).

3.1.1 Chemical Compatibility

When discussing chemical compatibility between two or more substances, this refers to the possibility of bringing them into contact without triggering exothermic reactions (i.e. reactions that lead to a temperature increase in the system, such as oxidations) or reactions that rapidly and violently release toxic and/or flammable gases or vapors (e.g. decompositions). Conversely, chemical incompatibility occurs when such reactions can be initiated. Particular attention should be paid to substances that may become hazardous when mixed with others or when coming into accidental contact with air or water (see CLP classification in Section 2 of the Safety Data Sheet).

The purpose of this analysis is to determine whether accidental contact between substances could lead to undesired events, without quantifying their magnitude. A detailed quantitative characterization should only be carried out for the reference substances identified.

Chemical interaction matrices (Figure 3.2) and chemical compatibility tables (Table 3.2) are fundamental tools for assessing not only the compatibility between different substances, but also the compatibility between the substances and the materials used for storage or equipment construction. These tools help reduce the risk of undesired reactions, corrosion, material degradation, or release of hazardous substances.

In SDSs and compatibility tables, the information usually refers to the pure substance. However, the chemical behavior in solution or in the presence of impurities may differ significantly. Whenever possible, reference should be made to the SDS of the solution rather than to that of its individual components.

The procedure for assessing chemical compatibility differs depending on whether the context involves simple storage operations or facilities where mixing and chemical reactions take place. In both cases, a good starting point is the use of the SDS, paying particular attention to the sections listed in Table 3.3.

For waste treatment plants performing mixing operations, a useful operational reference for chemical compatibility verification is the HSE guideline "Compatibility Testing Guidance for Bulking Operations in the Waste Treatment Industry". In more complex cases, it is good practice to divide the study into two stages:

1. Theoretical phase, information gathering through literature review:
    (a) Bretherick's Handbook of Reactive Chemical Hazards, 8th Edition, Peter Urben, Elsevier Health Sciences, 2017;
    (b) Journal of Loss Prevention in the Process Industries;
    (c) Journal of Hazardous Materials;
    (d) Specialized software such as:
        i. CAMEO Chemicals.
        ii. Cole-Parmer Technical Compatibility Database.
        iii. CHETAH
2. Experimental phase. Testing using calorimetric techniques.

A fundamental rule in chemical storage is to keep chemically incompatible substances separated to prevent accidental mixing that could lead to fires, explosions, or the release of toxic gases.

Hazardous reactions can be triggered by poor warehouse management, leading to the contact of incompatible materials as a result of:

- accidental rupture of drums, cans, or containers;
- fires or earthquakes;
- mixing of gases or vapors leaking from poorly sealed containers;
- incorrect labelling of containers;
- incompatibility between container material and stored substance.

It is essential to periodically verify the integrity of containers to prevent accidental leaks. A good practice is to store chemicals according to their hazard and compatibility classes, using separate cabinets or secondary containment, and applying clear labelling indicating their position. This same principle should be applied to industrial storage areas.

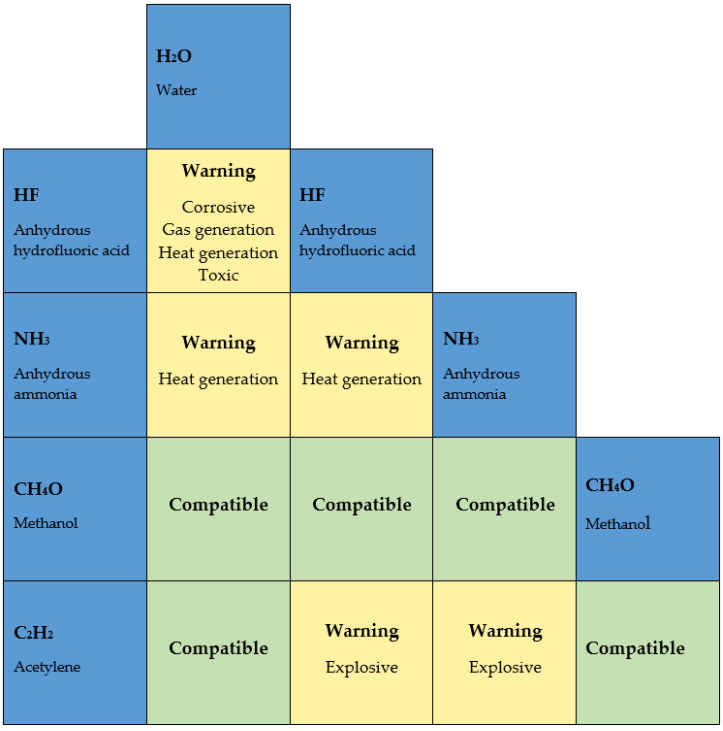

Figure 3.2: Example of interaction matrix.

Table 3.2: Example of chemical compatibility chart [4].

Substance A	Substance B	Type of Hazard
Corrosive acids or bases	Metals (e.g. aluminium, calcium, lithium, potassium, magnesium)	Fire
Hydrogen peroxide	Amines	Explosion
Acetylene	Copper	Formation of copper acetylide, explosive
Potassium permanganate	Sulphuric acid	Explosion
Carbon tetrachloride	Alkali metals	Explosion
Olefins	Air	Peroxides formation
Acrylates and Acrylic Acid	Nitric acid	Flammable reaction
Nitric acid	Amine	Explosive reaction
Cyanide–sulphur mixture	Acids	Fire
Chlorates	Ammonium salts	Formation of explosive ammonium salts
Isocyanates	Ammonia	Explosive reaction
Nitro compounds	Alkalis	Unstable mixture
Nitric acid	Aluminium powder	Flammable reaction

Table 3.3: Safety data sheet sections to be consulted to identify possible incompatibilities.

SDS Section	Title
2.1	Classification of the substance or mixture
5	Firefighting measures
7.2	Conditions for safe storage, including any incompatibilities
8.2	Exposure controls / Personal protection
9.1	Information on basic physical and chemical properties
10.1	Reactivity
10.2	Chemical stability
10.3	Possibility of hazardous reactions
10.4	Conditions to avoid
10.5	Incompatible materials
10.6	Hazardous decomposition products
11.1	Information on toxicological effects

3.2 Thermal Stability and Chemical Reactivity

Raw materials, intermediates, products, and wastes must be examined and assessed to determine potential hazards related to reactivity and thermal instability. In addition to the reaction of interest, undesired reactions (such as polymerizations and decompositions) as well as those that may occur due to the accidental mixing of incompatible substances, must also be considered.

The concept of thermal stability of a substance (or mixture) is linked to its behavior when it is:

- subjected to an increase in temperature over time;
- maintained at a given temperature for an extended period (e.g. longer than three days) within a container (made of a specific material) filled with a gas atmosphere of known composition (e.g. air, nitrogen, etc.).

The study of a substance's thermal behavior allows the identification of endothermic or exothermic phenomena, both of which may lead to the release of gases and/or vapors. In crystalline solids, a rearrangement of the crystal lattice may also be observed.

Chemical reactivity refers to the tendency of a substance or mixture to react and form new products. For safety assessment purposes, only exothermic phenomena involving the release of gases or vapors will be considered in the following sections. To identify hazards associated with chemical reactivity, the following steps are essential:

- collect all available information on reactivity from internal company sources, external databases, and dedicated software;
- when data from literature are insufficient, use theoretical predictive methods and thermal analysis techniques (see Table 3.4);
- analyze thermodynamic and kinetic data;
- assess the presence of potential risks such as accidental mixing, temperature increases, contamination, scale-up effects, and autocatalytic reactions that may initially appear stable but can be triggered after an induction period;
- consider the possibility of endothermic reactions capable of generating toxic and/or flammable gaseous products;
- estimate the consequences of deviations from normal process conditions;
- conduct a thorough and rigorous review of hazards, as well as prevention and protection measures, to ensure that the identified reactivity hazards are effectively addressed.

The flowchart proposed by the CCPS (Center for Chemical Process Safety) (Figure 3.3) represents a useful tool for identifying preliminary hazards related to chemical reactivity.

In particular, insufficient attention to safety in processes involving exothermic reactions greatly increases the likelihood of losing temperature control within an industrial reactor, a phenomenon known as thermal runaway. During a runaway reaction, an imbalance arises between the rate of heat generation within the reacting mass and the rate of heat removal by the cooling system. This imbalance leads to a further temperature increase, triggering a self-accelerating cycle: as the temperature rises, the reaction rate increases exponentially, resulting in loss of thermal control of the system.

A runaway reaction is always preceded by an induction period, during which self-heating of the reacting mass occurs. The temperature rise may trigger secondary exothermic reactions (in addition to the intended one), potentially generating gaseous by-products (e.g. from decompositions). In closed systems, this leads to a simultaneous increase in both temperature and pressure, which, in the worst-case scenario, may cause the physical explosion of the reactor.

Table 3.4 provides an overview of the most common experimental techniques used for calorimetric investigations.

Table 3.4: Experimental techniques for assessing thermal stability and chemical reactivity.

Technique	**Measured or Calculated Values**	**Advantages**	**Disadvantages**	**When to Use**
TGA	Sample mass loss/gain; Onset temperature of phenomena involving mass change (e.g., decomposition, oxidation, etc.)	Small sample quantity (1–100 mg); Fast (dynamic tests <2 h); Wide temperature range (30–1000 °C)	Does not provide reaction heat data (unless coupled with DSC); Cannot reproduce pressurized conditions	Initial screening to identify decomposition, oxidation of organic/metallic materials, and evaporation or sublimation phenomena
DTA	T_{onset}	Small sample quantity; Fast (dynamic tests <2 h); Wide temperature range (-150–2000 °C)	Not representative of plant operating conditions; Does not provide information on pressure, mixing, or reagent addition; High thermal inertia.	Initial screening to identify onset temperatures of endothermic and exothermic phenomena.
DSC	ΔH_{rx} Specific heat (c_p) Kinetics T_{onset}	Small sample quantity; Fast (dynamic tests <2 h); Wide temperature range (up to 600 °C)	Not representative of plant operating conditions; Does not provide information on pressure, agitation, or reagent addition; High thermal inertia; Provides global kinetic information but not detailed mechanisms.	Initial screening to determine onset temperatures and enthalpies of endothermic and exothermic events.

Technique	Measured or Calculated Values	Advantages	Disadvantages	When to Use
Isothermal Titration Calorimetry(e.g., C80)	ΔH_{rx} ΔP dP/dt Kinetics T_{onset}	Small sample quantity (<10 g); Good temperature range; Can reproduce process conditions.	Slow analysis (maximum heating rate 1–2 °C/min).	Detailed screening to determine onset temperatures, enthalpies, reaction kinetics, and catalytic effects.
ARC	ΔH_{rx} ΔP dP/dt Kinetics T_{onset}	Small sample quantity (<10 g); Fast (<2h); Good temperature range.	High thermal inertia; Small volumes (less representative); Magnetic stirring only; Long test duration.	Thermal stability; Autocatalysis; Runaway study.
PHI-TEC II	ΔH_{rx} ΔP dP/dt Kinetics T_{onset}	Wide temperature range; Thermal inertia factor between 1.02–1.2; Internal pressure compensation.	Medium volumes (≈120 mL); Magnetic stirring (motor-driven for glass cells); Long test times due to stepwise heating.	Thermal stability; Autocatalysis; Runaway study; Sizing of safety devices.
ARSST	ΔH_{rx} dP/dt dT/dt T_{onset} TMR	Low cost; Fast; Low thermal inertia (1.02–1.05).	Low heating rate (up to 2 °C/min).	Thermal stability; Autocatalysis; Runaway study; Sizing of safety devices.
Reaction Calorimeters (e.g., RC1, Peltier Cell Systems)	Reaction rate Kinetic constants Activation energy Specific heat transfer coefficient (U) Overall heat transfer coefficient (UA) Specific heat (C_p) ΔH_{rx}	Can accurately reproduce process conditions; Can operate under reflux.	Requires significant quantities of substances (tens of grams up to 1–2 kg).	Process reactivity studies; Peak heat flow determination; Evaluation of thermal conditioning systems.

3.3 Theoretical Predictive Methods

This section describes the main preliminary investigation methods used to assess the stability of substances and the production processes in which they are involved.

The chemical risk associated with a thermally unstable material or system can often be anticipated through thermodynamic analysis and a correct interpretation of the fundamental laws of physical chemistry.

The first step in identifying a thermal hazard consists of evaluating the thermodynamic potential of the system (that is, determining whether the reaction is thermodynamically

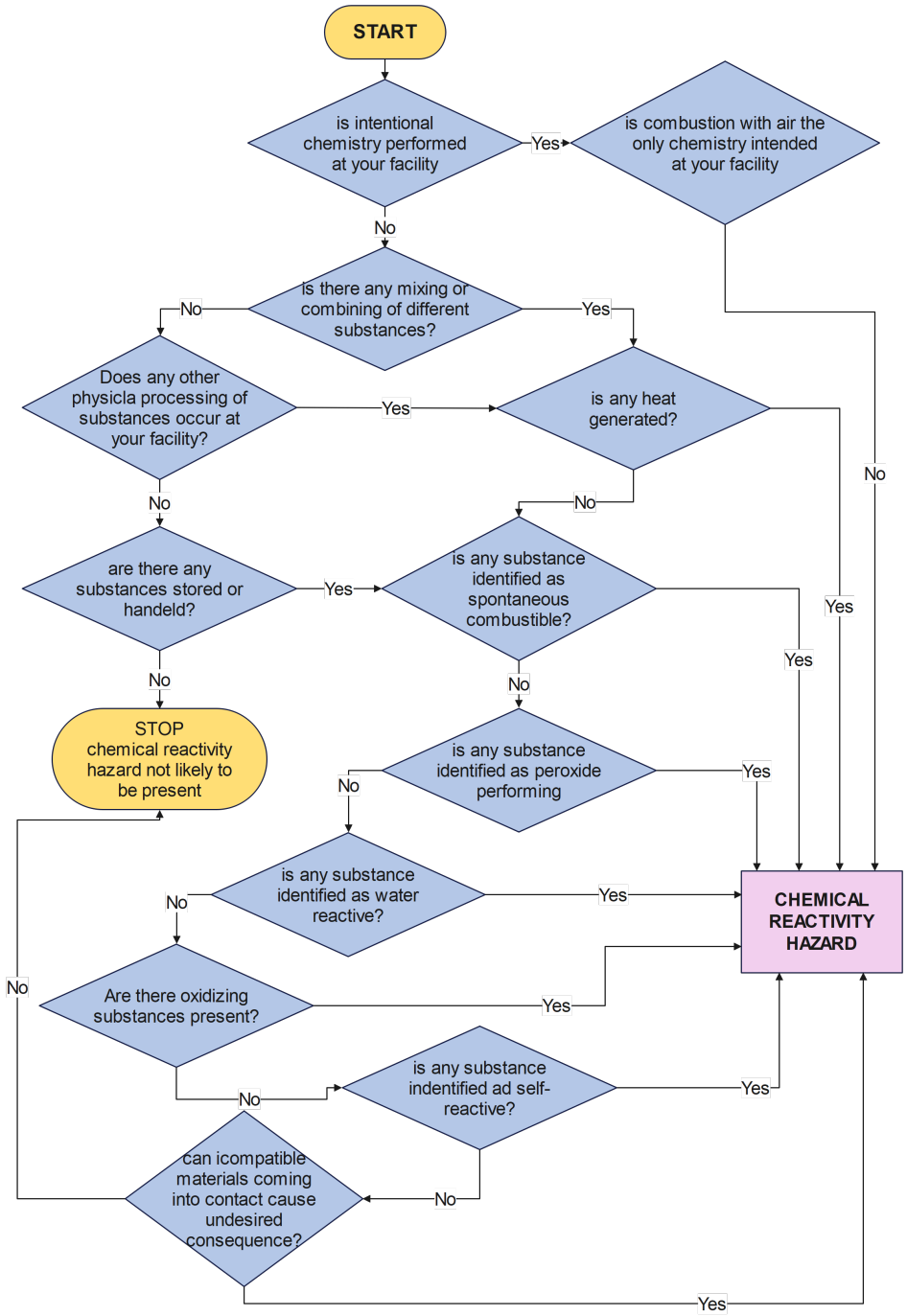

Figure 3.3: Example of a flowchart for the initial screening aimed at assessing the possible presence of substances that may present chemical reactivity hazards (adapted from [5]).

favored and, subsequently, estimating the amount of thermal energy released). The heat generated can be correlated with the adiabatic temperature rise, and therefore with the potential instability of reactants, products, or reacting mass. Consequently, if all the thermal effects of an undesired reaction can be predicted or calculated in advance, it is possible, at least as a first approximation, to estimate its hazardous potential [6].

Over the years, several theoretical methods have been developed to both identify and quantify the degree of hazardouness of a chemical substance in terms of reactivity and instability. Since these approaches are based on conservative assumptions, they provide screening-level assessments that, while not rigorous, are nonetheless valuable for preliminary hazard identification.

Applying a predictive method during the early stages of hazard identification and risk evaluation makes it possible to pinpoint the most critical aspects on which to focus subsequent, more rigorous investigations (primarily experimental studies) aimed at analyzing potential runaway reaction scenarios. It should be emphasized that theoretical predictive methods alone cannot (and should not) be neither considered exhaustive nor used as a substitute for experimental investigations, even at a screening level. Rather, they should be regarded as tools to either narrow the experimental domain or select the most appropriate techniques for the case under study [4].

3.3.1 Chemical Reactivity Worksheet

The Chemical Reactivity Worksheet (CRW) is a free software tool developed and distributed by the Emergency Management Office, in collaboration with the U.S. Environmental Protection Agency (EPA), the National Oceanic and Atmospheric Administration (NOAA), and the American Institute of Chemical Engineers (AIChE).

It is a comprehensive database containing information on more than 5,000 chemicals and mixtures, designed to help users identify potential chemical incompatibilities and predict the outcomes of accidental mixing.

Since the CRW adopts a conservative approach in predicting binary interactions, the results should be interpreted with caution. Moreover, the software provides compatibility information only under ambient temperature and pressure conditions. Therefore, care must be taken when applying CRW results to systems operating at different temperatures or pressures, as the chemical behavior may vary significantly [5].

3.3.2 Oxygen Balance

Violent oxidation reactions are often explosive reactions. The oxygen balance is a criterion used to estimate the potential hazard and instability of substances or reaction mixtures that contain oxygen.

The oxygen balance is the amount of oxygen, expressed as a weight percentage, released (or required) by the complete conversion of the material into CO_2, H_2O, SO_2, Al_2O_3, N_2 and other oxides. If the oxygen contained in the molecule is sufficient to achieve complete oxidation, the oxygen balance is zero and the maximum energy release occurs (a condition sometimes referred to as complete explosion). If the oxygen bound to

the molecule is insufficient for complete oxidation, the balance is negative; conversely, if oxygen is in excess, the balance is positive.

For a generic molecule with composition CxHyOz, the oxygen balance is defined as the difference between the oxygen content of the molecule and the oxygen required for complete oxidation:

$$B_O = -\frac{1600(2x + y/2 - z)}{\text{Molecular Weight}} \tag{3.1}$$

Equation (3.1) is not valid for substances that contain other elements (e.g., halogens, metals, or energetic substituents).

The oxygen – balance – based assessment of explosive potential is not an absolute measure, but rather an indicator. Its interpretation depends on how oxygen is chemically bound within the molecule. For example, acetic acid contains oxygen in its molecular structure, but it is not an explosive material because that oxygen cannot be efficiently used to oxidize the carbon atoms under typical conditions [7].

When estimating explosive power by means of the oxygen balance, it should be borne in mind that the oxidizing capacity of the oxygen atom depends not only on its proportion in the molecule but also on the molecular structure. If oxygen in the molecule is already tightly bound in stable combinations with hydrogen or carbon, it is not available to react further; conversely, labile oxygen - containing functionalities (for instance, N=O groups) may more readily participate in redox or decomposition processes. In principle, one could distinguish between total oxygen and active oxygen, but this distinction is difficult to implement in practice because many structural and electronic factors influence whether oxygen is available for oxidation.

Some explosives (for example, lead azide) do not rely on oxidation reactions during detonation and therefore cannot be characterized by an oxygen balance. Nevertheless, when oxygen is present in the molecule, it plays an important role in the thermal energy release associated with molecular dissociation into simpler fragments [8].

3.3.3 Reaction Hazard Index

Stull developed a classification system to establish the relative potential hazards of specific chemical substances by introducing the Reaction Hazard Index (RHI), an empirical index of reactivity. The RHI is related to the maximum adiabatic temperature reached by the products of a decomposition reaction and is defined as:

$$RHI = \frac{10\ T_d}{T_d + 30\ E_a} \tag{3.2}$$

where

T_d decomposition temperature [K];

E_a Arrhenius activation energy [kcal/mol].

Low-reactivity substances exhibit low RHI values (1÷3), whereas unstable substances show higher values (5÷8). Table 3.5 reports typical RHI values for selected compounds.

Table 3.5: Reaction Hazard Index (RHI) values for selected compounds [5].

Formula	Compound	Decomposition temperature (K)	Activation energy (kcal/mol)	RHI
$C_2H_4O_2$	Acetic acid	634	67.5	2.38
N_2H_4	Hydrazine	1,338	60.5	4.25
C_2H_2	Acetylene	2,898	40.5	7.05
$C_3H_5N_3O_9$	Nitroglycerin	2,895	40.3	7.05

3.3.4 Material Factor

The Material Factor (MF), used in the Dow Fire and Explosion Index (F&EI) method, represents a measure of the potential energy release of a substance under ambient temperature and pressure conditions.

It is evaluated based on the reactivity and flammability of the material, as indicated by the NFPA hazard numbers: the Flammability Number (N_f) and the Reactivity Number (N_r). If the substance is a combustible dust, the Dust Hazard Class Number (St) is used instead of the flammability rating (N_f).

Table 3.6 provides the criteria for determining the Material Factor (MF) based on the physicochemical characteristics of the substances and their hazard indices (N_f, N_r, St) [8].

3.3.5 CHETAH

The Chemical Thermodynamics and Energy Release Evaluation (CHETAH) program, developed by ASTM in 1974, is designed to predict thermochemical and flammability properties, as well as some reactive chemical hazards, for pure substances, mixtures, and chemical reactions. The software allows the user to:

- estimate the heat of reaction;
- estimate the heat of combustion;
- determine equilibrium constants of reactions;
- estimate thermodynamic properties of mixtures;
- predict the tendency of a compound or mixture to propagate deflagration or detonation.

All calculations are based solely on the molecular structure of the chemical species, using the heat of formation estimated by the Benson group contribution method, which assigns a heat of formation value to each functional group according to its molecular context.

Table 3.6: Criteria for the determination of the Material Factor (MF). FP is the flash point temperature measured in a closed cup, while BP is the boiling point at atmospheric pressure [8].

Material type	**Condition / Hazard index**		N_r**=0**	N_r**=1**	N_r**=2**	N_r**=3**	N_r**=4**
Flammable and combustible liquids or gases (including volatile solids)	Non-combustible	N_f=0	1	14	24	29	40
	FP>93.3°C	N_f=1	4	14	24	29	40
	37.8<FP<93.3°C	N_f=2	10	14	24	29	40
	22.8<FP<37.8°C or FP<22.8°C and BP>37.8°C	N_f=3	16	16	24	29	40
	FP<22.8°C and BP<37.8°C	N_f=4	21	21	24	29	40
Combustible dusts or mists	St-1	–	16	16	24	29	40
	St-2	–	21	21	24	29	40
	St-3	–	24	24	24	29	40
Combustible solids	Compact	N_f=1	4	14	24	29	40
	Granular	N_f=2	10	14	24	29	40
	Foams, fibers, powders, etc.	N_f=3	16	16	24	29	40

CHETAH does not provide kinetic data; therefore, reaction rate, activation energy, and reaction order must be determined experimentally. It is important to emphasize that CHETAH should not replace experimental tests. Instead, it should be regarded as a predictive screening tool, useful for identifying substances that require further investigation.

The database of the latest version (CHETAH 11.0) includes 397 Benson groups for liquids, 875 for aqueous species, and 306 for solids. When describing a molecule, it is essential not to mix Benson groups from different physical states; for example, for a liquid compound, only the liquid-phase Benson groups should be used. In most cases, corrections are applied by adding specific functional groups to improve accuracy. For instance, to estimate the thermochemical properties of ethanol (Figure 3.4), the following Benson groups are used:

- $CH_3-(C)$
- $CH_2-(C, O)$
- $OH-(C)$

The CHETAH model presents some limitations:

- It does not handle heterocyclic compounds and nitriles accurately.

- It does not yield valid results for very fast and highly exothermic reactions, such as vinyl polymerizations.
- The predicted decomposition enthalpy may differ by up to 50% from the experimental value, as since the program assumes decomposition products specifically aimed at maximizing the decomposition enthalpy.
- Reaction enthalpy estimates are accurate for gas-phase systems but less so for liquids.

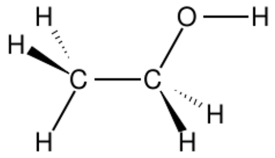

Figure 3.4: Chemical structure of ethanol.

The hazard potential of a substance is expressed through four risk criteria, each assigned a specific risk level by the software. CHETAH also provides an overall Energy Release Potential (ERP) value as an indicator of total chemical reactivity.

First Criterion – Maximum Decomposition Enthalpy

The program assumes that when a generic compound with the formula CHNO decomposes, the oxygen atoms within the molecule combine with hydrogen to form water (H_2O); any excess oxygen forms carbon dioxide (CO_2), while excess hydrogen may react with carbon to produce methane (CH_4).

The nitrogen present in the molecule usually converts to molecular nitrogen (N_2); however, if hydrogen or both hydrogen and oxygen are present in excess, ammonia (NH_3) or nitric acid (HNO_3) may be formed, respectively.

The software calculates the combination of these decomposition products that yields the maximum heat of decomposition. For example, in the case of the thermal decomposition of pure water, the set of products that maximizes the decomposition heat (calculated using Benson's group additivity method) is hydrogen (H_2) and oxygen (O_2).

The CHETAH program classifies the hazard level as high, medium, or low according to the value of the maximum decomposition enthalpy, as reported in Table 3.7. An example of the first criterion, computed with CHETAH, is shown in Table 3.8.

Second Criterion – Enthalpy Difference

The second criterion is based on the difference between the enthalpy of combustion and the enthalpy of decomposition. A compound containing sufficient oxygen in its structure may represent a hazard, since it can undergo oxidation with energy release.

Table 3.7: First CHETAH criterion.

High Risk	$\Delta H_{dec,\max} < -0.7$ kcal/g
Medium Risk	$-0.7 < \Delta H_{dec,\max} < -0.3$ kcal/g
Low Risk	$\Delta H_{dec,\max} > -0.3$ kcal/g

Table 3.8: Examples for the first CHETAH criterion.

Chemical formula	**Compound name**	$\boldsymbol{\Delta H_{dec,\max}}$ **(kcal/g)**	**Risk level**
$C_2H_4O_3$	Peracetic acid	−0.85	High
C_2H_3Cl	Vinyl chloride	−0.63	Medium
$C_2H_4O_2$	Acetic acid	−0.19	Low

Depending on the value of the enthalpy difference, the risk level can be classified as high, medium, or low (Table 3.9). Table 3.10 shows an example of the second criterion calculated using CHETAH.

Table 3.9: Second CHETAH criterion.

High Risk	$\Delta H_{comb} - \Delta H_{dec,\max} < -0.3$ kcal/g
Medium Risk	$-0.3 < \Delta H_{comb} - \Delta H_{dec,\max} < -5.0$ kcal/g
Low Risk	$\Delta H_{comb} - \Delta H_{dec,\max} > -5.0$ kcal/g

Third Criterion – Oxygen Balance

The third criterion, known as the Oxygen Balance (B_O), measures the amount of oxygen bound within a molecular structure that could potentially convert part or all of the molecule into the corresponding combustion products.

For a generic molecule with the formula CxHyOz, the oxygen balance can be calculated according to Equation 3.1. In practice, the oxygen balance expresses how many grams of oxygen are required to completely oxidize 100 grams of a compound. The closer this index is to zero (meaning that all the oxygen needed for complete oxidation is already contained within the molecule) the higher the potential risk associated with the substance, as shown in Table 3.11. However, the oxygen balance must be interpreted with caution. For example, two isomers having the same B_O value may exhibit completely different behaviors: one may be explosive, while the other is stable.

Table 3.10: Examples for the second CHETAH criterion.

Chemical formula	Compound name	$\Delta H_{dec,\max}$ (kcal/g)	Risk level
$C_2H_4O_3$	Peracetic acid	−1.85	High
C_2H_3Cl	Vinyl chloride	−3.79	Medium
$C_2H_4O_2$	Acetic acid	−5.38	Low

Table 3.11: Third CHETAH Criterion.

High Risk	$-80<B_O<120$
Medium Risk	$120<B_O<240$; $-160<B_O<-80$
Low Risk	$B_O<240$; $B_O<-160$

A typical case is represented by peracetic acid (explosive) and glycolic acid (stable), which share the same B_O value but differ in the nature of the chemical bonds involved (Figure 3.5). Indeed, when calculating B_O, all oxygen atoms are counted indiscriminately, regardless of the type of bond in which they are involved. Table 3.12 provides an example of the third criterion as estimated using CHETAH.

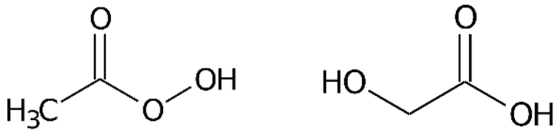

Figure 3.5: Left: structural formula of peracetic acid. Right: structural formula of glycolic acid.

Fourth Criterion: Modified Decomposition Enthalpy

The fourth criterion is defined by the following Equation 3.3:

$$Y = \frac{10\,\Delta H^2_{\mathrm{dec,max}}\,W}{n} \tag{3.3}$$

where

$\Delta H_{dec,\max}$	maximum heat of decomposition (kcal/g);
W	molecular weight;
n	total number of atoms in the molecule.

Depending on the value of Y, three different risk levels can be identified, as shown in

Table 3.12: Example of estimated risk level calculated using the third CHETAH criterion.

Chemical formula	Compound name	B_O	Risk level
$C_2H_4O_3$	Peracetic acid	−63.1	High
C_2H_3Cl	Vinyl chloride	−128.0	Medium
$C_2H_4O_2$	Acetic acid	−186.0	Low

Table 3.13. Table 3.14 presents an example of the risk level estimated using the fourth CHETAH criterion [9].

Table 3.13: Fourth CHETAH Criterion.

High Risk	Y>110
Medium Risk	30<Y<110
Low Risk	Y<30

Table 3.14: Example of estimated risk level calculated using the fourth CHETAH criterion.

Chemical formula	Compound name	Y	Risk level
$C_2H_4O_3$	Peracetic acid	61.1	High
$C_7H_5N_3O_6$	Trinitrotoluene	215.0	Medium
$C_2H_8O_2$	Ethyl acetate	6.0	Low

3.4 Calorimetry

Experimental investigation is essential for the complete characterization, in terms of both safety and control, of either the substances or the processes in which they are involved. Its purpose is to define the conditions that may trigger uncontrolled reactions, quantify the consequences of such reactions, and establish safety margins between normal operating conditions and the onset of hazardous exothermic effects.

When studying a reaction from a safety perspective, it is crucial to ask the following questions:

- is the reaction exothermic? If so, how fast is the heat released and within what temperature range does this occur?

- is there a temperature peak? If so, how many degrees above the normal process temperature?
- is there a possibility of pressure build-up within the system? If so, when and how rapidly, and within what temperature range does pressure accumulate in the system?
- can the pressure increase cause the reactor to rupture?

Indeed, insufficient attention to the safety of a process involving exothermic reactions significantly increases the likelihood of losing temperature control within an industrial reactor, giving rise to a phenomenon known as a "runaway reaction".

The experimental approach to study runaway phenomena is never straightforward. There is no single test capable of fully defining the hazard associated with such phenomena. Moreover, it is often difficult to fully understand the fundamental meaning of test methods and to correlate the obtained data with the physicochemical properties of the system under investigation. A hazardous reaction may have several origins and can be initiated in different ways.

Each testing method evaluates only the sensitivity of a substance or reaction mixture to a specific energy impulse, under the conditions imposed during the test. Therefore, a single calorimetric test cannot be absolute or conclusive in providing answers. The results must not be considered in isolation; rather, the hazard must be assessed based on a series of tests conducted under different conditions.

To evaluate the consequences of a runaway reaction, it is necessary to determine:

- the heat of reaction and peak heat flux under process conditions;
- the specific heat capacity of the reacting mass;
- the adiabatic temperature rise;
- the boiling point of the reacting mixture;
- the temperature range in which undesired reactions may be initiated and the corresponding heat of reaction (sometimes undesired polymerization reactions may lead to runaway phenomena);
- the quantity and rate of gas release (maximum pressure and maximum rate of pressure increase);
- the effects of impurities, operator errors, and other deviations [4].

Over the past thirty years, calorimetry has proven to be an effective tool for determining kinetic and process parameters, as well as for studying the behavior of exothermic and/or self-accelerating reactions. It provides all the necessary information for process optimization and scale-up.

The main data that can be derived from calorimetric analysis are:

- thermodynamic data;
- reaction kinetics;
- rate of heat generation;
- required cooling power;
- accumulation of reactants;
- maximum reaction temperature under adiabatic conditions;
- overall heat transfer coefficient.

Not all experimental analysis systems allow the extraction of this information, nor they can provide it with the same degree of accuracy. The choice of instrument depends therefore on the level of detail required in the investigation.

Table 3.15 lists the most common instruments and techniques used in calorimetric analysis. Table 3.4 summarizes the most commonly used techniques, highlighting their main advantages and disadvantages, the parameters that can be determined, and their respective fields of application [4, 8].

3.4.1 Operating Modes

The experimental investigation methodologies used in this field can be grouped into three main categories:

- thermal analysis;
- adiabatic calorimetry;
- reaction calorimetry.

There are several ways to classify calorimeters. Based on temperature control, they can be distinguished as follows:

- Programmed-temperature tests (conducted under dynamic conditions, i.e., temperature ramp): these tests can provide preliminary information on the likelihood and severity of self-heating phenomena.
- Constant-temperature tests (conducted under isothermal conditions): these tests provide information on the kinetic behavior of the reaction, such as the presence of autocatalysis and the apparent activation energy.
- Isoperibolic or heat-accumulation tests (performed under conditions where the reacting mixture exchanges heat with a wall or fluid at constant temperature): these can provide a direct indication of the safe storage temperature and help identify autocatalytic reactions.

- Adiabatic tests: these represent the ideal method for simulating the extreme case of poor heat dissipation; the results can be directly used to estimate the time to explosion.
- Reaction calorimetry tests: these tests allow the reproduction of actual process conditions and the determination of reaction heats, heat release rates, kinetic parameters, and heat-transfer data [4].

3.5 Thermal Analysis Techniques

The term thermal analysis refers to a set of techniques that measure a physical property (such as mass or heat/heat flow) of a sample subjected to a controlled thermal cycle as a function of temperature or time.

Table 3.15: Common instruments and techniques used in calorimetry (adapted from [4]).

Abbreviation	Technique/Instrument
TGA	Thermogravimetric Analysis
DTA	Differential Thermal Analysis
DSC	Differential Scanning Calorimetry
C80	Heat Flow Calorimeter
PHI-TEC II	Adiabatic Calorimeter
ARC	Accelerating Rate Calorimeter
RC	Reaction Calorimeter
Dewar	Dewar Vessel
EDM	Exothermal Decomposition Meter
RSST	Reactive System Screening Tool
-	miniautoclave
IET	Insulated Exotherm Test
STT	Sealed Tube Test
SEDEX	Sensitive Detector for Exothermic Processes
IST	Isothermal Storage Test
DPT	Decomposition Pressure Test
-	Sikarex
HET	Homogeneous Explosion Test
AST	Adiabatic Storage Test
VSP	Vent Sizing Package

This category includes:

- Thermogravimetric Analysis (TGA);
- Differential Thermal Analysis (DTA);
- Differential Scanning Calorimetry (DSC);
- Isothermal Titration Calorimetry (C80)

These techniques are primarily used to assess the thermal stability of a substance or mixture.

3.5.1 Thermogravimetric Analysis

Thermogravimetric Analysis (TGA) consists of measuring the change in mass of a sample as a function of temperature (when subjected to heating, typically at a constant rate, e.g. 5 or 10 °C/min) or as a function of time (for isothermal tests).

TGA provides information on:

- the thermal stability of the sample;
- the thermal stability of possible intermediate compounds (i.e., those that form or remain in the condensed phase after an initial mass loss);
- the stability of the sample in corrosive or reactive atmospheres;
- the determination of the content of low-boiling substances (residual monomers, solvents, or moisture);
- when coupled with a Fourier Transform Infrared (FTIR) spectrometer or a mass spectrometer, TGA can determine the composition of residues and intermediates.

Mainly referring to organic substances subjected to eventual devolatilization, useful information from this technique can be obtained only in case of significative volatile products release. If the goal is to investigate decomposition, the sample should not vaporize before decomposing, as otherwise this information would be lost.

Chemical or structural changes that do not involve a change in mass cannot be detected by TGA, and no direct information on degradation products or mechanisms can be obtained. However, by coupling the TGA with a Fourier Transform Infrared (FTIR) analyzer, it is possible to obtain detailed information about the nature of the decomposition products and volatile species released during heating or during an isothermal analysis period.

Factors that can affect precision, accuracy, and reproducibility of measurements include:

- heating rate of the furnace: an increase in heating rate generally shifts the initial and final decomposition temperatures to higher values, although the total weight change remains the same;

- furnace atmosphere: this includes both the gas flow rate over the sample and the composition and nature of the gas;
- sample characteristics: parameters such as sample quantity, homogeneity, particle size, and thermal conductivity are all relevant.

The effect of the furnace atmosphere on the TGA curve mainly depends on:

- the type of reaction;
- the nature of the decomposition products;
- the type of atmosphere used: for assessing thermal stability for safety purposes, tests are conducted both in an oxidizing atmosphere (air) and in an inert atmosphere (nitrogen). This allows one to distinguish between decomposition and combustion or oxidation reactions.

TGA can highlight both physical transformations (sublimation, evaporation, absorption, desorption, adsorption) and chemical transformations (decomposition, oxidation, reduction, combustion) through the weight loss experienced by the sample due to the evolution of gases resulting from decomposition reactions or evaporation of volatile species.

However, TGA is not always accompanied by a decrease in sample mass; in some cases, a weight gain is observed, as in the oxidation of a metallic powder or gas adsorption phenomena.

The result of the experiment is a thermogram that plots temperature (or time) on the x-axis and mass change (absolute or percentage) on the y-axis (Figure 3.6). In addition to the TGA curve, the first derivative with respect to time (DTG curve) is often shown. This highlights more clearly the onset and end temperatures of mass changes in the sample and the maximum rate of mass loss. It also emphasizes small slope variations that might otherwise be undetectable from the TGA curve alone [4, 8].

3.5.2 Differential Thermal Analysis

Differential Thermal Analysis (DTA) is a calorimetric technique in which both a test sample and an inert reference sample are heated or cooled simultaneously, while continuously measuring the temperature difference between them.

At the beginning of the analysis, the temperature of both samples increases (or decreases) until a physical or chemical transformation occurs in the test sample, resulting in heat absorption or release. At that point, a temperature difference is recorded between the test and the reference sample. The sign of this temperature difference indicates whether the event is endothermic or exothermic, allowing its classification (e.g., melting, decomposition reaction, etc.).

The test can be carried out in either an oxidizing atmosphere (air) or an inert atmosphere (e.g., nitrogen). The material of the sample holder and the thermocouple depends on the operating temperature range of the instrument. The most common sample holders are crucibles made of platinum, alumina, aluminum, and stainless steel.

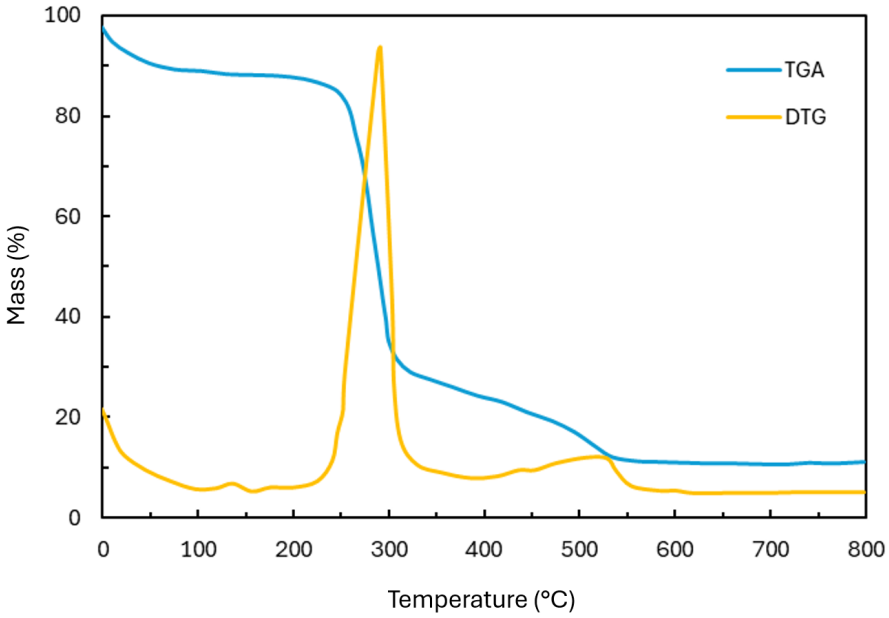

Figure 3.6: Example of TGA and DTG curves.

The factors influencing the test are similar to those observed for TGA:

- Heating rate: typically varies from 0.1 °C to over 100 °C. In general, lower heating rates produce better resolved but less sharp peaks. Moreover, decreasing the heating rate increases the duration of the experiment. A rate of 10 °C/min is commonly used.

- Furnace atmosphere: tests may be performed under static conditions (sealed environment) or under dynamic conditions by continuously purging the furnace with gas.

- Crucible material.

- Sample mass: smaller sample masses provide sharper peaks and less baseline drift, but the signal intensity is lower.

The DTA curve plots the temperature difference on the y-axis against time or temperature on the x-axis (Figure 3.7). The baseline corresponds to the heating of the substance in the absence of any transformation, while upward or downward peaks indicate exothermic or endothermic processes, respectively (Table 3.16).

Using this technique, it is possible to follow thermal events, identify their nature (e.g., melting, decomposition, crystalline transition, etc.), and determine the corresponding temperature, without directly measuring the heat involved.

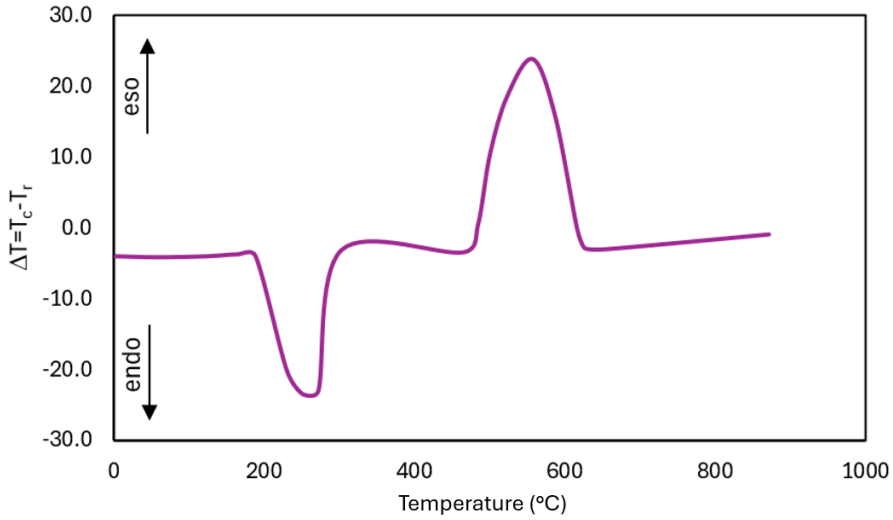

Figure 3.7: Example of a DTA curve.

Table 3.16: Enthalpy change in some important transformations.

Process	Exothermic	Endothermic
Crystallization	*	
Melting		*
Vaporization		*
Sublimation		*
Drying		*

Quantitative determination of the heat associated with these transformations can instead be obtained using another calorimetric technique: Differential Scanning Calorimetry (DSC) [4].

3.5.3 Differential Scanning Calorimetry

Differential Scanning Calorimetry (DSC) is a calorimetric technique used to measure the temperature and heat flow associated with a physical or chemical transition of a material as a function of time (at a fixed temperature) or as a function of temperature (varied over time).

In particular, the DSC technique is based on the measurement, as a function of temperature (or time), of the thermal power required to maintain zero temperature difference between the test sample and an inert reference, when both are subjected to the same thermal program in a heated (or cooled) environment at a controlled rate (in power-compensated instruments).

Each exothermic or endothermic event in the sample causes an imbalance in the system, which is corrected to restore temperature equality. The electrical power required to re-establish equilibrium represents a direct measure of the thermal energy released or absorbed during the transformation [4].

DSC is one of the most widely used preliminary screening techniques for identifying potential hazards associated with strongly exothermic reactions. There are two main types of instruments:

- Heat-flux DSC: the most common technique, allowing temperature scans at rates up to 30°C/min.
- Power-compensated DSC: used for precise and accurate calorimetric analyses, allowing very rapid heating/cooling rates up to 500°C/min.

Each instrument produces a graph of power or heat flow versus temperature or time, known as a thermogram (Figure 3.8). In heat-flux DSC, a single furnace is used to house both the crucible containing the sample and the reference crucible. The furnace is heated or cooled at a programmed rate. When a physical or chemical transition occurs in the sample, a temperature difference arises between the sample and the reference. This temperature difference, ΔT, is the key measured parameter. One or more temperature sensors detect this difference, which is then converted into heat-flow data.

Power-compensated DSC consists of two identical furnaces, one for the sample and one for the reference (usually an empty aluminium crucible). Both are heated or cooled at a programmed rate, and each furnace has its own temperature sensor that continuously monitors temperature. During the process, a compensating power is applied to maintain equal temperatures between the two furnaces, ensuring that the programmed heating (or cooling) rate is followed precisely.

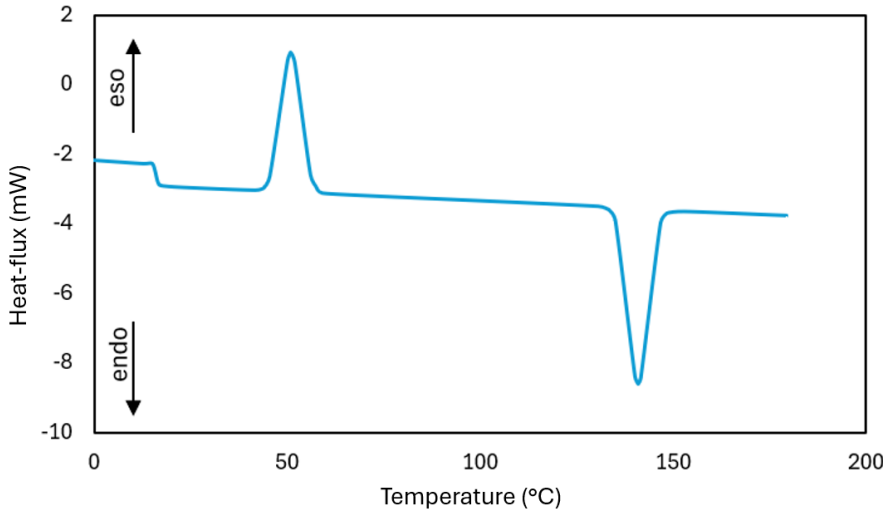

Figure 3.8: Example of a DSC thermogram.

Generally, DSC measurements can be conducted in two modes: isothermal mode, that is maintaining a constant temperature; or dynamic mode, that is applying a programmed temperature ramp and observing the sample behavior as temperature varies.

Dynamic heating tests are faster, cover a wider temperature range, and provide greater sensitivity.

Isothermal tests, on the other hand, are useful to determine significant initial decomposition temperatures and to identify substances whose thermal stability depends on time; particularly when the decomposition rate does not follow the Arrhenius law (i.e., when it requires a long induction period before decomposition becomes detectable).

DSC allows the determination not only of the enthalpy changes (ΔH) associated with the analyzed phenomena but also of the specific heat capacity (c_p) of the sample and its variation with temperature. In particular, it can be used to determine changes in heat flow associated with a chemical reaction, enabling kinetic studies based on suitable interpretative models.

At the end of the test, a graph is obtained in which the x-axis represents temperature (for dynamic tests) or reaction time (for isothermal tests, also known as isoaging), while the y-axis shows the thermal power released or absorbed by the sample (generally in mW, or normalized with respect to the initial sample mass, in W/g). After defining an appropriate baseline, the area under the heat-flow curve corresponds to the enthalpy associated with the analyzed event.

For a dynamic test with a known scanning rate, the enthalpy associated with a phenomenon can be calculated as:

$$\Delta H = \frac{\int_{T_i}^{T_f} (\dot{Q} - \dot{Q}_b) dT}{m_c} \tag{3.4}$$

where

ΔH enthalpy per unit mass of the tested sample associated with the analyzed event [J/g];

$\dot{Q}$ thermal power released or absorbed by the sample [W];

$\dot{Q}_b$ baseline thermal power, obtained by connecting the onset (T_i) and end (T_f) temperatures of the event;

m_c initial sample mass [g];

T_i, T_f onset and end temperatures of the thermal event [°C].

For an isothermal test, equation (3.4) takes an analogous form, where integration is performed with respect to time. However, there is no substantial difference between the two types of tests, as both since time and temperature are correlated even in a dynamic scan.

From the shape and size of the DSC curve, several types of information can be obtained:

- The area of a peak provides quantitative information about the heat involved in the transformation.

- For equal peak areas, a sharper rise in the curve indicates greater hazard potential, either due to a strong increase in reaction rate with temperature or a high enthalpy value.

- A Gaussian-shaped curve suggests a reaction following Arrhenius-type kinetics.

- An asymmetric shape indicates autocatalytic or chain radical polymerization mechanisms.

- Curves with multiple peaks correspond to complex reactions.

- Sharp, narrow peaks are typical of physical transitions (e.g., melting).

The test can be conducted in either an oxidizing (air) or an inert (e.g., nitrogen) atmosphere, although eliminating static air can pose operational challenges. Performing the test in an inert atmosphere allows differentiation between decomposition and oxidation phenomena. Test durations vary widely: from less than two hours, for dynamic scans, to 24 hours or more for isothermal tests. DSC requires only a small sample amount (a few milligrams), which is advantageous for preliminary screening of unknown substances that might decompose or explode violently. However, test conditions differ significantly from those of actual process operation: for example, there is no agitation, reagent addition is impossible, and no information on pressure evolution can be obtained. Therefore, DSC is not suitable for characterizing complex reactive systems, including end-of-reaction mixtures [4].

In heterogeneous mixtures, samples may also be poorly representative. Nevertheless, if compatible with the crucible material, DSC can still be employed for preliminary mixture characterization. Another concern may arise from the formation of gaseous products, such as during decomposition reactions, which can cause a pressure build-up. This may lead to rupture of the sealed crucible and the release of material into the furnace, potentially damaging the instrument. For this reason, in all safety-screening tests, it is recommended to perform the test in a sealed crucible, provided the crucible material is compatible with the sample.

The results of a DSC test are influenced by the following factors:

- Crucible material: it must be chemically inert with respect to the substance analyzed, to avoid distorting the thermogram. For example, aluminium crucibles are commonly used but may react with many chemicals, leading to incorrect conclusions.

- Atmosphere surrounding the sample: static air trapped inside the crucible can alter the curve, triggering secondary oxidation reactions, especially when stainless-steel crucibles are used. For small sample amounts (2 – 5 mg), oxidation can produce false exothermic peaks, leading to unnecessary safety measures. To prevent this, it is advisable to seal crucibles under an inert atmosphere (e.g., using a glove box). Tests in static air, however, can be useful to evaluate sample reactivity toward air.

- Sample mass: it depends on the material type and transition of interest. Excessive sample quantity during melting can introduce noise during and after the transition. In general, 1 – 3 mg are sufficient for pharmaceutical materials, while about 10 mg are adequate for polymers.

- Heating rate: it is a key parameter in DSC, as it affects both resolution and measurement accuracy. A typical heating rate is 5 °C/min.

Interpretation of DSC Test Results

Considering a standard "safety screening" test (see Table 3.17), the heat flow vs. time curves generated can be analyzed to characterize the identified thermal effects using appropriate software. These software tools allow, for instance, the integration of thermal curves to calculate the energy associated with a given thermal event.

Table 3.17: Typical operating conditions for a safety-screening test performed by Differential Scanning Calorimetry (DSC).

Temperature range	Atmosphere	Heating rate	Sample mass	Crucible
30 – 280 °C	Nitrogen	5 °C/min	2 – 5 mg	Steel, Viton (sealed)

To analyze a thermal effect, the software typically requires the following input parameters:

- Left limit: temperature (or time) at which the effect begins.

- Right limit: temperature (or time) at which the effect ends.

- Baseline: type of baseline selected (interpolated, horizontal, etc.).

The selection of these parameters is entirely at the analyst's discretion. It should be noted that in a dynamic DSC test, since the temperature profile is predefined, time and temperature are directly correlated. The software then provides the following output values (Figure 3.9):

- Onset/Endset: these temperatures are determined as the intersection points between the tangent at the maximum derivative of the heat-flow curve (on the left and right sides of the peak, respectively) and the chosen baseline. They can be interpreted as characteristic temperatures associated with the studied thermal event

- Integral: the area under the curve between the left and right limits (a small offset can be applied to both limits). This represents the heat associated with the thermal event: a positive value typically indicates an exothermic effect.

- Normalized Integral: the ratio between the integral heat and the sample mass. This is an intensive property, more suitable for comparing results or extending findings.
- Peak: the temperature at which the maximum (or minimum) heat flow occurs, depending on whether the event is exothermic or endothermic.

When the sample is subjected to a dynamic test (programmed heating), the most significant information sought from a DSC analysis is the temperature at which the instrument detects the onset of an exothermic (or endothermic) phenomenon. This temperature can be identified either as the left limit temperature or the onset temperature, but the choice must be properly justified. It should also be noted that the presence of impurities or catalysts can significantly lower the onset temperature of the observed effect.

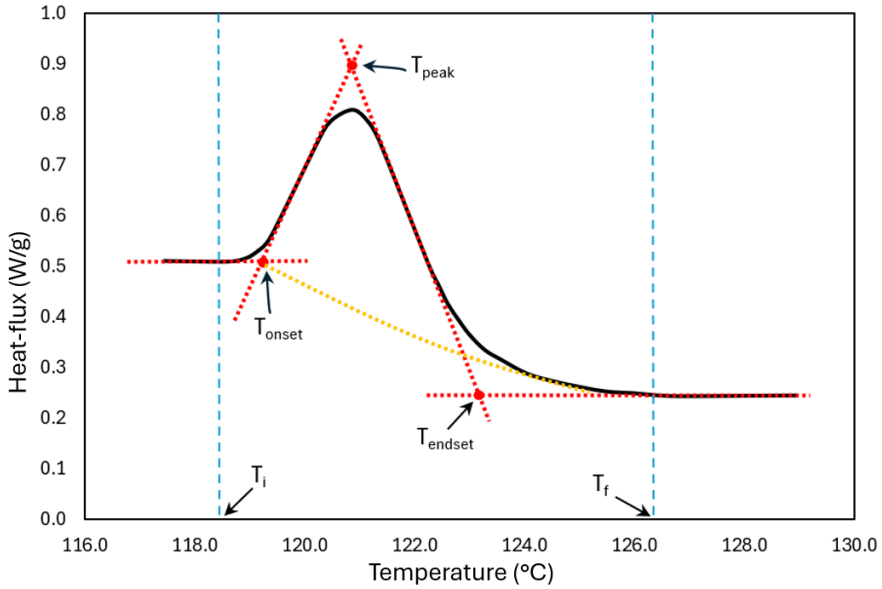

Figure 3.9: Example of a DSC curve. The blue dashed lines (–) indicate the start and end temperatures of the event. The red points(•) represent the onset, endset, and peak temperatures, obtained from the intersection of the tangential lines (–) to the curve. The yellow dotted line ( ) represents the interpolated baseline.

3.5.4 Isothermal Titration Calorimetry

The heat flow calorimeter operates basing on the Calvet principle, and the most well-known instrument of this type is C80.

The sample, together with the reference cell, is placed inside a calorimetric block that acts as a heat sink, under both either dynamic or isothermal conditions. The sample and reference cells are surrounded by a series of detectors and thermocouples, which

allow the measurement of all the heat released or absorbed, including that transmitted by radiation, convection, and conduction.

The 3D sensor consists of two cylindrical thermopiles, each made up of nine concentric rings, with each ring containing 38 thermocouples (a total of 324 thermocouples). This configuration forms a cylinder that completely surrounds both the sample and the reference cell, enabling the measurement of heat in all directions (Figure 3.10).

The sample, contained within a measurement cell, is positioned directly at the center of the detection zone. The cell can be a simple closed cylinder or can be equipped with instruments for mixing and stirring, as well as for measuring pressure and gas or liquid flow. Cells are typically made of metal, polymeric materials, or temperature- and corrosion-resistant glass [10].

The signal derived from the sample, measured with respect to that of the reference cell, is proportional to the heat flux passing through the surface surrounding the sample and its cell. This produces a characteristic curve that indicates the number, nature, and temperature of thermal events. The area under each peak can be integrated to obtain the energy change associated with the transformation.

Compared to DSC, the sample mass used in the C80 calorimeter can be up to 1000 times greater. This, combined with the excellent thermal stability of the instrument, contributes to its high sensitivity. However, the trade-off is an extremely slow thermal response: the heating rates range between 0.1 and 2 °C/min, making the tests very time-consuming [4].

Figure 3.10: Schematic representation of the 3D sensor of a C80 calorimeter.

3.6 Adiabatic Calorimetry

Adiabatic calorimetry is a fundamental tool in safety studies and risk analysis, as it allows for the laboratory simulation of the consequences of thermal runaway in exothermic processes. Such runaways may result from operational errors during synthesis (for example, an unintended "one-shot" addition) or from insufficient cooling due to malfunctioning of the thermal conditioning system.

In industrial plants, adiabatic conditions arise whenever the characteristic cooling times of equipment (where chemical reactions typically take place) are much longer than the characteristic times of heat generation.

To ensure that a system can be approximated as adiabatic, several factors can be controlled:

- Sample quantity: the larger the amount of material or mixture tested, the closer the conditions are to adiabaticity.
- Insulation of the container: to approach adiabatic conditions, the material of the container holding the sample must be highly insulating, minimizing any heat losses to or from the external environment.
- Control of ambient temperature: the external temperature must be regulated with respect to that of the sample so as eliminating any thermal gradient (this is particularly important when working with small sample quantities).

The main challenges in adiabatic testing include:

- Measurement accuracy: a process is ideally adiabatic if it occurs without any heat exchange. However, this is only an abstraction. In practice, every calorimeter involves some degree of heat transfer to or from the sample, which may cause signal drift in temperature measurements over time, even after the exothermic event has ended.
- Thermal inertia (Φ). Part of the heat produced by the reaction is absorbed by the sample holder (vessel), causing deviations from true adiabaticity [4]. The thermal inertia factor, or "Phi factor", is defined as:

$$\Phi = 1 + \frac{m_c \; c_{p,c}}{m_s \; c_{p,s}} \tag{3.5}$$

where

m_s mass of the sample [g];
m_c mass of the sample holder [g];
$c_{p,s}$ specific heat capacity of the sample [kcal/(kmol °C)] or [J/(kg K)];
$c_{p,c}$ specific heat capacity of the sample holder [kcal/(kmol °C)] or [J/(kg K)];

Under perfectly adiabatic conditions, $\Phi = 1$, meaning that the thermal inertia of the container is negligible compared to that of the sample. In industrial reactors

with agitation, Φ factors typically range from 1.05 to 1.1, while in laboratory-scale equipment, values between 1.05 and 8 are commonly observed.

- Limitations in temperature control at high heating rates. When the rate of heat release from the sample is very high, even advanced instruments cannot maintain perfect adiabaticity. This deviation, however, usually occurs only briefly, often toward the end of the test.

The main limitation of tests performed with adiabatic calorimeters is that the data cannot be directly used to evaluate kinetic parameters, and therefore reaction rates, without additional processing. This is because mathematical models and differential equations must be applied to extract the actual heat flow generated by the reaction, unlike techniques such as DSC, which can measure it directly.

In general, adiabatic calorimetry tests involve measuring the temperature and pressure variations of a sample contained in a closed cell, designed to minimize heat exchange with the external environment. The sample reacts inside the test cell without heat exchange with the surroundings. In practice, pseudo-adiabaticity is achieved by using electrical resistance heaters that, when exothermic phenomena begin, heat the outer walls of the sample container, compensating for any residual heat losses to the environment [8].

3.6.1 Accelerating Rate Calorimeter

The Accelerating Rate Calorimeter (ARC) was developed by Dow Chemicals in the 1970s. It is a microprocessor-controlled adiabatic calorimeter equipped with an advanced data acquisition and analysis system, specifically designed for studying potentially hazardous decomposition reactions.

The key feature of the ARC is its ability to maintain the sample under near-perfect adiabatic conditions through active control of heat losses. This is achieved by continuously adjusting the furnace temperature to match that of the sample cell, measured by a thermocouple located on the cell's external surface. As a result, there is no temperature gradient, and hence no heat flow, between the sample and its surroundings.

The main components of the ARC are illustrated in Figure 3.11:

- Sample holder (cell): a spherical vessel that can contain 8–10 g of liquid or solid sample, made from materials such as titanium, Hastelloy C, or stainless steel, suspended within the calorimeter chamber.
- Calorimeter enclosure (furnace or jacket): built from nickel-plated copper, it includes three thermocouples for temperature measurement and eight heaters to minimize temperature differences between the calorimeter walls and the sample during exothermic reactions.
- Thermocouple: mounted on the outer wall of the sample cell to record the sample temperature.
- Capillary tube: connects the sample cell to a diaphragm-type pressure transducer, which continuously measures the system pressure [4].

- Safety shield: the entire assembly is enclosed within a protective housing designed to contain any explosion resulting from cell rupture.

When planning the experiment, the thermal inertia of the cell must be taken into account. The cell material must be chosen carefully to simulate plant-scale conditions. Titanium cells offer low thermal inertia but may exhibit catalytic effects on the sample; in such cases, Hastelloy C cells are preferred to minimize these effects. If pressure and pressure-rate data are required, the degree of fill of the sample cell must also be considered.

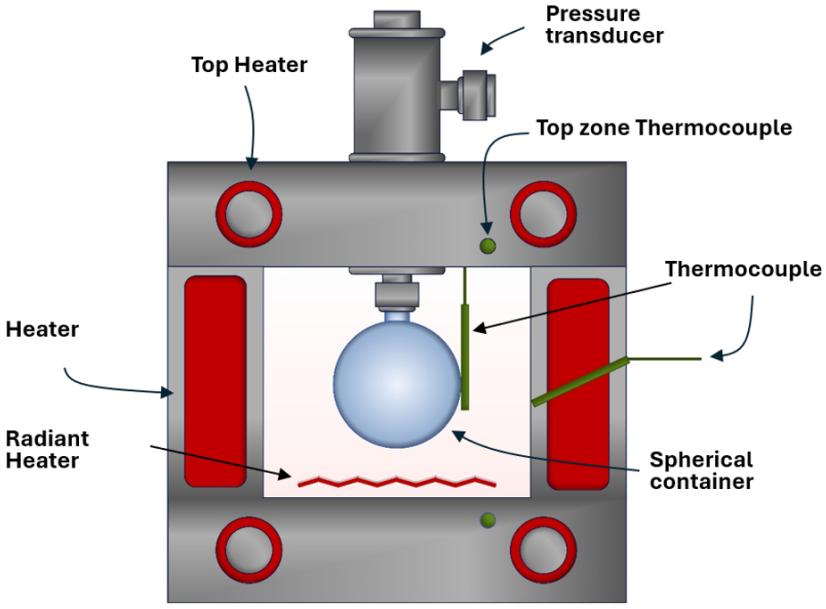

Figure 3.11: Schematic representation of the ARC instrument.

There are two operating modes for the ARC:

- HWS (Heat–Wait–Search) mode. The sample is heated to a predefined temperature using electrical heaters ("Heat" phase), while the surrounding environment is simultaneously heated to minimize heat loss from the hotter sample to the cooler furnace walls. During the "Wait" phase, heating is paused to allow any local temperature gradients to dissipate, ensuring thermal equilibrium between the sample and the calorimeter. In the "Search" phase, the controller switches to adiabatic mode: if the self-heating rate of the sample exceeds a preset threshold (typically 0.02 °C/min), the furnace temperature follows the sample temperature (adiabatic tracking mode); if the self-heating rate remains below this threshold, the system advances to the next heating step. In adiabatic tracking, direct heating of the sample is suspended, and the instrument continuously adjusts the heat supplied

to the calorimeter walls so that the wall and sample temperatures remain equal at all times, thereby maintaining adiabatic conditions (Figure 3.12) [8, 11].

- Iso-aging mode. The sample is heated directly to the desired temperature and maintained under isothermal conditions until an exothermic event is detected, at which point the test proceeds under adiabatic conditions.

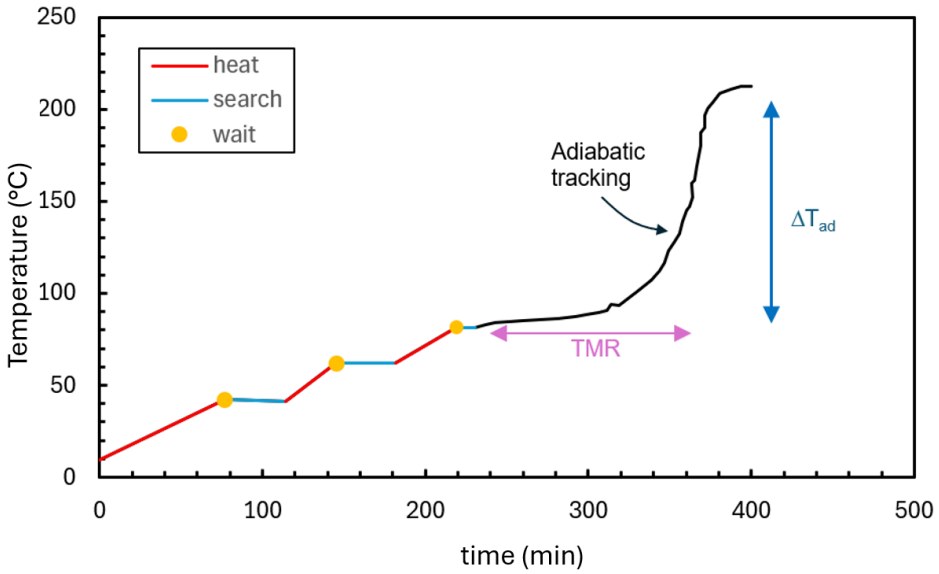

Figure 3.12: Example of a temperature-time trace obtained from an ARC experiment in HWS mode.

The ARC provides the following key results:

- onset and end temperatures of decomposition;
- self-heating rate at each temperature;
- pressure profile as a function of temperature;
- adiabatic temperature rise;
- pressure rise rate;
- Time to Maximum Rate (TMR) or time to explosion;
- kinetic parameters of decomposition.

The typical operating ranges are $25-500\,^{\circ}\mathrm{C}$ and $1-170$ bar; beyond these limits, built-in safety devices automatically engage. The ARC is primarily designed for homogeneous liquid systems.

Reliable results using standard sample cells require samples with high thermal conductivity and/or low viscosity, ensuring efficient heat transfer and minimal temperature or concentration gradients.

Non-conservative results may be obtained for solids that do not melt before decomposition or for multiphase samples where reactive liquid–liquid interactions occur [4]. The thermal inertia of the cell is relatively high ($\Phi = 2$ – 5, depending on the fill ratio), as the cell walls must be thick enough to withstand the pressure increase accompanying decomposition. To minimize the risk of cell rupture, a low fill level is typically used, which also limits the total energy released, particularly for systems generating non-condensable gases during decomposition.

Under truly adiabatic conditions, the heat released by the reaction should only warm the reacting system itself. In practice, due to thermal inertia, part of the heat also warms the cell walls. Therefore, experimental data must be corrected to account for this effect. The adiabatic temperature rise, reaction enthalpy, and final adiabatic temperature are calculated using the following equations:

$$\Delta T_{ad} = \phi \, \Delta T_{ad,s} \tag{3.6}$$

$$\Delta H_r = c_p \, \Delta T_{ad} \tag{3.7}$$

$$T_f = T_o \, \Delta T_{ad} \tag{3.8}$$

where

Φ	thermal inertia factor [–];
ΔT_{ad}	adiabatic temperature rise of the sample [K];
$\Delta T_{ad,s}$	apparent adiabatic temperature rise of the sample + cell system [K];
ΔH_r	reaction enthalpy [J/g];
c_p	specific heat capacity of the sample [J/g K];
T_f	final adiabatic temperature [K];
T_o	onset temperature of the exothermic event detected by the instrument [K].

The main limitations of the ARC are related to its high thermal inertia, which restricts the maximum achievable temperature rise and limits the ability to record temperature increase rates above $\approx 10-15\,^{\circ}\mathrm{C/min}$. This limitation also reduces the suitability of ARC data for the design or verification of pressure relief systems. Another drawback is the difficulty in obtaining accurate kinetic data from temperature-rise profiles. For reliable results, the test sample should possess high thermal conductivity and low viscosity to minimize internal gradients during testing. However, these conditions are rarely achieved given the small sample mass used. This is particularly critical for polymerization reactions, where viscosity increases rapidly as the reaction proceeds [8].

3.6.2 PHI-TEC II

PHI-TEC II low thermal inertia calorimeter was developed in the 1990s. It consists of a sample cell that can be manufactured from different materials such as aluminum, Hastelloy, stainless steel, or glass, to simulate various process conditions. The dimensions of the sample cells vary, but the one most commonly used in adiabatic calorimetry has a volume of approximately 110 cm^3 and very thin walls (about 0.15 mm thick).

The cell is placed inside a containment vessel designed to withstand pressures up to 200 bar. To prevent cell rupture caused by a sudden internal overpressure, the system includes a nitrogen compensation loop that maintains the internal pressure of the containment vessel equal to that inside the cell [4]. The cell is equipped with a stirrer, either mechanical or magnetic, and an internal thermocouple. Externally, it is surrounded by three independent radiant panels: two circular ones positioned above and below, and a lateral ring. These panels heat up when the sample starts to release heat, thereby minimizing thermal exchange between the outer surface of the cell and the surrounding environment and ensuring pseudo-adiabatic conditions. Two thermocouples measure the temperature of the sample and the cell surface (Figure 3.13) [8].

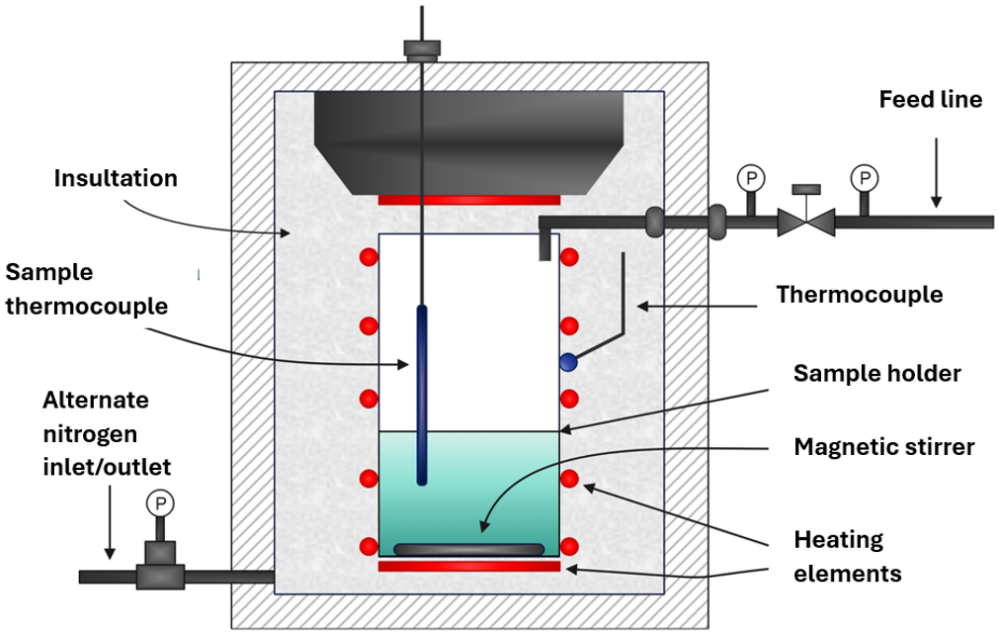

Figure 3.13: Schematic representation of the PHI-TEC II.

PHI-TEC II has a thermal inertia (Φ-factor) very close to that of large-scale systems, typically between 1.05 and 1.08. This represents a major advantage, as the data obtained can simulate full-scale behavior without the need for further extrapolation, unlike other techniques such as ARC.

Another important feature is the possibility of adding reagents, catalysts, etc., even

when the cell is at high temperature and pressure, thus reproducing actual plant operating conditions. The large cell volume allows for accurate measurement of gas generation rates and the resulting pressure increase. In smaller cells, significant pressure rises can cause complications, since deviations from ideal-gas behavior must be considered along with gas solubility in the liquid phase.

In PHI-TEC II, these issues of non-ideality and solubility are overcome thanks to the presence of a secondary containment reservoir connected to the sample cell. This additional volume not only improves accuracy but also reduces the risk of an explosive rupture of the main cell [13].

An additional advantage is that data obtained from PHI-TEC II tests can be directly applied in the DIERS (Design Institute for Emergency Relief Systems) methodology for design and sizing of pressure relief systems. Figure 3.14 shows a typical temperature and pressure profile of the sample as a function of time obtained during an adiabatic calorimetry test performed using a Phi-TEC apparatus. The pressure profile, in particular, highlights the generation of gases and/or vapours associated with the development of the exothermic reaction, providing relevant information for the assessment of the potential for overpressure and the risk of thermal runaway under conditions of loss of process control.

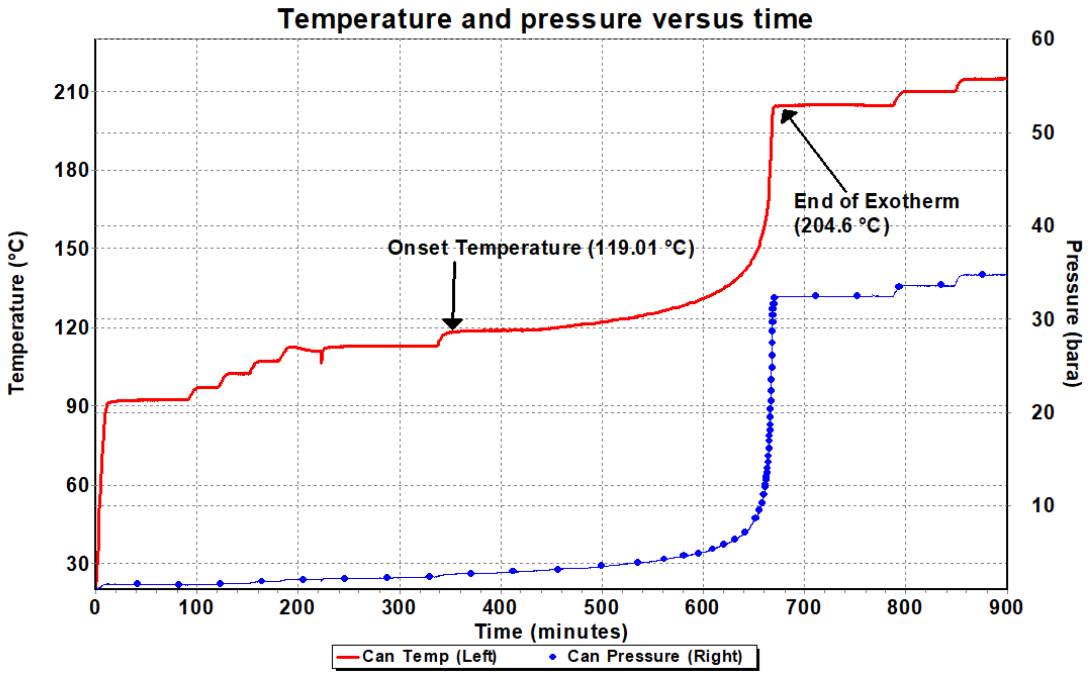

Figure 3.14: Example of a typical temperature–time plot obtained from a PHI-TEC II test [12].

3.6.3 Advanced Reactive System Screening Tool

Advanced Reactive System Screening Tool (ARSST) was developed as an alternative to VSP tests, known for their low thermal inertia. This calorimeter, simple to use and cost-effective, allows for the rapid identification of potential hazards in the process industry.

The main components of ARSST are shown in Figure 3.15:

- A spherical glass sample cell with a volume of 10 cm^3. Typically, 10 mL of sample are used, but tests have been conducted with as little as 1 g of sample, yielding reliable results. Using small sample quantities can be advantageous, especially in the early stages of process development when limited material is available, or when the reagent is highly reactive and the decomposition products are particularly hazardous.
- Insulating material surrounding the test cell to reduce heat loss.
- A thermocouple for measuring the sample temperature.
- A second thermocouple for online gas temperature measurement.
- A pressure transducer.
- A 350 mL stainless steel vessel equipped with a lid and a rupture disk.
- A magnetic stirrer.
- A heating element, placed either inside the cell (at the center) or externally when studying solid systems.

The experiments are carried out using a Heat – Wait – Search (HWS) mode. The heating rate depends on the specific heat capacity (c_p) of the sample and may vary from 0.25 °C/min to 2 °C/min. The obtained data include:

- temperature and pressure rise rates (dT/dt and dP/dt);
- onset temperature (T_{onset}), maximum temperature reached (T_{max}), and adiabatic temperature rise (ΔT_{ad});
- mixing enthalpy (ΔH_{mix});
- reaction enthalpy (ΔH_{rx});
- TMR (Time to Maximum Rate), or time to explosion.

The reaction enthalpy can be calculated as:

$$\Delta H_{rx} = c_{p,mix}\, \phi\, (T_{max} - T_{onset}) \tag{3.9}$$

The results obtained from ARSST tests can be employed for the sizing of pressure relief systems according to the DIERS methodology [7, 14].

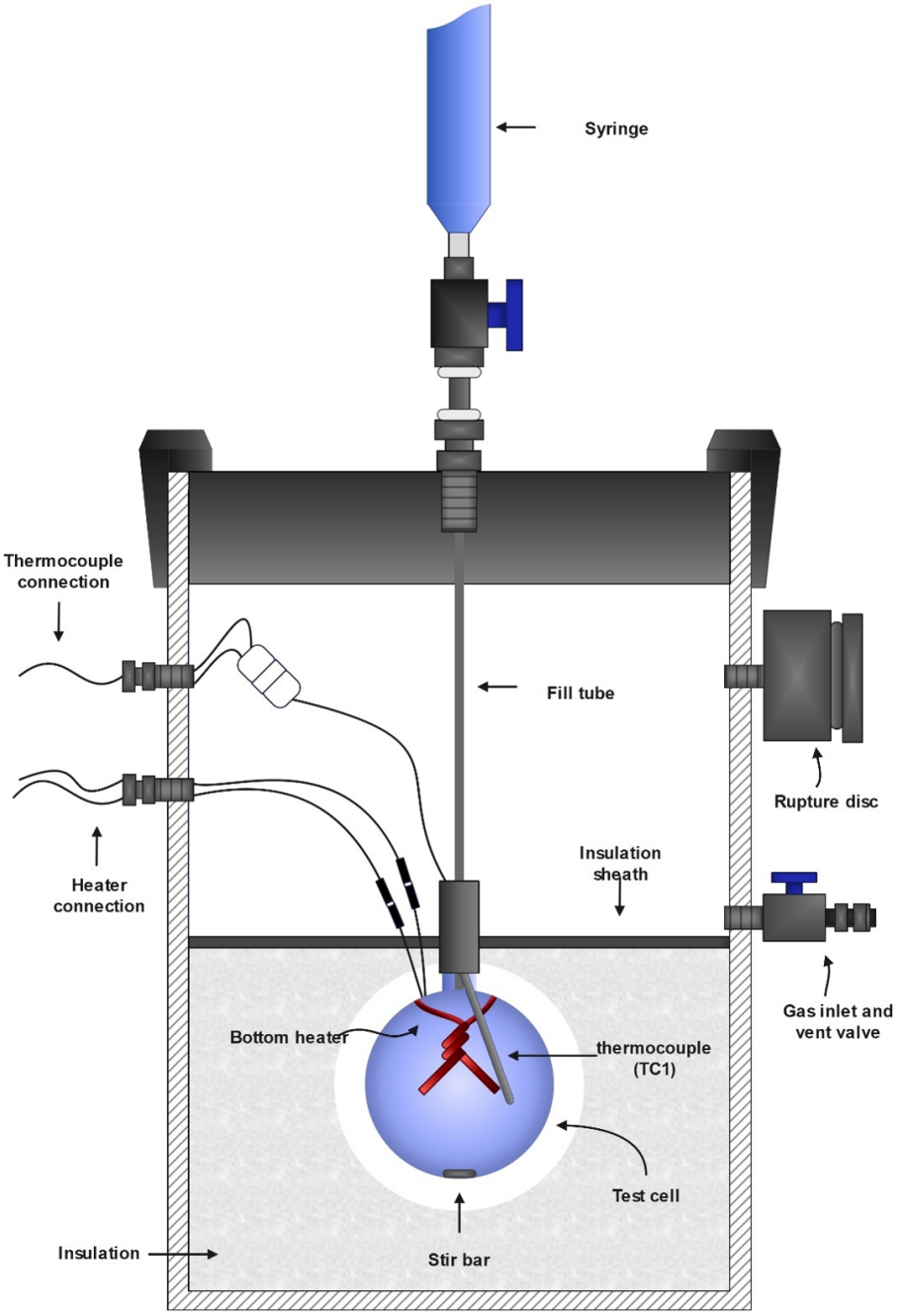

Figure 3.15: Schematic representation of the ARSST.

3.7 Reaction Calorimetry

Until 1980, research efforts in the field of process safety were mainly focused on the thermal stability properties of substances rather than on the analysis of processes themselves. In fact, decomposition temperatures were determined, and appropriate safety margins were set, for instance by applying the 100 °C/min rule. The focus was therefore placed on the chemical stability of a mixture or compound by measuring its heat of decomposition, while reaction rate and the parameters influencing it were largely neglected.

Thermal analysis and adiabatic calorimetry techniques enable the evaluation of hazards arising from secondary decomposition reactions. However, to assess the risks associated with the different stages of a chemical process, a different and more structured approach is required.

The reaction calorimeter is the most suitable instrument for simulating the process under the same operating conditions used on an industrial scale. It allows for the monitoring of processes characterized by high exothermicity and self-accelerating kinetics, such as polymerization reactions, and for improving chemical reactor control systems.

From a safety and risk assessment standpoint, it is essential to understand how reagents interact under industrial operating conditions. Parameters such as: the rate of heat release, the rate of temperature rise in case of cooling failure, and the reaction enthalpy, must be determined. It is also important to evaluate the influence of parameters such as agitation, temperature, molar ratio of reactants, feed rates, and catalyst concentration. All of this can be achieved through reaction calorimetry. Besides investigating process safety aspects, reaction calorimetry allows for the development of new processes and the optimization of existing ones, improving selectivity and yield while providing essential information for scale-up.

Furthermore, reaction calorimetry makes it possible to evaluate the adiabatic temperature rise (ΔT_{ad}) and the maximum temperature of the synthesis reaction (MTSR) that may be reached following a loss of process control, as defined later.

Table 3.18 summarizes the types of information that can be obtained from reaction calorimetry.

Modern instruments, in addition to monitoring agitation speed, temperature, pH, and reagent flow rates, can also measure the online concentration of chemical species by means of Fourier Transform Infrared Spectroscopy (FTIR) and turbidimetric probes. In this way, any exothermic behavior can be quantified and correlated to specific reaction stages and conversion levels. By coupling FTIR spectroscopy with reaction calorimetry, it is possible to record variations in functional groups during the course of the reaction and monitor the conversion of reactants into products, either directly or through the formation of intermediates.

However, FTIR probes have limitations when water is present in the reaction mixture (even when it is a reaction product), as well as in the presence of insoluble solids, gas bubbles (e.g., during hydrogenation reactions), or when species are present at concentrations below 5% [4, 8].

Table 3.18: Thermochemical data obtainable from reaction calorimetry.

Physical properties	Thermal data	Kinetic data	Heat transfer data
Specific heat capacity	Reaction temperature	Reaction rate	Overall heat transfer coefficient (UA)
Heat of mixing	Reaction enthalpy	Rate constants	Specific heat transfer coefficient (U)
Heat of solution	Temperature–time profiles	Activation energy	Required cooling capacity
Vapor pressure	Heat flow–time profiles		
	Adiabatic behavior		

3.7.1 Operating Principles

Depending on their operating mode, reaction calorimeters can be classified as:

- Heat flow calorimeters.
- Heat balance calorimeters.
- Compensation calorimeters.

The tests can be performed under different operating conditions:

- isothermal, isoperibolic, or adiabatic mode;
- with or without agitation;
- in continuous, semi-continuous, or batch operation.

3.7.2 Heat Flow Calorimeter

The heat produced in the reactor is exchanged with a thermal conditioning system (for example, a jacket through which a service fluid circulates). The heat flow is calculated by measuring the temperature difference between the reactor jacket and the reacting system, according to Equation (3.10):

$$Q_{flow} = U\,A\,(T_r - T_j) = Q_{rx} \tag{3.10}$$

where

U specific heat transfer coefficient [W/K m^2];
A effective heat transfer area [m^2];
T_r internal reactor temperature [K];
T_j jacket fluid temperature [K];
Q_{flow} heat flow exchanged with the jacket through the reactor walls [W];
Q_{rx} heat flow generated by the chemical reaction [W].

The heat flow generated by the reaction is defined as:

$$Q_{rx} = (-r_A)\, V\, (-\Delta H_{rx}) \tag{3.11}$$

where

$(-r_A)$ reaction rate [mol/s m^3];
V reacting mass volume [m^3];
$-\Delta H_{rx}$ reaction enthalpy [J/mol], obtained by integrating the heat flow curve generated by the reaction (Equation 3.10).

From a safety standpoint, it is important to note that the heat removed through the jacket increases with the surface area (A), which varies with the square of the linear dimension (L^2), whereas the heat generated by the reaction increases with the reactor volume (V), which varies with the cube of the linear dimension (L^3). This implies that during scale-up, the heat removal capacity grows more slowly than the heat generation rate, potentially making reactions that are safe at laboratory scale hazardous at industrial scale.

The product UA is determined through calibration. For this purpose, an electric heater with known power Q_c is used:

$$Q\,A = \frac{Q_c}{T_r - T_j} \tag{3.12}$$

where

Q_c electrical power supplied to the system [W].

Before starting the calibration, it is essential to verify that no thermal events are occurring. This procedure must be repeated each time the heat transfer coefficient or area changes, for instance, due to variations in viscosity, stirring speed, or feed rate in semi-batch operations.

The main advantage of these instruments lies in the fast heat transfer response of the fluid circulating in the jacket, which allows the study of reactions under runaway conditions. An example of a heat flow calorimeter is the RC1, which will be described later [11].

3.7.3 Heat Balance Calorimeter

The operating principle of these calorimeters is based on the thermal balance of the heat flow exchanged with the fluid circulating in the jacket:

$$Q_j = \dot{m}\, \dot{c_p}\, (T_{j,out} - T_{j,in}) \tag{3.13}$$

where

$\dot{m}$ mass flow rate of the service fluid in the jacket [kg/s];
$\dot{c_p}$ specific heat of the jacket fluid [J/kg K];
$T_{j,out}$ outlet temperature of the jacket fluid [K];
$T_{j,in}$ inlet temperature of the jacket fluid [K].

In these instruments, temperature control of the reacting mass is less precise, but they have the advantage of being independent of the heat transfer coefficient (U) and its variations. Therefore, continuous calibration is not required, unlike in heat flow calorimeters.

3.7.4 Compensation Calorimeter

Calorimeters operating on the compensation principle use an electric heater with a power output at least equal to the maximum heat release rate expected from the reaction or phenomenon being measured.

The heater is switched on before the reaction begins, while the reactor is cooled by a fluid circulating through the jacket.

When an exothermic phenomenon occurs, the temperature controller reduces the heater power to maintain the desired set-point temperature. Conversely, during an endothermic phenomenon, the controller increases the heater power. In this way, the measured heater power is mirror-symmetric (i.e., complementary) to the heat released or absorbed within the calorimeter, thus allowing accurate quantification of the thermal effects involved [11].

3.7.5 RC1 Calorimeter

Among the various types of reaction calorimeters, the Mettler Toledo RC1 is undoubtedly the most renowned. It is a heat flow calorimeter capable of operating under in different temperature control modes:

- Isothermal mode: the reacting mass is maintained at a constant temperature throughout the experiment (T_r=const). A cascade controller regulates the jacket fluid temperature to ensure isothermal conditions. This configuration allows evaluation of agitation and heat transfer efficiency, as well as reaction rate, making it possible to study separately the influence of reaction temperature and reactant concentration on reaction progress, and to determine the overall heat transfer coefficient (UA).

- Isoperibolic mode: the temperature of the jacket fluid is kept constant during the experiment (T_j=const). Isoperibolic calorimetry provides results similar to those obtained in isothermal mode and allows for the acquisition of kinetic data over a broad temperature range relevant to the process.
- Adiabatic mode: the jacket temperature is maintained equal to that of the reacting mass inside the reactor (T_r–T_j=0). Adiabatic operation provides thermokinetic data useful for process safety analysis, such as the adiabatic temperature rise and the rates of temperature and pressure increase. However, this mode is not always feasible, as the adiabatic temperature rise may lead to thermal decomposition of the reacting mixture.
- Reflux mode.

The calorimeter consists of a 2-liter double-jacketed glass reactor, with silicone oil circulating in the outer jacket as the service fluid (Figure 3.16). Smaller reactors (down to 1 L) are also available, allowing the appropriate scale to be selected depending on the process to be simulated. Various impellers with different geometries (anchor, turbine, etc.) and materials (stainless steel, glass, Hastelloy) can be chosen according to the reacting system.

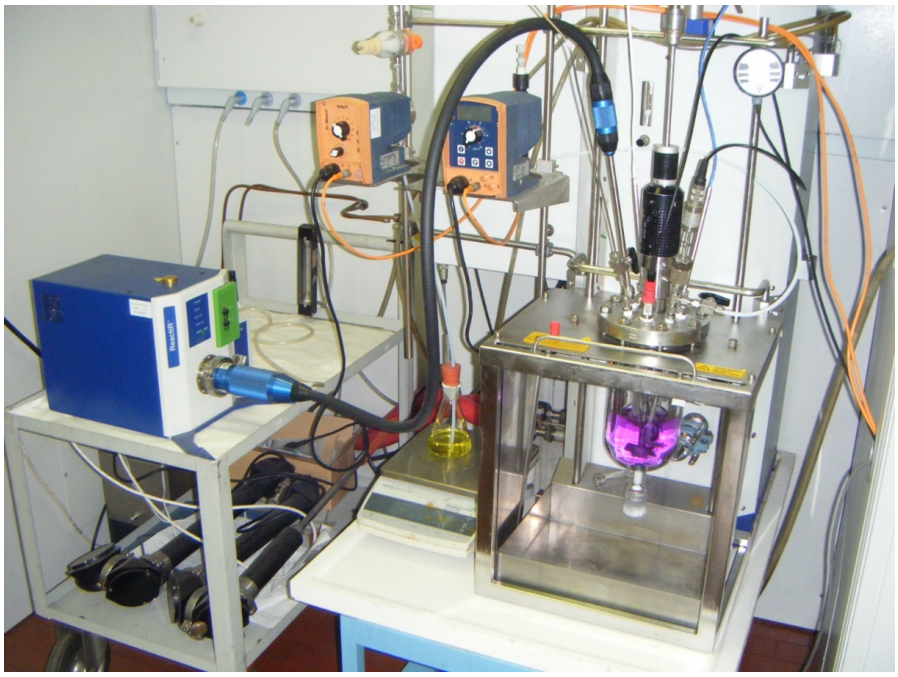

Figure 3.16: RC1 medium-pressure reaction calorimeter (6 bar), equipped with a mechanical stirrer, two feed pumps, and an FTIR probe [15].

The circulation system for the silicone oil consists of two parts: a heating circuit with an electrically heated circulator, and a cooling circuit connected to an external cryostat. The instrument is equipped with a calibration probe, a temperature sensor, and a feed pump for the addition of liquid reagents.

To determine the heat released or absorbed during the reaction, the RC1 performs an energy balance that accounts for different heat contributions:

$$\text{Heat in} = \text{Heat out} + \text{Accumulation} \tag{3.14}$$

$$Q_{rx} + Q_c + Q_{stirr} = Q_{dos} + Q_{loss} + Q_{acc} \tag{3.15}$$

where

Q_{rx} heat release rate due to the chemical reaction [W], as defined in Equation 3.11

Q_c calibration power [W];

Q_{stir} heat flow associated with mechanical stirring [W];

Q_{dos} heat flow due to reagent addition [W];

Q_{loss} heat flow lost through the reactor head [W];

Q_{flow} heat flow exchanged through the reactor wall [W], defined in Equation 3.10;

Q_{acc} heat flow accumulated by the reacting mass and internal inserts (thermocouples, stirrer, etc.) due to their specific heat [W].

Equation 3.15 represents the total energy balance when the reaction occurs below the boiling point of the reacting mass. Conversely, when operating above the boiling point or under reflux conditions, the contribution of the latent heat of vaporization must also be considered. By integrating the heat flow curve (Q_{rx}) over time, the reaction enthalpy can be calculated as:

$$\Delta H_{rx} = \int_{t_0}^{t_f} Q_{rx}\, dt \tag{3.16}$$

where

ΔH_{rx} reaction enthalpy per unit mass [kJ/kg];

t_0, t_f initial and final times of integration for the heat flow curve [s].

Figure 3.17 shows a graph obtained with the RC1 calorimeter.

The test was conducted using an isothermal temperature control mode at 55 °C and a stirring rate of 300 rpm. The reactor was pre-charged with an aromatic organic compound; once thermal stability was achieved and no thermal events were detected, a sulfonitric reagent mixture was fed to the reactor. The dosing time was set to 3 hours. The addition of the reagent generated a heat flow that ceased upon completion of the dosing.

3.7.6 Thermodynamic and Kinetic Parameters to be Evaluated to Determine Process Reactivity

The main physico-chemical and thermodynamic parameters that characterize a reaction in terms of hazard potential can sometimes be derived from literature data

or theoretical calculations. However, for a more reliable characterization, it is often necessary to employ experimental techniques that also reveal kinetic aspects.

Attention is primarily focused on exothermic reactions, as they pose a greater challenge from a process control and safety perspective. Nevertheless, conducting endothermic reactions is not without risks: in such cases, the reaction products possess a higher energy content than the reactants, making them thermally unstable and therefore more prone to exothermic decomposition reactions.

The key thermochemical parameters that must be known to assess the hazard potential of exothermic reactions include:

- reaction (or process) temperature (T_r);
- adiabatic temperature rise (related to the desired reaction) (ΔT_{ad});
- Maximum Temperature due to Synthesis Reaction (MTSR);
- Maximum Allowable Temperature (MAT);
- induction time (t_{ind});
- Time to Maximum Rate (TMR);
- boiling temperature of the reacting mixture (or solvent) (T_{eb});
- peak heat flow ($\dot{Q}_{\max}$) both during the dosing phase (if applicable) and throughout the overall process.

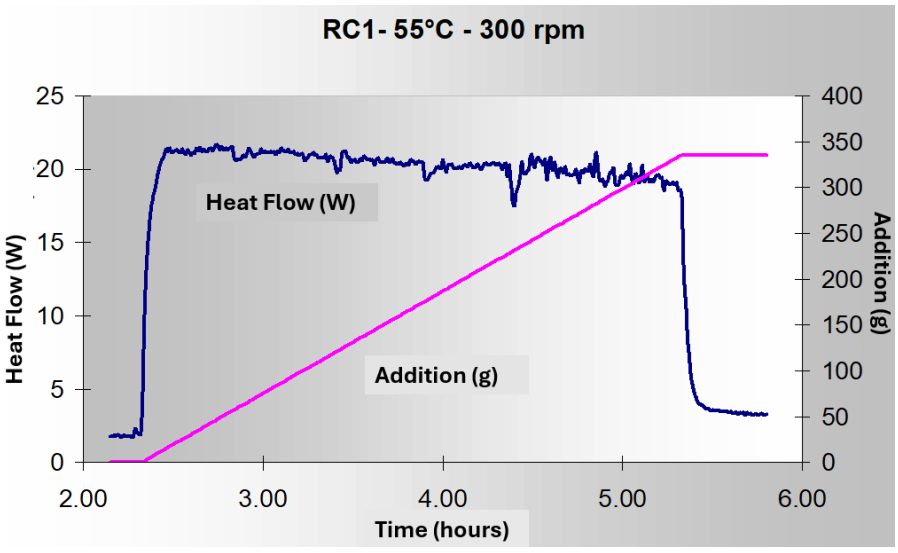

Figure 3.17: Example of a graph obtained using the RC1 calorimeter. The blue curve represents the heat flow released during dosing, while the pink curve indicates the reagent addition profile as a function of time [15].

These parameters will be briefly described in the following sections.

Reaction or Process Temperature (T_r)

This is the temperature at which the process is conducted under plant operating conditions. Such a temperature is the result of detailed studies performed during the Research and Development (R&D) phase within the company, aimed at identifying the optimal conditions for ensuring process efficiency, selectivity, and safety.

Adiabatic Temperature Rise (ΔT_{ad})

The adiabatic temperature rise is defined as the maximum temperature increase that can occur in a system under adiabatic conditions, i.e., in the absence of any heat exchange with the surrounding environment. Adiabatic conditions arise when the system is unable to transfer energy to the outside. In such a case, all the energy released by the reaction is used to increase the temperature of the system, making the temperature rise proportional to the released energy. A typical example of an adiabatic condition occurs in the event of a cooling system failure during a chemical reaction. The adiabatic temperature rise is one of the most widely used criteria for assessing the degree of exothermicity of a potentially runaway reaction.

It is defined as follows:

$$\Delta T_{ad} = \frac{\Delta H_{rx}\, n_{lim}}{m\, c_p} \tag{3.17}$$

where

ΔT_{ad} adiabatic temperature rise [K], calculated parameter;

ΔH_{rx} reaction enthalpy [kJ/mol], determined experimentally through reaction calorimetry tests or estimated using theoretical-predictive methods;

n_{lim} number of moles of the limiting reagent [mol];

m total reaction mass [kg];

c_p specific heat capacity of the reaction mixture [kJ/(kg K)], determined by reaction calorimetry calibration or from theoretical methods or literature data.

ΔT_{ad} is an important parameter because it provides an estimate of the maximum theoretical temperature that can be reached by the system during actual process conditions, especially when large volumes of reacting mixture are involved or abnormal situations occur, such as loss of agitation or cooling failure. Under such circumstances, conditions approaching adiabaticity can effectively be achieved.

The parameters influencing ΔT_{ad}, and on which it is possible to act to mitigate its value, are:

- the total mass of the system (which is the sum of the masses of reactants, products, catalysts, and solvents);

- the specific heat capacity of the reacting mass.

Therefore, a more diluted reacting system (i.e., with a total mass significantly greater than that of the limiting reagent) or one containing compounds with high specific heat capacity will reach lower ΔT_{ad} values, thus ensuring a higher safety margin for the process.

Maximum Temperature due to Synthesis Reaction (MTSR)

The MTSR (Maximum Temperature due to Synthesis Reaction) represents the maximum temperature that can be reached by a reacting system under adiabatic conditions, considering only the desired synthesis reaction. It is defined as:

$$MTSR = T_r + X_{acc}\,\Delta T_{ad} \tag{3.18}$$

where

T_r process temperature [K];

X_{acc} accumulation fraction of the unreacted limiting reagent (value between 0 and 1) [–];

ΔT_{ad} adiabatic temperature rise [K].

The MTSR can be calculated based on the definition of X_{acc}. Typically, it refers to a batch reaction (all reagents charged at the synthesis temperature) where $X_{acc} = 1$, meaning that after heating the reactor to the process temperature (T_r), the cooling system is assumed to fail, and no heat removal occurs.

Maximum Allowable Temperature

The Maximum Allowable Temperature (MAT) is defined as the temperature at which the onset of any exothermic effect is detected by a calorimetric instrument during the heating of a reacting mass.

The onset temperature of an exothermic reaction is defined as the point at which the thermal power generated by the system exceeds the lower detection limit of the measuring instrument. For the same exothermic reaction, more sensitive instruments will detect a lower onset temperature than less sensitive ones.

The MAT can be determined using the following calorimetric techniques (the applicability of each method to the reacting mixture under study must be properly justified):

- Adiabatic calorimetry (e.g., ARC, PHI-TEC II, VSP2, or ARSST), by performing a standard Heat – Wait – Search test with heating steps $\leq 5\,^{\circ}\mathrm{C}$ starting from the process temperature;

- Differential Scanning Calorimetry (DSC), by conducting a dynamic heating test at a scanning rate of $5\,^{\circ}\mathrm{C/min}$, either in inert atmosphere (nitrogen) or air, with crucible material selected according to the compatibility with the mixture under analysis;

- 3D heat – flow calorimetry (e.g., C80), by performing a dynamic heating test at a scanning rate of 0.5 °C/min in air.

Among these instruments, DSC calorimeters have the lowest sensitivity, followed by adiabatic calorimeters, while 3D heat-flow calorimeters are the most sensitive. Among the exothermic phenomena that can be detected, decomposition reactions are those that lead to the most severe effects in terms of magnitude.

A decomposition is defined as an undesired exothermic chemical transformation of a substance (or mixture) in the condensed phase, typically involving significant heat and non-condensable gas generation. These reactions usually occur through a multi-step mechanism with complex kinetics.

Their hazardous nature lies in the combination of exothermicity and gas evolution, which makes it virtually impossible to protect a reactor or storage vessel against the risk of a physical explosion, even with safety devices such as relief valves or rupture discs. In such cases, alternative emergency procedures (e.g., discharge into a quench pool) must be considered and executed within appropriate time frames (see the section on the TMR parameter).

Induction Time

The induction time is defined as the time elapsed before the onset of an exothermic event under isothermal conditions. It depends both on the temperature at which the system is maintained during the induction period and on the concentration of the substances in the mixture. Its value is generally determined through iso-aging calorimetric tests. Such experimental tests can be performed using either Differential Scanning Calorimeters (DSC) or adiabatic calorimeters.

Time to Maximum Rate

Once the MTSR has been reached, the system naturally tends to cool down (due to natural convective heat exchange with the surrounding air), unless the MAT has been exceeded, in which case a latent decomposition reaction may have been triggered. In this latter case, after a period of apparent isothermality, the system begins to self-heat.

The Time to Maximum Rate (TMR) is defined as the time required to reach the maximum rate of self-heating (i.e., the maximum derivative of temperature with respect to time) under adiabatic conditions. It depends on several factors, including the presence of secondary exothermic reactions, decomposition reactions, and the value of MTSR, among others.

The TMR can be determined directly from Heat – Wait – Search tests performed with adiabatic calorimeters, starting from the instant when the MTSR is reached.

It can be also estimated theoretically if either the thermochemical parameters of the system and the kinetic parameters of undesired exothermic reaction are known or using the following relation:

$$\mathrm{TMR} = \frac{c_p \, \mathrm{R} \, \mathrm{MAT}^2}{\mathrm{q} \, \mathrm{E}} \tag{3.19}$$

where

c_p specific heat capacity of the reacting mixture [kJ/kg K], determined from reaction calorimetry calibration tests, estimated by predictive methods, or derived from literature data;

R universal gas constant [8.314 J/mol K];

q maximum heat release rate [W/kg], determined from dynamic heating tests using Differential Scanning Calorimetry (DSC);

MAT onset temperature of the undesired exothermic reaction [K], determined from DSC dynamic heating tests or Heat–Wait–Search tests in adiabatic calorimetry;

E activation energy of the reaction [J/mol], estimated using the same dynamic DSC test employed for q and MAT determination, or following specific standards (e.g., ASTM E698), or by kinetic fitting of adiabatic calorimetry data.

The TMR value is directly proportional to:

- the heat capacity of the reacting system (a higher heat capacity slows down self-heating);
- the MAT (a higher onset temperature of exothermic reactions, such as decomposition, means longer energy accumulation times before initiation).

Conversely, the TMR is inversely proportional to:

- the maximum heat release rate (q) (a faster heat release leads to more rapid self-heating and shorter times to reach peak reaction rates);
- the activation energy (E) (a lower activation energy allows the exothermic reaction to start at lower temperatures, reducing the time to reach peak rates).

From an operational perspective, the TMR represents the minimum time available to perform corrective actions aimed at preventing thermal runaway and the resulting physical explosion of the system.

At the European level, experts recommend selecting suitable operating conditions such that the TMR is not shorter than 24 hours. This value originates from the Seveso accident experience, corresponding to a typical weekend shutdown period, during which small amounts of post-reaction or product mixtures might remain stagnant in pump housings or buffer tanks, potentially leading to decomposition. For continuous production processes, some company standards accept a TMR value equal to the duration of a work shift (i.e., 8 hours). Although this criterion is less conservative, it may be acceptable in specific cases.

Boiling Temperature of the Reacting Mixture or Solvent

The boiling temperature (T_{eb}) is defined as the temperature at which incipient boiling phenomena begin to appear within the reacting system. Boiling conditions can be visually observed during reaction calorimetry experiments, or alternatively estimated using appropriate theoretical or predictive methods.

For a reacting system undergoing transformation (i.e., during the conversion of reactants into products), the boiling temperature of the system may vary significantly over time. In some cases, it may be acceptable to assume, as the system's boiling temperature, the normal boiling point of the solvent (i.e., the substance present in the greatest amount). However, this assumption must be carefully justified, demonstrating its conservativeness with respect to process safety considerations.

Peak Heat Flow

The peak heat flow ($\dot{Q}_{max}$) is defined as the maximum thermal power released by the reactions occurring inside a system. This information reflects both the kinetics of the desired reaction and the operating conditions, namely:

- the actual process temperature;
- the temperature control mode (e.g., isothermal, isoperibolic, etc.);
- the dosing time (if applicable);
- the presence of auxiliary heat removal systems (e.g., reflux condensers).

The evaluation of $\dot{Q}_{max}$ is fundamental to determine whether the selected operating conditions are safe for conducting the process at the industrial scale. It also provides an indicative measure of the reliability margin of the reactor cooling system.

Figure 3.18 shows a typical thermal profile during a temperature runaway event in a batch reactor (i.e., one in which all reagents are charged before thermal conditioning to reach the process temperature).

Initially, all reagents are at ambient temperature (T_0) and are heated to the operating temperature (T_{proc}). Once this temperature is reached, the desired chemical reaction proceeds under controlled conditions for a given time (Phase 1).

At a certain moment (Point 3), due to a cooling system failure or an inappropriate choice of operating parameters, the reaction begins to proceed under quasi-adiabatic conditions, and the system temperature starts to increase uncontrollably. The maximum temperature that the system can reach as a result of the heat generated by the desired reaction is the MTSR.

The temperature increase associated with the exothermicity of the desired reaction is termed the adiabatic temperature rise (ΔT_{ad}) (Interval 2). Consequently, the system temperature becomes higher than the normal operating temperature.

If this temperature also exceeds the MAT parameter, the system temperature continues to rise, reaching a much higher temperature (T_{max}), typically associated with an explosive

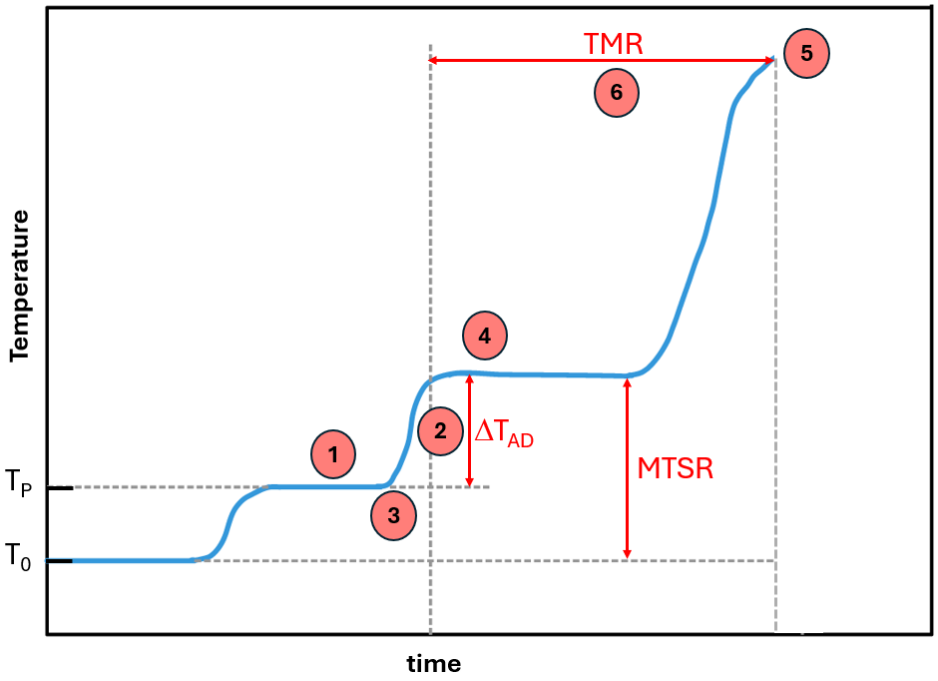

Figure 3.18: Typical thermal profile in a batch reactor during a runaway reaction.

event (Point 5). The temperature increase related to the decomposition of the reacting mass is referred to as the decomposition temperature rise (ΔT_{dec}).

The time required to reach the maximum rate of heat generation due to decomposition is the TMR (Phase 6). As discussed earlier, this parameter provides crucial insight for process risk characterization: a longer TMR offers operators more time to take corrective action before decomposition reactions actually occur. Naturally, these parameters depend not only on the reaction chemistry, but also on the process characteristics and the equipment design—including geometric configuration, materials of construction, and the type of cooling system employed.

Classification of Reaction Hazard: Stoessel–Ciba Method

Data obtained from reaction calorimetry can be used to evaluate the safety of a process and to estimate the potential consequences of a runaway reaction. The Stoessel–Ciba method allows classification of the hazard level of a reacting system based on the following parameters:

- process temperature (T_{proc});
- boiling temperature of the reacting system or solvent (T_{eb});
- onset temperature of decomposition (i.e., MAT, Maximum Allowable Temperature);

- maximum temperature due to the synthesis reaction under adiabatic conditions (MTSR).

Depending on the relative positions of these parameters, processes can be classified into five hazard classes (see Figure 3.19):

- Class 1 – The process is inherently safe since, after an eventual thermal loss of control of the desired reaction, the "decomposition temperature" T_d cannot be reached (MTSR $< T_d$). Even in case of an external fire forces the reacting mass temperature to increase, the reaching of the boiling temperature will remove heat acting as a safety barrier.

- Class 2 – The process is inherently safe because, even in case of thermal runaway, neither the boiling temperature nor the decomposition temperature is reached. This condition is similar to that of Class 1, but being T_d lower with respect to the boiling temperature, the mitigation effect due to the solvent evaporation is missed.

- Class 3 – The process remains safe from a thermal point of view, as in the event of a runaway phenomenon, T_d is not reached. However, the reaching of the boiling temperature could cause the system pressurization.

- Class 4 – The process is potentially runaway. After the loss of temperature control, both the boiling temperature and decomposition temperature may be reached. Process safety depends on the heat release rate of both the synthesis and

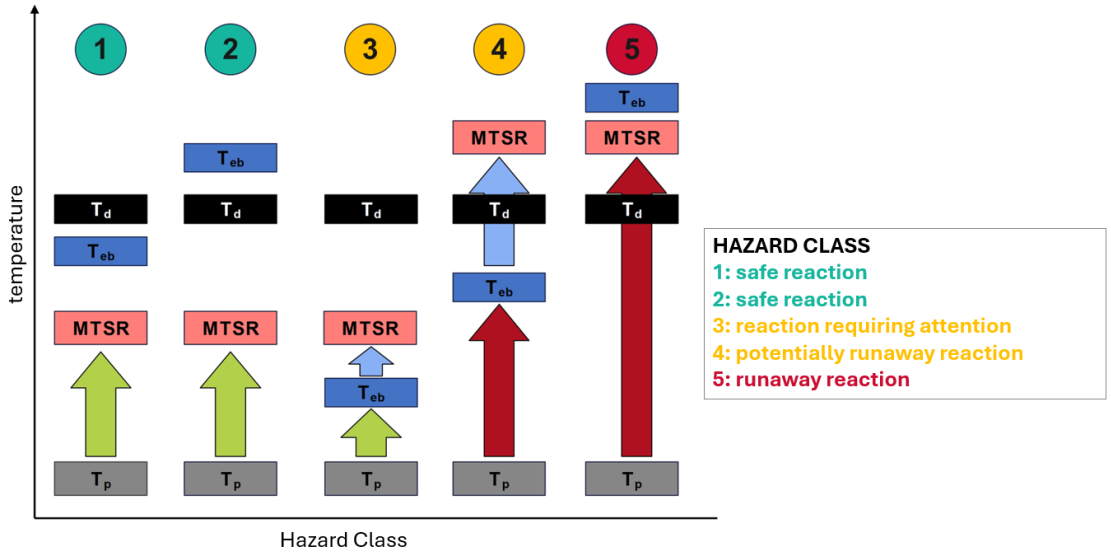

Figure 3.19: Classification of chemical reaction hazard according to the Stoessel–Ciba method.

decomposition reactions. As in Class 3, evaporative cooling may act as a temporary safety barrier, preventing the overcoming of T_d.

- Class 5 – The process is potentially runaway and represents the most critical case. After loss of temperature control, decomposition is initiated, but in this situation, evaporation of the reacting mass does not provide any effective safety barrier because the solvent boiling point is higher with respect to T_d. [8, 11].

3.8 Flammability and Explosivity

A fire (or combustion) can be defined as an exothermic chemical reaction in which a substance combines with an oxidizer, releasing energy. Part of the released energy sustains the combustion process itself, so that once initiated, it no longer requires an external energy source to continue.

An explosion, on the other hand, is defined as a rapid release of stored energy within a confined volume (e.g., a stored substance), occurring over a very short time period. The sudden expansion of gases generates a shock wave or a sudden pressure increase. This gas expansion may be: mechanical, caused by the rupture of a pressurized vessel, or the result of a rapid chemical reaction.

Depending on the propagation speed of the shock wave, explosive phenomena are classified as either detonations or deflagrations:

- Detonation: the energy release propagates the shock front at a supersonic speed.
- Deflagration: the energy release propagates the shock front at a subsonic speed (below the speed of sound).

Explosions can further be categorized into two main types:

- Confined explosion: the most common type, occurring inside a tank or building, often resulting in severe structural damage and potential casualties near the event.
- Unconfined explosion: occurring outdoors, generally following the release of a flammable gas. The gas disperses and mixes with air until it encounters an ignition source. Although less frequent than confined explosions (since wind dilution often reduces gas concentration below the lower flammability limit), when they occur, unconfined explosions can be highly destructive, affecting large areas and involving significant quantities of gas [5, 16].

3.8.1 Definition of Fire

As previously discussed, a fire is a chemical reaction that generates heat and light, often producing smoke due to incomplete combustion. Combustion can occur with or without visible flames: in the first case, it is referred to as flaming combustion, while in the second case, it is known as smoldering combustion, since the long characteristic times of the phenomenon prevent light emission.

For a fire to occur, three factors must be present simultaneously, as summarized in the so-called fire triangle (Figure 3.20):

- Fuel. It may be solid (e.g., metal dusts), liquid (e.g., gasoline), or gaseous (e.g., hydrogen), and is defined as the substance that increases its oxidation number during combustion. Regardless of its physical state, combustion always takes place in the vapor phase; therefore, liquids must first vaporize, while solids may sublimate or decompose to release vapors or gases.
- Oxidizer. Any substance that decreases its oxidation number during the combustion reaction. It may be gaseous (e.g., oxygen, chlorine), liquid (e.g., hydrogen peroxide), or solid (e.g., ammonium nitrate).
- Ignition source. The initial energy required to initiate combustion. Examples include sparks, open flames, static electricity, or heat.

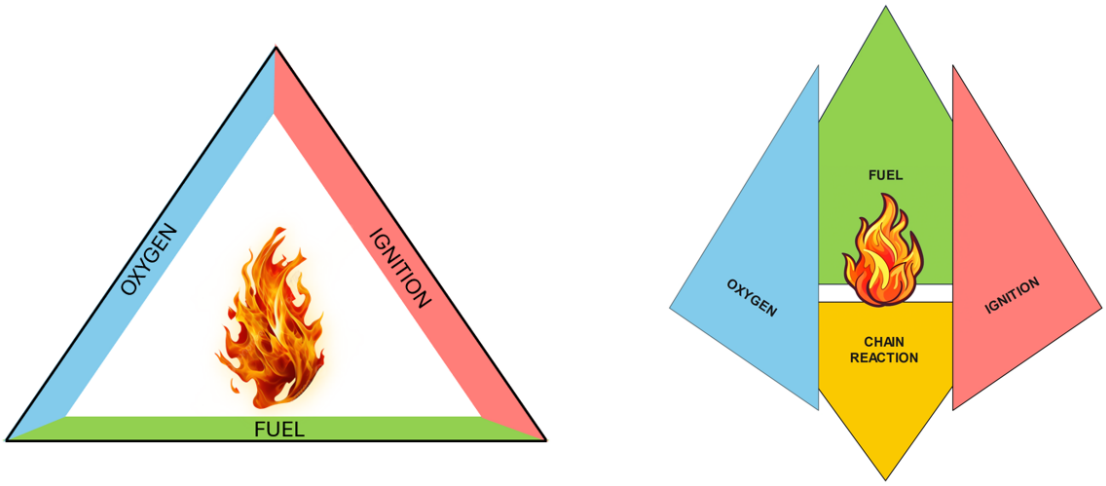

Figure 3.20: On the left, the fire triangle; on the right, the fire tetrahedron.

The fire tetrahedron also considers the chain reaction responsible for the formation of free radicals, which release the heat necessary to sustain combustion. Some extinguishing agents are capable of interrupting this chain reaction, effectively suppressing the fire [5, 16].

3.8.2 Flammability

To assess the risks associated with fire hazards, it is essential to understand the flammability properties of substances, whether they are liquids, gases, vapors, or dusts.

The most important parameters influencing flammability characteristics include: nature of the fuel, temperature, pressure, humidity, presence of inert gases, and particle size distribution, among others.

Variations in temperature or pressure can cause changes in vapor pressure, flammability limits, reaction rates, and flame propagation velocity, among other factors. Below are the physico-chemical parameters useful for determining the flammability of a substance.

Vapor Pressure

When a liquid is placed in a closed container at constant temperature, its molecules initially evaporate until a dynamic equilibrium is reached between the liquid phase and the vapor phase. The pressure exerted by the vapor at this equilibrium is called the vapor pressure (or equilibrium vapor pressure).

This property applies to all liquids and depends not only on the nature of the molecules and the strength of their intermolecular interactions, but also on the temperature of the liquid. The vapor pressure provides an indication of a substance volatility: the higher the vapor pressure, the more easily the substance evaporates.

Autoignition or Self-Ignition Temperature

The autoignition temperature (AIT), also referred to as self-ignition temperature (SIT), is the minimum temperature at which a fuel–oxidizer mixture begins to burn spontaneously and continuously, without any external source of heat or energy. It is important to note that the AIT represents the minimum temperature measured under laboratory conditions, and it depends on the characteristics of the test vessel, such as its size, shape, and material.

This parameter is useful for comparing different flammable substances, but in real operating conditions, the actual AIT is generally higher than the laboratory value, because ignition sources in industrial or accidental scenarios may have different confinement, geometry, or size than those in standardized tests [17] (Table 3.19).

Table 3.19: Autoignition Temperature (AIT) of selected substances.

Substance	**CAS Number**	**AIT (°C)**
Acetone	67-64-1	465
Benzene	71-43-2	498
n-Hexane	110-54-3	225
Methanol	67-56-1	464

Fire point

The fire point is the lowest temperature at which the vapors of a liquid, once ignited, will continue to burn for at least 5 seconds after the ignition source has been removed. Typically, the fire point is slightly higher than the flash point measured in an open cup test, as it represents the condition at which sustained combustion can occur rather than just a momentary ignition [5].

Flash point

The flash point is the lowest temperature at which a combustible liquid emits enough vapor to form a flammable mixture with air near its surface. At the flash point, the vapor briefly ignites in the presence of an ignition source, but the combustion does not sustain because the vapor concentration is insufficient to maintain the flame.

The flash point temperature generally increases with pressure; conversely, a decrease in pressure lowers it. This effect is important since liquids that have a flash point above ambient temperature at atmospheric pressure can still form explosive mixtures if stored under reduced pressure.

The flash point of a liquid in a closed cup can be interpreted as the temperature at which the vapor pressure of the fuel corresponds to a vapor concentration equal to the lower flammability limit (LFL) in air.

The flash point is a key safety property of flammable liquids, as it helps assess fire and explosion hazards during storage, handling, and transportation. Liquids with low flash points require special precautions, whereas those with flash points above $50 - 60\,^{\circ}\mathrm{C}$ are considered progressively less hazardous in terms of flammability (Table 3.20).

When determining the flash point of multicomponent mixtures, the relationship is not always linear. Adding a liquid with a higher flash point to one with a lower flash point does not necessarily yield an intermediate value, as the mixture might form an azeotrope with a vapor pressure higher (or lower) than that of its individual components. Consequently, the flammable vapor concentration may be reached at a temperature lower (or higher) than the flash points of the pure substances [5, 8].

Table 3.20: Flash point temperatures of selected substances.

Substance	**CAS Number**	**Flash Point (°C) - Closed Cup**	**Flash Point (°C) - Open Cup**
Acetaldehyde	75-07-0	4	-
Acetone	67-64-1	-18	-9
Benzene	71-43-2	-11	-
Cyclohexane	110-82-7	-20	-
Methanol	67-56-1	12	-
p-Xylene	106-42-3	25	31
Toluene	108-88-3	4	7

Flammability Limits (LFL, UFL)

The flammability limit represents the range of gas or vapor concentrations in air that can burn or explode in the presence of an ignition source. These limits are typically expressed as a percentage by volume of fuel in air at ambient temperature and pressure.

They are divided into two categories:

- Lower Flammable Limit (LFL): the lowest concentration of vapor or gas in air below which combustion cannot occur due to an insufficient amount of fuel.
- Upper Flammable Limit (UFL): the highest concentration of vapor or gas in air above which combustion cannot occur due to an excess of fuel.

In general, both temperature and pressure influence the flammability limits, as temperature increases, the LFL tends to decrease and the UFL increases, thus widening the flammability range. Conversely, a decrease in pressure narrows the range, making ignition less likely (Figure 3.21). Many gases and vapors have narrow flammability ranges, making them easier to handle safely. Others, such as hydrogen, exhibit very wide flammability ranges, which require strict control over fuel concentration to ensure safe operation. In certain cases, one of the limits may be absent, for example, acetylene has no upper flammable limit, meaning its vapors can explode even in the absence of an oxidizer (Table 3.21) [5].

Table 3.21: Flammability limits of selected substances at atmospheric pressure (1 atm).

Substance	**CAS Number**	**LFL (% vol fuel/air)**	**UFL (% vol fuel/air)**
Acetaldehyde	75-07-0	4	57
Acetylene	74-86-2	2.5	100
Ammonia	7664-41-7	16	25
Benzene	71-43-2	1.4	8.0
Hydrogen	1333-74-0	4	75
Cyclohexane	110-82-7	-20	-
Methane	74-82-8	5.0	15.0
Ethylene oxide	75-21-8	3	100

Flammability Range

The flammability range is the interval between the lower and upper flammability limits, expressed as the percentage of fuel gas in the air, within which ignition and flame propagation can occur in the mixture when an ignition source is present.

Minimum Ignition Energy

The Minimum Ignition Energy (MIE) is the minimum amount of energy required to initiate the combustion process. All flammable materials, including dusts, have a specific MIE value that depends on their chemical nature, concentration, pressure, and temperature.

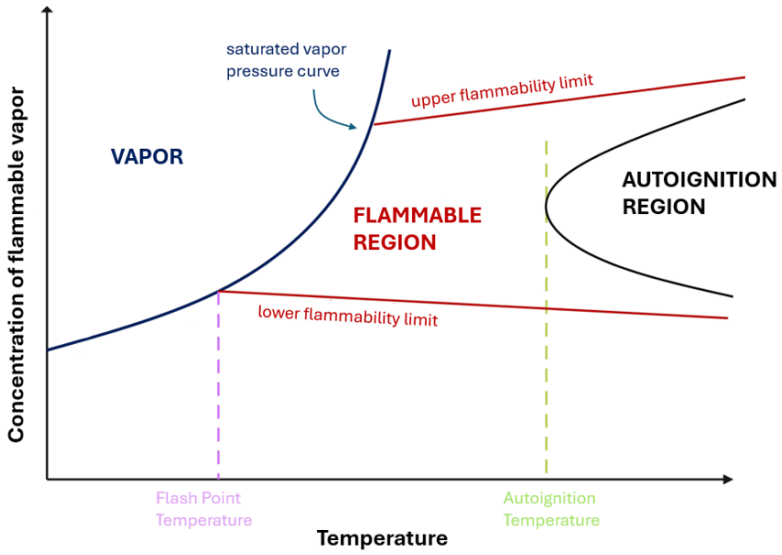

Figure 3.21: Flammable vapor concentration as a function of temperature.

Experimental data show that for flammable vapors, MIE:

- decreases with increasing pressure;
- decreases with increasing temperature;
- increases with increasing nitrogen concentration.

Dusts generally have higher MIE values than combustible gases. Many hydrocarbons have MIE values around 0.25 mJ, while for dusts the values are typically several tens of millijoules (Table 3.22).

Table 3.22: Minimum Ignition Energy (MIE) of selected gases and vapors.

Substance	CAS Number	MIE (mJ)
Acetaldehyde	75-07-0	0.4
Acetylene	74-86-2	0.020
Ammonia	7664-41-7	80
Benzene	71-43-2	0.225
Hydrogen	1333-74-0	0.016
Methane	74-82-8	0.21
Propane	75-21-8	0.250
Ethylene oxide	75-21-8	0.06

Limiting Oxygen Concentration

The Limiting Oxygen Concentration (LOC) is defined as the lowest concentration of oxygen below which combustion can no longer occur. This parameter is also known as the Minimum Oxygen Concentration (MOC) or the Maximum Safe Oxygen Concentration (MSOC). LOC is expressed as the oxygen content in the gas mixture, in percent by volume (% vol).

Determining the LOC is a key aspect in explosion prevention and represents a fundamental design parameter for inerting systems. For a given combustible substance, the LOC value depends on the type of inert gas used, for instance, nitrogen (N_2), carbon dioxide (CO_2), or water vapor (Figure 3.23).

The addition of an inert gas significantly reduces the upper flammability limit of a fuel-oxidant mixture, while the lower limit remains nearly constant. This leads to a progressive narrowing of the flammable range (flammability gap), until a further addition of inert gas causes the upper and lower limits to overlap, making the mixture completely non-flammable.

The experimental determination of LOC is carried out according to ASTM E2931 or EN 14034-4, using standardized apparatus such as the 20-L sphere or the 1 m^3 explosion chamber. Both methods employ an ignition source of 10 kJ in the 1 m^3 vessel, while in the 20-L sphere the ignition energy may vary depending on test conditions.

In the absence of experimental data, the LOC can be estimated using the reaction stoichiometry and the lower flammability limit (LFL). This estimation method is applicable to many hydrocarbons.

Table 3.23: Limiting Oxygen Concentration (LOC) of selected substances.

Substance	**N_2/Air**	**CO_2/Air**
Acetone	11.5	14
Benzene	11.4	14
Hydrogen	5	5.2
Methane	12	14.5
Propane	11.5	14.5
Toluene	9.5	-

3.8.3 Flammability Triangle Diagram

In the literature, the lower and upper flammability limits are generally referred to vapor–air mixtures. However, under certain operating conditions, it is necessary to consider the presence of a third component, such as an inert gas, which can influence the combustion behavior of the mixture. For this reason, it is particularly useful to represent experimental results using a ternary diagram, as shown in Figure 3.22 and Figure 3.23. The two graphs are formally identical and provide the same information. In this type of

diagram, each side of the triangle represents one component of the mixture: nitrogen, oxygen, and methane.

A key feature of the graph is the AB line, also known as the "air line", which describes all possible combinations of the methane – air mixture. Point A corresponds to 100% methane, while point B represents the typical air composition, consisting of 21% oxygen and 79% nitrogen.

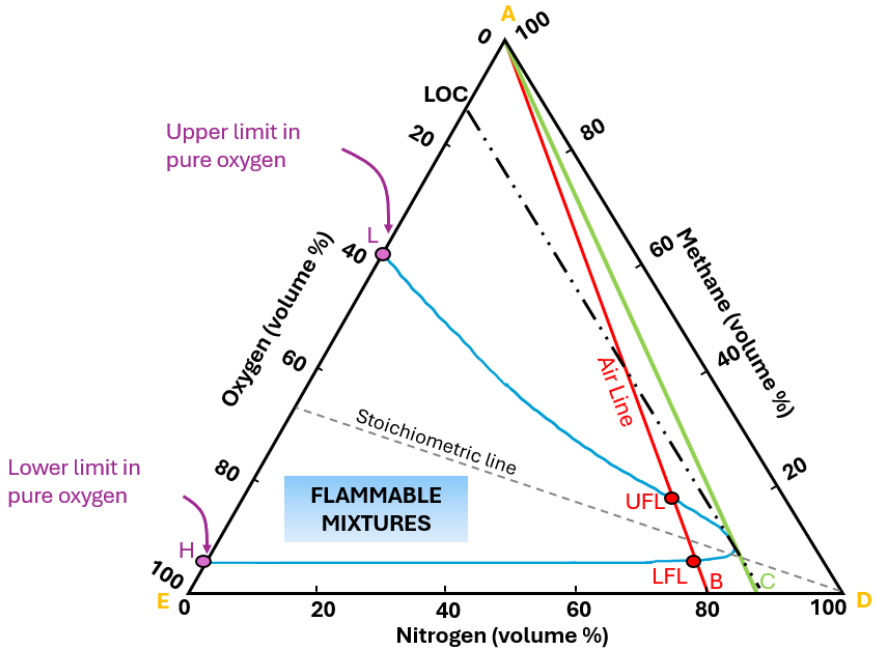

Figure 3.22: Flammability diagram for the $CH_4/O_2/N_2$ mixture at atmospheric pressure and ambient temperature.

This line intersects the flammability region at two points corresponding to the lower and upper flammability limits of methane in air, equal to 5% and 15% methane, respectively. The area enclosed by the blue curve is defined as the flammability envelope, representing all the mixtures that can sustain combustion. Outside this region, the mixture is not capable of supporting a flame. The shape of this envelope depends on several parameters, including the type of fuel, temperature, pressure, and type of inert gas used.

The diagram also shows the stoichiometric line, which includes all combinations of methane and oxygen in stoichiometric ratio; that is, the conditions where the fuel and oxidizer are present in exactly the right proportions for complete combustion.

Finally, another crucial piece of information derived from the graph is the Limiting Oxygen Concentration (LOC), defined as the maximum oxygen concentration at which flammability is inhibited in the presence of an inert gas. To determine the LOC experimentally, a line parallel to the methane axis is drawn tangent to the flammability

envelope. This value is particularly important for industrial inerting strategies, as it defines the minimum amount of inert gas required to prevent explosion hazards.

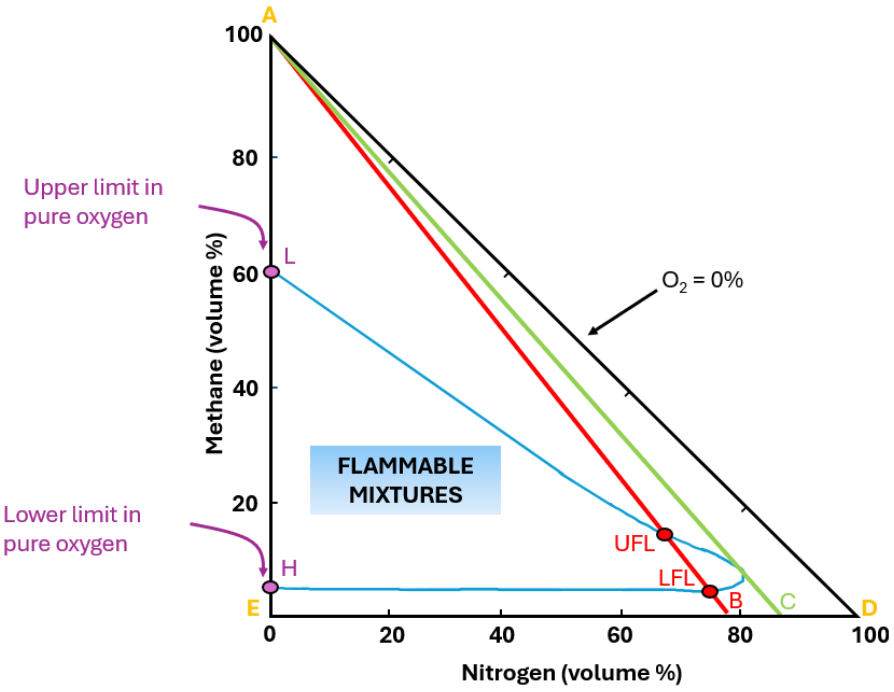

Figure 3.23: Flammability diagram for the $CH_4/O_2/N_2$ mixture at atmospheric pressure and ambient temperature.

3.8.4 Experimental Techniques for the Determination of Flash Point and Flammability Limits

The accurate determination of flash point and flammability limits is essential for assessing the fire and explosion hazards associated with chemical substances and mixtures.

This section presents the main experimental techniques commonly used to determine flash point and flammability limits, followed by a description of the predictive methods available in the literature for estimating these values based on chemical structure and thermodynamic properties.

Several experimental methods are available, each of which may provide slightly different results. The two most commonly used techniques are the open cup and closed cup methods. In general, the flash point temperature measured with the open cup method is a few degrees higher than that obtained using the closed cup method.

Open Cup Method

The most widely used technique for determining the flash point by the open cup method is known as the Cleveland Open Cup (COC) method (Figure 3.24).

The liquid to be tested is placed in an open container equipped with a thermometer to measure the temperature and a Bunsen burner to provide heat. Above the cup, a movable rod with a small test flame fixed at its end is slowly passed back and forth over the surface of the liquid during heating. When the liquid reaches a sufficiently high temperature to generate an ignitable vapor, a momentary flash occurs: the temperature recorded at that instant is defined as the flash point temperature. Upon further heating, the temperature rises until a sustained flame is observed; this temperature is known as the fire point.

A limitation of the open cup method is that air movement above the liquid surface can alter the vapor concentration, thereby affecting the measured flash point temperature. To overcome this drawback, the closed cup method was developed [5].

To determine the flash point temperature, the equipment and test procedures must comply with the following standards:

- ASTM D92-24 – Standard Test Method for Flash and Fire Points by Cleveland Open Cup Tester;
- ISO 2592:2017 – Petroleum and related products – Determination of flash and fire points – Cleveland open cup method;
- DIN EN ISO 2592:2018-01 – Petroleum and related products – Determination of flash and fire points – Cleveland open cup method.

Figure 3.24: Determination of the flash point temperature using the open cup method.

Closed Cup Method

The most widely used procedure for determining the flash point using the closed cup method is the Pensky – Martens method (Figure 3.25).

Figure 3.25: Pensky – Martens closed cup apparatus used for flash point determination.

In this test, the liquid sample is placed inside a container equipped with a perforated lid and a shutter. The liquid is heated at precisely controlled and constant temperature increments. As the temperature increases, vapors are generated and mixed with the air present inside the cup. At predetermined intervals, the shutter is momentarily opened and a small ignition source is directed toward the opening. The operation is repeated until a brief flash is observed. The temperature at which this flash occurs, corrected for the barometric pressure measured at the time of the test, is defined as the flash point temperature of the material.

To determine the flash point temperature, the apparatus and testing procedures must comply with the following standards:

- ASTM D93-20 – Standard Test Methods for Flash Point by Pensky–Martens Closed Cup Tester;
- ISO 2719:2016 – Determination of flash point – Pensky–Martens closed cup method;
- ASTM D3934-20 – Standard Test Method for Flash/No Flash Test – Equilibrium Method by a Closed-Cup Apparatus;
- ISO 3679:2022 – Determination of flash point – Method for flash/no-flash and flash point by small-scale closed cup tester;
- ISO 13736:2021 – Determination of flash point – Abel closed cup method;
- ISO 1523:2002 – Determination of flash point – Closed cup equilibrium method.

Experimental Determination of Flammability Limits

Flammability limits are experimentally determined using a closed vessel apparatus, consisting of a glass chamber placed inside an insulated enclosure and equipped with a magnetic stirrer. The lid of the vessel includes ports for the controlled introduction of air and the test sample.

The sample, at a known concentration, is mixed with air and loaded into the vessel; the presence of the stirrer ensures uniform mixing of the gas mixture. Subsequently, a spark is generated as the ignition source, and the occurrence of a flame is observed.

The test is repeated several times, starting with a low concentration and gradually increasing it until the mixture becomes flammable. The temperature at which ignition occurs corresponds to the Lower Flammable Limit (LFL). Similarly, to determine the Upper Flammable Limit (UFL), the procedure is reversed: the test starts from the highest concentration of the sample and is repeated while gradually decreasing the concentration until ignition is observed. To ensure accuracy and reproducibility, the apparatus and test procedure must comply with the following international standard: ASTM E681-09 (Reapproved 2023) – Standard Test Method for Concentration Limits of Flammability of Chemicals (Vapors and Gases).

3.8.5 Theoretical Predictive Methods for Estimating the Flash Point Temperature

Several predictive methods for estimating the flash point temperature are available in the literature. The most common ones are summarized below.

Satyanarayana and Rao Correlation

Satyanarayana and Rao developed a method to estimate the flash point temperature of organic compounds and petroleum fractions based on the boiling point of the liquid, using the following correlation [5]:

$$T_f = a + \frac{b\left(\frac{c}{T_b}\right)^2 e^{-c/T_b}}{\left(1 - e^{-c/T_b}\right)^2} \tag{3.20}$$

where

T_f flash point temperature [K];

T_b boiling point temperature [K];

a, b, c empirical constants [K], tabulated values (Table 3.24).

Hshieh Correlation

Hshieh developed a closed-cup correlation for estimating the flash point temperature from the boiling point, applicable to both silicone and organic compounds.

Table 3.24: Constants for estimating flash point temperature and absolute error for different chemical groups [18].

Group	Number of compounds	Absolute error %	a	b	c
Hydrocarbons	230	0.410	225.1	537.6	2,217
Alcohols	150	0.186	230.8	390.5	1,780
Amines	70	0.200	222.4	416.6	1,900
Acids	40	0.531	323.2	600.1	2,970
Ethers	80	0.343	275.9	700.0	2,789
Sulfur compounds	40	0.484	238.0	577.9	2,297
Esters	120	0.186	260.8	449.2	2,217
Ketones	80	0.722	260.5	296.0	1,908
Halogenated compounds	200	0.672	262.1	414.0	2,154
Aldehydes	45	0.771	264.5	293.0	1,970
Phosphorus compounds	20	0.815	201.7	416.1	1,666
Nitrogen compounds	125	0.622	185.7	432.0	1,645
Petroleum fractions	21	0.294	237.9	334.4	1,807

For silicone compounds, the correlation (Equation 3.21) was tested on 207 samples, yielding a standard error of estimation of 11.06 °C:

$$T_f = -51.2835 + 0.4994\,T_b + 0.00047\,T_b^2 \tag{3.21}$$

For organic compounds, the correlation (Equation 3.22) was derived from 494 compounds (including 250 organics, 207 silicones, 31 sulfur-containing, and 6 phosphorus-containing compounds). The standard estimation error remains 11.06 °C [19]:

$$T_f = -54.5377 + 0.5883\,T_b + 0.00022\,T_b^2 \tag{3.22}$$

where

T_f flash point temperature [K];

T_b boiling point temperature [K].

Prugh Correlation

Prugh proposed a method to estimate the flash point temperature based on the boiling point and the chemical structure of the substance. The procedure consists of two steps [19]:

1. Calculation of the stoichiometric vapor concentration in air:

$$\chi_{st} = \frac{83.8\%}{4(C) + 4(S) + H - X - 2(O) + 0.84} \tag{3.23}$$

where

C, S, H, X, O number of carbon, sulfur, hydrogen, halogen, and oxygen atoms in the molecule.

2. Calculation of the flash point temperature from the boiling point.
For alcohols:

$$\frac{T_b}{T_f} = 1.3611 - 0.0697 \ln(\chi_{st}) \tag{3.24}$$

For all other compounds:

$$\frac{T_b}{T_f} = 1.4420 - 0.08512 \ln(\chi_{st}) \tag{3.25}$$

where

χ_{st} stoichiometric vapor concentration in air [vol %];
T_b boiling point temperature [K or °R];
T_f flash point temperature [K or °R].

Flash Point Temperature of Binary Mixtures

The flash point temperature of a flammable or combustible liquid is defined as the temperature at which the vapor pressure of the substance produces, in air, a vapor concentration equal to the Lower Flammable Limit (LFL).

$$\mathrm{LFL_i} = \frac{P^{sat}_{i,fp}(T_f)}{P} \tag{3.26}$$

where

i component index;
$P^{sat}_{i,fp}$ vapor pressure of component i at the flash point temperature [kPa];
P ambient pressure [kPa].

Each component i in the liquid phase is in equilibrium with the vapor phase at the same temperature and pressure:

$$y_i \, \Phi_i \, P = x_i \, \gamma_i \, f_i \tag{3.27}$$

where

x_i, y_i mole fraction of component i in liquid and vapor phases, respectively;

Φ_i fugacity coefficient of component i in the vapor phase;

γ_i activity coefficient of component i in the liquid phase;

f_i fugacity of the pure component i [kPa].

At low pressures, the vapor phase can be approximated as an ideal gas, so the fugacity coefficient is assumed to be 1. The fugacity of the pure component equals its vapor pressure at the system temperature. Equation 3.27 can therefore be rewritten as:

$$y_i = \frac{x_i \, \gamma_i \, P_i^{sat}}{P} \tag{3.28}$$

where P_i^{sat} is the vapor pressure of component i at temperature T.

Applying Le Chatelier's rule for a binary mixture:

$$1 = \frac{y_1}{\mathrm{LFL}_1} + \frac{y_2}{\mathrm{LFL}_2} \tag{3.29}$$

Substituting Equations 3.26, 3.27 and 3.28 into Equation 3.29, we obtain:

$$\sum_{i=1}^{2} \frac{x_i \, \gamma_i \, P_i^{sat}}{P_{i,fp}^{sat}(T_f)} = 1 \tag{3.30}$$

The temperature satisfying Equation 3.30 corresponds to the flash point temperature of the mixture [20, 21].

3.8.6 Theoretical Predictive Methods for the Estimation of Flammability Limits

The estimation of the lower and upper flammability limits can be performed using theoretical predictive methods, some of which are briefly presented below.

It is important to emphasize that these methods are suitable only for preliminary assessments and should not be considered as substitutes for experimental determinations.

Jones Method

The Jones method allows for the estimation of the flammability limits in air based on the stoichiometric concentration of the fuel [5]:

$$\mathrm{LFL} = 0.55 \, C_{st} \tag{3.31}$$

$$\mathrm{UFL} = 3.50 \, C_{st} \tag{3.32}$$

where C_{st} is the stoichiometric concentration of the fuel in the fuel – air mixture [% vol].

For most organic compounds, the stoichiometric concentration can be determined using the general combustion reaction:

$$C_m H_x O_y + z O_2 \longrightarrow m CO_2 + \frac{x}{2} H_2 O \tag{3.33}$$

From the stoichiometric balance, the following relationship is obtained:

$$z = m + \frac{x}{4} - \frac{y}{2} \tag{3.34}$$

where z is expressed as moles of O_2 per mole of fuel.

Finally, the stoichiometric concentration can be expressed as:

$$C_{st} = \frac{\text{moles of fuel}}{\text{moles of fuel} + \text{moles of air}} 100 = \frac{100}{1 + \frac{z}{0.21}} \tag{3.35}$$

Suzuki and Koide Method

This method correlates the lower and upper flammability limits with the heat of combustion of the fuel. It has shown good agreement for approximately 30 organic compounds containing carbon, hydrogen, oxygen, nitrogen, and sulfur [5].

$$\text{LFL} = -\frac{3.42}{\Delta H_c} + 0.569\,\Delta H_c + 0.0538\,\Delta H_c^2 + 1.80 \tag{3.36}$$

$$\text{UFL} = 6.30\,\Delta H_c + 0.567\,\Delta H_c^2 + 23.5 \tag{3.37}$$

where ΔH_c is the heat of combustion of the fuel [kJ/mol].

3.8.7 Explosibility

An explosion is defined as a rapid release of energy occurring within a sufficiently short period of time and within a sufficiently confined volume to generate a pressure wave of significant intensity, which propagates outward from the point of release and can often be perceived acoustically.

The behavior of an explosion is influenced by several key factors, including [5]:

- ambient temperature;
- ambient pressure;
- composition of the explosive material;
- physical properties of the explosive material;
- nature of the ignition source (type, energy, and duration);
- geometry of the environment (confined or unconfined);
- quantity of combustible material;

- time prior to ignition;
- turbulence of the combustible mixture;
- rate of release of the combustible material.

As shown in Figure 3.26, explosions can be grouped according to their nature into the following categories:

- Physical explosions: occur as a result of the rapid release of mechanical energy and include phenomena such as the rupture of pressurized vessels, boiling liquid expanding vapor explosions (BLEVEs), and rapid phase transitions.
- Atomic explosions: result from nuclear transformations in which mass is converted into energy (these will not be considered in this document).
- Dust explosions: result from the rapid combustion of finely divided solid particles suspended in an air stream.
- Chemical explosions: occur due to rapid chemical reactions, decomposition, or combustion of substances or mixtures.

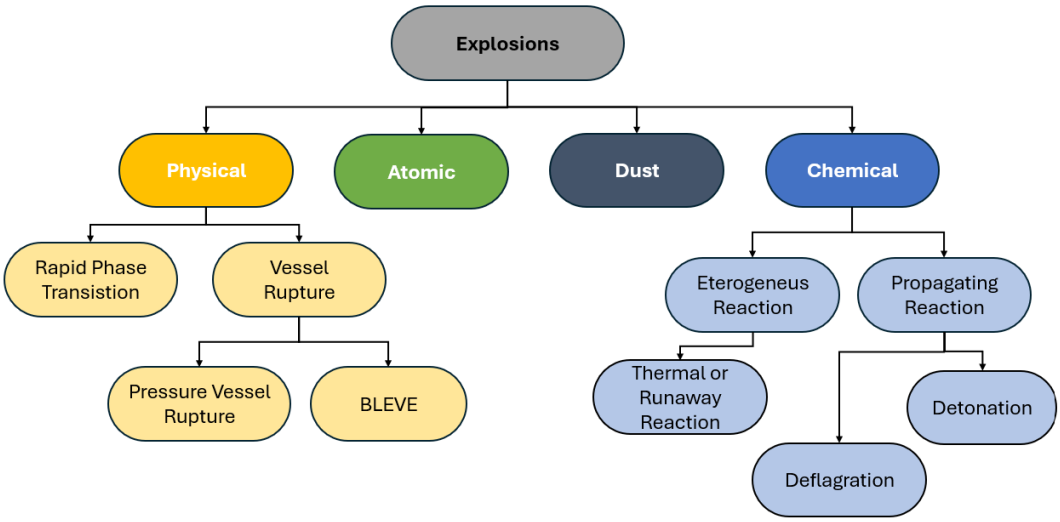

Figure 3.26: Classification of explosions.

Physical Explosions

Physical explosions occur as a result of the sudden rupture of a vessel containing a substance under high pressure. The conditions leading to such an internal overpressure

are typically identified through hazard identification and incident scenario analysis procedures.

The main methods used to estimate the energy released following the explosion of a pressurized gas are: Brode equation, isoentropic expansion, isothermal expansion, and thermodynamic availability method. Among these, the Brode method is the simplest approach.

The mechanism responsible for generating a shock wave in a physical explosion can be related to the difference between the internal energy of the substance inside the vessel before rupture and that in the surrounding environment after rupture.

An approximate estimation of this energy can be made by assuming that the substance undergoes a violent isoentropic expansion during vessel failure. In such a case, the released energy E can be expressed as:

$$E = \int_{V_0}^{V} P \, \mathrm{d}V = \int_{V_0}^{V} P_0 \left(\frac{V_0}{V} \right)^{\gamma} \mathrm{d}V = \frac{P_0 V_0 - P_a V_a}{\gamma - 1} \approx \frac{V_0 \left(P_0 - P_a \right)}{\gamma - 1} \tag{3.38}$$

where

V_0 internal volume of the vessel [m^3];

P_0 internal pressure of the vessel [Pa];

P_a external (atmospheric) pressure [Pa];

γ isentropic expansion coefficient of the substance [–].

Under real accidental conditions, the fraction of internal energy converted into a shock wave typically ranges between 40% and 80% of the maximum available energy estimated by Equation 3.38.

Chemical Explosions

A chemical combustion or decomposition reaction becomes explosive when heat exchange with the surroundings is nearly negligible (pseudo – adiabatic conditions). Under these circumstances, all the thermal power released by the reaction is used to increase the temperature of the reacting mass, thereby accelerating the reaction rate. This leads to an exponential rise in temperature, which can only be stopped once the reactants are completely consumed.

Chemical explosions can be further classified as homogeneous (occurring in the gas phase) or heterogeneous (involving liquid and/or solid phases).

In homogeneous chemical explosions, the entire gas mixture reacts uniformly throughout its volume. A typical example is the Unconfined Vapour Cloud Explosion (UVCE), in which large volumes of fuel – air mixtures are ignited, and the combustion reaction proceeds almost instantaneously in every region where fuel and oxidizer are present.

In contrast, heterogeneous chemical explosions involve a condensed phase (liquid or solid, e.g., an explosive substance). These reactions, usually triggered by decomposition, release very large volumes of high-temperature gases almost instantaneously. The rapid expansion of these gases, which may or may not react further with atmospheric oxygen,

produces a shock wave (i.e., the collapse of overlapping pressure fronts). Depending on the propagation velocity of the shock front, the phenomenon can be classified as either deflagration or detonation [16].

3.9 Dust Explosions

Any combustible solid material, when finely divided and dispersed in air in the form of a dust cloud, can cause an explosion upon ignition.

This potential explosibility is observed not only in substances classified as hazardous under current regulations (e.g., aluminum and other metal powders, pharmaceutical products, etc.) but also in materials commonly considered non-hazardous, such as flour, grains, milk powder, sugar, and wood dust.

According to the UNI EN 14034 standard, a material is classified as a dust when the particle size does not exceed 500 μm. Analogously to the fire triangle that represents the conditions for flammability, the case of dust explosions is described by the so-called explosion pentagon (Figure 3.27).

Figure 3.27: Explosion pentagon for dust explosions.

For an explosion to occur, the following five conditions must coexist:

- the dust must be combustible;
- the dust must be dispersed in air or another oxidizing atmosphere at a concentration equal to or greater than the Minimum Explosible Concentration (MEC);
- the presence of an ignition source, such as an electrostatic discharge, spark, hot surface, open flame, or heat generated by friction;
- mixing between the fuel (dust) and the oxidizer (air);
- partial or total confinement, which allows a pressure build-up, enabling the flame front to propagate rapidly and generate an explosion.

The parameters used to assess the ignition sensitivity of a dust cloud are (Table 3.25):

- Minimum Ignition Energy (MIE);
- Minimum Explosible Concentration (MEC);
- Minimum Ignition Temperature (MIT) of a dust cloud or Layer Ignition Temperature (LIT) of a dust layer;
- Limiting Oxygen Concentration (LOC).

The parameters commonly used to quantify the violence of a dust explosion are (Table 3.25):

- Maximum explosion pressure (Pmax);
- Maximum rate of pressure rise (dP/dt)max;
- Deflagration index (Kst).

A brief description of each parameter listed in Table 3.25 is provided below. Some of these parameters have been already discussed in the context of flammability of liquids, gases, and vapors.

Table 3.25: Main explosion/flammability parameters of combustible dusts.

Parameter	**Unit**	**Description**	**Application**
MIE	mJ	Minimum ignition energy of the dust cloud (electrical spark).	Elimination of ignition sources; grounding.
MEC	g/m^3	Minimum explosible concentration of the dust in air.	Control of dust concentration.
MIT (or LIT)	°C	Minimum ignition temperature of the dust cloud (or of a dust layer).	Control of surface temperatures.
LOC	Vol. %	Minimum (or limiting) oxygen concentration in the atmosphere required for flame propagation through a dust cloud.	Inerting.
P_{max}	bar(g)	Maximum explosion pressure under constant volume conditions.	Containment; venting; suppression; isolation; inerting.
$(dP/dt)_{max}$	bar/s	Maximum rate of pressure rise under constant volume conditions.	Containment; venting; suppression; isolation; inerting.
K_{st}	bar m/s	Deflagration index.	Containment; venting; suppression; isolation; inerting.

Minimum Ignition Energy

Already defined in Section 3.8.2.

3.9.1 Minimum Explosible Concentration

The Minimum Explosible Concentration (MEC) is defined as the lowest concentration of a combustible dust that is capable of supporting the propagation of a deflagration within a well-dispersed dust/air mixture under specified test conditions (ASTM E1515 or UNI EN 14034-3:2011).

The MEC is analogous to the Lower Flammable Limit (LFL) for vapors. However, unlike vapors, dusts generally do not exhibit a practical upper flammability limit that can be used for explosion prevention purposes. It is important to note that LFL and UFL are intrinsic properties of vapors, whereas the MEC is an extrinsic property, since it depends on the particle size of the dust. The MEC increases significantly with increasing particle diameter, particularly for dusts with particle sizes above 60 μm.

Most combustible dusts have MEC values between 30 and 125 $\mathrm{g/m^3}$. For practical safety assessments, a conservative value of 30 $\mathrm{g/m^3}$ is often assumed. Although this may appear low, a dust cloud at this concentration visually resembles a dense fog.

Experimentally, the MEC is determined using a 20-liter sphere apparatus. The test begins with an initial dust concentration, which is progressively adjusted to identify the minimum value capable of producing an explosion. According to ASTM E1515, the test typically starts at a concentration of 100 $\mathrm{g/m^3}$ or lower. If an explosion occurs, the test is repeated while decreasing the concentration in 10 $\mathrm{g/m^3}$ increments until no explosion is observed. If the initial concentration exceeds 100 $\mathrm{g/m^3}$, it is reduced by 25% in subsequent trials until the threshold concentration sustaining flame propagation is determined. Under UNI EN 14034-3, the initial concentration is set to 500 $\mathrm{g/m^3}$.

If an explosion occurs, the concentration is halved until no explosive event is observed. If no deflagration occurs at 500 $\mathrm{g/m^3}$, the concentration is increased by 250 $\mathrm{g/m^3}$ and the test is repeated. The ignition energy significantly influences MEC determination and is regulated by the relevant standards:

- ASTM (20-L sphere): 2.5–5 kJ;
- ASTM (1 $\mathrm{m^3}$ chamber): not specified, but typically 10 kJ;
- EN 14034-3 (20-L sphere): 2 kJ;
- EN 14034-3 (1 $\mathrm{m^3}$ chamber): 10 kJ.

Test results are based on the assumption of a homogeneous dust cloud. In practice, the MEC is affected by both the uniformity of dust dispersion and the ignition energy applied during testing [22, 23] .

3.9.2 Minimum Ignition Temperature

The Minimum Ignition Temperature (MIT) is defined, according to CEI EN 50281-2-1:1999 and ASTM E1491, as the lowest temperature of a hot surface capable of causing the spontaneous ignition of a dispersed dust/air mixture.

The MIT can be determined using two different types of apparatus: the Godbert–Greenwald (G–G) vertical furnace, and the BAM horizontal furnace.

These two instruments yield different results. The BAM furnace generally produces lower MIT values than the G–G furnace, due to the longer residence time of the dust in the heated zone. In the BAM setup, dust particles that do not ignite immediately upon dispersion tend to settle on the hot lower surface of the furnace, promoting the release of volatile components that can ignite more easily at lower temperatures than the dust itself.

It should be emphasized that the MIT is not an intrinsic property of the dust. Instead, it depends on several factors, including the test method, the type of apparatus, the geometry of the heated surface, and the dynamic state of the dust cloud. It should be emphasized that before using the MIT value in the design of deflagration risk mitigation systems, it is essential to verify which method was used to determine it [22, 23].

3.9.3 Layer Ignition Temperature

The Layer Ignition Temperature (LIT) is defined as the minimum temperature at which a layer of deposited combustible dust ignites spontaneously on a hot surface, without the presence of an external flame or spark. This parameter is critical for assessing the risk of fires and explosions in environments where combustible dust may accumulate, such as in manufacturing, material processing, and handling industries.

The determination of LIT is regulated by international standards that provide standardized methods to ensure accurate and reproducible results. The primary reference standard is ASTM E2021-15 (2023): Standard Test Method for Hot-Surface Ignition Temperature of Dust Layers.

3.9.4 Limiting Oxygen Concentration

The Limiting Oxygen Concentration (LOC) was previously defined in Section 3.8.2. For dusts, the procedure for determining the LOC is similar to that used for the Minimum Explosible Concentration (MEC). The dust sample is weighed and placed either in the storage chamber or directly above the dispersion nozzle. The chamber is then evacuated, and a known amount of oxygen and nitrogen is introduced until a final absolute pressure of 1 bar is reached. After a delay time of 60 ms for the 20-L sphere or 600 ms for the $1\,m^3$ vessel, the dispersion nozzles are activated, and a computer records the resulting overpressure, thereby determining the maximum explosion pressure. To determine the LOC, the test is repeated while varying the oxygen concentration until the value is reached below which no deflagration occurs. The LOC depends on temperature, pressure,

and the type of inert gas used. For most combustible organic dusts, the LOC typically ranges between 5 and 10% vol [22, 23].

3.9.5 Maximum Explosion Pressure

The Maximum Explosion Pressure (P_{max}) represents the highest overpressure developed during an explosion within a closed vessel. It is determined through a series of tests conducted in accordance with ASTM E1226 or EN 14034-1, over a wide range of dust concentrations.

Tests are carried out in closed vessels using either the 20-L sphere or the 1 m^3 chamber. In general, the 20-L sphere yields a slightly lower P_{max} value than the 1 m^3 vessel.

A high P_{max} value indicates a particularly hazardous dust, as it represents the maximum mechanical stress that a process vessel could be subjected to in the event of an explosion [22, 23].

3.9.6 Maximum Rate of Pressure Rise

The Maximum Rate of Pressure Rise ($(dP/dt)_{max}$) is defined as the maximum rate of increase in pressure over time during an explosion in a closed vessel.

This parameter is determined through a series of tests carried out in accordance with ASTM E1226 or EN 14034-1, using either the 20-L sphere or the 1 m^3 explosion chamber.

3.9.7 Deflagration Index

The Deflagration Index (K_{st}) represents the maximum rate of pressure rise normalized to a reference volume of 1 m^3. It is defined by the cubic law (Equation 3.39):

$$K_{st} = \left(\frac{dP}{dt}\right)_{max} V^{1/3} \tag{3.39}$$

where

P Pressure [bar];
t Time [s];
V Volume of the test vessel [m^3];
K_{st} Deflagration index [bar m/s].

The deflagration index K_{st} is determined using either the 20-L sphere or the 1 m^3 explosion chamber, following ASTM E1226 or EN 14034-1 standards. The deflagration index is considered independent of the test vessel size and is assumed to remain constant for a given dust type. This parameter is used to classify combustible dusts into four explosion hazard classes, as summarized in Table 3.27.

Table 3.26: Maximum explosion pressure and deflagration index of selected dusts.

Dust	$\mathbf{P_{max}}$ **(bar)**	$\mathbf{K_{st}}$ **(bar m/s)**
Cellulose	7.2	2.4
Polyethylene	7.5	67
Aluminum	12.9	515
Polypropylene	8.4	101

Table 3.27: Classification of dust explosion severity ($1\,m^3$ chamber, 10 kJ ignition source).

Explosion Class	$\mathbf{K_{st}}$ **(bar m/s)**	**Explosion Type**
St 0	0	None
St 1	$0 < K_{st} \leq 200$	Weak to moderate
St 2	$200 < K_{st} \leq 300$	Strong
St 3	$300 < K_{st} \leq 800$	Very strong

3.9.8 Primary and Secondary Explosions

Dust explosions in process industries are often initiated inside equipment such as storage silos, cyclones, filters, or mills. This type of explosion, which occurs at the point of ignition, is referred to as a primary explosion.

If the explosion propagates outside the initial enclosure, the shock wave and flame front generated by the primary explosion can lift and disperse dust layers deposited on surrounding surfaces, forming a secondary dust cloud that may, in turn, ignite and result in a secondary explosion (Figure 3.28). Depending on the amount of accumulated dust, even a weak primary explosion can trigger secondary explosions of considerable intensity. Furthermore, the initiating event of a secondary explosion is not necessarily a dust explosion; an external ignition source, such as a flammable vapor mixture, may also trigger a subsequent dust explosion. A primary explosion can therefore initiate a chain of successive explosions, creating a domino effect that significantly increases both structural damage and risk to personnel. The most effective way to prevent secondary explosions is to minimize dust accumulation on surfaces. Good industrial practices include [23]:

- regular cleaning of work areas;
- proper design and maintenance of equipment to prevent dust leaks;
- use of well-maintained dust collection systems;
- minimization of flat surfaces where dust can accumulate;
- sealing of areas that are difficult to access or clean.

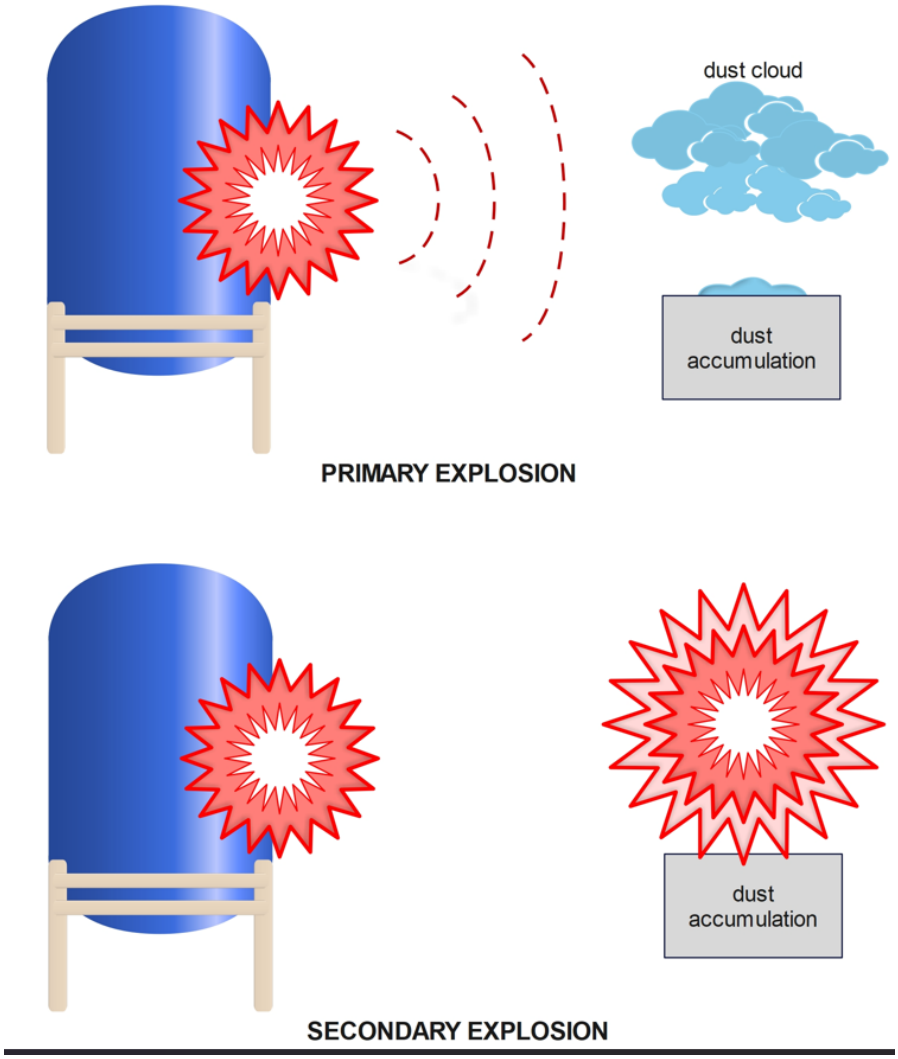

Figure 3.28: Sequence of a primary explosion followed by a secondary explosion.

3.9.9 Guideline for Dust Fire and Explosion Risk Assessment

The Occupational Safety and Health Administration (OSHA) has developed a general approach for assessing the risk of fire and explosion in dust-handling operations. The steps to be followed are illustrated in the flowchart shown in Figure 3.29.

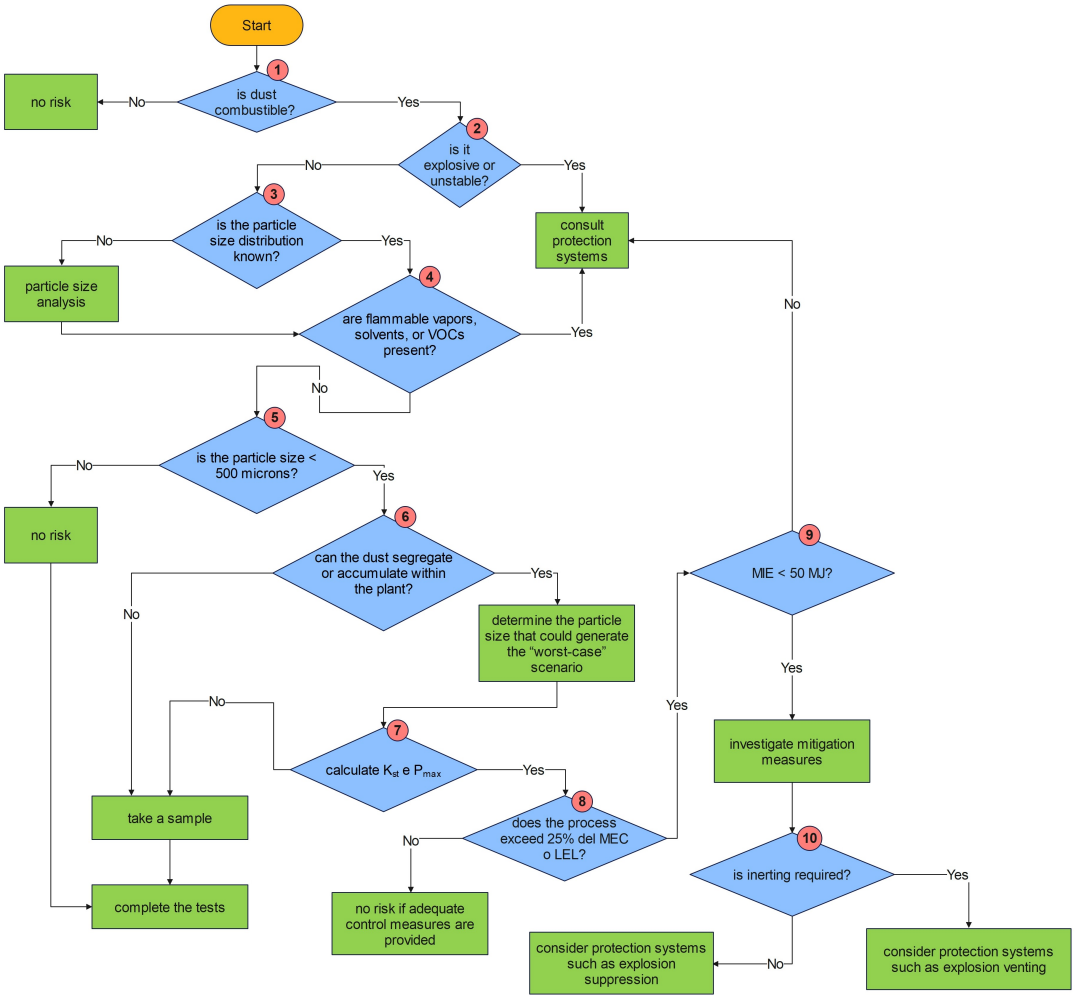

Figure 3.29: Logical flowchart for dust explosion hazard analysis (has been adapted and redrawn based on reference [23]).

The first step is to determine whether the dust is combustible. While the flammability of organic and metallic dusts is well documented, new products or intermediates may be present whose flammability properties are unknown. In such cases, a literature review should be conducted, and if the available information is insufficient, laboratory testing must be performed. If the dust is found to be non-combustible, the analysis can be considered complete; otherwise, the next step should be carried out.

The second step involves assessing whether the dust is explosive or unstable. Certain materials, such as organic peroxides, may be sensitive to impact, friction, or heat, increasing the likelihood of explosion.

The third step concerns evaluating the particle size distribution of the dust. Particle size is typically expressed in micrometers (μm). Unlike flammable liquids, solids require a specific surface-to-volume ratio to sustain combustion. If particle size exceeds a certain critical dimension, the explosion hazard becomes negligible, although the potential for fire may still remain.

In the fourth step, the presence of flammable or combustible solvents or the potential for the dust to release volatile organic compounds (VOCs) should be verified. Mixtures of solid dusts with liquid or gaseous solvents, known as hybrid mixtures, are particularly dangerous because they can lead to explosive events even when the individual components, taken separately, are not explosive. In such cases, a comprehensive experimental analysis is essential, since parameters such as particle size and LFL may not always be reliable indicators of the actual risk level.

The fifth step consists of verifying whether the particle size is below 500 μm. Experience and laboratory tests have shown that non-reactive dusts, even if combustible, do not generate explosions if their particle size exceeds 500 μm.

The sixth step is generally performed in parallel with the fifth. If particle fractions smaller than 500 μm are present, it is necessary to evaluate whether segregation or accumulation could occur within the plant. If the dust is well dispersed, the explosion hazard may be negligible; however, a representative sample must still be tested. If the dust tends to accumulate or segregate, further testing is required to determine the level of risk.

The seventh step is the most critical. As previously mentioned, risk evaluation should be based on the worst-case scenario. Therefore, attention should focus on determining the four key parameters: K_{st}, P_{max}, MIE, and MEC. The first two parameters (K_{st} and P_{max}) are used for designing explosion protection systems, while the latter two (MIE and MEC) help assess the need for venting or pressure relief systems. In general, dusts have a higher MIE than flammable vapors or gases. If the MIE exceeds 50 mJ, the explosion risk is considered insignificant, and preventive measures such as grounding may be sufficient, although in some cases, additional precautions may be necessary.

The eighth step involves verifying that the dust concentration in air does not exceed 25% of the MEC. If the concentration is below this threshold, the explosion risk is minimal, and neither inerting nor venting systems are required. If the concentration exceeds 25% of the MEC, the next step is to verify whether the MIE is greater than 50 mJ. If so, even in the presence of an electrostatic discharge, the mixture will not ignite. If the MIE is lower than 50 mJ, it is necessary to evaluate inerting systems or, if the risk is excessive, adopt explosion relief systems, as recommended by NFPA 68 (`https://www.nfpa.org/codes-and-standards/6/8/nfpa-68`).

3.9.10 Experimental techniques for the determination of dust explosibility

The following paragraphs describe some of the experimental techniques used to determine the parameters required for assessing the explosion and ignition hazard of a dust. Table 3.28 provides an overview of the most commonly used tests for determining dust hazard parameters, indicating for each test the parameters obtained and the corresponding reference standards.

Table 3.28: Overview of the most common tests used to determine the hazard parameters of a dust, the parameters obtained from each test, and the corresponding reference standards.

Test	**Parameters Determined**	**Reference Standard**	**Notes**
$1\,\mathrm{m}^3$ chamber	P_{max} $(dP/dt)_{max}$ LFL K_{st} LOC MEC	UNI EN 14034	Not applicable for dusts that do not require oxygen for combustion.
20-L sphere	P_{max} $(dP/dt)_{max}$ LFL K_{st} LOC MEC	UNI EN 14034	Not applicable for coarse, poorly flowable, fibrous, or voluminous dusts. Not applicable for dusts that do not require oxygen for combustion.

20-L Sphere Test

The 20-L sphere is a standard method used to determine the explosibility of combustible dusts. The data obtained provide a measure of the deflagration intensity and are used for the design of explosion protection systems.

The apparatus consists of a closed stainless-steel vessel (Figure 3.30) equipped with a rebound nozzle for dust dispersion, two chemical ignitors, each with an energy of 5 kJ connected to a voltage generator, and two pressure transducers for measuring the pressure rise. Time–pressure data are recorded by a high-speed data acquisition system, and the entire test sequence is controlled by computer. The vessel is also fitted with an external water jacket for heat removal during the explosion. The dust sample is weighed and either placed in the 600-mL storage chamber (pressurized to 20 bar) or directly on top of the nozzle for larger quantities. The ignition source is located at the center of the vessel, and all valves are closed to seal the system. Before the test begins, a vacuum

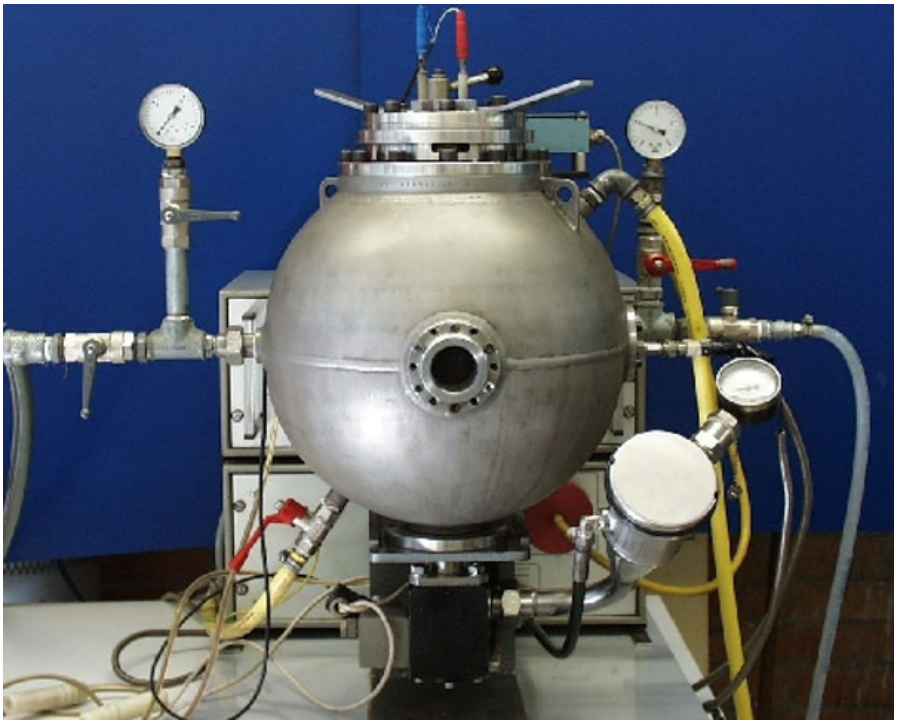

Figure 3.30: 20-L Sphere apparatus. Source: Adinex, Dust Explosion Testing – 20 L Sphere. `https://www.adinex.be/en/stofexplosies/20-liter-bol/.`

pump is used to achieve a pressure of 0.4 bar absolute. When the dust is dispersed, the nominal pressure inside the vessel reaches 1 bar absolute, at which point the test can begin. The solenoid valve is opened to allow the dust to enter the chamber. After a delay of $60 \pm 5\,\mathrm{ms}$, the ignitors are fired. The pressure rise is recorded by the two transducers, and the time–pressure data are stored for analysis.

The test is repeated for several dust concentrations, typically starting from $250\,\mathrm{g/m^3}$, and then increased or decreased as specified in the relevant standard. The only exception is the determination of the Lower Flammability Limit (LFL), where the initial concentration is $500\,\mathrm{g/m^3}$ [22].

$1\,\mathrm{m^3}$ Explosion chamber

The operating principle of the $1\,\mathrm{m^3}$ explosion chamber is similar to that of the 20-L sphere. It consists of a closed, pressure-resistant vessel, either spherical or cylindrical in shape, with an internal volume of $1\ 1\,\mathrm{m^3}$. The chamber is equipped with a dust dispersion system composed of a $5.4\,\mathrm{dm^3}$ reservoir connected to the chamber through a pipe and fitted with a valve that enables controlled release of the dust.

The ignition source, positioned at the center of the chamber, consists of two pyrotechnic ignitors electrically activated with a total energy of 10 kJ. The dust sample is weighed

and placed inside the dispersion container, which is pressurized to 20 bar before the test.

The experiment is repeated for different dust concentrations, typically starting from $250\,\mathrm{g/m^3}$, and the concentration is subsequently increased or decreased according to the procedure specified in the relevant standard. The only exception is for the determination of the LFL, where the initial concentration is $500\,\mathrm{g/m^3}$.

Horizontal BAM furnace

The BAM furnace is a horizontally oriented tubular electric furnace made of high-temperature-resistant steel (Figure 3.31).

The apparatus consists of the following main components:

- a cylindrical heated chamber (60 mm in diameter, 125 mm in length, with a volume of 0.35 L) closed either by a venting flap or an open outlet to the atmosphere;
- an electric heating element and a thermocouple to measure the internal temperature;
- a disperser for generating a homogeneous dust cloud inside the chamber;
- a fast-response thermocouple connected to a recording system capable of detecting the temperature rise during ignition.

To determine the Minimum Ignition Temperature (MIT) according to ASTM standards, the furnace is typically pre-heated to a maximum temperature of 600 °C and then switched off. As the temperature decreases, dust samples are introduced into the tube at 50 °C intervals. The tube is inserted into the furnace, the dust is dispersed by an air jet, and the presence or absence of a flame at the rear opening is observed. The test starts with an initial dust volume of 1 mL.

To determine the exact MIT, the test is repeated while decreasing the temperature in 10 °C increments until no flame is observed within 5 seconds. Once the temperature at which no ignition occurs is found, the experiment is repeated using three dust loadings (0.5, 1.0, and 2.0 mL). The MIT is then reported as the lowest temperature at which flame ignition is observed for the different loadings.

Before each new test, it is essential to ensure that the chamber is completely clean, as residual burnt dust from previous runs may influence the results. Moreover, the material of construction of the chamber can have catalytic effects on ignition and must therefore be considered when interpreting the results.

Vertical Godbert–Greenwald (G–G) furnace

The Godbert–Greenwald (G–G) furnace consists of a vertical cylindrical electric furnace with an external stainless-steel structure and a hollow ceramic inner tube with a diameter of 365 mm (Figure 3.32).

The internal walls are made of refractory ceramic capable of withstanding temperatures up to 1000 °C. The upper end is connected to a glass observation elbow, which in turn

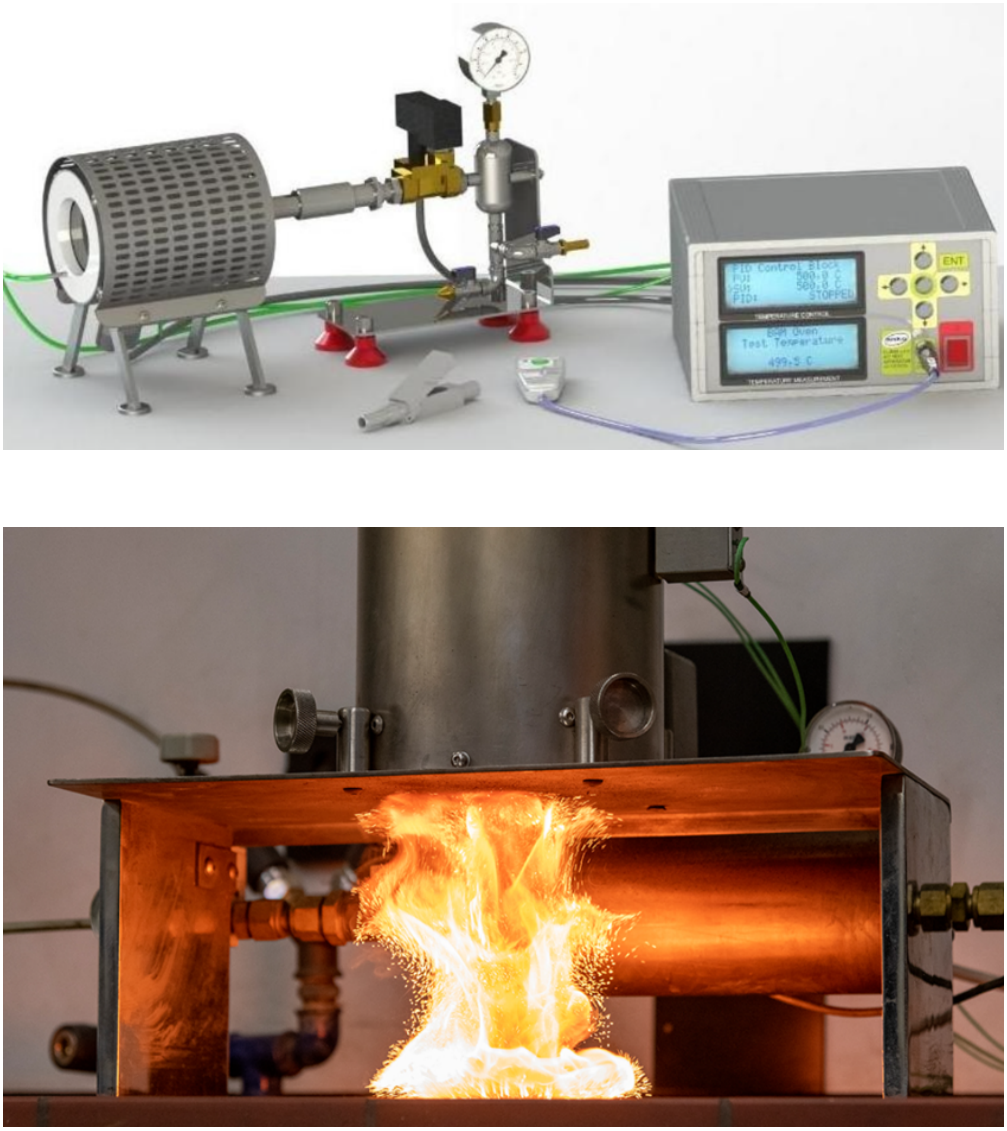

Figure 3.31: Horizontal BAM furnace. Source (top): ANKO-Lab, www.anko-lab.com; (bottom): BAM, www.bam.de.

is linked to the dust loading chamber. The lower end is open, allowing the operator to visually confirm ignition using a mirror plate placed beneath the furnace.

The inner ceramic cylinder includes a spiral groove to accommodate the heating element and two thermocouple ports for internal temperature measurement. The dust is dispersed into the furnace through a compressed-air jet released from a reservoir via a solenoid valve. The jet intensity is regulated by overpressure, monitored with a manometer installed along the supply line.

The procedure for determining the Minimum Ignition Temperature (MIT) is similar to that used for the BAM furnace. The furnace temperature is first set to 500 °C; once stabilized, after 5 minutes, a 0.1 g dust sample is dispersed. If no ignition occurs, the test is repeated at 50 °C increments until ignition is observed, not exceeding 1000 °C. Sparks without flame are not considered ignition.

Once ignition has occurred, the sample mass and dispersion pressure are varied to identify the most vigorous ignition conditions. The MIT is then defined as the lowest furnace temperature at which no ignition occurs in ten consecutive tests, reduced by 20 °C for temperatures above 300 °C, or by 10 °C for temperatures below 300 °C [23].

Figure 3.32: Vertical Godbert–Greenwald (G–G) furnace. Source: Sigma-HSE, "Dust and Powder Testing," `https://sigma-hse.com/testing/dust-powder-testing-`

3.10 Toxicity

The release of toxic substances represents a significant hazard to both the population and the environment in the immediate vicinity of an industrial site. The extent of the resulting damage depends on several factors, including the type and quantity of the released substance, meteorological conditions, and terrain characteristics.

Historically, toxicology has been defined as "the science of poisons." As early as the 1500s, Paracelsus, one of the first scholars in this field, stated:

> All substances are poisonous; there is none which is not a poison. The right dose differentiates a poison from a remedy.

The impact of a toxic substance depends mainly on three factors:

- the intrinsic properties of the substance;
- the duration of exposure;
- the route of exposure (cutaneous, oral, or inhalation).

The toxicity of a substance refers to its ability to cause harm to a living organism and is classified into:

- chronic toxicity, which examines the effects of multiple exposures over a long period of time;
- acute toxicity, which studies the effects resulting from a single exposure or multiple exposures occurring within a short period.

To evaluate acute toxicity, the following indicators are commonly used:

- Lethal Dose (LD_{50}): represents the amount of substance that causes death in 50% of a test animal population within five days following a single administration. Exposure may occur via oral or dermal routes and is expressed in mg/kg of body weight, specifying the animal used for testing.
- Lethal Concentration (LC_{50}): represents the concentration of a toxic substance in air that is lethal to 50% of the test animals after a single exposure lasting five days. Inhalation exposure is expressed in mg/kg of body weight, again specifying the animal used.

In addition to these, other acute toxicity indicators can be used for both atmospheric dispersions and releases in confined environments (3.29). Each of these parameters will be discussed in the following sections.

Table 3.29: Toxicity Indicators.

Toxicity indicators used for atmospheric dispersion	Toxicity indicators used for confined environments
IDLH	TLV – TWA
AEGL	TLV – STEL
ERPG	TLV – C
PAC	

3.10.1 Regulatory Framework

According to Annex E (Table II – Threshold values for incapacitating effects for workers involved in plant control and/or emergency response) of Legislative Decree No. 105/2015, and Annex C (note 1, paragraph A.2.1), which in turn refers to the Ministerial Decree of 9 May 2001, published in the Gazzetta Ufficiale No. 138 of 16 June 2001, the reference parameters for the evaluation of damage areas resulting from the dispersion of toxic gases or vapors are:

- IDLH (Immediately Dangerous to Life or Health). It represents the concentration of a toxic substance below which a healthy individual can be exposed for 30 minutes without suffering irreversible health effects or experiencing symptoms that would prevent escape or protective action.
- LC_{50}. It indicates the concentration of a toxic substance in air that is lethal by inhalation to 50% of exposed individuals within a 30 minute exposure period.

3.10.2 Toxicity Indicators for Atmospheric Dispersion

IDLH

The IDLH (Immediately Dangerous to Life or Health) value, as defined by NIOSH, represents the maximum concentration of a toxic substance to which a healthy individual can be exposed for 30 minutes without suffering irreversible health effects or experiencing symptoms that would prevent escape.

IDLH limits were originally developed to assist in decisions regarding the use of respiratory protective equipment. In particular:

- above the IDLH value, only self-contained breathing apparatus (SCBA) must be used;
- below the IDLH value, air-purifying respirators may be used.

Until 1994, the IDLH definition explicitly included a 30-minute exposure period. However, in the current definition, no specific duration is mentioned: workers should never be exposed to IDLH concentrations without adequate respiratory protection.

The determination of IDLH values follows a standardized procedure based on toxicological data obtained from animal studies, which are then corrected and extrapolated to estimate the effects on humans, assuming a 30 minute exposure. When selecting IDLH limits, two key criteria are considered:

- absence of permanent health damage in exposed workers;
- absence of severe eye or respiratory tract irritation (or other conditions) that could impair escape ability.

IDLH values for more than 380 substances are available in the following databases:
`https://cameochemicals.noaa.gov/`
`https://www.cdc.gov/niosh/idlh/intridl4.html`
Since IDLH limits were developed to protect healthy workers, they may not be adequate for more vulnerable individuals such as the elderly, persons with disabilities, or those with pre-existing medical conditions.

AEGL

The AEGL (Acute Exposure Guideline Levels) were developed by the U.S. Environmental Protection Agency (EPA) and are used by emergency planners and responders as guidance for managing accidental chemical releases. AEGL values represent the airborne concentrations at which most of the general population, including sensitive individuals such as elderly, children, and those with pre-existing health conditions, could begin to experience adverse health effects from exposure to a hazardous chemical for a given period of time. For each exposure duration, a chemical may have up to three AEGL levels, each corresponding to a different severity of health effect (Figure 3.33):

- AEGL-3. The airborne concentration (in ppm or mg/m^3) above which it is predicted that the general population, including susceptible individuals, could experience life-threatening health effects or death.
- AEGL-2. The airborne concentration above which it is predicted that the general population could experience irreversible or long-lasting health effects, or effects that could impair escape capability.
- AEGL-1. The airborne concentration above which it is predicted that the general population could experience notable discomfort, irritation, or other mild and transient effects. These effects are non-disabling and disappear once exposure ceases.

All three AEGL levels (AEGL-1, AEGL-2, AEGL-3) are established for five exposure durations: 10 minutes, 30 minutes, 1 hour, 4 hours, and 8 hours. AEGL values for various chemicals can be found in:
`https://cameochemicals.noaa.gov/`
`http://www.epa.gov/aegl`

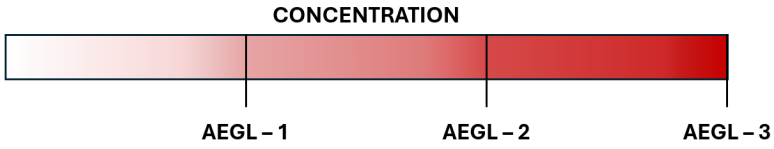

Figure 3.33: Graphical representation of AEGL levels as a function of airborne concentration. As concentration increases, health effects progress from mild and transient (AEGL-1), to serious and long-lasting (AEGL-2), and finally to potentially lethal (AEGL-3) outcomes.

As shown for AEGL-2 in Table 3.30, AEGL values generally vary with exposure duration, since physical effects are typically related to the dose, i.e., the combination of concentration and exposure time. However, in some cases, often for AEGL-1, values remain constant across exposure durations, because this level represents the threshold for non-disabling effects. For example, odor perception depends only on concentration, not on exposure duration.

Table 3.30: AEGL values for acetone.

Exposure period	**AEGL-1**	**AEGL-2**	**AEGL-3**
10 min	200	9,300	16,000
30 min	200	4,900	8,600
60 min	200	3,200	5,700
4 h	200	1,400	2,500
8 h	200	950	1,700

AEGLs are a valuable tool for protecting the public during short-term chemical releases, allowing responders to estimate how the population might react and to delineate risk zones, (i.e., areas where concentrations exceed specific AEGL limits for a given exposure time). For instance, in areas just above AEGL-1, most individuals may experience mild and reversible effects. In areas slightly above AEGL-2, most individuals may experience significant but non-life-threatening health effects.

However, AEGLs should not be used in the following situations:

- for evaluating occupational exposure of workers regularly exposed to chemicals for extended periods; in such cases, occupational exposure limits (OELs) should be applied, as they account for chronic exposure and safety factors.
- For issues concerning ambient air quality, where National Ambient Air Quality Standards (NAAQS) or similar regulatory benchmarks are more appropriate than emergency response guidelines.

ERPG

The ERPG (Emergency Response Planning Guidelines), developed by the American Industrial Hygiene Association (AIHA), provide estimates of airborne chemical concentrations at which most individuals could begin to experience health effects following an exposure duration of one hour.

Sensitive populations (such as elderly, very young, or individuals with pre-existing health conditions) are not included in these guidelines and may experience adverse effects at concentrations below ERPG levels. Up to three ERPG levels can be defined for each chemical, each corresponding to a different degree of health severity. Table 3.31 summarizes the ERPG-1, ERPG-2, and ERPG-3 values for ammonia.

Table 3.31: ERPG values for ammonia.

Chemical	ERPG-1	ERPG-2	ERPG-3
Ammonia	25 ppm	150	750

The three ERPG levels are defined as follows (Figure 3.34):

- ERPG-3. The maximum airborne concentration below which nearly all individuals could be exposed for up to 1 hour without experiencing or developing life-threatening health effects.
- ERPG-2. The maximum airborne concentration below which nearly all individuals could be exposed for up to 1 hour without experiencing or developing irreversible or serious health effects, or symptoms that could impair their ability to take protective action.
- ERPG-1. The maximum airborne concentration below which nearly all individuals could be exposed for up to 1 hour without experiencing more than mild, transient health effects, or without perceiving a clearly unpleasant odor.

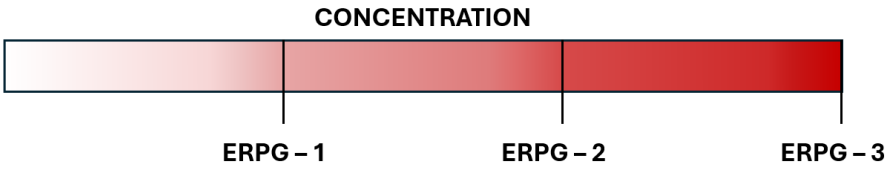

Figure 3.34: ERPG levels as a function of airborne concentration. With increasing concentration, effects progress from mild and transient (ERPG-1), to serious but non-lethal (ERPG-2), to potentially fatal (ERPG-3).

ERPG values are particularly useful for protecting the public in the event of short-term accidental releases, especially when AEGL values are not available. They allow estimation

of how most of the population (excluding sensitive individuals) might respond to a given exposure and can therefore be used to delineate hazard zones. For example:

- in areas with concentrations slightly above ERPG-1, most people may experience temporary, non-disabling effects;
- in areas where concentrations slightly exceed ERPG-2, significant but non-fatal effects may occur.

It is important to note that ERPG values are based on a standard exposure duration of 1 hour. Although real-life exposures may be shorter or longer, the AIHA strongly discourages extrapolating ERPG values to durations different from those for which they were derived. As with AEGLs, ERPG values also have limitations and should not be used as:

- Occupational exposure guidelines for workers regularly exposed to chemicals over long periods. In such cases, OELs should be applied, as they incorporate safety factors specific to chronic exposure.
- Public air quality standards for long-term releases. For air quality issues, NAAQS or equivalent national regulations should be used instead of emergency response guidelines.

Toxicity indicators for worker protection – relevant to Seveso Directive

ERPG and AEGL values are based on short-term exposures and are primarily intended to support industrial safety and emergency response planning in the event of accidental chemical releases. However, other indicators—such as Threshold Limit Values (TLVs)—are used to assess long-term worker exposure, for instance during maintenance or cleaning operations.

It is important to emphasize that the exposure levels discussed above refer to specific durations. In an occupational setting, however, it is crucial to know both: the level at which a chemical may produce immediate effects, and the level below which no adverse effects are expected to occur.

TLV

Threshold Limit Values (TLVs) represent the airborne concentrations of chemical substances to which nearly all workers may be repeatedly exposed, day after day, throughout their working lifetime, without adverse health effects.

There are three types of TLVs:

- TLV–TWA (Time-Weighted Average);
- TLV–STEL (Short-Term Exposure Limit);
- TLV–C (Ceiling Limit).

For most substances, a greater amount of toxicological data is available for TLV–TWA compared to the other two. It is essential that users always consult the most recent ACGIH documentation, as both the quantity and quality of available information for each chemical may vary over time.

It should also be noted that two chemicals with identical TLV values do not necessarily produce the same toxic effects. TLVs do not represent sharp boundaries between "safe" and "unsafe" workplace conditions, nor precise thresholds above which health damage occurs. Therefore, they cannot guarantee protection for all workers. Some individuals may experience adverse or more severe health effects when exposed to a substance at or even below its TLV. This increased sensitivity can result from various factors, including age, sex, genetic predisposition, lifestyle (e.g., diet, smoking, alcohol or drug use), medication use, or pre-existing medical conditions such as asthma or cardiovascular disease.

For estimating the magnitude of toxic substance releases in confined environments, it is preferable to use TLV–STEL and TLV–C values.

TLVs are expressed in different units, including ppm, $\mathrm{mg/m^3}$, or $\mathrm{mg/100\,cm^2}$, depending on the physical state of the substance and the route of exposure.

Conversions between ppm and $\mathrm{mg/m^3}$ can be made using the following equations:

$$\mathrm{TLV_{ppm}} = \frac{\mathrm{TLV_{mg/m^3}} \cdot 24.45}{\text{Molecular Weight (g/mol)}} \tag{3.40}$$

$$\mathrm{TLV_{mg/m^3}} = \frac{\mathrm{TLV_{ppm}} \cdot \text{Molecular Weight (g/mol)}}{24.45} \tag{3.41}$$

where 24.45 represents the molar volume of air (in liters) at 25 °C and 760 Torr (1 atm). Example: Suppose we wish to convert the TLV–TWA for ammonia from 25 ppm to $\mathrm{g/m^3}$:

$$\mathrm{TLV_{mg/m^3}} = \frac{25\,\mathrm{ppm} \cdot 17.03\,(\mathrm{g/mol})}{24.45} = 17.4\,\mathrm{mg/m^3} \tag{3.42}$$

TLV – TWA

The TLV–TWA (Time-Weighted Average) represents the average concentration of a substance for a conventional 8-hour workday and 40-hour workweek, to which nearly all workers may be repeatedly exposed without adverse health effects throughout their working lifetime. Although in certain cases it may be appropriate to calculate the average exposure concentration on a weekly basis rather than daily, ACGIH provides no specific recommendations for this adjustment.

TLV – STEL

The TLV–STEL (Short-Term Exposure Limit) represents the concentration to which workers may be continuously exposed for a short-term period of 15 minutes without suffering from: irritation, chronic or irreversible tissue damage, dose-dependent toxic effects, or narcosis sufficient to increase the likelihood of accidental injury, impair self-rescue ability, or significantly reduce work efficiency.

The TLV–STEL does not guarantee protection if the daily TLV–TWA is exceeded. This value is typically used in addition to the TLV–TWA, especially for substances that have primarily chronic toxic effects but can also produce acute effects. Exposures between the TLV–TWA and TLV–STEL (15-minute TWA) should :last no longer than 15 minutes, occur no more than four times per day, and be separated by at least 60 minutes between successive exposures.

TLV – C

The TLV–C (Ceiling Limit) represents the concentration that must not be exceeded at any time during occupational exposure.

If instantaneous measurements are not available, sampling should be conducted over the shortest feasible time period necessary to identify any exceedances of the limit value. This limit is primarily applied to substances that have immediate irritant or narcotic effects, which can quickly impair a worker's alertness, potentially leading to injury or errors in technical operations.

Final Considerations

Below are some remarks on the use of toxicity indicators that should be taken into account when preparing a Safety Report.

It is essential not to confuse the release duration of a substance or mixture with the exposure time to it. The release duration determines, under otherwise identical source conditions, the total quantity of substance discharged into the environment. Conversely, the exposure time refers to the period during which an exposed individual is in direct contact with a given concentration of the substance or mixture. The concentration of a substance/mixture at a specific location may decrease over time once the release has stopped, particularly for gases or vapours. However, this trend depends on several factors, such as: the relative density of the substance,whether the release occurs in a confined space or open area, whether the source is located in underground rooms or basements, and the meteorological conditions at the time of release.

If no IDLH value is available for a given substance, other toxicological indicators may be used, such as AEGL, ERPG, or TLV–STEL. However, these values must not be adjusted for exposure durations other than those for which they were originally derived.

When a substance or mixture is released into the environment in the form of a gas, vapour, or aerosol and exhibits irritant or corrosive properties to the skin and eyes, or sensitising effects on the respiratory system or via dermal contact, and shows toxicity by inhalation as well as by dermal or ocular exposure, such effects must be explicitly considered in the risk assessment.

Chapter 4

Hazard Identification

The identification of hazards and potential accident scenarios represents one of the most critical stages in the risk assessment process. The main techniques commonly adopted for hazard identification include (Table 4.1):

- Index-based methods;
- Historical analysis;
- Checklists;
- What-if analysis;
- FMEA (Failure Modes and Effects Analysis);
- HAZOP (Hazard and Operability Study);
- ROA (Recursive Operability Analysis).

The selection of the most appropriate methodology depends on several factors, including:

- the type of process under consideration;
- the size and complexity of the installation;
- the level of available knowledge about the system;
- the objectives of the analysis.

There is no single methodology that can be universally applied to all situations, and the adoption of one technique does not preclude the use of others. On the contrary, the most effective approach is often based on a combination of multiple methods, each providing complementary insights into process hazards and potential failure scenarios.

Table 4.1: Overview of hazard identification techniques.

Method	Advantages	Disadvantages	When to apply*
Index-based method	Identifies critical areas in complex installations.	Not exhaustive; Requires integration with other techniques.	A, E.
Historical analysis	Enhances corporate knowledge and learning from past events.	Not exhaustive; Accident databases often lack detailed descriptions of incident dynamics.	A, B, C, D, E, F, G, H.
Checklist	Easy to use; Applicable at any stage of the plant lifecycle; Incorporates historical analysis.	The list of questions may not always be applicable to the specific case; Cannot predict unusual or unexpected hazards; Identifies hazards but not scenarios.	A, B, C, D, E, F, G, H.
What-if analysis	Simple to apply; Suitable for any stage of the plant lifecycle; Applicable to a wide variety of situations; Useful for reviews following process modifications.	Lacks a structured framework; The quality of results depends on the experience and expertise of the assessment team.	A, B, C, D, E, F, G, H.
FMEA	Useful for analysing complex equipment (e.g. compressors).	Time-consuming; Cannot be used as a standalone technique for hazard identification in chemical plants.	B, C, D, E, F, G, H.
HAZOP	Highly structured technique; Provides a detailed understanding of potential deviations from standard operating conditions.	Time and cost intensive; The quality of results depends on the preparation and experience of the team; Not suitable for identifying scenarios related to mechanical failures or external events (e.g. collisions).	A, B, C, D, E, F, G, H.
ROA	Well suited for process plants; Less time-consuming than HAZOP; Facilitates fault tree construction.	The quality of results depends on the competence of the analysis team; Limited use and recognition in academic settings.	A, C, D, E, F, G, H.

** Letters correspond to Seveso establishment categories (Table 2.1).*

4.1 Index-based method

The index-based method is particularly useful for conducting a preliminary analysis in complex industrial facilities. At the international level, the most widely recognized methods are:

- F&EI (Fire and Explosion Index), developed by Dow Chemical Company;
- Mond Index, developed by Imperial Chemical Industries (ICI).

In Italy, the regulatory references defining the index-based approach depend on the type of plant, namely:

- DPCM 31 March 1989 – Annex II: "Preliminary analysis for the identification of critical areas within industrial activities";
- Ministerial Decree of 15 May 1996: "Criteria for the analysis and evaluation of Safety Reports related to LPG storage facilities";
- Ministerial Decree of 20 October 1998: "Criteria for the analysis and evaluation of Safety Reports related to liquid storage facilities", applicable to flammable and/or toxic liquid storage sites.

The application of the index-based method involves the following steps:

- Subdivision of the establishment into units. A unit is defined as a section of the plant that can be logically characterized as a physically separate or potentially separable entity from adjacent units. Each unit is distinguished by its process type, the substances involved, and their operating conditions. For each unit, the corresponding risk indices are evaluated.
- Selection of the predominant substance. The predominant substance is defined as the compound or mixture present in the unit that, due to its intrinsic properties and inventory, provides the highest potential for energy release in the event of combustion, explosion, or exothermic reaction. It may be a reactant, intermediate, product, solvent, or catalyst.
- Evaluation of the substance factor (B). This factor represents a numerical value assigned to a substance or mixture that accounts for its flammability (Nf) and reactivity (Nr) characteristics.
- Calculation of penalty factors, which consider risks arising from different aspects of the process within the unit under assessment. The penalty factors include:
  - M: specific hazards of the substances;
  - P: general process hazards;
  - S: special process hazards;

  - Q: hazards associated with quantities;
  - L: layout-related hazards;
  - s: health risks in case of an accident.

- Calculation of intrinsic risk indices. Once the substance factor and penalty factors have been determined, the intrinsic risk indices are calculated, that is, values obtained before considering any prevention or protection measures. The intrinsic indices are (Table 4.2):

  - F: Fire Load Index;
  - C: Confined Explosion Index;
  - A: Air Explosion Index;
  - T: Toxic Risk Index;
  - G: General Risk Index.

Table 4.2: Estimation of intrinsic risk indices [24].

Index	**Symbol**	**Formula**
Equivalent Dow	D	$D = B\left(1+\frac{M}{100}\right)\left(1+\frac{P}{100}\right)\left[1+\frac{S+Q+L+S}{100}\right]$
Fire Load	F	$F = D \cdot \frac{K}{N}$
Confined Explosion	C	$C = 1+\frac{M+P+S}{100}$
Air Explosion	A	$A = B(1+\frac{M}{100})(1+P)(Q \cdot H \cdot \frac{C}{1000})(\frac{T+273}{300})$
Toxic Risk	T	$T = (PCF' + PT + PET)\,BC\,(PED + DA \cdot PE)\,\frac{100}{976.5}$
General Risk	G	$G = D[1+0.2\,C\,(A \cdot F)^{1/2}]$

K = total quantity of substance [ton]

N = standard working area of the process unit [m^2]

PCF′ = coefficients related to chemical-physical properties relevant to toxicity

PT = coefficients related to toxicological properties

PET = coefficients related to ecotoxicological properties

BC = bioconcentration coefficient

PED = coefficient for multiple direct exposure

DA = coefficient for environmental dispersion

PE = persistence coefficient

- Calculation of compensating factors. These factors account for the existing prevention and protection measures, at technical, organizational, and management levels.

The compensating factors are:

  - K_1: containment;
  - K_2: process control;
  - K_3: safety culture and attitude;
  - K_4: fire protection;
  - K_5: elimination or substitution of substances;
  - K_6: emergency response support.

- Calculation of compensated risk indices. These indices include the positive effects of compensating measures (except for index D, for which no compensation is applied). The corresponding formulas are reported in Table 4.3.

Table 4.3: Calculation of compensated risk indices [24].

Compensated Index	**Symbol**	**Formula**
Fire Load	F'	$F' = F \cdot K_1 \cdot K_3 \cdot K_5 \cdot K_6$
Confined Explosion	C'	$C' = C \cdot K_2 \cdot K_3$
Air Explosion	A'	$A' = A \cdot K_1 \cdot K_2 \cdot K_3 \cdot K_5$
Toxic Risk	T'	$T' = T \cdot K_1 \cdot K_2 \cdot K_3 \cdot K_4 \cdot K_5 \cdot K_6$
General Risk	G'	$G' = G \cdot K_1 \cdot K_2 \cdot K_3 \cdot K_4 \cdot K_5 \cdot K_6$

- Categorization of logical units. The calculated indices are compared with the reference qualitative/quantitative evaluation table (Table 4.4) [24].

Based on the analysis results, it is possible to identify the logical units presenting the highest risk levels. In general, the following considerations apply:

- according to DPCM 31 March 1989, for logical units with a General Risk Index (G or G′) classified as High or above, one or more accident scenarios should be developed;

- according to DM 15 May 1996 and DM 20 October 1998, for logical units with a moderate or higher General Risk Index, one or more accident scenarios should also be developed.

Where the index-based method can be applied, it is necessary to explicitly report all values assigned to the considered parameters, the criteria and justification for assigning those values, and the calculation formulas used.

Table 4.4: Risk level of a unit as a function of calculated risk indices [24].

Risk level	**Risk index**				
	G/G'	F/F'	A/A'	C/C'	T/T'
Low	0-20	0-2	0-10	0-1.5	0-5
Minor	20-100	2-5	10-30	1.5-2.5	5-10
Moderate	100-500	5-10	30-100	2.5-4	10-15
High (grade I)	500-1100	10-20	100-400	4-6	15-20
High (grade II)	1100-2500	20-50	-	-	-
Very High	2500-12500	50-100	400-1700	>6	> 20
Severe	12500-65000	100-2500	>1700	-	-
Extremely Severe	>6500	>250	-	-	-

4.2 Historical Analysis

Historical analysis consists in the collection and examination of all undesired events that have occurred in the past in plants similar to the one under study, with the aim of predicting potential future events. This analysis should not be considered an alternative to other hazard identification techniques, but rather a complementary tool that enhances their effectiveness. The incident experience to be considered may derive from:

- International and globally recognized accident databases, such as:
  - MARS (Major Accident Reporting System);
  - ARIA (Analisi, Ricerca e Informazioni sugli Incidenti);
  - FACTS (Failure & Accident Technical Information System);
  - MHIDAS (Major Hazard Incident Data Service);
  - SONATA (Summary of Notable Accidents in Technical Activities).
- The plant's own operational experience, including incidents or near misses that have occurred within the establishment over the last ten years.

Historical analysis makes it possible to statistically organise and extract information such as:

- causes that can lead to an accidental situation;
- factors that may aggravate it;
- potential consequences;
- availability and effectiveness of mitigation and containment measures.

Data obtained must be evaluated with great caution, since the final outcome depends on the reliability, completeness, and level of detail of the available information. Among all hazard identification techniques, historical analysis is the only one that provides useful input for the subsequent consequence analysis phase.

When performing a historical analysis, it is essential to consider both the operational and managerial experience of the company. The databases used must be relevant to the specific type of installation being analyzed and to the substances or mixtures involved.

4.3 Checklist Analysis

The Checklist analysis method involves the use of a detailed list of questions related to the design and operation of equipment or specific sections of a plant. The answers to these questions are usually expressed as "yes", "no", "not applicable", or "further information required". The level of detail can vary considerably depending on the process under analysis.

The questions are generally grouped into categories such as: accident causes, process equipment, human errors, external events, plant functions, alarms, construction materials, control systems, documentation, training, instrumentation, piping, pumps, vessels, etc.

This is a versatile and easy-to-use methodology that can be applied at any stage of a process's life cycle, both during the design phase, to identify design-related risks, and prior to plant start-up. In situations where experienced personnel are not available, the use of checklists represents a valuable tool for identifying potential hazards. However, checklist analysis has also several limitations:

- it does not allow for the identification of new or unexpected hazards, due to its schematic approach based on existing systems;
- the results strongly depend on the competence and experience of the person completing the checklist;
- when using checklists taken from manuals or general references, many items may not be applicable to the specific process or system under consideration;
- it highlights the existence of hazards, but does not identify the possible accident scenarios associated with them.

To improve its effectiveness, checklist analysis is often combined with other hazard identification methods, such as the "What-If" analysis or the HAZOP study, which allow a deeper and more systematic examination of process deviations and potential failure scenarios [25].

4.4 What – If Analysis

The What-If analysis is a creative, brainstorming-based technique that can be applied to processes, systems, or operations. It is conducted by a multidisciplinary team of

experienced personnel capable of posing questions (or expressing concerns) about potential equipment malfunctions or undesired events.

Unlike other structured methodologies, such as HAZOP or FMEA (described in the following sections), the What-If technique is less formal and less structured, and its outcome largely depends on the competence and experience of the participants.

The What-If analysis encourages the team to formulate questions beginning with "What would happen if…", for example: "What would happen if the seal of pump X started leaking?" ora "What would happen if valve Y failed to open?"

Through a systematic series of such questions, the team identifies possible accidental events, their potential consequences, the existing safety barriers, and proposes additional measures to reduce the associated risks. The events identified are not classified or quantified in terms of probability or consequence magnitude.

The information required for a What-If analysis includes detailed process descriptions, operating parameters, up-to-date P&IDs and plant layouts reflecting the actual configuration, operating and maintenance procedures.

The main steps of the What-If analysis are:

- division of the system into nodes;
- formulation of deviations or failures by asking the question "What if…?";
- evaluation of each "What-If" question in terms of:
  - expected consequences;
  - existing preventive or protective measures that could prevent the event or mitigate its effects;
  - potential accident scenario (expected damages);
  - additional descriptive information, actions, or recommendations.
- Review and organization of results. The outcomes of the analysis are typically summarized in a tabular format, listing each identified hazardous situation, its consequences, current safeguards, and possible recommendations (Table 4.5) [26].

Table 4.5: Typical format of a What-If worksheet.

LINE/VESSEL		**DATE / /**		
WHAT-IF	**CAUSE**	**CONSEQUENCE**	**EXISTING PROTECTIONS**	**RECOMMENDED ACTIONS / COMMENTS**
The pump P-101 leaks HCl?	Seal wear; corrosion	Release of corrosive substance. Personnel exposure hazard	Containment basin; automatic shut-off valves	Install pH sensors in the containment basin

4.5 FMEA

The Failure Mode and Effects Analysis (FMEA) is a systematic procedure used to identify potential failure modes of system components and determine their possible effects on the system's overall performance. The objective is to identify all elements for which it may be necessary to modify design, operating strategies, or inspection and maintenance activities to reduce the severity of the effects resulting from the failure.

There are two main approaches to perform a FMEA: the functional approach and the hardware approach. The term "functional" or "hardware" refers to the way in which system components are classified in the FMEA worksheet, either according to their function within the system or their physical (hardware) nature.

The functional FMEA is generally used for complex systems. It follows a top-down approach, where the system is broken down into subsystems and equipment depending on the information available and the scope of the analysis. Subsystems or equipment are treated as "black boxes" capable of providing information about the system functionality, and the analysis evaluates the impact of each failure on the overall system performance.

The hardware FMEA follows a bottom-up approach, in which each system component is examined individually for each of its physical failure modes to determine its potential effect on the system.

For both functional and hardware FMEA, the analysis can be extended to include failure rates or semi-quantitative estimates of the probability and severity of consequences. When this is done, the method becomes FMECA (Failure Mode, Effects and Criticality Analysis).

FMEA typically consists of three main stages:

- definition of the process;
- execution of the analysis;
- documentation of results.

The process definition and documentation can be performed by a single person, while the analysis itself should be conducted by a multidisciplinary team. During the process definition phase, equipment and instrumentation to be included in the study are identified, along with their operating conditions. The level of detail is determined by the objectives of the analysis (from subsystem level to system level) with a preference for analyzing major components to balance time requirements with the usefulness of the results. Typical steps of a FMEA procedure (Figure 4.1):

- define the system and reliability performance requirements;
- build a block diagram showing interconnections among subsystems and components;
- record assumptions made in defining system and subsystem failure modes;
- prepare a component list and identify failure modes for each component;

- complete the FMEA worksheet (Table 4.6), analyzing the effects of each failure mode on system performance;
- list failure effects for each subsystem or component.
- identify existing protective measures or controls that can prevent or mitigate the failure effects;
- Propose corrective actions (if needed) to prevent or reduce the likelihood of failure [26].

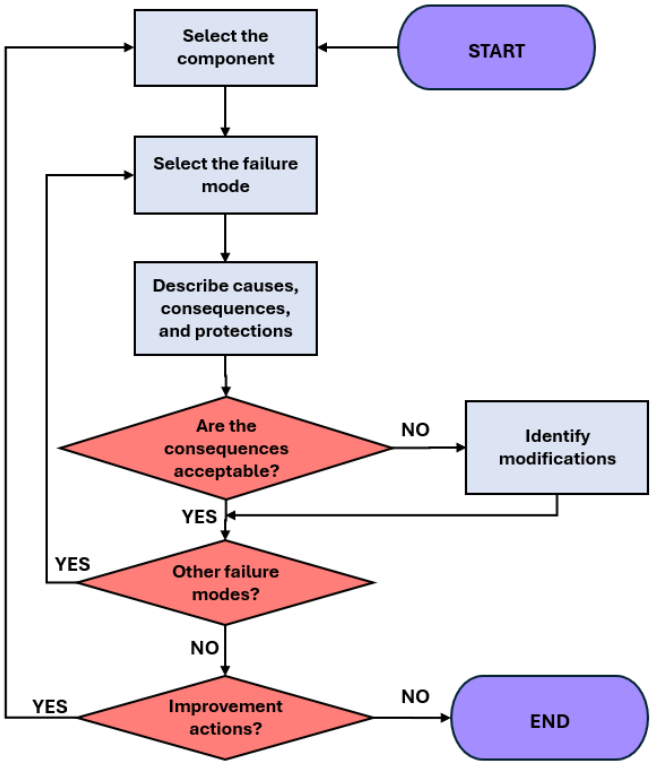

Figure 4.1: Main steps of the FMEA process.

Each component is uniquely identified by a code indicating its type and location within the plant. The second column describes the function of the component within the system. For each element, possible failure modes and their main causes are identified. The worst-case consequence is then evaluated assuming all protective systems fail, allowing assessment of the true criticality of the component. The Protections column lists alarms, manual and automatic safeguards. If operator intervention is required, the analysis must describe the safety conditions under which the operator would act. Where possible, a failure probability for each protective measure should be indicated, or at least a subjective

estimate. The Recommended Actions column includes suggestions for improving plant safety, enhancing protective systems, or revising operational and emergency procedures.

Finally, the Severity Class column categorizes the consequence severity according to the MIL-STD-1629A standard [25]:

- Category I – Catastrophic: may cause death or total system loss.
- Category II – Critical: may cause severe injury or major damage to the system or plant.
- Category III – Marginal: may cause minor injury or limited system damage.
- Category IV – Minor: not serious enough to cause injury or system damage.

The FMEA method presents some limitations that should be taken into account when interpreting the results of the analysis:

- it does not explicitly account for human errors, as these are typically treated as a component failure mode;
- it does not consider multiple simultaneous failures, since each failure is analyzed as an independent event.

Table 4.6: Typical FMEA worksheet format.

DATE / /							**PAGE**	
PLANT							**SYSTEM**	
ITEM							**REFERENCE**	
ID	**Component Function**	**Failure Mode**	**Causes**	**Consequences**	**Protections**		**Severity Class**	**Notes**
					Manual	**Automatic**		
1.0	Valve RV-10 – Process fluid transfer	Leakage from pump	Seal wear; corrosion	Flammable fluid release; jet fire hazard	Firewater hose line; operator isolation	Automatic shut-off valves; containment basin	II	Check for ignition sources nearby

4.6 HazOp

The Hazard and Operability Study (HAZOP) is a structured and systematic technique developed to identify potential hazards in process plants and to detect operability problems that, although not necessarily critical, could compromise plant productivity. The underlying concept of HAZOP studies is that processes perform well when operating under design conditions; however, deviations from these conditions can lead to operability problems or accidents.

It is one of the most widely used methodologies for process risk analysis and can be applied at virtually any stage of a plant's lifecycle. It has become so common that any detailed process risk review is often colloquially referred to as a "HAZOP."

Before initiating a HAZOP study, detailed process information must be collected, including process flow diagrams (PFDs), updated P&IDs, technical data sheets, operating and maintenance procedures, emergency procedures, construction materials, and mass and energy balances.

A thorough understanding of the process, instrumentation, and operating conditions is essential. The HAZOP team typically includes members with diverse technical backgrounds, such as design, engineering, operations, and maintenance.

A typical HAZOP team consists of:

- A team leader (facilitator): guides the discussion, ensures participation from all members, and keeps the analysis on track. The leader should have experience with HAZOP studies but does not necessarily need to be an expert on the specific process.
- A secretary (scribe): responsible for accurately recording the results of the discussions; should have strong listening skills and a technical background.
- Other team members: such as process engineers, operators, instrument technicians, and electricians.

The HAZOP method uses guide words to assist the analysis team in identifying possible causes and consequences of process deviations (Table 4.7). These guide words are applied to specific process parameters (Table 4.8) to identify potential deviations from the design intent (Table 4.9).

Table 4.7: Examples of HAZOP guide words.

Guide Words	
No	More (High)
Less (Low)	Part of
Before / After	Early / Late
Partial	Faster / Slower
Reverse / Opposite	Instead of (Substitution)

Table 4.8: Examples of process parameters.

Process Parameter		
Flow	Agitation	Pressure
Pressure	Reaction	Flow
Temperature	pH	Sequence
Level	Viscosity	Time
Composition	Phase	Mixing
Separation	Start/Stop	

Table 4.9: Examples of guide word and parameter combinations.

Process Parameter	**Deviation**	**Process Parameter**	**Deviation**
Flow	None, High, Low, Reverse	Pressure	High, Low
Temperature	High, Low	pH	High, Low
Level	High / Overflow, Low / Empty	Viscosity	High, Low
Mixing	Excessive, Insufficient, No, Reverse	Reaction	None, Slow, Fast, Excessive

The analysis consists of the following steps (Figure 4.2):

- Divide the plant system into nodes. The node selection is arbitrary and depends on team experience. A node can represent a single equipment item (e.g., a reactor) or several interconnected units (e.g., reactor, recirculation system, and pump).
- Select the node to be analyzed.
- Define the design intent of the node. For example, "The tank V-101 is designed to store caustic soda and deliver it to the reactor upon request".
- Choose a process parameter (e.g., flow, level, temperature, pressure, concentration, pH, viscosity, phase, agitation, reaction rate, etc.).
- Apply a guide word to the process parameter to suggest possible deviations.
- If a deviation is applicable, determine possible causes and note any existing protection systems.
- Evaluate the potential consequences of the deviation.
- Recommend corrective or preventive actions (what, by whom, and by when).
- Record all results in a dedicated worksheet (Table 4.10) [26, 27].

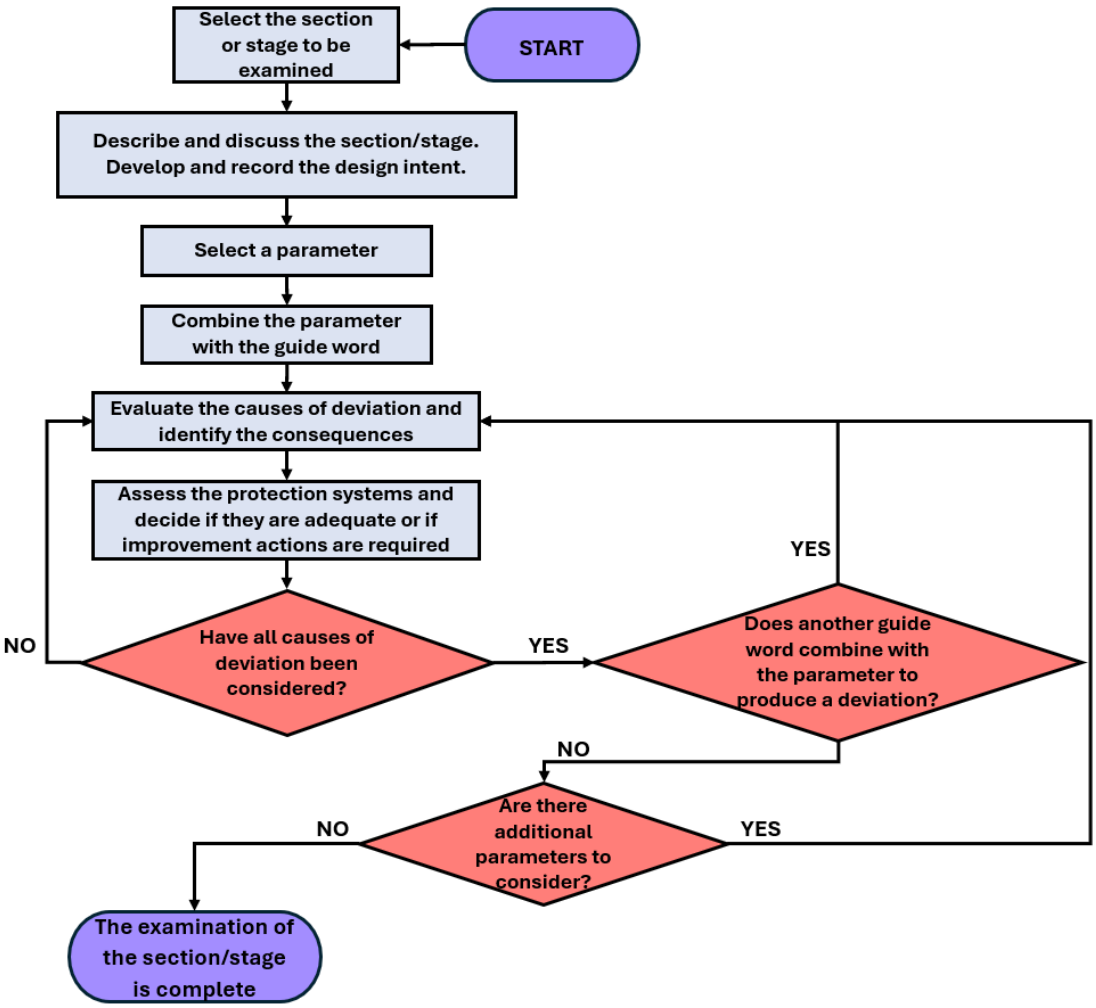

Figure 4.2: Flowchart for the HAZOP analysis.

Table 4.10: Typical HAZOP worksheet format.

LINE/VESSEL				**DATE / /**			
Guide Word	**Deviation**	**Possible Causes**	**Consequences**	**Protection Systems**	**Interventions**	**Actions / Notes**	**Top Event**
More	Tank level	Operator error OR malfunction of level transmitter (LT-10)	Tank overpressure	High and high-high level alarms on LT-10	Operator intervention on alarm	–	–

4.7 ROA

The Recursive Operability Analysis (ROA), also known by its Italian acronym AOR (Analisi di Operabilità Ricorsiva), was developed in the 1980s by the engineering company Snamprogetti – SAIPEM for application in chemical and petrochemical plant design.

One of the main limitations of the HAZOP analysis lies in the difficulty of systematically deriving explicit cause–consequence relationships, especially when the analyst responsible for constructing the fault trees (FTA) was not part of the original HAZOP team. Indeed, the HAZOP worksheet format was designed primarily to identify potential hazardous deviations (hazards) and to verify or improve operating procedures, rather than to structure information for the logical modelling of failures.

The ROA methodology was developed precisely to overcome this limitation. It employs a worksheet format that makes the relationships between process variable deviations, their causes, and consequences more explicit, while also highlighting the logical links with protective systems, both automatic and manual. This structure facilitates the systematic and traceable construction of fault trees, improving consistency between operability studies and quantitative risk assessment.

A typical worksheet used in the ROA is shown in Table 4.11.

The first column, called NDV (Node – Deviation – Variable), collects the same information contained in the first three columns of a HAZOP worksheet. The information concerning protective systems is, however, more detailed and is divided into: Optical/acoustic alarms, capable of triggering the operator's intervention; Automatic protection systems, designed to act without human intervention.

The last column includes a progressive numbering of the Top Events, i.e. the events whose consequences are deemed significant enough by the team to require probabilistic quantification for risk estimation purposes.

The ROA approach was therefore conceived to simplify and systematize the construction of fault trees. Although it already contains all the necessary information to build complete fault trees, experience has shown the usefulness of first deriving a graphical representation of the relationships among process variables, known as the Incident Sequence Diagram (ISD).

This diagram is submitted to the original HAZOP team to verify the completeness and accuracy of the data recorded in the ROA worksheets before proceeding with the fault tree construction and subsequent analysis.

Nevertheless, despite its methodological advantages, the ROA has found limited industrial application and has not achieved the same level of standardization and dissemination as the HAZOP technique, remaining mostly confined to academic or research contexts.

Table 4.11: Typical worksheet format for conducting a ROA.

NDV	**Cause**	**Consequences due to protection system failure**	**Protective systems**		**Note**	**Top Event**
			Optical / acoustic alarm	**Automatic protection systems**		

Chapter 5

Estimation of Expected Frequency

Once the potential hazards have been identified using one of the techniques described in Chapter 4, the next step in the risk analysis process is the estimation of risk, which, as previously discussed, is defined as the product of the likelihood (or frequency) of occurrence of an accidental event and the magnitude of its consequences.

This chapter illustrates the methodologies used to evaluate the probability or frequency of occurrence of hazardous events, while the following chapters will focus on the assessment of consequences, such as toxic releases, fires, or explosions.

When referring to the expected frequency of an accidental event, it may be expressed either in terms of frequency or probability.

The frequency represents the number of times an event occurs within a specified time period, usually one year. For instance, if an event occurs on average once every 100 years, its frequency will be equal to 0.01 per year.

The probability, on the other hand, is a dimensionless quantity. For example, if an operator is required to perform a task 100 times over a given period and fails 5 times while performing it correctly 95 times, the probability of failure is 0.05. As can be easily understood, the rarer the event, the smaller its probability of occurrence within a given time frame.

In this chapter, a brief introduction will also be given to the basic principles of reliability theory, which underpins the estimation of the probability of failure of systems and components. The most widely used techniques for estimating the expected frequency of accidental events are:

- Fault Tree Analysis (FTA);
- Event Tree Analysis (ETA).

5.1 Overview of Reliability Theory

The objective of this section is to describe the methods that can be used to predict the performance of a component, a system, or a subsystem. Even when components are carefully designed and manufactured, failures are inevitable over time.

The most useful probabilistic parameters for describing system performance over time are availability/unavailability and reliability.

Throughout this chapter, the terms component, system, and subsystem will often be used interchangeably, as the difference among them is primarily a matter of scale. In this section, some basic definitions are introduced, starting from the concept of reliability and availability/unavailability of a component or system.

System components can be classified into three categories:

- Non-repairable components: these are components that, once failed, cannot be restored without being replaced; in other words, the transition from the operating state to the failed state is irreversible. Examples include chemical reactors, storage tanks, and similar equipment.

- Repairable components with self-revealing failures: these components are equipped with internal self-diagnostic systems capable of detecting and signaling a fault to the user, allowing timely repair. Typical examples include measuring instruments (e.g., temperature or pressure sensors).

- Repairable components with non-self-revealing failures: these components lack internal diagnostic systems, and their failures remain latent over time, at least until the component is called upon to perform its intended function. Examples include pumps and similar devices.

From an operational point of view, the lifetime of a repairable component consists of alternating phases between operating and failed states, repeating throughout its service life (see Figure 5.1). A performance indicator for non-repairable components is reliability, whereas for repairable components the relevant measure is availability, or its complement, unavailability.

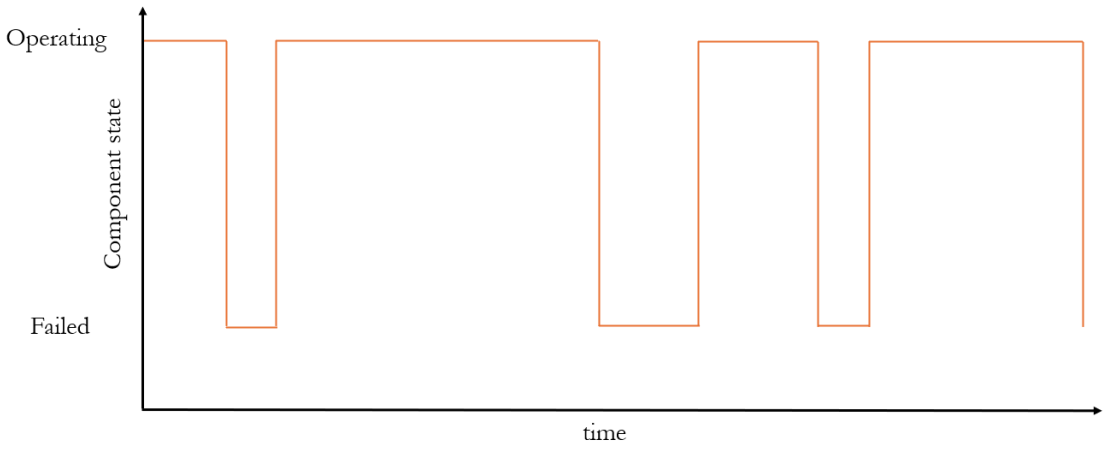

Figure 5.1: Example of the life history of a repairable component.

An important aspect of risk quantification is identifying the most appropriate reliability characteristic to be evaluated. Depending on the system under study, it may be necessary to calculate:

- Probability of failure on demand (PFD): used for protective or standby systems (e.g., rupture disks, safety valves, emergency generators). These are typically passive components whose failures are discovered either during inspection or when the component is required to operate ("on demand").
- Reliability or unreliability: used for systems that must perform an active function over a specific period of time, known as the mission time, without experiencing any failure.
- Unavailability and expected number of failures (within a given time interval): used for evaluating reliability in systems operating in continuous mode [28, 29].

5.1.1 Expressions of Reliability and Failure Rate for Non-Repairable Components

Reliability

According to the EN 13306 standard, reliability is defined as:

> *The ability of an item to perform a required function under given conditions for a stated period of time.*

Reliability, denoted as R(t), represents the probability that a component, equipment, or system will operate for a specified period of time or at a given instant under stated environmental and operational conditions without experiencing failure. It is not a deterministic quantity that can be directly derived through fixed mathematical equations, but rather a random variable that can be evaluated through probabilistic and statistical methods, assuming values between 0 and 1.

Reliability R(t) can be expressed as [29]:

$$R(t) = \frac{1 - n_f(t)}{n_0} = \frac{n_v}{n_0} \tag{5.1}$$

where

R(t)	reliability as a function of time t [–];
$n_f(t)$	number of failed components at time t;
n_v	number of operating components at time t;
n_0	total number of identical components in operation at time $t = 0$;
t	time.

It follows that:

$$n_0 = n_f + n_v \tag{5.2}$$

Unreliability or Cumulative Failure Distribution

The cumulative failure distribution, also referred to as unreliability or failure probability, and denoted as F(t), expresses the probability that a component or system which was operating at time zero is in a failed state at time t. Being a probability, it is a dimensionless quantity, and its values range between 0 and 1.

$$F(t) = \frac{n_f(t)}{n_0} = \frac{n_0 - n_v}{n_0} = 1 - R(t) \tag{5.3}$$

where

$F(t)$ cumulative failure distribution as a function of time.

Reliability is therefore the complement to 1 of the failure probability, as illustrated in Figure 5.2, which shows the typical trends of R(t)and F(t)as functions of operating time [29].

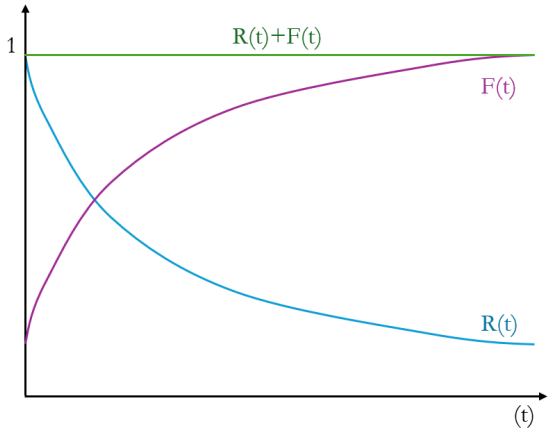

Figure 5.2: Trend of reliability and unreliability functions over operating time.

Failure Density

By differentiating the cumulative failure distribution with respect to time, the failure density function f(t), also known as mortality, is obtained:

$$f(t) = \frac{dF(t)}{dt} \tag{5.4}$$

Dimensionally, $f(t)$ is expressed as the inverse of time, and it applies to all components, whether failed or still operating. The product $f(t)\ dt$ represents the probability that the component under consideration fails within the time interval between t and $t + dt$,

assuming it was operating at $t = 0$. The reliability and failure probability can be expressed in terms of the failure density function as follows:

$$F(t) = \int_0^t f(t)\, dt \tag{5.5}$$

$$R(t) = 1 - \int_0^t f(t)\, dt = \int_t^\infty f(t)\, dt \tag{5.6}$$

Failure Rate

A concept frequently encountered in risk analysis is the conditional failure rate, also known as the failure rate or hazard rate, denoted by $\lambda(t)$. The failure rate is defined as the probability that a component fails within the time interval between t and $t + dt$, given that it was operating just before time t. Dimensionally, it represents the fraction of failures per unit time, and it can assume values between:

- 0, when no failures occur within the time interval $[t]$ and $[t, t + dt]$;
- ∞, when all components fail simultaneously.

The failure rate can be expressed as the ratio between the number of components failing in the unit time and the number of components exposed to failure [29]:

$$\lambda(t) = \frac{n_f(t + \Delta t) - n_f(t)}{n_v(t) \cdot \Delta t} = \frac{f(t)}{R(t)} = \frac{f(t)}{1 - F(t)} \tag{5.7}$$

Integrating both sides of Equation 5.7 yields the general expressions of unreliability, reliability, and failure density as functions of the failure rate:

$$F(t) = 1 - e^{-\int_0^t \lambda(t)\, dt} \tag{5.8}$$

$$R(t) = e^{-\int_0^t \lambda(t)\, dt} \tag{5.9}$$

$$f(t) = \lambda(t)\, R(t) = \lambda(t) - e^{-\int_0^t \lambda(t)\, dt} \tag{5.10}$$

The value of $\lambda(t)$ can be obtained either through statistical evaluation or from data provided by manufacturers or reliability handbooks. The failure rate describes how the likelihood of failure evolves during the component lifecycle and can be represented graphically by the well-known "bathtub curve", shown in Figure 5.3. Under identical operating and environmental conditions, similar components experience different types of failures throughout their useful life, which can be classified as follows:

- Infant failures;
- Random failures;
- Wear-out failures.

Infant failures are typical of the early life of a component and are mainly due to design, installation, or manufacturing defects. Since these are caused by intrinsic weaknesses, their probability tends to decrease over time during the initial "burn-in" period.

Random failures may occur at any point in the component's life and their probability of occurrence is independent of time. Unlike infant failures, which can be reduced through post-production quality control, random failures cannot be completely eliminated.

Wear-out failures occur during the final phase of the component's life and are caused by aging, corrosion, creep, or fatigue. Their probability increases over time, although they can be mitigated through appropriate maintenance strategies. Random failures typically overlap with infant failures during the early life of the component and with wear-out failures during the final phase of its lifecycle.

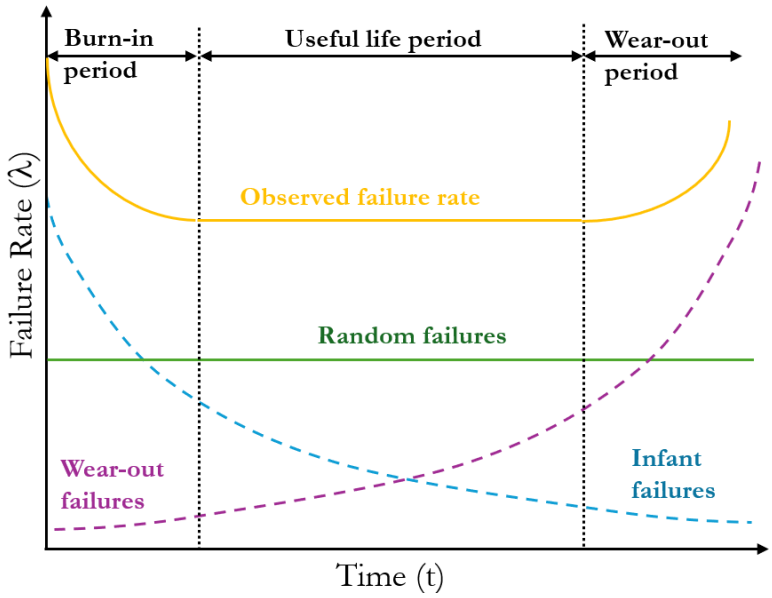

Figure 5.3: Typical "bathtub curve" showing the trend of failure rate over time.

Mean Time To Failure (MTTF)

The Mean Time To Failure (MTTF) represents the average time between time zero, when the component is operating, and the instant when a failure occurs. It is expressed in hours, or more commonly, in years. The MTTF can be calculated using the following equation [29]:

$$MTTF = \int_0^\infty t\, f(t) = \int_0^\infty t\, \frac{dF(t)}{dt}\, dt = -\int_0^\infty t\, \frac{dR(t)}{dt}\, dt = \int_0^\infty R\, dt \qquad (5.11)$$

This parameter is used to describe the reliability of non-repairable components manufactured in series, such as bearings, transistors, and similar devices.For identical types

of equipment, the one with the higher MTTF is considered to have greater reliability. Table 5.1 summarizes the relationships among the reliability functions $R(t)$, $F(t)$, $f(t)$, and $\lambda(t)$ derived in the previous sections.

Table 5.1: Relationships among the functions $R(t)$, $F(t)$, $f(t)$, and $\lambda(t)$.

Function	$\boldsymbol{R(t)}$	$\boldsymbol{F(t)}$	$\boldsymbol{f(t)}$	$\boldsymbol{\lambda(t)}$
$R(t)$	–	$F(t) = 1 - R(t)$	$\int_t^\infty f(t)\,\mathrm{d}t$	$e^{-\int_0^t \lambda(t)\,\mathrm{d}t}$
$F(t)$	$R(t) = 1 - F(t)$	–	$\int_0^t f(t)\,\mathrm{d}t$	$1 - e^{-\int_0^t \lambda(t)\,\mathrm{d}t}$
$f(t)$	$-\dfrac{\mathrm{d}R(t)}{\mathrm{d}t}$	$\dfrac{\mathrm{d}F(t)}{\mathrm{d}t}$	–	$\lambda(t)\, e^{-\int_0^t \lambda(t)\,\mathrm{d}t}$
$\lambda(t)$	$-\dfrac{\mathrm{d}}{\mathrm{d}t}\ln R(t)$	$\dfrac{\frac{\mathrm{d}F(t)}{\mathrm{d}t}}{1 - F(t)}$	$\dfrac{f(t)}{\int_0^t f(t)\,\mathrm{d}t}$	–

5.1.2 Probability Distributions

In reliability theory, probabilistic distributions are often used to describe the behavior of components or systems over time, allowing the evaluation of quantities such as reliability and maintainability.

In this section, two of the most widely used distributions are presented: the negative exponential distribution, and the Weibull distribution.

Negative Exponential Distribution

The failures of components or systems during their useful life are often the result of random events.

Assuming a constant failure rate offers several advantages: on one hand, it simplifies calculations, and on the other, it compensates for the lack of detailed information in cases where the time dependency of the failure rate is unknown. In this model, the past history of the component does not influence its future behavior in terms of failure probability [29]. The most commonly used model to represent a constant failure rate is the negative exponential distribution.

For a constant λ, the reliability function can be expressed as:

$$R(t) = e^{-\lambda t} \tag{5.12}$$

Once the reliability function is known, the failure probability and failure density function can be expressed as follows:

$$F(t) = 1 - R(t) = 1 - e^{-\lambda t} \tag{5.13}$$

$$f(t) = \frac{dF(t)}{dt} = \frac{f(t)}{1 - F(t)} = \lambda e^{-\lambda t} \tag{5.14}$$

A typical trend of these functions is shown in Figure 5.4. For a constant λ, the Mean Time To Failure (MTTF) becomes:

$$MTTF = \int_0^\infty R\, dt = \frac{1}{\lambda} \tag{5.15}$$

Two other parameters are also widely used to assess the reliability of a component:

- Mean Time To Repair (MTTR);
- Mean Time Between Failures (MTBF).

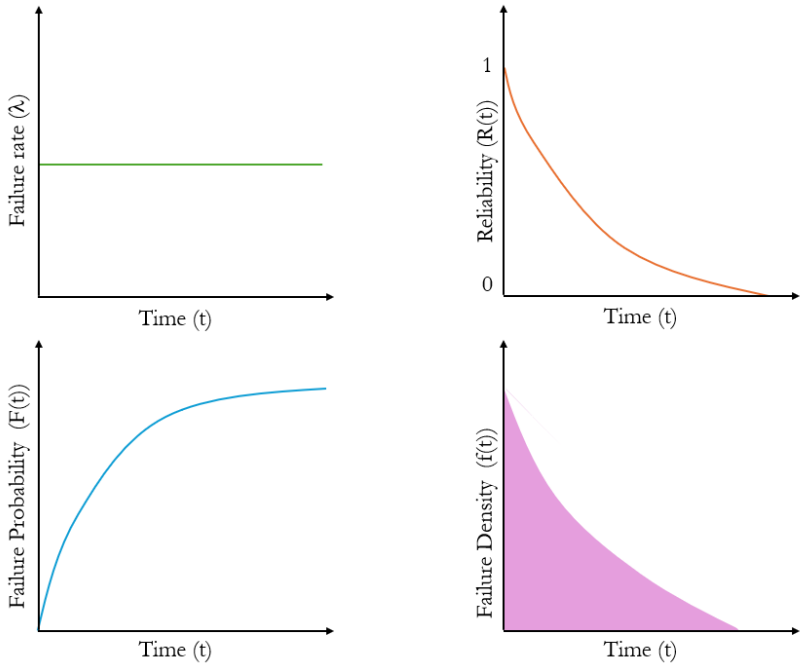

Figure 5.4: Example of reliability, failure probability, and failure density functions for a constant failure rate.

The Mean Time To Repair (MTTR) represents the average time required to restore a failed component to its operating condition. It is a useful parameter for assessing availability and the effectiveness of maintenance activities, and can be calculated as:

$$MTTR = \theta = \frac{1}{\mu} \tag{5.16}$$

where

θ repair time [hours];

μ repair rate [1/hour].

The Mean Time Between Failures (MTBF), applicable to repairable components, represents the average time between two consecutive failures and is defined as the sum of MTTF and MTTR (Figure 5.5):

$$MTBF = MTTF + MTTR = \frac{1}{\lambda} \tag{5.17}$$

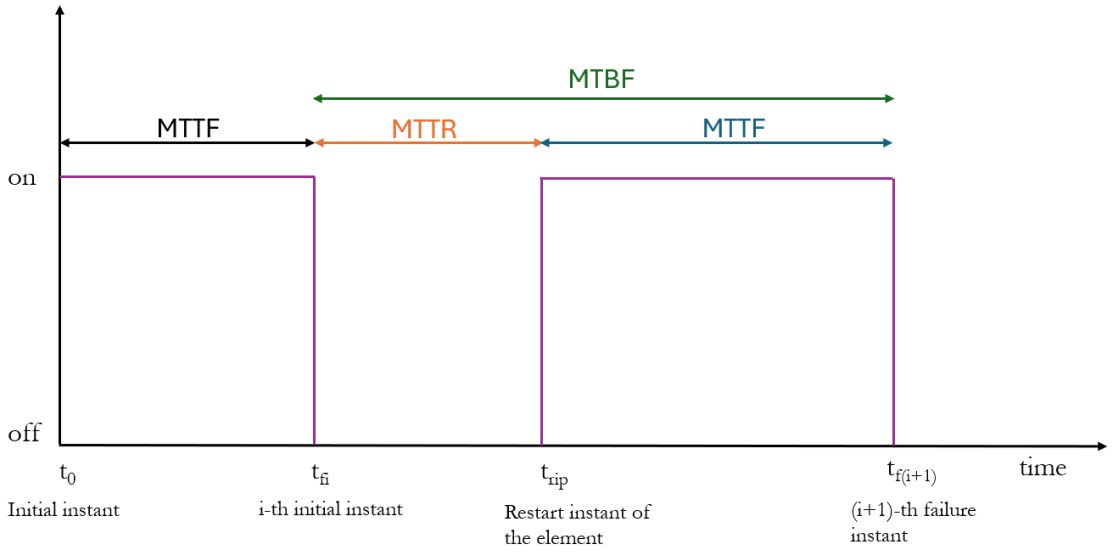

Figure 5.5: Reliability parameters.

Weibull Distribution

The Weibull distribution is widely used in data analysis to assess either the lifetime of components or the strength of materials over time. For instance, many companies employ the Weibull distribution to estimate warranty costs and durations of their products. What makes this distribution particularly attractive is its versatility, as it can fit increasing, decreasing, or constant failure rates as a function of time, thus being able to model all phases of a component lifecycle according to the bathtub curve [28].

The probability density function (PDF) of the two-parameter Weibull distribution is defined as:

$$f(t) = \frac{\beta\, t^{\beta-1}}{\alpha^{\beta}}\, e^{-\left(\frac{t}{\alpha}\right)^{\beta}}, \qquad t \geq 0;\ \alpha, \beta > 0 \tag{5.18}$$

where

α scale parameter or characteristic life [hours];

β shape parameter [–];

t time.

Once the probability density function is known, the failure probability $F(t)$, the reliability function $R(t)$, and the failure rate $\lambda(t)$ can be derived as follows:

$$F(t) = \int_0^t f(t)\, dt = 1 - e^{-\left(\frac{t}{\alpha}\right)^{\beta}} \tag{5.19}$$

$$R(t) = 1 - F(t) = e^{-\left(\frac{t}{\alpha}\right)^{\beta}} \tag{5.20}$$

$$\lambda(t) = \frac{f(t)}{1 - F(t)} = \frac{\beta\, t^{\beta-1}}{\alpha^{\beta}} \tag{5.21}$$

The parameter β, known as the shape parameter, determines the form of the curve, as shown in Figure 5.6:

- For $\beta > 1$, the failure rate increases with time, indicating that the component is approaching the end of its useful life.
- For $\beta < 1$, the failure rate decreases with time, which is typical of the burn-in phase.
- For β=1, the failure rate is constant, and the distribution approximates the negative exponential distribution.
- For $\beta = 3.33$, the Weibull distribution approximates the normal distribution, with a standard deviation equal to one-third of the mean.

The parameter α, known as the scale parameter, determines how far the curve extends along the time axis (see Figure 5.7). It represents the time by which 63.2% of the components have failed, since when $t = \alpha$:

$$1 - e^{-\left(\frac{t}{\alpha}\right)^{\beta}} = 1 - e^{-1} = 0.632 \tag{5.22}$$

5.1.3 Reliability Expressions for Repairable Components

For repairable components or systems, the statistical distributions presented in Section 5.1.2 cannot be directly applied, because failed units cannot be permanently removed from the population. This would lead to a cumulative failure distribution exceeding 1, which is mathematically impossible. For this reason, stochastic processes are used to model the behavior of repairable systems.

For repairable systems or components, the classical concept of reliability applies only up to the first failure. After the first failure, the system behavior becomes a sequence of operating, failed, and repaired states. In such cases, the most appropriate parameter to describe the system's performance is no longer reliability, but availability (A).

Several definitions of availability (A) and unavailability (U) are used in reliability analysis. The most common are described below.

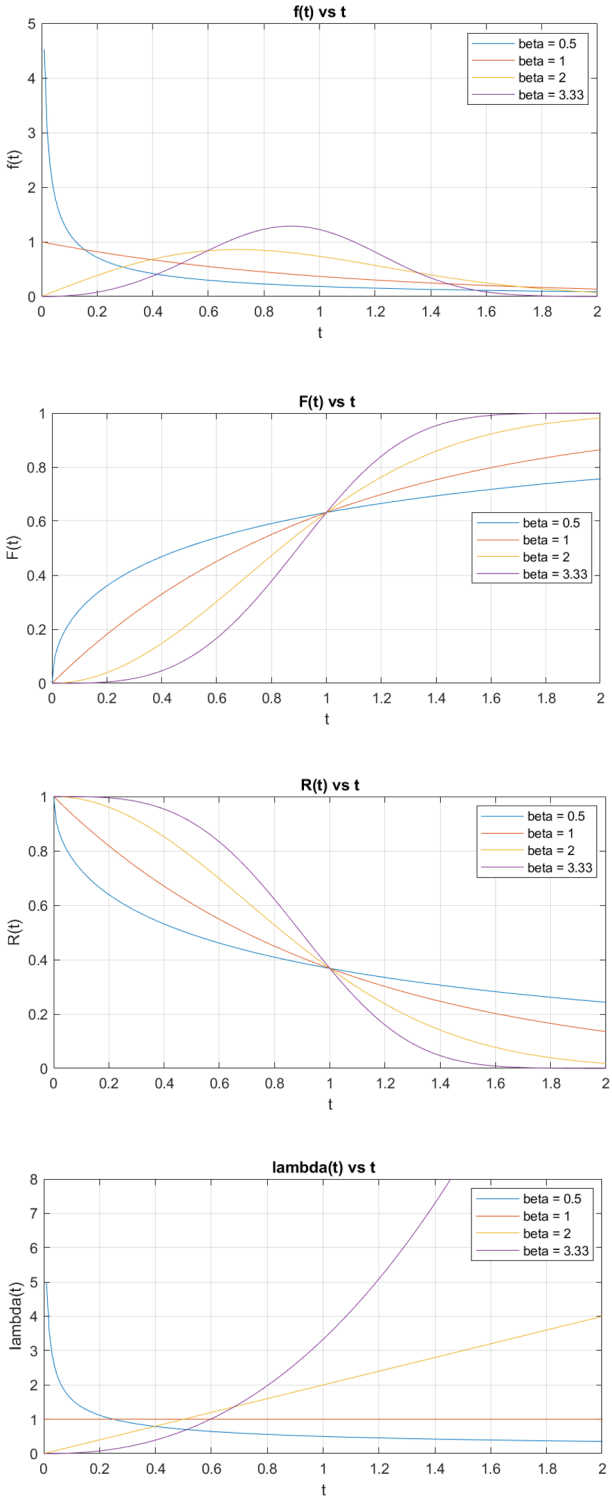

Figure 5.6: Influence of the shape parameter on the Weibull distribution ($\alpha = 1$).

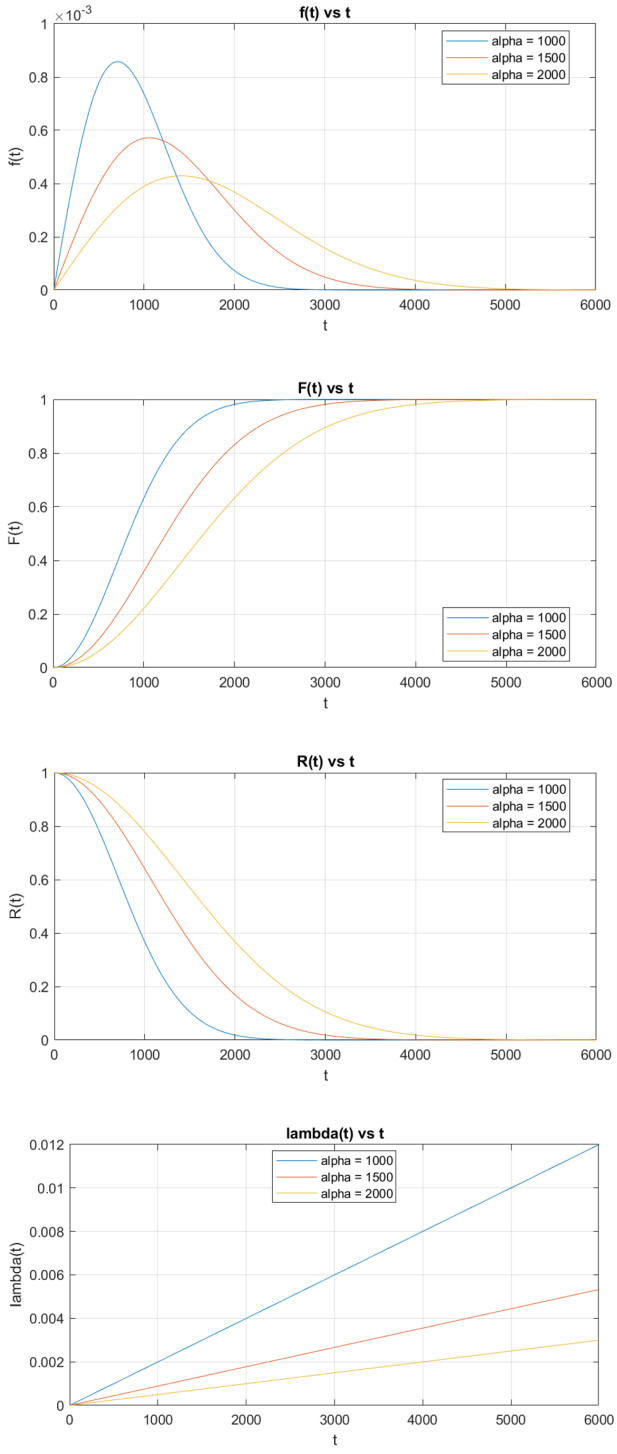

Figure 5.7: Influence of the scale parameter on the Weibull distribution ($\beta = 2$).

1. Instantaneous Availability.

   The instantaneous availability, $A(t)$, is defined as the probability that a component operating at the initial time $t = 0$ is not in a failed state at time t. Similarly, the unavailability, $U(t)$, is defined as the complementary probability that the component is in a failed state at time t:

   $$U(t) = 1 - A(t) \tag{5.23}$$

2. Limiting (Steady-State) Availability.

   The limiting availability is defined as the limit of the instantaneous availability as time tends to infinity:

   $$A = \lim_{t \to \infty} A(t) \tag{5.24}$$

   For a simple system, the steady-state availability can be expressed as:

   $$A(t) = \frac{\text{operating time}}{\text{operating time + downtime}} \tag{5.25}$$

   or, equivalently:

   $$A(t) = \frac{MTTF}{MTTF + MTTR} = \frac{\mu}{\lambda + \mu} \tag{5.26}$$

   Likewise, the unavailability can be expressed as:

   $$U(t) = 1 - A(t) = \frac{\lambda}{\lambda + \mu} \tag{5.27}$$

3. Mean Availability.

   The mean availability, $\bar{A}$, over a time interval T, is defined as:

   $$\bar{A} = \frac{1}{T} \int_0^T A(t)\,\mathrm{d}t \tag{5.28}$$

4. Limiting Mean Availability.

   The limiting mean availability over an infinite time horizon is defined as:

   $$\bar{\bar{A}} = \lim_{T \to \infty} \frac{1}{T} \int_0^T A(t)\,\mathrm{d}t \tag{5.29}$$

   For non-repairable components or systems, the availability coincides with reliability. In this case, recalling Equation 5.9:

   $$A(t) = R(t) = e^{-\int_0^t \lambda(t)\,\mathrm{d}t} \tag{5.30}$$

From a modelling perspective, repairable systems can be classified into two main categories:

- Repairable systems with self-revealing failures, i.e. systems equipped with diagnostic features that automatically indicate a fault condition;
- Repairable systems with non-self-revealing failures, where the failed state is detected only during inspections or when the system is required to operate[29].

Availability and Unavailability for Self-Revealing Failures

Components operating in online mode, such as controllers, are able to detect failures immediately. In such cases, assuming a constant failure rate $\lambda(t) = \lambda$ and a constant repair rate $\mu(t) = \mu$, the instantaneous unavailability $U(t)$ and availability $A(t)$ can be expressed as follows [29]:

$$U(t) = \frac{\lambda}{\lambda + \mu} \left(1 - e^{-(\lambda+\mu)t}\right) \tag{5.31}$$

$$A(t) = 1 - U(t) = \frac{\mu + \lambda e^{-(\lambda+\mu)t}}{\lambda + \mu} \tag{5.32}$$

where

μ repair rate [1/hour].

Availability and Unavailability for Non-Self-Revealing Failures

Some components, such as automatic protection systems (e.g., fire protection systems or electrical emergency systems), operate in stand-by mode, where failures are detected only when the component is required to perform its intended function.

In such cases, it is advisable to carry out periodic proof tests during the year, in order to reduce the exposure time of the component to an undetected failure condition. Assuming a constant failure rate $\lambda(t) = \lambda$, the instantaneous unavailability can be expressed as:

$$U(t) = 1 - e^{-\lambda t} \approx \lambda T \qquad \lambda T < 0.01 \tag{5.33}$$

where

T time interval between inspections [hours].

Since unavailability is a probability, its value ranges between 0 and 1: a system with $U = 0$ is perfectly reliable, whereas $U = 1$ indicates a complete failure.

The mean unavailability is given by:

$$\bar{U}(T) = \frac{1}{T} \int_0^T \left(1 - e^{-\lambda t}\right) \mathrm{d}t = 1 + \frac{1}{\lambda T} \left(e^{-\lambda T} - 1\right) \tag{5.34}$$

Equation 5.34 can be simplified by applying the Taylor series expansion of the exponential function and neglecting higher-order terms:

$$\bar{U}(T) = 1 + \frac{1}{\lambda T} \left(e^{-\lambda T} - 1\right) \approx \frac{\lambda T}{2} \tag{5.35}$$

5.2 Fault Tree Analysis

The Fault Tree Analysis (FTA) is a systematic and deductive technique used both to identify the logical sequence of intermediate events leading to a specific final event and to estimate the probability of its occurrence. It is particularly suitable for analyzing systems composed of multiple redundant elements and it is typically developed on the basis of hazard identification techniques, such as HAZOP.

A fault tree is a graphical model showing the combinations of failures, such as mechanical failures or human errors, that can lead to a well-defined accidental event, referred to as the Top Event, due to failed, ineffective, or missing safety barriers that should have interrupted the accidental sequence.

This approach allows the analyst to both identify and adopt preventive or mitigative measures to reduce the likelihood of the undesired event. Figure 5.8 shows an example of a fault tree.

FTA employs Boolean logic symbols to represent the relationships between failure events and the main event (Top Event), as summarized in Table 5.2 and Table 5.3. The analysis begins from the Top Event and proceeds downward, identifying the causes that led to it. Each cause, referred to as an intermediate event, is then examined in the same way until all basic events are identified. It is important to note that the fault tree does not represent all possible failures of a system but only those that contribute to the Top Event. Typical Top Events may include reactor rupture, tank failure, or liquid release. The FTA can be performed both qualitatively and quantitatively:

- Qualitatively. It is used to identify all necessary and sufficient failure combinations that can cause the Top Event.
- Quantitatively. It is used to estimate the frequency or probability of the Top Event.

In the quantitative phase, each basic event must be assigned a failure probability or, more precisely, an unavailability value. Both qualitative and quantitative analyses require the generation of all Minimal Cut Sets (MCS) of the fault tree, i.e., the smallest combinations of basic events capable of causing the Top Event. The probability of the Top Event is always expressed as the logical sum of the probabilities of the MCSs of the tree.

Different methods can be used to quantify the MCSs, including: probabilistic analysis applied to the logical resolution of the fault tree, Markov models, and Monte Carlo simulations.

During the construction of a fault tree, it is essential to distinguish between the concepts of failure and fault. This can be clarified by an example: if a valve fails to close when receiving a control signal, this is considered a failure; if the valve closes at the wrong time due to a malfunction in an upstream component, it is considered a fault. Both failures and faults represent malfunctions: a failure requires repair before the component can operate again, while a fault is a malfunction that is automatically corrected once the abnormal condition causing it is resolved. System components (whether mechanical parts, procedures, or human actions/omissions) can exist only in two states: operational or failed. No other states are allowed.

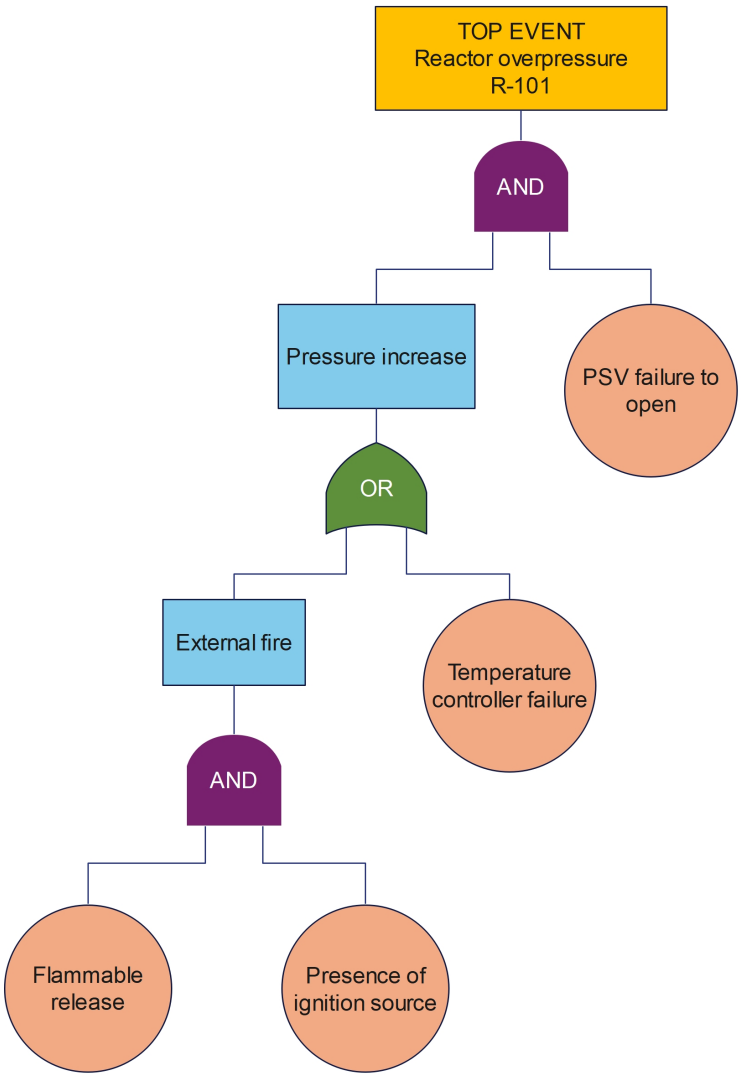

Figure 5.8: Example of Fault Tree.

Table 5.2: Logic gate symbols.

Symbol	Name	Description
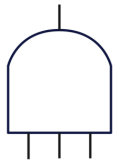	Gate AND	The output event occurs only if all input events occur simultaneously. The AND gate may have two or more inputs.
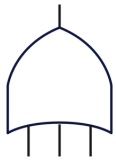	Gate OR	The output event occurs if any of the input events occurs. The OR gate may have two or more inputs.
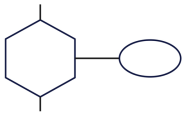	Gate INHIBIT	A special case of an AND gate. The output event occurs only if the input event occurs and a conditioning event (represented by an ellipse) has already taken place. The conditioning event can itself be a sub-tree.
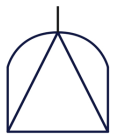	Gate PRIORITY AND	The output event occurs only if all input events occur in a specific sequence.
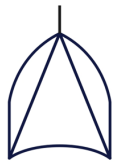	Gate EXCLUSIVE OR	A special case of an OR gate. The output event occurs only if one of the input events occurs, but not all of them.
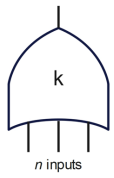	Gate k/n	The output event occurs if at least k out of n input events occur.
	Gate NOT	The output event occurs only if the input event does not occur.

Table 5.3: Event symbols.

Symbol	Name	Description
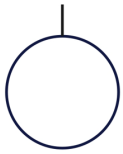	Primary Event	Describes basic component failures or human errors that do not require further development. Represents the limit of tree development.
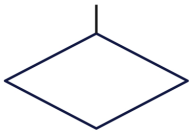	Undeveloped Event	Corresponds to a failure that is not analysed further either due to lack of information or because its development goes beyond the scope of the study.
	Intermediate Event	Describes events that occur as a result of one or more other failure events.
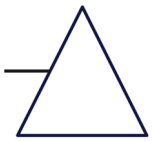	Transfer Symbol (OUT)	Used to simplify the tree structure and avoid the repetition of identical branches. The Transfer IN symbol indicates that the fault tree continues from a Transfer OUT symbol (e.g., on another page). These are labelled with numbers or codes for reference.
	Transfer Symbol (IN)	
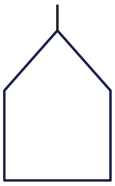	External or House Event	Used to identify events that are normally expected to occur during system operation.

Failures and faults can be classified into three categories:

- Primary failures: they occur when a component fails while performing its intended function, usually due to an intrinsic defect (e.g., a vessel rupturing below design pressure due to a weld defect).

- Secondary failures: they occur when a component fails while operating under conditions different from those for which it was designed (e.g., a vessel designed for a certain pressure fails due to overpressure caused by another component failure).

- Command (or control) failures: they occur when a component performs its function at the wrong time or under the wrong conditions (e.g., a relief valve opens without overpressure or too late after the pressure rise). System components can also be classified as passive or active.

- A passive component transmits a signal; its failure results in the absence of signal transmission. Typically, passive components have failure rates two or three orders of magnitude lower than active ones.

- An active component modifies the signal from a passive component (e.g., a valve that opens or closes to adjust flow). Active components usually require an input signal to produce an output signal; if they fail, either no output or an incorrect output is generated.

Developing a fault tree requires a detailed understanding of the plant or system, the failure modes of its components, and their effects. To ensure accuracy, the analyst must have access to comprehensive process information and collaborate closely with engineers and operators who are familiar with the system and equipment involved [28, 29].

5.2.1 Fault Tree Analysis Procedure

The development of a Fault Tree Analysis (FTA) involves the following main steps:

- system or process definition;

- fault tree construction;

- qualitative analysis of the fault tree;

- quantitative analysis of the fault tree;

- results collection and interpretation.

Each of these steps is described in detail in the following sections.

Definition of the System or Process

The first phase consists of selecting the Top Event and defining the boundary conditions of the analysis. The choice of the Top Event is one of the most critical aspects of this stage. It must correspond to a clearly defined critical event.

For example, a generic "plant failure" cannot be chosen as a Top Event, since it would not allow the identification of specific causes or the logical relationships among component failures within the system.

The boundary conditions include:

- Physical boundaries of the system: identifying which items of equipment are to be included in the tree and the required level of resolution. For example, should the analysis be extended to the subsystem level or further down to individual components? A valve, for instance, may be treated as a single piece of equipment or broken down into its parts (body, actuator, etc.). The selected level of detail determines the depth of the analysis.

- Initial configuration or standard operating conditions: specify which pumps are running, which valves are open/closed, and the normal process state.

- Excluded events: events considered highly improbable that are not to be taken into account in the analysis.

- Existing conditions: conditions that are assumed to certainly occur. These do not appear typically in the final fault tree but must be considered when evaluating causal relationships.

- Additional assumptions: any other modelling assumptions or simplifications adopted during the study [28, 30].

Construction of the Fault Tree

The construction of the fault tree begins with the Top Event placed at the top of the diagram and proceeds step by step downward, until all failure events are reduced to basic events whose probability (or, more precisely, unavailability) is known. For each intermediate failure event (also called a sub-event), the possible causes are identified and represented in the fault tree using the appropriate logic gate. Basic events may include equipment failures, sensor or controller malfunctions, and human errors, among others.

For example, in the fault tree shown in Figure 5.8, the Top Event is the overpressure of a reactor. For overpressure to occur, two events must take place simultaneously: a pressure increase and failure of the pressure safety valve (PSV) to open. The causes of the pressure increase may be a temperature controller malfunction or an external fire. The external fire may in turn be caused by the release of a flammable substance in the presence of an ignition source.

Qualitative Analysis of the Fault Tree

Once the fault tree has been constructed, a logical evaluation (or qualitative analysis) is carried out using the Minimal Cut Set (MCS) approach. The MCSs represent the smallest combinations of basic events that, if they occur simultaneously, would cause the Top Event to occur.

Quantitative Analysis of the Fault Tree

This stage, also referred to as fault tree resolution, involves calculating the probability of the Top Event once the probabilities of the basic events are known.

Using Boolean algebra, AND and OR logic gates can be converted into appropriate multiplicative and additive expressions.

Several methods can be used to quantify the MCSs, such as: application of standard probability equations, Markov models, or Monte Carlo simulations. In practical applications, this process is often supported by specialized software tools [29].

Table 5.4 summarizes the general relationships used to calculate both probability (P) and frequency (F) of events in a fault tree based on AND and OR logic gates.

Table 5.4: General rule for the calculation of probability (P) and frequency (F) in a fault tree.

Symbol	Gate	Input	Output
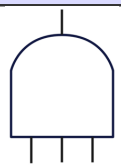	AND	$P(B)$ AND $P(C)$	$P(A) = P(B) \cdot P(C)$
		$F(B)$ AND $F(C)$	Unusual combination $F(A) = F(B) \cdot P(C)$ $F(A) = P(B) \cdot F(C)$
		$F(B)$ AND $P(C)$	$F(A) = F(B) \cdot P(C)$
	OR	$P(B)$ OR $P(C)$	$P(A) =$ $P(B) + P(C) - P(B) \cdot P(C)$ $\approx P(B) + P(C)$
		$F(B)$ OR $F(C)$	$F(A) = F(B) + F(C)$
		$F(B)$ OR $P(C)$	*Not permitted*

Results Collection and Documentation

The construction of the fault tree and the placement of logic gates (AND, OR, INH, etc.) must be consistent with both logical and procedural sequence of events leading to the accidental event.

The final step consists of documenting the results obtained from the analysis. This includes a detailed description of the system analyzed, the assumptions and boundary conditions adopted, and a complete list of all Minimal Cut Sets (MCSs) identified.

Furthermore, when reporting the results, particular attention should be paid to the data used in the analysis. If the failure rate value provided by the equipment or device manufacturer is available, it should be preferred over other sources (including literature values), provided that the manufacturer's instructions and conditions of use are respected. In the absence of such references, the most conservative approach shall be adopted, and the choice must always be properly justified.

5.3 Event Tree Analysis

The Event Tree Analysis (ETA) is an inductive risk analysis technique that provides information on how an initiating event may evolve and the probability of occurrence of the various accidental sequences. It is a complementary technique to the Fault Tree Analysis (FTA): while FTA investigates the causes leading to the Top Event, ETA focuses on the consequences of the initiating event, exploring all possible outcomes that may result from it.

The construction of an Event Tree begins with the identification of the initiating event, represented on the left-hand side of the diagram. The branches extend to the right, each representing a different sequence of events depending on the success or failure of protective systems.

When an accident occurs, several safety barriers or protection systems are activated to contain the event and prevent its escalation. These systems may either succeed or fail.

The ETA approach analyses the activation of the initiating event and evaluates the effects determined by the success or failure of the subsequent protection systems.

The main steps for constructing an Event Tree are:

- identify the initiating event;
- identify the protection barriers (or safety systems) designed to manage the event;
- graphically construct the event tree;
- describe the resulting sequences, identifying all possible accidental scenarios.

An example of an Event Tree structure is shown in Figure 5.9. Each branch is associated with a probability, allowing the calculation of the probability of each sequence and the identification of potential areas for improvement in the protection systems. The ETA is written from left to right, the initiating event is shown on the left; a horizontal line is drawn toward the first protection barrier. By convention:

- if the barrier succeeds, a straight line upward is drawn;
- if the barrier fails, a line downward is drawn.

From each node (success/failure), new horizontal lines extend toward the next barrier until all possible combinations are covered. The sum of the probabilities of success and failure for each barrier is equal to one.

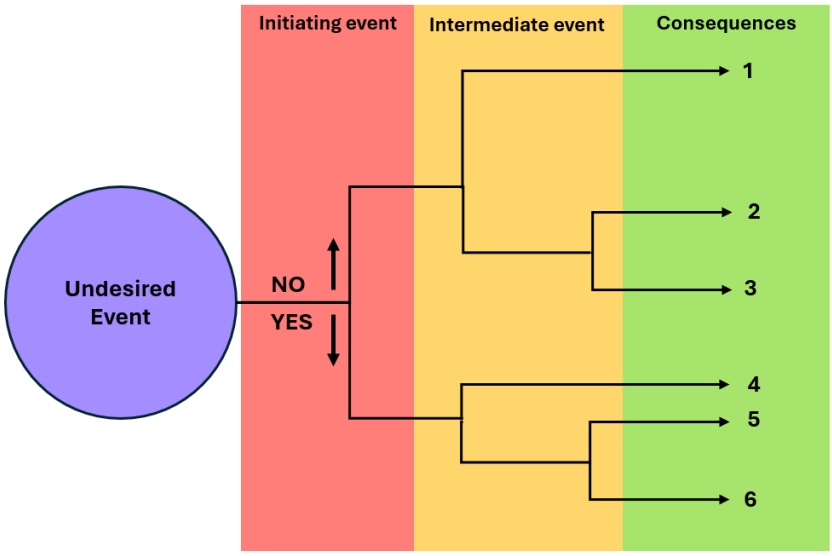

Figure 5.9: Structure of an Event Tree.

The Event Tree can be used as both a qualitative and quantitative technique: it allows estimation of the frequency of occurrence of each final scenario, given the frequency of the initiating event (often derived from FTA results). It is a powerful yet complex tool requiring operational experience and in-depth system knowledge.

The accuracy of the analysis strongly depends on a comprehensive understanding of the system, the undesired events, and the protection systems involved. To obtain meaningful results, it is essential to anticipate all possible evolutions of the initiating event. An example of an Event Tree is shown in Figure 5.10.

5.4 Human Error

The analysis of past accidents clearly shows that human errors play a predominant role in the occurrence of major accident. For this reason, it is essential to identify potential human errors, reducing their probability of occurrence as much as possible.

Over the last decades, the introduction of automated control systems has led to a significant reduction in technical failures, thanks to the implementation of protective measures and redundancy systems that have made industrial processes increasingly reliable. Nevertheless, when assessing the reliability of a component or system, the human factor must also be taken into account, as human interaction can influence the failure rate and/or error probability of components.

It has been observed that human errors contribute to 60–80% of accidents, whereas the remaining portion is attributable to technical deficiencies. Therefore, when conducting a reliability study, the role of the human operator cannot be neglected, as it significantly affects both the sequence of accidental events and the estimation of their consequences.

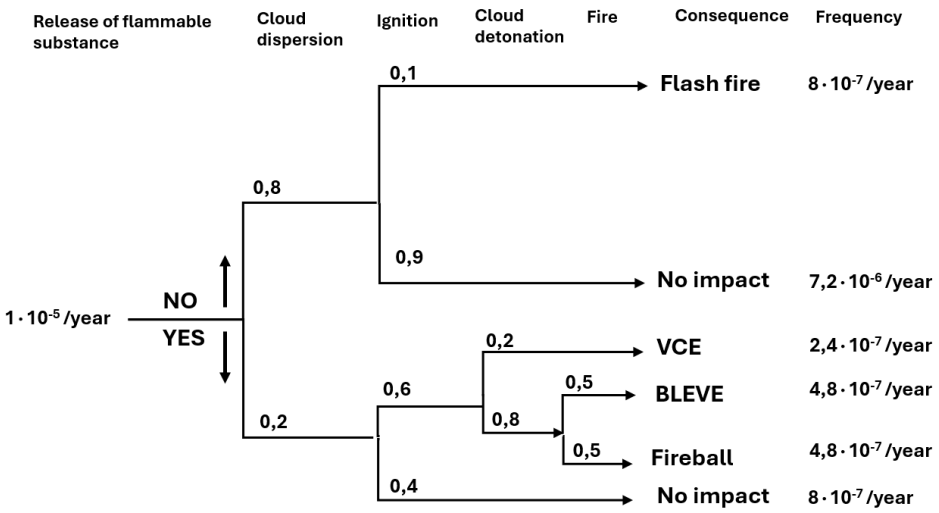

Figure 5.10: Example of an Event Tree.

5.4.1 Human Reliability Analysis (HRA)

The purpose of Human Reliability Analysis (HRA) is to identify potential human errors and their effects. The outcome of the analysis may be qualitative or quantitative, and it consists of a list of: possible human errors that could occur during either normal plant operation or emergency situations, the factors contributing to such errors, and the corrective actions or system modifications needed to reduce their probability of occurrence.

When used for quantification of human error, the results of the HRA can be integrated into fault trees (FTA) and event trees (ETA). The method also provides useful recommendations for reducing human error and improving system performance.

Human reliability is defined as the probability that personnel successfully complete a task or activity during any operational phase of the system, within the minimum required time, if a time constraint exists.

HRA represents a systematic assessment of the factors that influence the performance of operators, technicians, maintenance staff, and personnel in general. Since it follows a structured methodology, its results can be easily updated whenever plant modifications occur. The main steps of an HRA include:

- identifying all critical operations in which human error could lead to an accident and/or operational problems;
- identifying types of human errors, their causes, and performance-shaping factors influencing them;
- determining, for each type of human error, the corresponding Human Error Probability (HEP).

5.4.2 Human Error: Definition and Probability

The term "human error" is often used incorrectly. It is a generic expression that describes all situations in which a planned sequence of physical or mental activities fails to achieve the intended goal.

Human error is closely related to the concept of a task, understood as the set of actions performed by operators to achieve a specific outcome. Tasks can be further divided into sub-tasks and, if necessary, into even more detailed levels down to individual actions. Examples of human error include:

- Physical actions: errors in operational or maintenance procedures (e.g., failure to close a valve);
- Cognitive actions:
  - errors during maintenance, calibration, or verification of control and protection systems;
  - failure of the operator to intervene when necessary to restore the plant to safe operating conditions.

The result of a Human Reliability Analysis (HRA) is expressed either in terms of Human Error Probability (HEP) or Human Error Rate (HER). The Human Error Probability (HEP) is defined as the probability of an error occurring when an action is performed:

$$\text{HEP} = \frac{\text{number of errors}}{\text{number of opportunities for error}} \tag{5.36}$$

The Human Error Rate (HER) is defined as:

$$\text{HER} = \frac{\text{number of errors}}{\text{total duration of the action}} \tag{5.37}$$

The value assigned to human error must be clearly justified, specifying all algorithms, parameters, and data sources used for its determination. A value of 10^{-2} is generally considered acceptable for manual and repetitive operations. Less conservative values must be explicitly justified and proven applicable to the specific case.

Examples of reference values proposed in the literature:

- THERP: According to the NUREG/CR-1278 manual, error rates for routine operations range between 10^{-3} and 10^{-2}, depending on task complexity and operating conditions.
- HCR: Studies indicate variable error rates, generally similar to those of THERP for complex tasks performed under high-stress conditions.
- SLIM: Using expert judgment, error rates can be estimated for critical tasks, often suggesting values on the order of 10^{-4} or lower for highly critical operations.

5.4.3 Classification of Human Error

The study of human reliability focuses on analyzing the internal and external factors that influence the effectiveness and reliability of human performance. External factors include random technical or systemic events (such as environmental conditions, equipment, materials, organization, and workplace layout) that may alter the operational context and lead operators to erroneous behavior. Internal factors, on the other hand, are more difficult to predict because they are related to individual psychophysical conditions, which by their nature are not easily represented through systematic behavioral models.

The analysis of human factors is a highly interdisciplinary research field, still evolving and not yet fully defined. As a result, a comprehensive and universally accepted classification of human error types and their underlying causes has not yet been developed.

The most commonly used classification systems can be summarized as follows (Figure 5.11):

- the Skill–Rule–Knowledge (SRK) model proposed by Rasmussen;
- the Reason model, which distinguishes between slips, lapses, mistakes, and violations;
- the Swain and Guttmann model, which classifies errors as omissions or commissions [31].

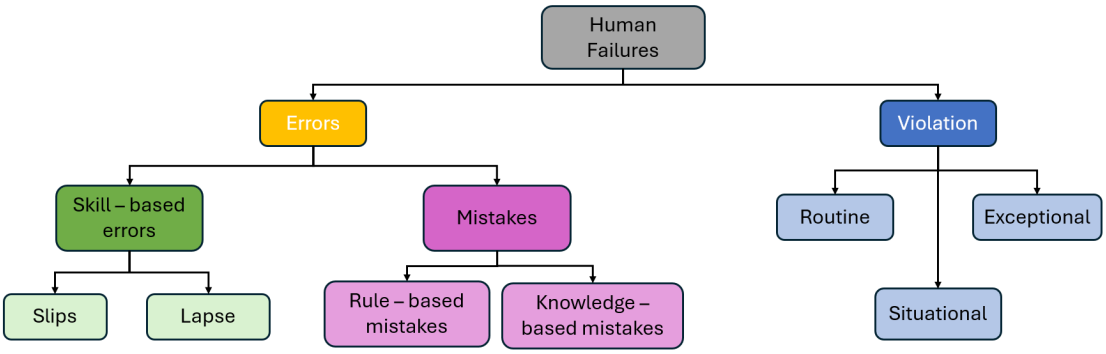

Figure 5.11: Classification of human failure types.

The Skill–Rule–Knowledge (SRK) Model by Rasmussen

Rasmussen's model classifies human behavior into three distinct categories:

- Skill-based behavior: these are automatic, subconscious actions requiring minimal or no cognitive effort. Errors at this level are typically associated with routine activities performed under familiar conditions.

  Example: opening or closing a valve, starting an agitator, etc.

- Rule-based behavior: this level requires greater cognitive effort, as it involves executing a specific procedure. Unlike skill-based behavior, the operator is less familiar with the task, which may lead to memory errors, incorrect application of a rule, or inaccurate execution of certain steps.

  Example: responding to a control panel alarm.

- Knowledge-based behavior: this refers to novel or unfamiliar situations that require significant mental effort to analyze the problem and make decisions. The operator must carefully assess the situation, interpret available information, and adopt appropriate solutions.

  Example: responding to an emergency following a sudden pressure loss in a chemical reactor for which no predefined procedure exists: the operator must quickly analyze the available data and decide on corrective action [32].

The Human Error Model by Reason: Slip, Lapse, Mistake, Violation

According to Reason, human errors can be classified into four main categories:

- Slip (attention failure): occurs when an action is performed differently from what was intended, due to a lapse in attention. The operator knows the correct action but performs it incorrectly or unintentionally.

  Examples: pressing the wrong button, transposing digits while reading an indicator.

- Lapse (memory failure): caused by a malfunction of memory, leading the operator to forget an intended action or omit an important step. Unlike slips, lapses may not be visible to others: only the person committing them may notice. These errors can be dangerous and difficult to detect.

  Example: forgetting to disconnect a hose after unloading and starting the tanker.

- Mistake (decision or planning failure): these errors arise from failures in diagnosis, decision-making, or planning. They are intentional actions that the operator believes to be correct, but they are actually wrong. Causes may include unclear operating instructions, a stressful work environment, or organizational issues.

  Example: shutting down the wrong motor or applying an incorrect procedure. Adequate training can help prevent such errors.

- Violation (rule-breaking): occurs when a person deliberately violates a rule or procedure, often to achieve a faster result or solve an immediate problem. Unlike mistakes, which are unintentional, violations are deliberate deviations from established rules. Several subtypes can be identified:

  – Routine violations: repeated deviations from rules or procedures that become habitual;

– Exceptional violations: rare deviations occurring under special or unforeseen circumstances (e.g., during an emergency, acting outside procedure may nevertheless solve the problem);
– Situational violations: occur when work demands make compliance difficult under certain conditions;
– Acts of sabotage: intentionally harmful actions, such as vandalism or terrorism, often linked to demotivation or other complex issues [32].

Errors of Omission and Commission

Swain and Guttmann classified human errors into two main types:

- Errors of omission: occur when a required action is not performed.
- Errors of commission: occur when an assigned action is performed incorrectly, or when an unnecessary action is taken.

5.4.4 Human Reliability Analysis (HRA) Techniques

In the literature, numerous Human Reliability Analysis (HRA) techniques are available to estimate the Human Error Probability (HEP) associated with the execution of specific operational tasks. A study conducted by the UK Health and Safety Executive (HSE) identified 72 different approaches for HRA, of which 17 were deemed suitable for application in high-hazard industries.

These techniques are classified into first-, second-, and third-generation methods, as well as expert-judgement-based methods (Table 5.5) [33].

First-generation methods were the earliest to be developed, primarily designed to both predict and quantify human error probabilities. Among these, the most well-known is THERP. Although often criticized for their inability to account for organizational factors and errors of commission, these methods remain widely used for quantitative risk assessment.

Since the 1990s, second-generation methods have been developed to include contextual factors and errors of commission. Among these, the most recognized are CREAM and MERMOS. However, these approaches have not yet been fully validated, and their use remains limited. In the 2000s, third-generation methods emerged, building upon first-generation methods such as HEART.

Expert-judgement-based techniques gained popularity in the 1980s and continue to be used today, particularly in less critical contexts. In high-hazard industries, however, quantitative or structured techniques are generally preferred.

According to the HSE, a HEP value of 0.1 can be considered conservative. In all other cases, lower-order values must be adequately justified. Although the literature provides a wide range of published human error probabilities, one of the main issues is the frequent lack of contextual information (such as time frame, operational environment, or task complexity) necessary to assess their quality. This does not imply that historical data are unreliable, but rather highlights the need for analysts to adopt a cautious and

well-justified approach when using such data for risk and consequence assessment. The following sections describe some of the most widely used techniques in HRA, useful for quantifying the probability of human error.

Table 5.5: Main Human Reliability Analysis (HRA) methods classified by generation.

Generation	Acronym	Full Name	Application
1st	THERP	Technique for Human Error Rate Prediction	Primarily used in the nuclear sector, but applicable to other industries
	ASEP	Accident Sequence Evaluation Programme	Nuclear
	HEART	Human Error Assessment and Reduction Technique	General
	SPAR-H	Simplified Plant Analysis Risk Human Reliability Assessment	Primarily used in the nuclear sector, but applicable to other industries
	HRMS	Human Reliability Management System	Nuclear. Not publicly available
	JHEDI	Justified Human Error Data Information	Nuclear. Not publicly available
	INTENT	Not an acronym	Nuclear. Not publicly available
2nd	ATHENA	A Technique for Human Error Analysis	Primarily used in the nuclear sector, but applicable to other industries
	CREAM	Cognitive Reliability and Error Analysis Method	Primarily used in the nuclear sector, but applicable to other industries
	CAHR	Connectionism Assessment of Human Reliability	General. Not publicly available
	CESA	Commission Errors Search and Assessment	Nuclear. Not publicly available
	CODA	Conclusions from Occurrences by Descriptions of Actions	Nuclear. Not publicly available
	MERMOS	Méthode d'Évaluation de la Réalisation des Missions Opérateur pour la Sûreté	Nuclear. Not publicly available
3rd	NARA	Nuclear Action Reliability Assessment	Nuclear. Not publicly available
Expert judgement	APJ	Absolute Probability Judgement	General
	PC	Paired Comparisons	General
	SLIM-MAUD	Success Likelihood Index Methodology – Multi - Attribute Utility Decomposition	Primarily used in the nuclear sector, but applicable to other industries

THERP

The Technique for Human Error Rate Prediction (THERP) was developed in the early 1960s for the U.S. Nuclear Regulatory Commission and still represents one of the most widely used methods for the quantitative analysis of human reliability. This method makes possible to both predict the probability of human error and assess the potential degradation of a man–machine system as a consequence of human errors (either

occurring independently or in combination with the performance of equipment, procedures, operational practices, or other system or human characteristics that influence overall behavior).

THERP methodology is based on the assumption that human success or failure can be treated analogously to functioning or failure of a technical component, where a human error is considered equivalent to a failure. In practice, each activity performed by the operator is analyzed using the same approach adopted for component reliability assessment, with specific corrections applied to account for the peculiar characteristics of human behavior.

Errors made by operators are classified into two main categories: Omission errors, and Commission errors. The main steps of the THERP methodology are as follows:

- Decomposition of tasks into individual elements;
- Assignment of nominal human error probability (HEP) values to each element;
- Determination of Performance Shaping Factors (PSFs), which allow the transition from nominal to effective error probabilities. PSFs are divided into three main categories:
  - External factors: including aspects related to the work environment, operational conditions, and human–machine interface quality;
  - Internal factors: related to individual operator characteristics such as experience, skill, motivation, and expectations;
  - Stress factors: including all elements that induce pressure or emotional tension and may impair concentration.
- Representation of operator performance through the construction of an event tree;
- Quantification of HRA, by assigning a human error probability to each node of the event tree

The event tree is a binary structure in which each node represents an operator action. An example of an event tree used for human reliability analysis is shown in Figure 5.12. From each node, two branches are generated: the left branch indicates success, while the right branch indicates failure. Each branch ends with a final event. Knowing the human error probability associated with each node, it is possible to determine the probability of the final events. To avoid overestimation, it is essential to also consider error recovery, which occurs when the operator detects the error and performs corrective actions.

The manual "*Handbook of Human Reliability Analysis with Emphasis on Nuclear Power Plant Applications*" provides 27 tables and guidance schemes to facilitate the identification and assignment of appropriate nominal human error probabilities.

Among the main advantages of the THERP methodology is its broad applicability, ranging from the nuclear and chemical sectors to the healthcare industry, making it a robust and well-established technique. Moreover, the availability of a detailed handbook

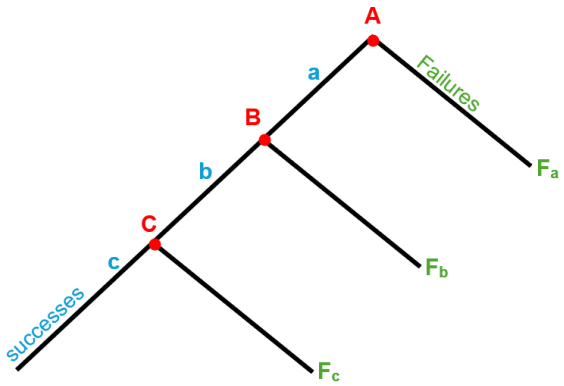

Figure 5.12: Example of an event tree. Nodes shown in red (•) represent operator actions, identified by red letters. Letters in blue (a, b, c) correspond to successful actions, while letters in green (Fa, Fb, Fc)indicate failures associated with the different actions.

and reference tables simplifies the analytical process. However, this methodology also presents some limitations: it is time- and resource-intensive, requiring detailed analyses that may be excessive for certain applications. Another limitation is the lack of explicit consideration of cognitive errors, as the method primarily focuses on omission and commission errors, neglecting other types of human errors which may significantly influence outcome [31, 32].

HEART

The Human Error Assessment and Reduction Technique (HEART) was developed in the late 1980s. It is a rapid and straightforward method for quantifying human error, and it can be applied across a wide range of industrial sectors. The method is based on the following assumptions:

- the basic level of human reliability depends on the generic nature of the task to be performed;
- under "perfect" conditions, this level of reliability tends to be achieved consistently within a defined probabilistic range;
- since such perfect conditions rarely exist, the predicted human reliability may deteriorate depending on the extent to which Error Producing Conditions (EPCs) are present.

In the HEART method, activities are classified into nine Generic Task Types (GTTs):

1. Totally familiar, performed rapidly without consideration of possible consequences.
2. Restoring or changing the system to a new or original state in a single attempt, without following a written procedure.

3. A complex task requiring a high level of skill.
4. A routine task performed rapidly or with limited attention.
5. A routine and well-practised task, executed quickly with a low level of skill.
6. Restoring or changing the system to its original or a new state, following procedures and carrying out checks.
7. A familiar, well-designed task, repeated several times per hour.
8. Correctly responding to a system command, even in the presence of an automated supervisory system.
9. Any other activity not covered by the above categories.

Each Generic Task Type is associated with a nominal Human Error Probability (HEP) and 38 Error Producing Conditions (EPCs) that may influence task reliability. Each EPC is characterized by a maximum multiplier by which the nominal HEP can be increased.

HEART is one of the few human reliability assessment methods that has undergone empirical validation. Its main advantages include: speed and simplicity of application, availability of supporting documentation, and the ability to identify corrective actions for each condition contributing to error generation. However, the method also has some limitations: it can only evaluate single tasks, the origin of the HEP data is not entirely transparent, and the EPC dataset is not publicly available, making independent validation of the database challenging [33].

SPAR – H

The SPAR-H (Standardized Plant Analysis Risk – Human Reliability Analysis) methodology classifies each Human Failure Event (HFE) into two main categories:

- Diagnosis phase: includes the entire spectrum of cognitive processes, from the interpretation of complex information to the formulation of simple decisions, such as whether or not to act.
- Action phase: involves no cognitive processing, but only the physical execution of the task.

Once the HFEs have been categorized as diagnosis and/or action, the next step is to identify the Performance Shaping Factors (PSFs) influencing operator performance. Each PSF must be analyzed by addressing the following questions:

- Is sufficient information available to assess the influence of the PSF?
- Does the PSF under consideration actually affect the probability of operator failure (i.e., is it a performance driver)?

Only those PSFs for which adequate information is available and that are identified as performance drivers are quantified. The eight Performance Shaping Factors (PSFs) used in SPAR-H are:

- Available time: evaluates the ratio between the time available and the time required to complete a task. This PSF does not account for perceived time pressure, as such stress-related aspects are considered separately under the stress/stressor PSF.
- Stress/stressors: includes both mental stress (e.g., excessive workload) and physical stress caused by environmental factors. It considers all conditions that may hinder task completion by the operator. Environmental factors such as excessive heat, noise, or poor ventilation can induce stress and negatively affect physical and mental performance. Stress levels are classified into four categories: extreme, high, nominal, and insufficient information. The stress/stressors PSF is not independent from the others, so care must be taken to avoid double counting.
- Complexity: refers to the degree of difficulty of performing an action in a given context. Generally, the more complex the task, the higher the likelihood of errors. The complexity PSF accounts for both mental effort (e.g., performing mental calculations) and physical effort (e.g., performing complex movements). Five levels are identified: highly complex, moderately complex, nominal, obvious diagnosis, and insufficient information.
- Experience/training: considers the years of experience of the operators or teams involved in the task, the training specific to the scenario under analysis, and the time since and frequency of the most recent training. Levels are classified as low, nominal, high, and insufficient information. When experience/training is considered a performance driver, the quality of the training must also be evaluated.
- Procedures: refers to the existence and use of formal operating procedures for the diagnostic or action tasks under consideration. Levels include not available, incomplete, available but poor, nominal, diagnostic, and insufficient information.
- Ergonomics/Human–Machine Interface (HMI): relates to the quality and quantity of information provided by instrumentation, displays, and controls, and the interaction between the operator (or team) and the instrumentation. This PSF evaluates both the HMI and the adequacy of the software. Levels are missing/misleading, poor, nominal, good, and insufficient information.
- Fitness for duty: refers to the physical and mental suitability of the individual to perform the task. Fatigue, substance use, and personal issues are all factors that may impair fitness for duty. Levels are unfit, degraded fitness, nominal, and insufficient information.
- Work processes: covers organizational aspects related to task performance, including safety culture, work planning, communication, support, and management policies. Levels are poor, nominal, good, and insufficient information.

Each PSF is assigned both a level and a corresponding numerical value. The Human Error Probability (HEP) is calculated as the product of the Nominal Human Error Probability (NHEP) and the composite PSF score ($\text{PFS}_{\text{composite}}$):

$$\text{HEP} = \text{NHEP} \cdot \text{PFS}_{\text{composite}} \tag{5.38}$$

The NHEP is assumed to be 0.001 for action and 0.01 for diagnosis.

If diagnosis and action are combined into a single HFE, the two HEPs are first calculated separately and then combined to produce a single probability value:

$$\text{HEP}_{\text{diagnosis+action}} = \text{HEP}_{\text{diagnosis}} + \text{HEP}_{\text{action}} - \text{HEP}_{\text{diagnosis}} \cdot \text{HEP}_{\text{action}} \tag{5.39}$$

If three or more PSFs negatively affect the $\text{PFS}_{\text{composite}}$ value, resulting in a HEP greater than 1, a corrective factor must be applied. In such cases, Equation 5.39 is replaced by:

$$\text{EP} = \frac{\text{NHEP} \cdot \text{PFS}_{\text{composite}}}{\text{NHEP} \cdot (\text{PFS}_{\text{composite}} - 1)} + 1 \tag{5.40}$$

The next step in determining the final HEP value involves considering dependency. Dependency exists when the occurrence of one event affects the likelihood of another event occurring. However, having two or more HFEs in sequence does not automatically imply dependency.

The analyst must evaluate the situation and context, taking into account the following factors:

- Time;
- Location;
- Whether the same operator or different teams are involved;
- The cues or stimuli that might cause the operator to respond differently.

The combined effect of these parameters determines a dependency level, which can be low, moderate, high, or complete. Depending on the level of dependency, correction factors are applied to adjust the final Human Error Probability accordingly [33].

Chapter 6

Estimation of the magnitude of consequences

The objective of this chapter is to provide an overview of the models used to estimate the initial stages of an accidental event and its related consequences and effects. Typical accidents that can occur in industrial environments include the partial or total rupture of a pipeline or tank, the development of an external fire near a reactor, or the onset of a runaway reaction. The consequences of such events involve the release of substances that, as discussed in the previous chapters, may be toxic, flammable, explosive, and/or reactive.

In general, predictive models used to simulate fires, explosions, and releases of hazardous substances consist of three specific sub-models referring to:

- the source (Source Model);
- the transmission of the physical effect (Effect Transmission Model);
- the impact on people, assets, and the environment (Consequence Assessment Model) (Figure 6.1).

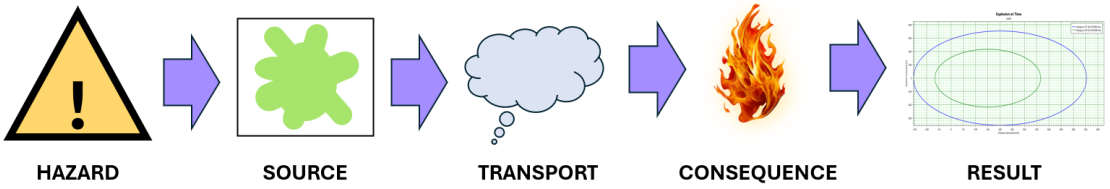

Figure 6.1: Phases for the final calculation of consequences.

Once the accidental scenario has been identified, the next step is to select the source model. The Source Model describes the spatial and temporal evolution of the release event during the initial moments of the accident and in the immediate vicinity of the

release point. To correctly apply the source model, the following input information is required:

- chemical – physical properties of the substance (density, vapor pressure, latent heat, etc.);
- storage conditions: temperature, pressure, etc.;
- characteristics of the vessel or pipeline: dimensions, shape, diameter, etc.;
- parameters of the orifice: shape, position, size, etc.

From these parameters, it is possible to derive:

- the release rate;
- the release duration;
- the total quantity of substance released;
- the physical state of the release (solid, liquid, vapor, or a two-phase liquid–vapor mixture).

The transport or dispersion model describes the behavior of a gas or vapor cloud released into the atmosphere, estimating its spatial distribution and concentration over time. This model takes as input the results of the source model and considers the physical properties of the substance (such as density and volatility) and meteorological conditions (wind speed, atmospheric stability, temperature, etc.), which significantly influence how the gas or vapour spreads in the atmosphere.

Transport models can be divided into three main categories:

- dispersion models, used to describe how the released material is dispersed by the wind and the resulting concentration profiles;
- fire models, used to estimate the thermal radiation in the case of flammable substance releases;
- explosion models, used to determine the overpressures generated by explosive events.

Consequence models process the results of the transport model to estimate the effects on humans and the environment resulting from a hazardous release. In particular:

- in the case of flammable substance releases, they allow the evaluation of the thermal radiation generated by fires or the overpressure associated with potential explosions;
- in the case of toxic releases, they enable the estimation of concentration levels in the atmosphere and the potential exposure of individuals within the affected area.

The ultimate goal of applying these calculation models is to obtain damage areas, also known as consequence maps, corresponding to the resulting concentrations from toxic releases, thermal radiation from fires, and overpressures from explosions (Figure 6.2).

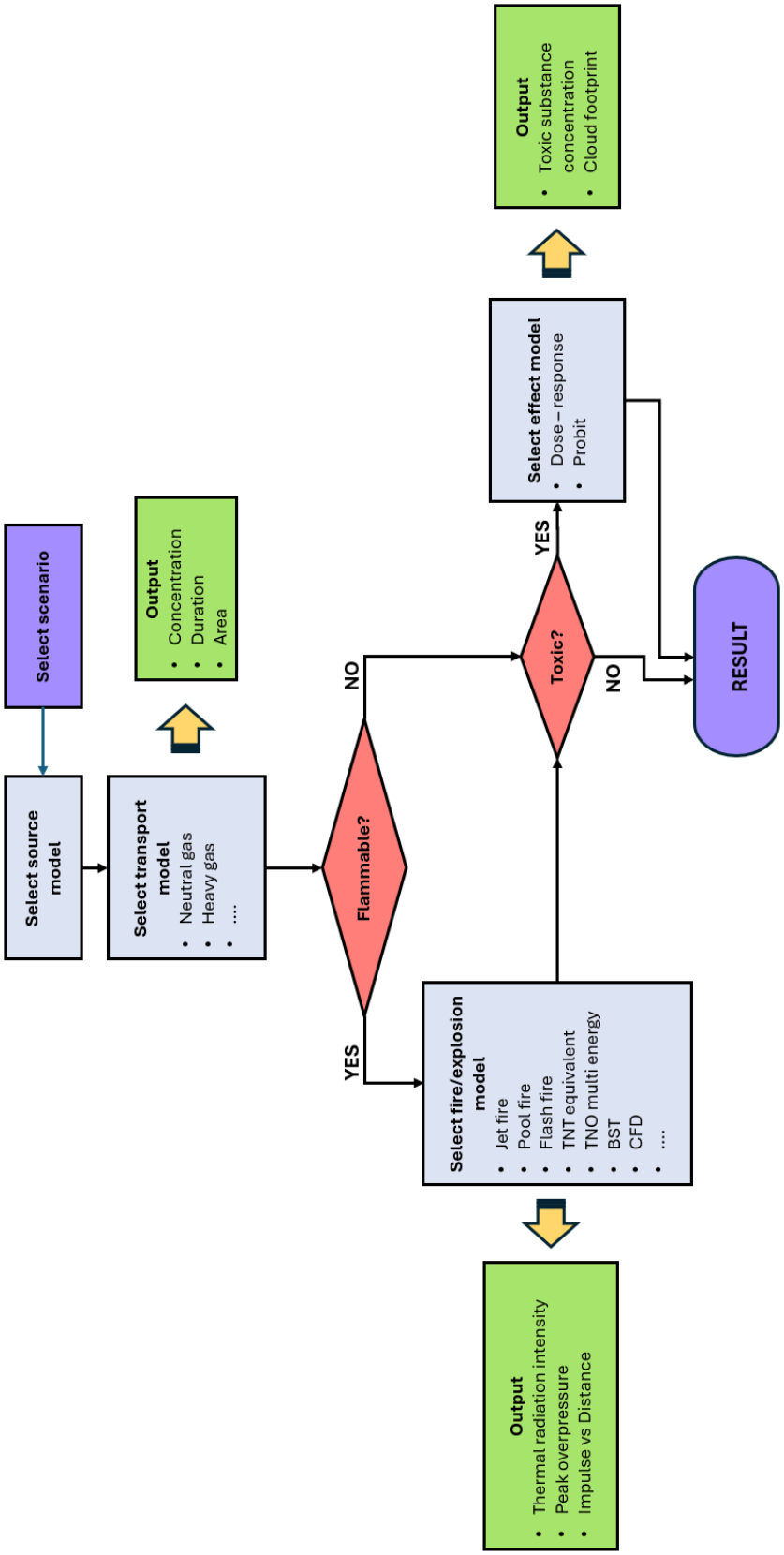

Figure 6.2: Flow diagram for consequence estimation.

All possible scenarios should be evaluated based on the physical state of the substance and the process conditions under which it is stored or handled, in order to ensure a realistic and comprehensive representation of the potential accident outcomes.

Throughout the various stages of the analysis, it is also essential to maintain a Register of Assumptions, which systematically records all the decisions made—both those based on the information provided by the operator (such as plant type, substances involved, process characteristics, etc.) and those resulting from the technical evaluations carried out by the risk analyst. Maintaining such a register represents good practice, as it allows clear traceability of the reasoning behind each assumption and supports transparency in the entire risk assessment process.

6.1 Overview of Available Models

Models used to simulate accidental events and estimate their consequences can be divided into four main categories:

- empirical correlations;
- integral models;
- shallow-layer models;
- computational fluid dynamics (CFD) models.

6.1.1 Empirical Correlations

Models based on empirical correlations are known for their ease of use and low computational requirements, making them ideal for preliminary screening analyses. However, it should be noted that applying these models to situations that differ significantly from the original experimental or validation conditions may lead to underestimation or overestimation of the results.

Despite these limitations, several empirical correlations have been validated through comparisons with experimental data, showing good levels of accuracy. In general, such models are readily available in scientific literature, including research papers and academic textbooks [34].

6.1.2 Integral Models

Integral models use simplified differential equations to describe the overall phenomenon (e.g. dispersion, thermal radiation, etc.). For instance, when applied to the dispersion of toxic or flammable substances in open fields, they allow the representation of idealized atmospheric conditions (e.g. D5 and F2), and some models also account for orographic and environmental features, as well as the presence of fences or other obstacles.

These models do not require advanced computing power, are very user-friendly, and provide clear and easily interpretable results. However, they do not consider the site

geometry or the presence of boundary conditions (such as buildings, obstacles, or other structures). As a result, modelling complex sites can be difficult, and the predictions may be imprecise or inapplicable in certain areas.

Regarding validation, many of these models have been compared with experimental data, and the companies that own the models tend to continuously improve them based on such comparisons [34].

6.1.3 Shallow-Layer Models

Shallow-layer models, also known as surface layer models, combine features of both integral models and computational fluid dynamics (CFD) models. For example, they can simulate dense gas dispersions as low and wide clouds, and some of them allow the incorporation of complex terrain orography into the solution algorithm.

These models use both the Navier–Stokes equations and one-dimensional integral formulations. Generally, they require more computational time than integral models [34].

6.1.4 Computational Fluid Dynamics (CFD) Model

Computational Fluid Dynamics (CFD) models use the Navier–Stokes equations to provide three-dimensional and time-dependent solutions.

They can account for complex geometries and physical effects (such as dispersion patterns influenced by obstacles). The inclusion of these features, however, requires considerably greater computational time and resources compared to other modelling approaches, to obtain both numerical and graphical solutions. As for reliability, some CFD models have been validated using both experimental data and information derived from actual industrial accidents [34].

6.1.5 Overview of Modelling Tools

This section presents some of the most widely used modelling software tools for predicting the dispersion of substances and simulating their consequences. The list provided in Table 6.1 is not exhaustive but it includes the most employed tools in risk analysis.

When using computational tools to estimate the extent of damage areas, it is essential to provide both input and output reports of the models used. Furthermore, the principles and algorithms underlying the selected methods should be clearly described, together with a justification of their application to the specific case under study.

The resulting damage areas should be presented referenced to ground level (zero elevation) and, where possible, should also include a side view representation to better illustrate the spatial distribution of effects.

Table 6.1: Comparison of consequence modelling software tools.

Modelling capability	ALOHA	DNV Phast	TNO EFFECT	SAFETI	AERMOD	CALPUFF
Gas dispersion	Dense gas; Neutral gas	Neutral gas; Dense gas	Neutral gas	Neutral gas	Neutral gas	Neutral gas
Release types	Pool; Tank; Pipe; Direct	Pool; Tank; Jet; Pipe; BLEVE	Pool; Tank; Jet; Pipe; BLEVE	Pool; Tank; Pipe; Jet	Point; Surface; Volume; Multiple	Point; Linear; Surface; Volume
Release duration	Continuous / Instantaneous	Continuous / Instantaneous	–	Continuous / Instantaneous	Continuous	Continuous / Instantaneous
Indoor release	No	Yes (limited)	–	–	No	No
Maximum time	1 h	–	–	–	1 h – year	Up to 5 years
Maximum distance	10 km	20–30 km	30 km	30 km	50 km	Hundreds of km
Chemical reactions	No	–	–	–	First-order reactions for pollutants	Yes (for some)
Cost	Free	Commercial licence	Commercial licence	Commercial licence	Free	Free

6.2 Source Model

The choice of the term source is not trivial, as it depends on several factors such as the physical state of the substance, the release time scale (continuous and steady, continuous and unsteady, or instantaneous), and the type of equipment involved. For instance, losses may occur through a crack in a storage tank, in a pressurized or refrigerated system, or through a hole in a pipeline or valve.

The location of the release orifice is also a key element to consider. For example, in a tank containing a two-phase liquid–vapour system, the behaviour will differ depending on whether the rupture occurs in the liquid or in the vapour phase. Similarly, the release dynamics change if it occurs directly onto the ground, into water, or within a confined environment. All these parameters introduce uncertainties in the modelling process; therefore, particular care must be taken at this stage.

The source model characterizes the release scenario by providing information such as the release rate, the amount of material released, and its physical state, including possible flash phenomena, pool evaporation, or aerosol formation. The results obtained from this model serve as input data for the transmission (or dispersion) model, showing a clear interdependence between the two. In addition, source model outputs can be directly used in consequence models for jet fires and fireballs. The source models currently used for consequence assessment studies are reported in Table 6.2.

Table 6.2: Initiating events, conditions and corresponding source models.

Initiating event	**Condition**		**Source model**
Fire	Localized	Liquid phase	Tank fire Pool fire
		Gas/Vapor phase	Jet fire
	In air	Gas/Vapor phase	Fireball
Explosion	Confined		Runaway reaction Flammable gas/vapor mixtures Combustible dusts
	Unconfined		Flammable gas/vapor mixture (UVCE)
	Rapid phase transition		e.g. cryogenic liquids
Hazardous substance release	Liquid phase	In water	Liquid/liquid dispersion Liquid/liquid emulsification Liquid evaporation
		On soil	Dispersion Evaporation
	Gas/Vapor phase	High or low release velocity	Turbulent dispersion (cloud density lower than air) Gravitational dispersion (cloud density higher than air)

For each source model applied, it is essential to explicitly state all calculations and the process conditions considered, to ensure the traceability and reproducibility of the results. Transparency at this stage is critical, as undocumented simplifications or assumptions may compromise the accuracy of the subsequent dispersion modelling and, ultimately,

the reliability of the consequence assessment. Particular attention should also be given to the determination of the discharge orifice size, which represents one of the most sensitive parameters in defining the release scenario. Whenever specific technical references (such as guidelines, standards, or ministerial decrees) are available for the type of installation or release under consideration, these must be adopted in full, ensuring that their applicability conditions are verified against the case study. It is important to emphasize that such guidelines should be applied consistently and in their entirety: it is not methodologically sound to combine portions of different documents to derive the desired information, as this practice could introduce inconsistencies and undermine the technical validity of the results.

6.2.1 Identification of Isolatable Sections

Before carrying out the modelling and calculation phases within the consequence analysis, it is essential to accurately define the release scenario. A process unit is composed of numerous components, such as tanks, pipelines, valves, flanges, pumps, and heat exchangers. Therefore, it is crucial to determine where the hazardous substance is located within the plant and, consequently, where a Loss of Containment (Loss of Containment, hereafter referred to as LOC, not to be confused with Limiting Oxygen Concentration discussed in Chapter 3) may occur.

In general, a LOC can occur along pipelines or at connection points between pieces of equipment, such as flanges. However, precisely identifying the exact point of failure is extremely complex due to the extensive distribution of the equipment and the numerous possible failure modes. For this reason, it is standard practice to divide the plant into isolatable sections, defined at the locations of isolation devices, rather than attempting to identify every single potential leakage point.

The term Loss of Containment refers to the accidental release of material contained within a piece of equipment or pipeline into the surrounding environment. Such events can range from minor releases, such as fugitive emissions from seals, pump or compressor gaskets, or valves, to major releases resulting from pressurized vessel ruptures, process line breaks, or BLEVE (Boiling Liquid Expanding Vapor Explosion) events.

The subdivision of the plant into isolatable sections, also known as the Parts Count Section, is fundamental for the estimation of release frequencies and it is supported by technical guidelines, such as those issued by the International Association of Oil & Gas Producers (IOGP) [36]. The limits of isolatable sections are identified at the position of isolation valves, such as:

- ESD (Emergency Shut Down valves);
- PSV (Pressure Safety Valves);
- BDV (Blowdown Valves);
- LC (Locked Closed) and NC (Normally Closed);
- ROSOV (Remotely Operated Shut-Off Valves).

Figure 6.3 shows an example of plant sectioning. The boundary of each section corresponds to the isolation valves. For valves equipped with remote control or automatic closing mechanisms, it is important to consider that closure is not instantaneous. Therefore, when estimating the release duration, the time required for the activation signal to reach the actuator and for the operation to be completed must be included.

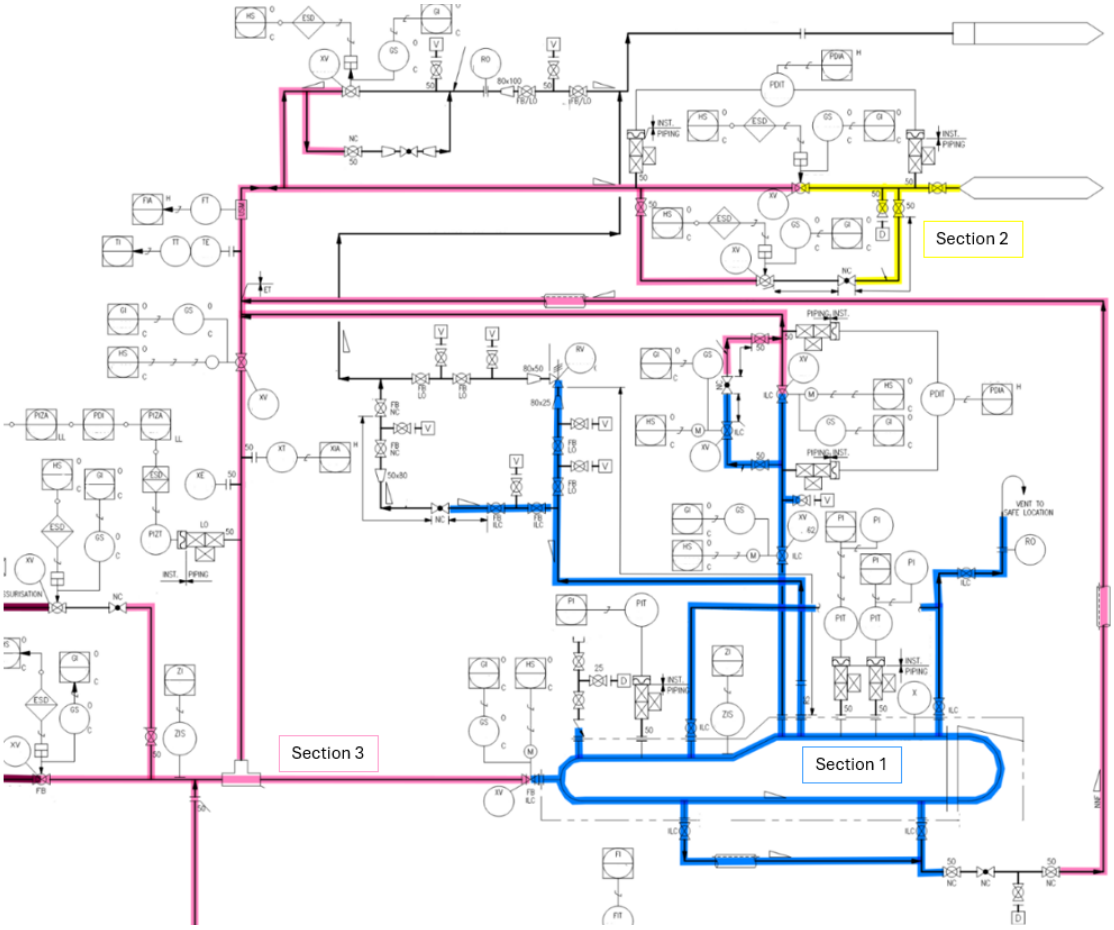

Figure 6.3: Example of sectioning.

For manually operated remote valves, the operator's intervention time must also be taken into account. Generally, full isolation of a section occurs within a range of 15 to 20 minutes, depending on both the plant complexity and the emergency systems in place. In long pipelines, valve closure cannot occur abruptly to avoid water hammer effects, which may significantly influence the release duration. Within each isolatable section, it is essential to distinguish between the fluid phases. For example, a tank containing both a liquid and a vapour phase should be divided into two subsections: an upper one containing vapour and a lower one containing liquid (Figure 6.4). This subdivision allows for a more accurate quantification of the potential release.

During release estimation, the following assumptions are generally applied:

- the released volume cannot exceed the total capacity of the tanks and pipelines included in the isolatable section;
- the release rate tends to decrease over time due to the progressive reduction of pressure upstream of the leak point [37].

Once the isolatable sections have been defined, the next step is to identify all the units within each section. A technical inventory is then compiled, including:

- unit name;
- substance contained;
- physical phase;
- operating temperature and pressure;
- chemical composition.

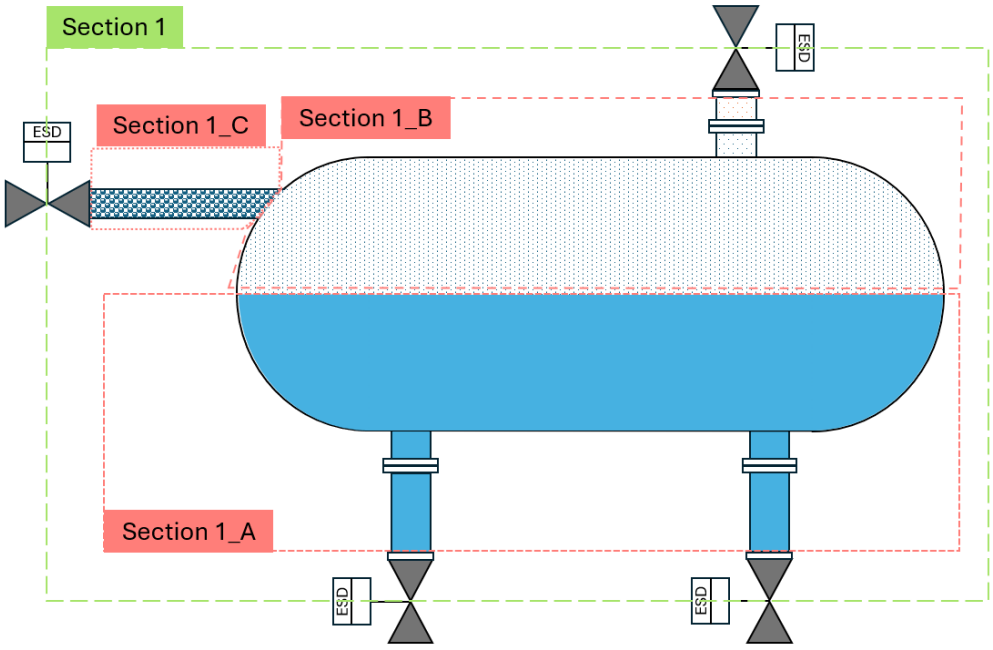

Figure 6.4: Section 1 is further subdivided into three subsections: Section 1_A for the liquid phase, Section 1_B for the gaseous phase, and Section 1_C for the two-phase mixture.

This data collection phase requires consultation of the following technical documentation:

- P&ID (Piping and Instrumentation Diagram);
- Heat & Material Balance (H&MB);
- Plant layout drawings;
- Cause & Effect Matrix.

The accuracy of this activity is essential to ensure the reliability of either the subsequent release modelling or the entire Quantitative Risk Assessment (QRA).

6.2.2 Physical State of the Substance

For an accurate evaluation of accidental scenarios, it is essential to identify the physical state of the substance or mixture at the time of release, based on thermodynamic principles. The most common types of release involve liquid, gas, vapor, or two-phase (liquid–vapor) flows, although in some cases the formation or presence of a solid may also occur.

Simulation software allows the prediction of phase behavior when the initial and final conditions are known. The final conditions are generally known, as they correspond to ambient temperature and atmospheric pressure at the time of the release. The initial conditions, on the other hand, may correspond to either normal operating conditions or an anomalous state reached by the system immediately before the release event [37]. Table 6.3 presents some typical accidental release scenarios that are frequently encountered in industrial facilities.

For example, in the case of a tank containing a liquid at ambient pressure and temperature, the position of the leak significantly affects the phase of the released material:

- if the hole is below the liquid level, the release will occur in the liquid phase;
- if the hole is above the liquid level, the release will occur as a two-phase mixture (liquid + vapor).

Gases can be stored in different ways; they are often liquefied by manipulating pressure and temperature. Depending on their physical state, gases can be classified as follows:

- Compressed gases. Gases that cannot be liquefied at ambient temperature and at a maximum operating pressure of 200 bar (e.g. oxygen and nitrogen);
- Liquefied gases. Gases that, at ambient temperature and at the maximum pressure allowed by the vessel, exist in equilibrium between liquid and vapor phases. To prevent overpressure and container damage, sufficient headspace must be provided for vapor expansion;

- Cryogenic liquefied gases. Compressed gases cooled below their boiling temperature, which is characteristic of each gas and typically below $-160\,^{\circ}\mathrm{C}$ (e.g. nitrogen, oxygen, nitrous oxide).

For liquefied gases, the location of the hole relative to the liquid level in the tank is crucial to determine the phase of the release:

- if the hole is well above the liquid level, the release occurs in the vapor phase;
- if the hole is just above the level, a two-phase mixture forms;
- if the hole is within the liquid region, the release is in the liquid phase.

Table 6.3: Typical release scenarios.

Release phase	**Scenario**
Liquid	Rupture or hole in a storage tank or pipeline operating at atmospheric pressure and containing a liquid phase. Rupture or hole in a tank or pipeline containing a pressurized liquid below its boiling point.
Gas	Hole in a pipeline or tank containing a gas under pressure. Discharge from a safety or process valve. Evaporation of volatile substances from a liquid pool. Formation of toxic combustion products following a fire. Leakage from the upper part of a pressurized tank containing liquid at the bottom and vapor in the headspace.
Two-phase	Hole in a pressurized storage tank or pipeline containing a liquid above its boiling point. Discharge from a safety or process valve.

6.2.3 Discharge Orifice Size

Another key parameter in the evaluation of accidental scenarios is the size of the discharge orifice, as it directly affects both the quantity and the release rate of the substance. In practice, three representative orifice sizes are generally considered: small, medium, and large.

From a consequence standpoint, it has been observed that intermediate sizes often lead to the most critical scenarios, since they allow the release of a significant quantity of material within a relatively short time. Conversely:

- small orifices result in limited but prolonged releases;
- large orifices cause rapid and intense releases, but of shorter duration.

The Italian Legislative Decree D.Lgs. 105/2015 does not provide specific guidance on how to determine the discharge orifice size, and no universally standardized methodology currently exists. Therefore, the approach generally relies on established good practice and criteria derived from the experience of risk analysts. Although not formally codified, these methodologies are widely recognized and applied in the industrial safety sector.

Several reference values are commonly adopted for practical estimations, as summarized below:

- some analysts assume an orifice diameter of 2 or 4 inches (i.e. 5.08 cm and 10.16 cm), regardless of the pipe diameter;
- for pressurized vessels, a complete rupture of inlet and outlet lines is often assumed, with a total release duration of 10 minutes;
- for pumps, the orifice size is generally associated with the diameter of the suction or discharge lines and can be assumed to be 5 mm, 25 mm, or 100 mm, depending on the specific case [38].

Table 6.4 and Table 6.5 present typical reference values used in consequence modelling for estimating the equivalent diameter of the discharge orifice based on pipeline size and equipment type.

Another useful reference for estimating the dimensions of discharge orifices is provided by the "Manual of Industrial Hazard Assessment Techniques", which reports empirical correlations derived from experimental and field data.

During the modelling phase, it is good practice to evaluate different orifice sizes corresponding to potential failure modes and to adopt, in accordance with the precautionary principle, the worst-case scenario for consequence assessment.

Table 6.4: Estimated discharge orifice diameter for pipelines with nominal diameter < 6 in.

Pipeline category	**in**	**cm**
DN < 6 in (15.24 cm)	0.2	0.508
	1	2.54
	4	10.16
	6	15.24

6.2.4 Release Duration

The release duration is another critical parameter in the simulation of an accidental scenario, as it significantly influences both the evaporation model and the dispersion model selected for the analysis.

Table 6.5: Typical discharge orifice diameters by pipe size [38].

Pipeline category	**Orifice diameter**			
Pipe < 1.5 in (3.81 cm)	5 mm			Total rupture
Pipe 2–6 in (5.08–15.24 cm)	5 mm	25 mm		Total rupture
Pipe 8–12 in (20.32–30.48 cm)	5 mm	25 mm	100 mm	Total rupture

The Italian Legislative Decree D.Lgs. 105/2015 does not provide specific guidance on how this parameter should be estimated. In the absence of regulatory references, good engineering practice suggests considering:

- the moment when the initiating event occurs (e.g. pipeline rupture, flange leak);
- the time required to activate mitigation measures, such as valve closure, pump shutdown, or the intervention of containment systems.

A useful reference for estimating release duration can be found in the Ministerial Decree of 15 May 1996, "Criteria for the analysis and evaluation of Safety Reports relating to liquefied petroleum gas (LPG) storage facilities." This document provides indicative average release durations for pipeline rupture events involving non-toxic hazardous substances, depending on the type of shutdown system installed:

- 20 – 40 s when motorized valves with automatic actuation are present;
- 1 – 3 min when motorized valves are equipped with emergency push-button controls located at several points within the facility;
- 3 – 5 min when motorized valves are operated manually from a single remote control point;
- 10 – 30 min when only manual valves are available.

These indicative times can be used as reference values in consequence modelling, provided that the specific characteristics of the plant and the actual operating conditions are taken into account. In every case, the duration of the release should be estimated in a realistic yet conservative manner, ensuring that the assumptions adopted reflect both the reliability of safety systems and the response time of operators during emergency situations.

6.3 Transmission Models

The transmission (or dispersion) model uses the information obtained from the source model, such as the type of substance released, its physical state, and the release conditions, to estimate the concentration of the substance within the resulting gas or vapour cloud and the extent of the area affected by the release.

As discussed in the previous section, the release may occur in a liquid, gaseous, or two-phase form. In the case of purely liquid substances, a phase change to the gaseous or aerosol state is required for the material to be transported through the atmosphere [38].

Dispersion models can be classified according to several criteria, including:

- buoyancy. Depending on the density of the released fluid, the dispersion can be classified as neutral, positively buoyant, or negatively buoyant;
- momentum: low or high initial momentum;
- source geometry: point, line, or area source;
- release duration: instantaneous (puff), continuous (plume), or intermediate;
- source elevation: ground level or elevated release;
- meteorological conditions: wind speed, atmospheric stability, temperature;
- topography: ground roughness, presence of obstacles or buildings, coastal or marine environments, and complex terrain [34].

When applying a transmission model, it is essential to justify all assumptions made in the selection of parameters and input data. Each parameter (e.g. wind speed, surface roughness, or atmospheric stability class) should be chosen carefully and supported by reliable information, as it can significantly influence the dispersion pattern and concentration profiles obtained.

6.3.1 Buoyancy

The buoyancy of a gas cloud depends on the density difference between the released gas and the surrounding air. Three main types of buoyancy can be identified:

- Neutral buoyancy: the gas has a density similar to that of air or a very low concentration. Such releases are often referred to as passive dispersions;
- Positive buoyancy: the gas is less dense than air and tends to rise quickly. This occurs with hot gases or substances with low molecular weight (e.g. hydrogen);
- Negative buoyancy: the gas is denser than air and tends to spread close to the ground. These are typically referred to as dense gases (e.g. chlorine). Over time, dense gases gradually mix with the surrounding air and may eventually behave like neutrally buoyant gases.

According to the ideal gas law, the density (ρ) of a gas depends on its temperature and molecular weight:

$$\rho = \frac{P \cdot MW}{R \cdot T} \tag{6.1}$$

where

ρ density;

P pressure;

MW molecular weight;

R universal gas constant;

T temperature.

The dispersion of neutrally or positively buoyant gases is well described by Gaussian models, in which atmospheric mixing is mainly driven by turbulence. In these cases, the contaminant concentration along the wind direction can be approximated by Gaussian profiles in both the horizontal and vertical directions.

Transport models can be either plume or puff models. Both allow the prediction of average concentrations and time-dependent profiles of flammable or toxic substances:

- the plume model describes a continuous release over time;
- the puff model represents a short-duration release compared to the sampling or transport time (Figure 6.5 , Figure 6.6).

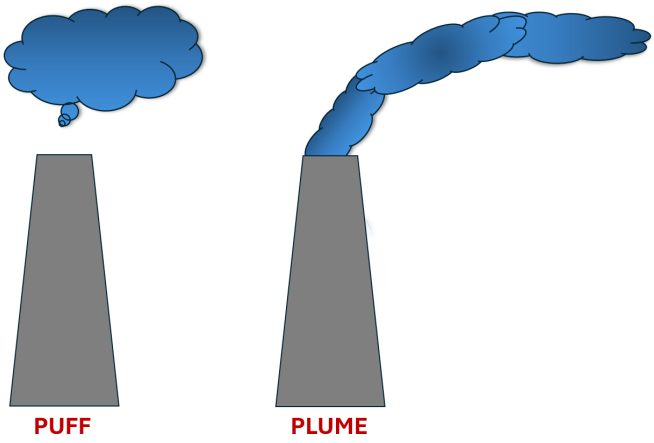

Figure 6.5: The puff represents an instantaneous release, while the plume corresponds to a continuous release.

A dense gas is a gas with a molecular weight higher than that of air or a lower temperature due to cooling during release or other thermodynamic processes. The dispersion behaviour of dense gases differs substantially from that of neutrally buoyant clouds.

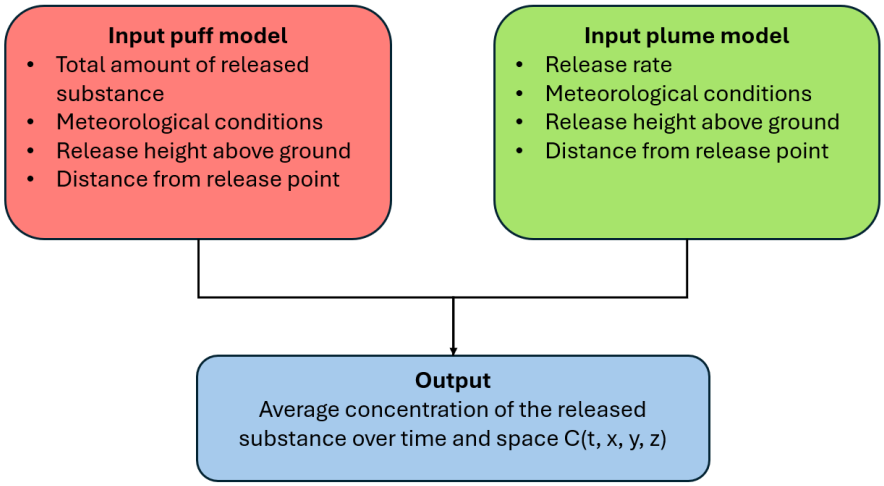

Figure 6.6: Input and output data for puff and plume dispersion models [37].

When a dense gas is released, it initially tends to move downward and spread along the ground, propagating both upwind and downwind. In the early stages, density effects may cause the cloud to flow uphill faster than it is transported downwind by the ambient wind. Although dense gases exhibit greater lateral spreading, they usually travel shorter distances than neutrally buoyant gases. For this reason, Gaussian models, which are commonly used for neutral gas dispersion, are not suitable for accurately describing the behaviour of dense gas clouds [37, 38].

6.3.2 Atmospheric Stability

The meteorological conditions during the release phase significantly influence the extent of the dispersion. In particular:

- stable atmosphere: minimal mixing and reduced dispersion;
- unstable atmosphere: increased turbulence and greater dispersion [37].

Atmospheric stability is classified according to the six Pasquill stability classes, indicated by the letters A to F (Table 6.6).

As shown in Table 6.6, the stability class is determined by both wind speed and solar radiation intensity. During the day, increasing wind speed and strong solar radiation, which heats the ground surface, promote unstable atmospheric conditions (e.g. class D). Conversely, during the night or under cloudy conditions, neutral or stable conditions (e.g. class F) typically prevail.

In the absence of site-specific meteorological data, standard conditions are conventionally adopted: stability class D with a wind speed of 5 m/s (D5), and stability class F with a wind speed of 2 m/s (F2), as established in Annex C, Section C.4.2 of D.Lgs. 105/2015.

Table 6.6: Meteorological conditions defined according to Pasquill's stability classes.

Surface wind speed	**Solar radiation intensity (daytime)**			**Cloud cover (night)**	
[m/s]	**Strong**	**Moderate**	**Slight**	**$\geq$ 50%**	**$<$ 50%**
< 2	A	A–B	B	E	F
2–3	A–B	B	C	E	F
3–5	B	B–C	C	D	E
5–6	C	C–D	D	D	D
> 6	C	D	D	D	D

A: Extremely unstable B: Moderately unstable C: Slightly unstable

D: Neutral E: Slightly stable F: Moderately stable

6.3.3 Wind Speed

The wind speed is a key factor influencing the dilution and transport of the released gas. As wind speed increases, the gas cloud is carried further downwind and becomes more diluted in the surrounding air. Wind speed and direction (i.e. the direction from which the wind originates) are typically represented using a wind rose.

Meteorological data are usually referenced to a height of 10 meters above ground level. Since wind velocity decreases significantly near the surface due to friction, corrections are required when the release occurs below this reference height [37].

The wind rose is divided into 16 sectors and it is based on three parameters: persistence, direction, and speed (Figure 6.7). Persistence represents the number of occurrences in which the wind blows from a specific direction during a defined period of time within a year.

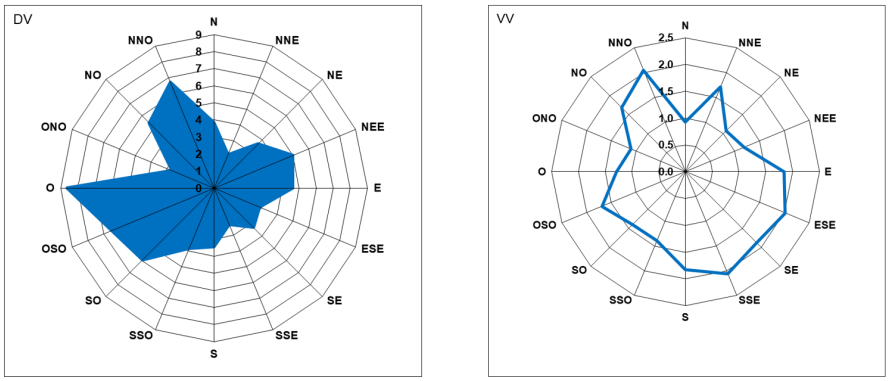

Figure 6.7: Example of a wind rose. The left side shows the wind direction as a percentage of occurrence, while the right side shows the wind speed in m/s.

6.3.4 Topography

The topographic characteristics of the terrain—such as surface roughness and the presence of obstacles, affect the degree of mixing during gas dispersion. For instance, dispersion behavior in a suburban area will differ from that in a densely built urban environment. The presence of buildings, vegetation, or irregular terrain increases turbulence and modifies the trajectory of the cloud, potentially enhancing dilution or, conversely, creating zones of recirculation and accumulation [37].

6.3.5 Source Height

The height of the release point above ground level influences the ground-level concentration of the gas downwind. As the source height increase:

- the ground-level concentration tends to decrease, since the plume has more opportunity to mix with the ambient air before reaching the surface;
- the distance of the maximum impact area (or deposition zone) increases (Figure 6.8).

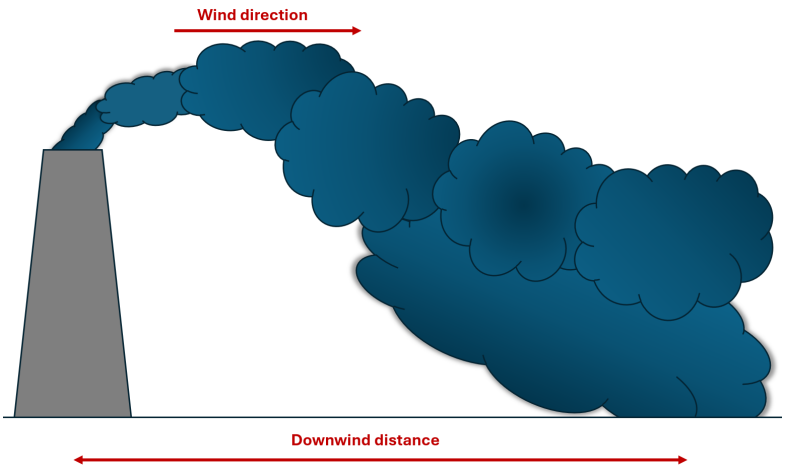

Figure 6.8: As the release height increases, the deposition distance becomes greater and the ground-level concentration decreases.

It should be noted that the release height primarily affects the ground-level concentration, while the concentration in the immediate downwind direction near the release point remains largely unchanged [38].

6.3.6 Geometry of the Release

In Gaussian dispersion models, the release is represented as a fixed point source. However, in real situations, release geometries are often more complex. Releases may take

the form of linear sources, such as the jet produced by a rupture or crack in a pressurized pipeline, or area sources, as in the case of a boiling liquid pool. Understanding the geometry of the release is essential, as it determines the initial dispersion characteristics, influences the momentum and buoyancy effects, and ultimately affects the concentration distribution in the atmosphere.

6.3.7 Momentum and Buoyancy

A plume generated by a dense gas release typically exhibits a combination of behaviors characteristic of both Gaussian dispersion and dense gas flow. In the initial phase, the release is dominated by the upward motion of the jet; subsequently, the plume begins to bend and descend due to its higher density compared to the surrounding air. At a certain distance from the release point, intense mixing with ambient air leads to cloud dilution, and the behaviour gradually approaches that of a neutrally buoyant gas.

Since in practice most releases occur in the form of jets rather than plumes, it is crucial to evaluate the influence of initial momentum and its interaction with ambient air on the jet behavior.

In the case of a neutrally buoyant jet, the vertical momentum remains nearly constant while the entrained mass increases with distance. As the exposed surface area grows, drag forces increase, and at a certain point the horizontal wind component becomes dominant, causing the jet to deflect in the direction of the airflow.

A positively buoyant jet is characterized by the predominance of buoyancy forces over the initial momentum, and thus tends to behave as a rising plume.

Conversely, in a negatively buoyant jet, the upward momentum is rapidly lost; once the maximum height is reached, the jet begins to descend, assuming the behavior of an inverted plume.

It is important to emphasize that there is no single combination of atmospheric stability and wind speed that universally represents the worst-case scenario. For example, F2 conditions (very stable atmosphere with low wind speed) typically produce long, narrow plumes. However, if the release occurs in a densely populated but spatially limited area, the plume width may be a more critical parameter than its length [37]. For this reason, risk analysts generally simulate several combinations of meteorological conditions to ensure a conservative assessment of potential impacts under various atmospheric regimes.

6.4 Consequence Models

The main consequences associated with an accidental release are fire, explosion, and toxic dispersion. Consequence models are used to estimate:

- the thermal radiation effects from fires;
- the overpressure and fragment projection effects from explosions;
- the toxic concentration levels from releases of hazardous substances.

Several models have been developed to represent different accidental scenarios depending on the physical state of the substance at the time of release (Figure 6.9):

- if the release occurs in the liquid phase, a flammable pool may form, potentially igniting and developing into a pool fire;
- if the released substance is a high-pressure flammable gas that ignites rapidly, a jet fire will occur. For instantaneous releases, the event results in a flash fire;
- the released gas is flammable at low pressure and does not ignite immediately, it may form a flammable vapour cloud that could ignite at a later stage.

As outlined in Chapter 3, explosions may originate from either physical or chemical phenomena.

A physical explosion occurs, for example, when a pressurized vessel ruptures, suddenly releasing the stored energy. A particular type of physical explosion is the BLEVE (Boiling Liquid Expanding Vapor Explosion), which occurs when a pressurized, superheated liquid is suddenly released to the atmosphere. If the released substance is flammable, a fireball may form.

Models used to estimate the consequences of a BLEVE are generally based on empirical correlations (e.g. fireball diameter, duration, and radiative fraction) and fundamental physical relationships (e.g. view factor, transmissivity).

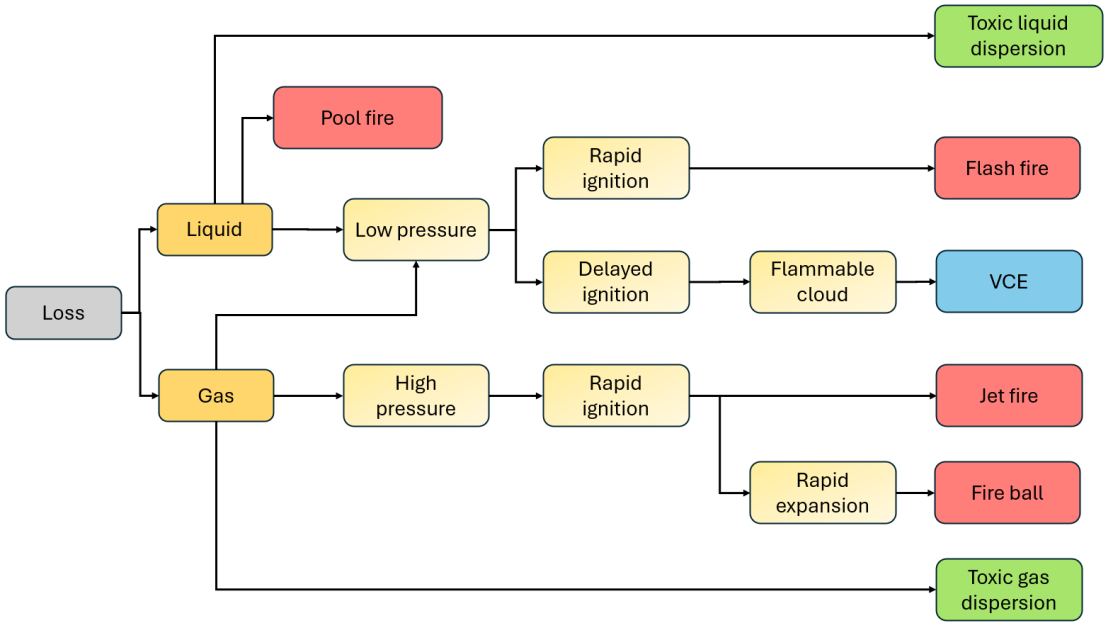

Figure 6.9: Likely accidental scenarios following the release of a liquid or gaseous substance.

Input parameters typically include: heat of combustion, vapour pressure, mass released, and atmospheric humidity. Errors in these parameters may lead to highly inaccurate results.

A VCE (Vapor Cloud Explosion) is another example of a physical explosion, occurring when a flammable gas cloud dispersed in air ignites before its concentration falls below the Lower Flammable Limit (LFL). Ignition often takes place at the edges of the cloud. The most commonly used models for vapour cloud explosions are summarized in Figure 6.10:

- TNT equivalency model: one of the earliest explosion models, which estimates the effects as if the explosion was equivalent to the detonation of a corresponding mass of TNT (trinitrotoluene). It is no longer recommended for modelling VCEs, as it does not account for combustion rate or flame acceleration.
- TNO Multi-Energy model: it assumes that only the confined portion of the cloud contributes to the explosion. It uses blast curves representing overpressure and impulse as functions of distance.
- Baker–Strehlow–Tang (BST) model: it employs blast curves that incorporate the flame speed, which depends on fuel reactivity, obstacle density, and degree of confinement.
- Computational Fluid Dynamics (CFD): CFD-based explosion models combine a transport model and an explosion model. They are time-dependent and provide more detailed results. CFD models are preferred when dealing with complex or confined geometries, such as offshore installations, although they require significant computational resources and a detailed geometric description of the domain [37].

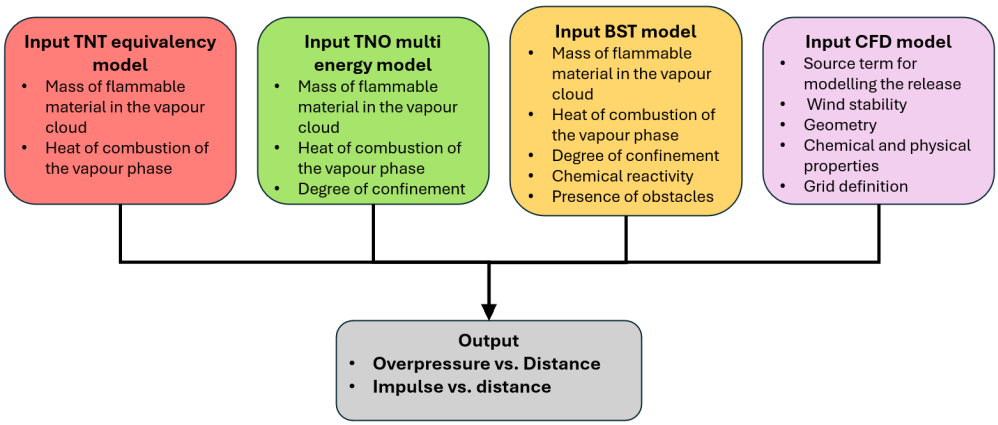

Figure 6.10: Comparison of input data required by the four models used to simulate a vapour cloud explosion [37].

6.5 Results

The evaluation of the effects of "credible" accidental scenarios on the potentially exposed population is carried out in terms of land-use planning compatibility, based on the threshold values established by the Ministerial Decree of 9 May 2001 – "Minimum safety requirements for urban and territorial planning in areas affected by major accident hazard establishments" (Table 6.7).

Table 6.7: Criteria for assessing the effects according to D.M. 9 May 2001.

Accidental scenario	**High lethality**	**Start of lethality**	**Irreversible injury**	**Reversible injury**	**Structural damage / domino effects**
	1	**2**	**3**	**4**	**5**
Fire (steady-state thermal radiation) [kW/m^2]	12.5	7	5	3	12.5
BLEVE / Fireball (time-varying radiation)	Fireball radius	350 kJ/m^2	200 kJ/m^2	125 kJ/m^2	200–800 m (*)
Flash fire (instantaneous radiation)	LFL	$\frac{1}{2}$ LFL			
VCE (peak overpressure) [bar]	0.3 (0.6 open space)	0.14	0.07	0.03	0.3
Toxic release (absorbed dose)	LC_{50} (30 min, hmn)		IDLH		

(∗) Depending on tank type.

As stated in D.M. 9 May 2001:

> The threshold values for fires (pool fire, jet fire) are expressed as incident thermal radiation power per unit area (kW/m^2). The numerical values refer to the likelihood of damage to unprotected individuals, initially located outdoors and directly exposed to the flames, while considering the possibility for a person to move away from the irradiated area under favorable conditions. The threshold value for structural damage represents a minimum limit, applicable to particularly vulnerable objects (e.g. atmospheric tanks, plastic-laminate panels) for long exposure times. For less vulnerable structures, higher values may be more appropriate, depending on exposure duration and material resistance.

The time-varying thermal radiation (BLEVE / fireball), typical of pressurized flammable liquid vessels, is characterized by a short-duration, high-intensity radiation lasting approximately 10–40 seconds, depending on the quantity involved. Because the duration of exposure significantly affects the expected damage, the physical effect must be expressed in terms of absorbed thermal dose (kJ/m^2).

For flash fires (instantaneous radiation), due to the very short exposure time (1–3 seconds), lethal effects are assumed to occur only within the flammable limits (LFL) of the cloud. However, sporadic lethal effects may occur slightly beyond the LFL, due to non-homogeneous flame fronts or local ignition pockets. Therefore, as a conservative assumption, the onset of lethality zone can be extended up to 1/2 LFL.

For Vapor Cloud Explosions (VCE), the reference threshold for high lethality (0.3 bar) mainly represents indirect lethality, caused by falls, impacts with obstacles, flying debris, or building collapse. In open areas without vulnerable structures, a threshold of 0.6 bar may be more appropriate, as it corresponds to direct lethality from the blast wave itself. Thresholds for irreversible and reversible injuries are related to distances where glass breakage and fragment projection are likely to occur.

The domino effect threshold (0.3 bar) takes into account the average range of projected fragments or objects capable of damaging tanks, equipment, or pipelines. The projection of large individual fragments from a VCE is generally considered a minor contributor to overall individual risk (unless domino effects occur), due to the limited area affected and low probability of human presence at the exact impact location.

Regarding toxic releases, the following parameters are typically adopted to determine the extent of damage zones for toxic gas or vapour dispersion:

- IDLH;
- LC_{50} (30 min, human).

If only LC_{50} values are available for non-human species or for different exposure times, they must be converted to human 30-minute reference values using the TNO method. The 30-minute exposure time is adopted as a conservative assumption, representing the maximum plausible duration of a release, pool evaporation, or cloud passage. Under favorable plant conditions (e.g. continuous monitoring, automatic alarms, remote shut-off systems, effective safety management), the operator may reasonably assume different exposure times, allowing the use of adjusted threshold values compared to those in Table 6.7.

It is essential to distinguish between: the release duration, which determines the total amount of substance emitted into the environment; and the exposure duration; i.e. the time during which an individual is directly in contact with a specific concentration.

When defining damage zones, the use of IDLH implies reversible effects, whereas methods based on toxic load or Probit functions imply acceptance of a certain lethality level (e.g. 1%, 3%, etc.). This choice greatly influences the extent of the damage area. Where available, the IDLH-based damage area must always be reported in the Safety Report.

For the definition of the Level of Concern (LOC) in external emergency planning, a minimum exposure time of 30 minutes with reversible health effects should be considered. The priority value to be used is 1/10 of the IDLH, although alternative parameters such as AEGL or ERPG may also be adopted. The results obtained from consequence modelling, compared against the threshold values established in D.M. 9 May 2001, are used to define the extent of the damage zones and to assess territorial compatibility.

Chapter 7

Risk Calculation and Evaluation

The final stage of the risk analysis process consists of risk evaluation, that is, combining the information related to the frequency and magnitude of the Top Events identified in the previous phases.

At this point, a large amount of data is available (concerning the likelihood of occurrence, the quantity of substance released, and the expected effects) which must be synthesized to support decision-making. The way in which the results are presented depends on the objective of the analysis. For instance: one may wish to compare the effectiveness of different mitigation measures; or to assess whether the risk level complies with a predetermined target or acceptability criterion.

The main approaches used to combine frequency and magnitude include:

- risk indices;
- risk matrices;
- individual risk;
- societal risk.

Risk can be expressed in terms of the number of injuries, fatalities, or economic losses expected within a given time interval. When the analysis focuses on safety aspects, the most relevant parameter is the number of fatalities per unit of time, resulting from events such as toxic releases, fires, or explosions. The calculation of the risk index (or simply risk) is conventionally expressed as:

$$R = P \cdot M \tag{7.1}$$

where

P is the probability (or frequency) of occurrence of the Top Event;

M is the magnitude or severity of its consequences.

7.1 Application within the Italian Regulatory Framework

Within the framework of risk analysis as required by D.Lgs. 105/2015, the explicit calculation of risk (i.e., the numerical combination of frequency and magnitude) is not required.

The Safety Report, prepared in compliance with Annex C of the decree, must include the identification of credible accident scenarios and the assessment of the corresponding damage areas, but not the quantitative evaluation of risk or the comparison with numerical acceptability criteria. Conversely, the risk calculation is applied in land-use planning, where it serves to assess the compatibility of territorial uses with the presence of Seveso establishments.

In this context, the regulatory reference is the Ministerial Decree of 9 May 2001, "Minimum safety requirements for urban and land-use planning in areas affected by establishments at risk of major accidents" (D.M. 9 maggio 2001).

The following Table 7.1 and Table 7.2, taken from this decree, define the compatible land-use categories as a function of the event probability class and the severity of the effects.

Table 7.1: Compatibility between Land-Use Categories and Establishments. (Reference: Table 3a of D.M. 9 May 2001).

Event	**Effect Categories**			
Probability Class	**High lethality**	**Start of lethality**	**Irreversible injury**	**Reversible injury**
$< 10^{-6}$	DEF	CDEF	BCDEF	ABCDEF
$< 10^{-4}$ - $< 10^{-6}$	ED	DEF	CDEF	BCDEF
$< 10^{-3}$ - $< 10^{-4}$	F	EF	DEF	CDEF
$> 10^{-3}$	F	F	EF	DEF

Table 7.2: Land-Use Categories (Reference: Table 1 of D.M. 9 May 2001)

Category	**Description**
A	1. Areas with predominantly residential use, where the building density index exceeds 4.5 m^3/m^2. 2. Places with concentration of people with limited mobility, e.g. hospitals, nursing homes, hospices, nurseries, primary schools, etc. (more than 25 beds or 100 persons). 3. Places subject to high outdoor crowding, e.g. permanent markets or other commercial destinations (more than 500 persons).

Category	Description
B	1. Areas with predominantly residential use, where the building density index ranges between 4.5 and 1.5 m^3/m^2. 2. Places with concentration of people with limited mobility (up to 25 beds or 100 persons). 3. Places subject to high outdoor crowding (more than 500 persons). 4. Places subject to high indoor crowding (more than 500 persons). 5. Places subject to crowding during limited exposure periods (more than 100 persons if outdoors, more than 1,000 if indoors). 6. Railway stations and other transport hubs (passenger flow greater than 1,000 persons/day).
C	1. Areas with predominantly residential use, where the building density index ranges between 1.5 and 1.0 m^3/m^2. 2. Places subject to high indoor crowding (more than 500 persons). 3. Places subject to crowding during limited exposure periods (more than 100 persons if outdoors, up to 1,000 if indoors; any size if used no more than weekly). 4. Railway stations and other transport hubs (passenger flow greater than 1,000 persons/day).
D	1. Areas with predominantly residential use, where the building density index ranges between 1.0 and 0.5 m^3/m^2. 2. Places subject to crowding with exposure no more than once per month, e.g. fairs, periodic markets, cemeteries.
E	1. Areas with predominantly residential use, where the building density index is below 0.5 m^3/m^2. 2. Industrial, craft, agricultural, and livestock facilities.
F	1. Area within the boundaries of the establishment. 2. Adjacent area where there are no buildings or structures intended for the regular presence of groups of people.

7.2 Risk Indices

Risk indices include a range of techniques, such as the "index method" of Chapter 4. These methods are generally simple and intuitive, often derived from simplified versions of more complex analytical approaches. In some cases, indices are expressed as numerical values presented in tabular form, possibly associated with a unit of measure; in other cases, they are dimensionless parameters used to classify different levels of risk, such as in the Dow Fire and Explosion Index.

Some examples of commonly used risk indices include:

- Dow Fire and Explosion Index (F&EI): estimates the relative risk associated with fire and explosion hazards;
- Dow Chemical Exposure Index (CEI): evaluates the risk related to the release and dispersion of toxic substances;
- Average Rate of Death (ARD): determines the average number of fatalities per unit of time.

Further details and additional examples can be found in the technical literature. The main limitations of risk indices are the lack of absolute criteria to determine whether a risk is acceptable or not, and their inability to provide the same level of detail achievable through quantitative measures of individual or societal risk [38].

7.3 Risk Matrix

The risk matrix is a useful tool that provides a graphical representation of risk through a matrix combining frequency and magnitude (Figure 7.1).

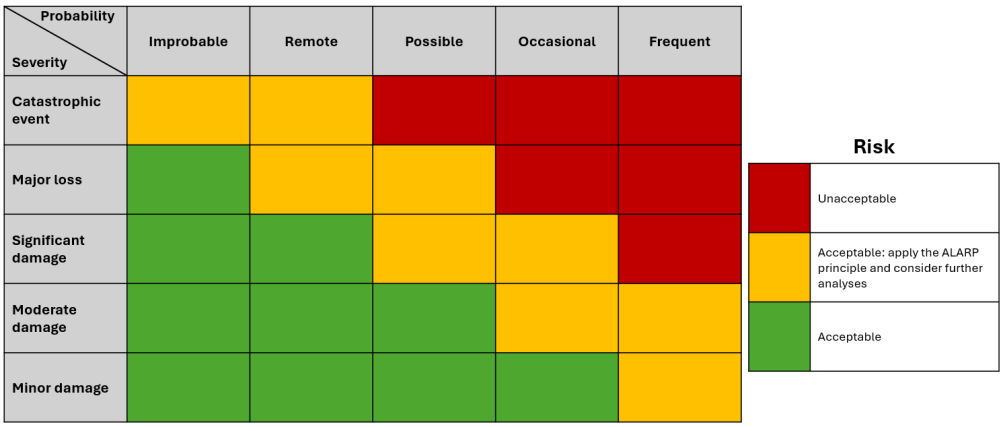

Figure 7.1: Example of a Risk Matrix.

There are no defined standards regarding the size of the matrix or the labelling of its axes. In general, the axes represent frequency and severity of damage. Each parameter is divided into several levels or classes, which can be expressed either by letters (e.g., A, B, C, etc.) or by numbers (e.g., 1, 2, 3, etc.) (see Table 7.3 and Table 7.4). The number of cells may range from as few as four to as many as thirty-six or more. Cells can be grouped to reduce the number of risk categories; however, a smaller number of classes may provide insufficient information for identifying appropriate protection measures, whereas an excessive number of classes may make the matrix more complex and difficult to use.

Table 7.3: Example of consequence classes for accident scenarios.

Damage Class	Definition of the Class
A	High lethality near the release point (5–15 m); onset of lethality within plant boundaries.
B	High lethality within the plant boundaries; onset of lethality within the establishment boundaries; irreversible injuries outside the establishment but within a multi-company site (if present).
C	High lethality within the establishment; onset of lethality near non-bunkered offices and control rooms; potential domino effects on large tanks and tall structures; irreversible injuries outside the multi-company site (if present).
D	High lethality in external industrial areas; onset of lethality outside the multi-company site (if present).
E	High lethality in non-industrial areas outside the multi-company site; events causing overpressures exceeding the design pressure of bunkered control rooms; domino effects on large liquefied storage tanks; onset of lethality on protection systems (e.g., fire-fighting pumps) or on nearby residential areas.

Table 7.4: Example of frequency classes for accident scenarios.

Frequency [events/year]	Definition	Class
$F \geq 10^{-3}$	Non-negligible scenario	F1
$10^{-4} \leq F < 10^{-3}$	Unlikely scenario	F2
$10^{-5} \leq F < 10^{-4}$	Rare scenario	F3
$10^{-6} \leq F < 10^{-5}$	Very rare scenario	F4
$F < 10^{-6}$	Extremely rare scenario	F5

The risk matrix is particularly applied in semi-quantitative and qualitative analyses. In semi-quantitative analyses, the frequency of occurrence is expressed in terms of events per year, while consequences are represented by a numerical level indicating the severity of the outcome, from the least severe (level 1) to the most severe.

An example of a risk matrix is shown in Figure 7.1. Each identified accident scenario is evaluated according to a pair of parameters (frequency and consequence) and placed within one of the three regions of the risk matrix. Depending on its position, the risk can be considered tolerable or may require the implementation of an improvement plan aimed at reducing the identified risk level.

A scenario located in the red region indicates an unacceptable risk, requiring the immediate shutdown of the activity. A scenario in the yellow region may require an ALARP study (As Low As Reasonably Practicable), with the objective of adopting additional mitigation measures. However, a risk in this zone is not necessarily unacceptable: if

further reduction is technically unfeasible or would involve a disproportionate economic effort compared to the expected benefit, it may be deemed tolerable. Risks located in the green region are considered acceptable, and therefore no additional mitigation actions are required [27].

7.4 Individual Risk

Individual risk represents the probability that a person, located in the immediate vicinity of a hazard source, will suffer harm. It can be evaluated with reference to:

- the most exposed individual;
- groups of people present in a hazardous area;
- an average individual located within a risk area.

Based on these approaches, several ways of expressing individual risk are defined:

- Individual risk contour: it indicates the frequency with which harmful events may occur at a specific location, regardless of whether a person is actually present there. Risk is represented by means of a map showing the spatial distribution of risk, assuming that a person remains continuously at that point throughout the year (8,760 hours).
- Maximum individual risk: it indicates the highest risk level to which a person may be exposed, such as a plant operator or a resident living near the industrial area.
- Average individual risk for the exposed population: it represents the mean value of individual risk calculated only for those actually exposed. This measure is meaningful if the risk is uniformly distributed.
- Average individual risk for the total population: it represents the average risk calculated for a predefined population, even if not all individuals are truly exposed. If the considered population is too large, the average risk may be underestimated.
- Time-weighted average individual risk: it takes into account the amount of time an individual is exposed to the hazard during the working day.

The unit of measurement of individual risk is [1/year]. Depending on the purpose of the analysis, individual risk can be expressed in various forms:

$$IR_{x,y} = \sum_{i=1}^{n} IR_{x,y,i} \tag{7.2}$$

where

$IR_{x,y}$ individual risk at the geographical point (x,y) (expressed as frequency of fatality per year);

$IR_{x,y,i}$ individual risk at point (x,y) resulting from the i-th accident scenario (expressed as frequency of fatality per year);

n total number of accident scenarios considered in the analysis.

The term $IR_{x,y,i}$ can be expressed as:

$$IR_{x,y,i} = f_i \cdot P_{F_i} \cdot P_i \tag{7.3}$$

where

f_i frequency of the i-th event (occurrences/year), derived from frequency estimation;

P_{F_i} probability that the effects of the i-th event cause a fatality at the geographical point (x,y);

P_i weighting factor accounting for release directionality, meteorological conditions, and other scenario-specific parameters.

To visualize individual risk, two main tools are commonly used (Figure 7.2):

- Iso-risk curves (individual risk contours): lines connecting points with the same risk level on a map. They help identify sensitive areas such as schools, hospitals, or residential zones. When the effects of the accident are symmetrically distributed, the contours appear circular (radial risk), as in the case of BLEVEs. When the intensity varies spatially, the contours become irregular (directional risk), as in the dispersion of toxic substances influenced by wind direction and atmospheric stability.
- Risk profile: a two-dimensional representation of individual risk as a function of the distance from the source. This approach is applicable when:
  - the hazard source can be approximated as a point;
  - the risk distribution is symmetrical in all directions [38]

The procedure to determine the iso-risk curves includes the following steps:

1. Divide the study area into a grid (25 m × 25 m cells for distances below 300 m, and 100 m × 100 m cells for larger distances).
2. Identify the coordinates of the accident source.
3. Determine the frequency of the event.
4. Define meteorological data: stability class and corresponding probability. Typically, a value of 0.8 is assumed for class D and 0.2 for class F.
5. Establish the probability of wind direction for each sector (wind rose) (P_w). For scenarios generating thermal radiation, P_w=1 is usually assumed.

6. Determine the probability of the accident scenario.
7. Calculate the impact area of the event for each stability class and wind direction.
8. Compute the overall individual risk at each grid point.

These calculations are typically carried out using dedicated computational software. The obtained results must then be compared against risk acceptability criteria recognized by technical or regulatory standards.

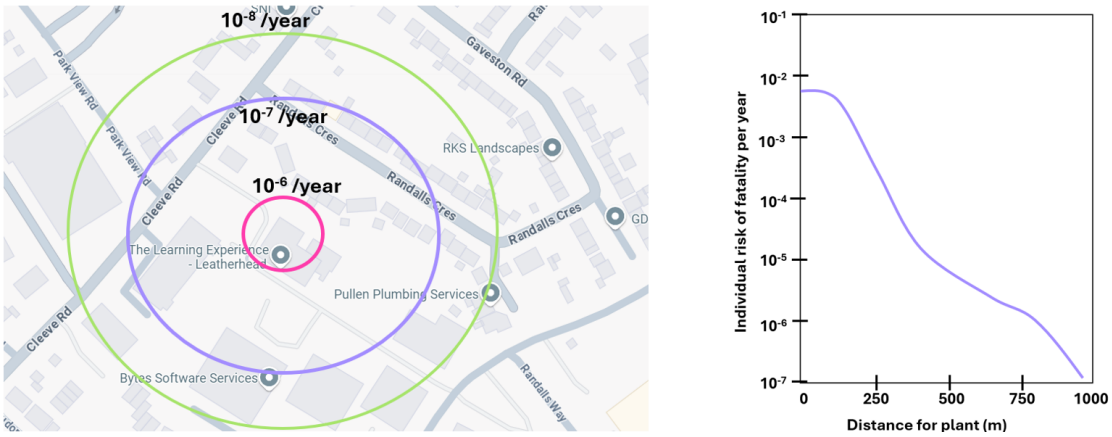

Figure 7.2: On the left: example of iso-risk curves. On the right: example of a risk profile.

7.5 Societal Risk

The evaluation of societal risk is generally considered a complementary technique to the assessment of individual risk. Although this methodology is widely applied in Anglo-Saxon countries, its implementation within the Italian national context remains rather limited.

Societal risk represents a measure of the risk associated with a group of people exposed to a specific hazard. Its estimation requires the same basic input data used for individual risk (namely, the frequency of accident scenarios and their associated consequences) but the processing method differs. As a result, individual risk and societal risk cannot be directly derived from one another. In addition to frequency and consequence data, the calculation of societal risk requires the definition of the exposed population, including:

- the density and geographical distribution of the population;
- the type of population involved (e.g., residential, school, industrial);
- the probability of presence, i.e. the number of hours per day during which people are located within the hazardous area.

Societal risk is typically represented using F–N curves (Frequency–Number of fatalities) (Figure 7.3). These curves are obtained by plotting the cumulative frequency of accident scenarios against the number of fatalities. Given the wide variability in both frequency and the potential number of victims, a logarithmic scale is normally adopted [38].

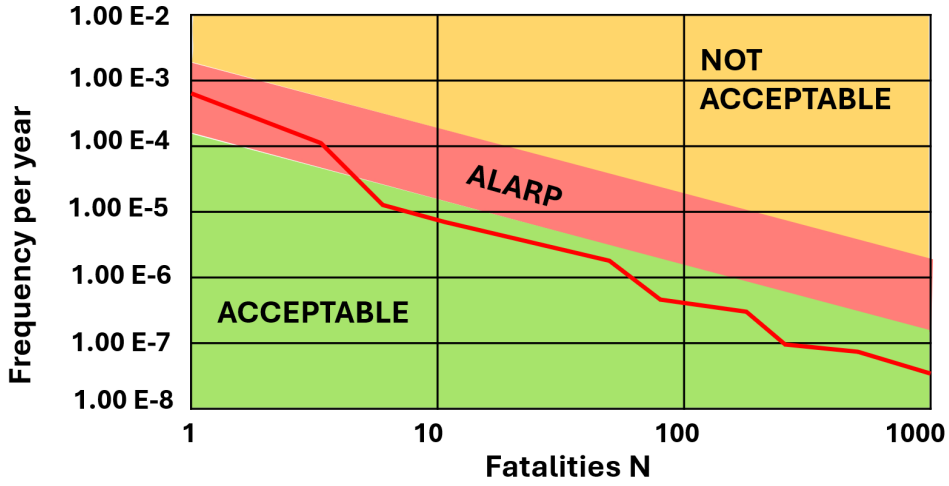

Figure 7.3: Example of an F–N curve.

The number of fatalities N_i associated with each i-th accident scenario is calculated according to the following expression:

$$N_i = \sum_{i=1}^{n} p_{x,y,i} \cdot P_{F_i} \cdot P_i \tag{7.4}$$

where

$p_{x,y,i}$ number of people located at the geographical point (x,y);

P_{F_i} probability that the effects of the i-th event cause a fatality at point (x,y);

P_i factor associated with the event, accounting for release directionality, meteorological conditions, and other contextual elements.

Chapter 8

Case Study

This chapter presents a case study involving three substances that are frequently present in installations subject to the Seveso Directive: ammonia, chlorine, and methane.

The objective is to analyze how differences in calculation models and simulation assumptions can influence the estimation of the hazard areas associated with the dispersion of hazardous substances.

It is important to clarify that the purpose of this case study is not to assess the quality or reliability of the software used, nor to determine which of them provides the most accurate results. The comparative analysis is conducted solely for academic and research purposes, with the aim of highlighting how the choices made in scenario definition and the assumptions adopted by the risk analyst can lead to different outcomes in terms of the extent of the impact areas.

Since the simulation results are strongly affected by the input data, an effort was made, where possible, to maintain comparable initial and meteorological conditions among the different software tools, in order to ensure a neutral and consistent comparison.

8.1 Modelling Software Used

For the simulations, the software tools used were ALOHA (version 5.4.7), PHAST (version 9.1), and ADAM (version 3). A brief description of each tool is provided below.

8.1.1 ALOHA

ALOHA (Areal Locations of Hazardous Atmospheres) is a program jointly developed by the National Oceanic and Atmospheric Administration (NOAA) – Office of Response and Restoration – and the Environmental Protection Agency (EPA) – Office of Emergency Management.

The software allows simulation of toxic gas dispersion, fires, and explosions, providing a threat zone corresponding to concentration levels exceeding specific threshold values known as Levels of Concern (LOCs).

ALOHA is based on Gaussian dispersion models and can simulate short-duration scenarios ranging from one minute up to one hour, with a maximum distance of approximately 10 km. It can model several types of release events, including BLEVEs, flash fires, jet fires, pool fires, and vapor cloud explosions.

8.1.2 PHAST

PHAST (Process Hazard Analysis Software Tool) is a commercial consequence modeling package originally developed in 1989 by the company Technica and later acquired by DNV in 1992. It was initially designed as the consequence engine of SAFETI, a software developed for the Dutch Government to assess major hazard facilities under the Seveso Directive.

PHAST can simulate a wide range of complex accidental scenarios involving releases, fires, and explosions, but its correct use requires a solid understanding of the underlying modeling assumptions. The software employs integral models, specifically the Unified Dispersion Model (UDM), which provides a continuous description of the different phases of dispersion, including jet release, dense gas behavior, and passive dispersion.

8.1.3 ADAM

ADAM (Accident Damage Analysis Module) is a software tool developed by the Joint Research Centre (JRC) of the European Commission to assess the physical effects and damages associated with industrial accidents resulting from unintended releases of hazardous substances. It was designed to assist EU Competent Authorities in implementing the Seveso Directive.

For atmospheric dispersion, ADAM uses the SLAB model, a well-established and validated approach primarily applied to heavy gas clouds but also suitable for neutral or lighter-than-air gases. The model accounts for different types of releases (evaporating puddle, horizontal or vertical jets, instantaneous sources) and solves spatially averaged conservation equations for mass, momentum, and energy.

Depending on the release characteristics, dispersion can be modeled as a steady-state plume (for continuous releases) or as a transient puff (for instantaneous or finite-duration releases), ensuring a consistent representation of the transition between the active release and subsequent cloud dispersion.

8.2 Description of Substances and Accident Scenarios

For the simulation of the accidental scenarios, three representative substances commonly found in establishments covered by the Seveso Directive were selected: chlorine, ammonia, and methanol.

It should be noted that all input data are hypothetical and do not refer to any specific facility. The purpose of this study is purely comparative, aiming to evaluate how the extent of the hazard areas may vary depending on the mathematical model applied and on the selected input parameters.

The scenarios modelled are as follows:

- Scenario 1: pressurized chlorine release due to tank rupture;
- Scenario 2: ammonia release resulting from a full-bore pipe failure;
- Scenario 3: methanol release caused by a tank fissure and subsequent pool formation in the loading bay, followed by ignition.

Before running the simulations, it is essential to collect all relevant physicochemical information about the substances involved, typically available in the Safety Data Sheets (SDS).

8.2.1 Chlorine

Under ambient conditions, chlorine (Cl_2) is a yellow-green gas with strong oxidizing properties. In contact with moisture, it reacts to form hydrochloric acid and hypochlorous acid, both highly corrosive. Facilities handling chlorine must adopt specific operational procedures and mitigation systems to minimize accidental releases. In the event of a release, chlorine vapors can be scrubbed using water sprays, and the resulting contaminated water should be collected and neutralized with sodium hydroxide solution to prevent pollution of sewers or surface waters.

According to Regulation (EC) No 1272/2008 (CLP), chlorine is classified as reported in Table 8.1. Chlorine is also listed among the hazardous substances in Annex I, Part 2 of

Table 8.1: Substance classification under Regulation (EC) No 1272/2008 (Annex VI, Table 3.1).

Hazard Class and Category	**Hazard Statement**
Press. Gas	-
Ox. Gas 1	H270: May cause or intensify fire; oxidizer
Skin Irrit. 2	H315: Causes skin irritation
Eye Irrit. 2	H319: Causes serious eye irritation
Acute Tox. 3 (inhalation)	H331: Toxic if inhaled
STOT SE 3	H335: May cause respiratory irritation
Aquatic Acute 1	H400: Very toxic to aquatic life

Legislative Decree 105/2015, as shown in Table 8.2. Human exposure to concentrations below 15 ppm generally causes irritation of the nasal, ocular, and throat mucosa without significant clinical effects. At concentrations above 30 ppm, symptoms such as respiratory burning, coughing, rhinorrhea, and lacrimation may occur. Prolonged exposure can lead to delayed effects such as pulmonary edema, bronchopneumonia, and, in severe cases, lung abscess.

Table 8.2: Classification of the substance according to Legislative Decree 105/2015 (Annex 1, Part 2).

Hazardous Substance	CAS Number	Lower-Tier Quantity (t)	Upper-Tier Quantity (t)
10.Chlorine	7782-50-5	10	25

8.2.2 Anhydrous Ammonia

Under ambient conditions, ammonia (NH_3) is a colorless gas with a strong, pungent odor. It is generally marketed either as a liquefied gas under pressure or as an aqueous solution at various concentrations.

Ammonia is both toxic and flammable: in confined spaces, it can form explosive mixtures with air, while in open environments the vapor cloud may behave as a heavy gas due to the cooling caused by rapid evaporation. Similarly to chlorine, in the event of an accidental release, vapors should be suppressed using water spray systems. However, a collection and neutralization system for the contaminated water must be provided to prevent pollution of surface waters or sewage networks.

According to Regulation (EC) No 1272/2008 (CLP), anhydrous ammonia is classified as shown in Table 8.3. Ammonia is also listed among the hazardous substances in Annex 1, Part 2 of Legislative Decree 105/2015, as shown in Table 8.4.

Table 8.3: Substance classification under Regulation (EC) No 1272/2008 (Annex VI, Table 3.1).

Hazard Class and Category	Hazard Statement
Press. Gas	–
Flam. Gas 2	H221: Flammable gas
Skin Corr. 1B	H314: Causes severe skin burns and eye damage
Acute Tox. 3 (inhalation)	H331: Toxic if inhaled
Aquatic Acute 1	H400: Very toxic to aquatic life

Table 8.4: Classification of the substance according to Legislative Decree 105/2015 (Annex 1, Part 2).

Hazardous Substance	CAS Number	Lower-Tier Quantity (t)	Upper-Tier Quantity (t)
35. Anhydrous Ammonia	7664-41-7	50	200

When in contact with moisture, ammonia reacts to form ammonium hydroxide (NH_4OH), which is responsible for its caustic effects on skin and mucous membranes. Exposure causes immediate irritation of the eyes and respiratory tract, and severe cases may lead to bronchospasm or pulmonary edema. Systemic effects can appear several hours after exposure, making prolonged medical observation advisable.

8.2.3 Methanol

Under ambient conditions, methanol (CH_3OH) is a colorless liquid. It is a toxic and highly flammable substance; its vapors are heavier than air and may accumulate near the ground, forming explosive mixtures in confined spaces. As for the other substances, a collection and treatment system for contaminated water must be provided in case of spills or fires to prevent environmental contamination. According to Regulation (EC) No 1272/2008 (CLP), methanol is classified as shown in Table 8.5. Methanol is also listed among the hazardous substances in Annex 1, Part 2 of Legislative Decree 105/2015, as shown in Table 8.6.

Table 8.5: Classification of the substance according to Regulation (EC) No 1272/2008 (Annex VI, Table 3.1)

Hazard Class and Category	**Hazard Statement**
Flam. Liq. 2	H225: Highly flammable liquid and vapor
Acute Tox. 3 (oral)	H301: Toxic if swallowed
Acute Tox. 3 (dermal)	H311: Toxic in contact with skin
Acute Tox. 3 (inhalation)	H331: Toxic if inhaled
STOT SE 1	H370: Causes damage to organs

Table 8.6: Classification of the substance according to Legislative Decree 105/2015 (Annex 1, Part 2).

Hazardous Substance	**CAS Number**	**Lower-Tier Quantity (t)**	**Upper-Tier Quantity (t)**
22. Methanol	67-56-1	500	5000

Acute exposure may cause headache, nausea, visual disturbances, dizziness, and loss of consciousness; in severe cases, it can lead to permanent blindness and respiratory failure.

8.3 Modelling of the Accident Scenarios

For the simulation of the three accident scenarios, the same input parameters were used across the three software tools, as far as possible, to ensure comparability of the results.

All simulations were carried out under standard ambient conditions, assuming two representative meteorological combinations: stability class F with wind speed of 2 m/s (stable conditions) and stability class D with wind speed of 5 m/s (neutral conditions).

8.3.1 Scenario 1 – Pressurized Chlorine Release

This scenario involves the accidental release of pressurized chlorine. Under these storage conditions, chlorine is maintained in a liquefied state. The postulated event assumes the occurrence of a fissure in the tank wall, leading to the discharge of the liquefied chlorine and the subsequent formation and dispersion of a toxic vapor cloud in the atmosphere.

The main input parameters adopted for the dispersion modelling are summarized in Table 8.7. These input data were used consistently across all three software tools (ALOHA, PHAST, and ADAM) in order to ensure comparability of the results. The dispersion simulations were performed under the same meteorological conditions and with equivalent assumptions regarding the release geometry and boundary parameters.

Toxic concentrations were evaluated with reference to the IDLH values for chlorine. Two thresholds were considered, 10 ppm and 30 ppm, corresponding respectively to the lower and upper reference concentrations commonly adopted in toxic dispersion analyses.

The outcomes of the simulations, including the cloud footprints and the toxic concentration contours obtained from each model, are presented and discussed in Section 8.4.1.

8.3.2 Scenario 2 – Pressurized Ammonia Release

The second scenario concerns the release of pressurized anhydrous ammonia following a leak in a process pipeline connected to the storage tank. The accidental discharge is assumed to occur through an orifice of 50 mm diameter located on the pipeline at an elevation of 1 m above ground level. The simulations were carried out under two representative meteorological conditions:

- stability class F, wind speed 2 m/s (stable conditions);
- stability class D, wind speed 5 m/s (neutral conditions).

For the assessment of toxic effects, an IDLH value of 300 ppm was adopted as the reference concentration threshold (Table 8.8).

Table 8.7: Input data for Scenario 1 (pressurized chlorine release).

Substance	
Substance	Chlorine
Storage Conditions	
Storage pressure	5.5 bar
Temperature	18.5 °C
Volume	30 m^3
Mass	42,365 kg
Tank Geometry	
Type	Horizontal
Length	8.22 m
Diameter	2.41 m
Leak Geometry	
Orifice diameter	45 mm
Elevation	1 m
Discharge coefficient (C_d)	0.88
Meteorological Conditions	
Stability class (wind speed)	F (2 m/s)
	D (5 m/s)
Toxicity Parameter	
IDLH	10 ppm
	30 ppm

Table 8.8: Input data for Scenario 2 (pressurized ammonia release).

Substance	
Substance	Ammonia
Storage Conditions	
Storage temperature	15 °C
Pressure	6.25 bar
Volume	180 m^3
Mass	111,006 kg
Tank Geometry	
Type	Horizontal
Length	15 m
Diameter	4.3 m
Leak Geometry	
Orifice diameter	50 mm
Elevation	1 m
Meteorological Conditions	
Stability class (wind speed)	F (2 m/s)
	D (5 m/s)
Toxicity Parameter	
IDLH	300 ppm

8.3.3 Scenario 3 – Release of methanol

This scenario considers the accidental release of methanol stored in an atmospheric tank under ambient temperature and pressure conditions. The loss of containment is assumed to occur through an orifice located near the bottom section of the tank, resulting in the discharge of liquid methanol and the subsequent formation and dispersion of a flammable vapour cloud.

As in the previous two cases, simulations were performed under two representative meteorological conditions in order to ensure comparability of results:

- stability class F with wind speed of 2 m/s (stable conditions).
- stability class D with wind speed of 5 m/s (neutral conditions).

The main input data adopted for the modelling are summarized in Table 8.9.

Table 8.9: Input data for Scenario 3 (Release of methanol).

Substance	
Substance	Methanol
Storage Conditions	
Storage pressure	1.13 bar
Temperature	20 °C
Volume	25 m^3
Mass	19,800 kg
Tank Geometry	
Type	Horizontal
Length	10 m
Diameter	1.95 m
Leak Geometry	
Orifice diameter	45 mm
Elevation	0.3 m
Discharge coefficient (Cd)	0.62
Meteorological Conditions	
Stability class (wind speed)	F (2 m/s)
	D (5 m/s)
Toxicity Parameter	
IDLH	6000 ppm
	600 ppm

8.4 Result

8.4.1 Results for the Pressurized Chlorine Release Scenario

Chlorine is initially stored in the liquid phase inside the pressurized vessel. Following the rupture of the tank wall, the liquid is released through the opening. Considering that chlorine has a boiling point of $-34.4\,^{\circ}\mathrm{C}$, at the moment of the release, when it is suddenly exposed to atmospheric pressure, it undergoes rapid vaporization.

This phase transition is accompanied by the absorption of latent heat from the surrounding air, which consequently cools down together with the nearby surfaces. In the early stages of the release, the resulting cloud consists of a two-phase mixture of chlorine vapor, fine liquid droplets, air, and condensed water droplets formed due to the humidity of the air and ground.

Part of the liquid chlorine may also form a pool on the ground; the subsequent evaporation of this pool further contributes to the cooling of both the liquid and the underlying surface.

All three software tools used for the modelling account for this physical behaviour by describing the two-phase release that occurs upon depressurization of the vessel. This phase involves the simultaneous presence of liquid and vapor chlorine during the initial stage of the release, which significantly affects the mass flow rate, the jet temperature, and consequently the subsequent dispersion of the toxic cloud. The release phase is independent of meteorological conditions.

According to PHAST, the discharge occurs with an initial release rate of 58.69 kg/s and an exit velocity of 103 m/s. The total release duration is approximately 722.5 seconds, during which a mass of about 42,000 kg is discharged, corresponding to the entire tank inventory (see Figure 8.1).

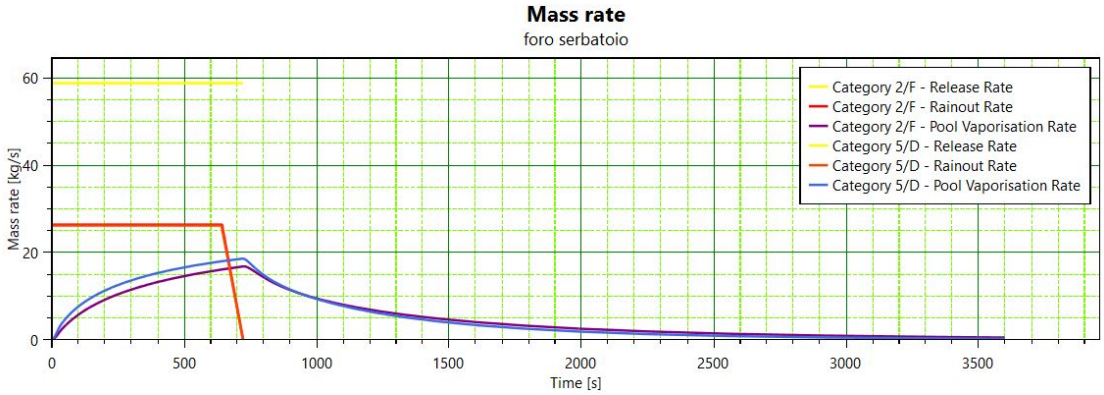

Figure 8.1: Time evolution of release rate, rainout rate, and pool vaporization rate simulated with PHAST for the pressurized chlorine release.

In ALOHA, the release rate is estimated to be 2,360 kg/min (39.3 kg/s), with a total release duration of 25 minutes (1500 s) (see Figure 8.2).

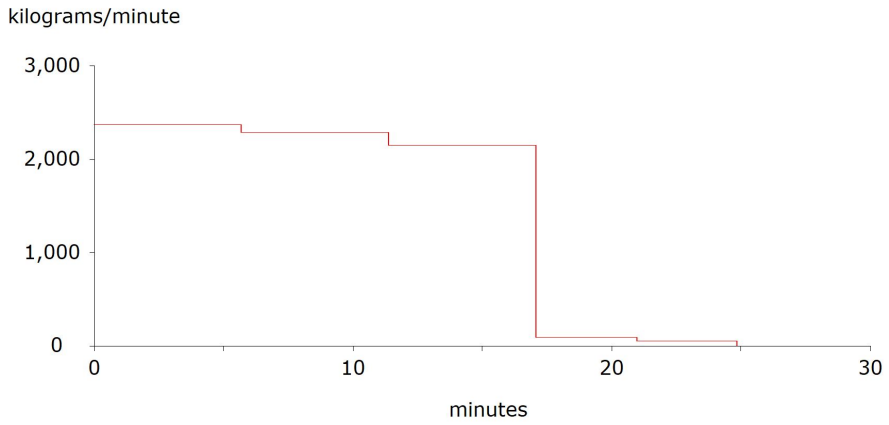

Figure 8.2: Release rate profile simulated with ALOHA for the pressurized chlorine release.

In ADAM, the release rate varies over time, as shown in Figure 8.3. The total duration of the release is about 1,700 seconds. During the first 493 seconds, the effluent is mainly in the liquid phase, with a release rate ranging between 55 and 52 kg/s. The total mass released is approximately 29,000 kg.

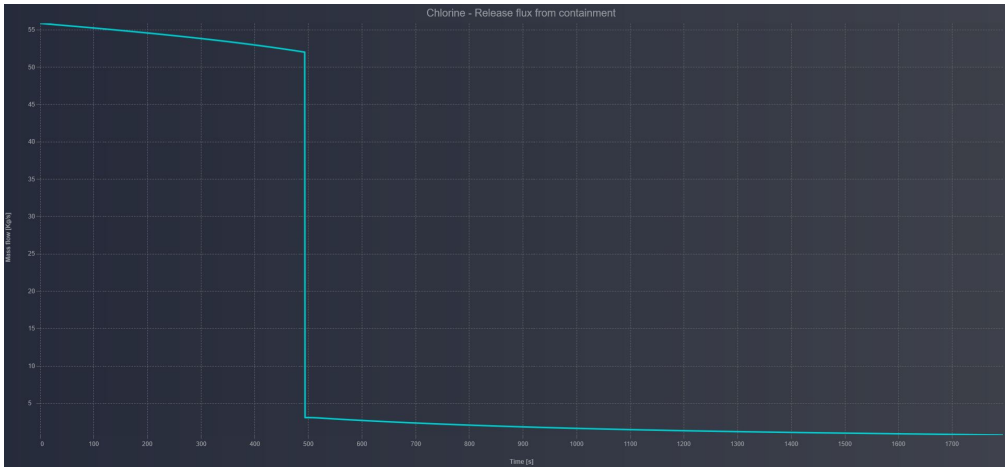

Figure 8.3: Time evolution of the release flux simulated with ADAM for the pressurized chlorine release.

All three models describe the release as a two-phase discharge (liquid and vapor) resulting from the depressurization of the vessel, but they differ in how they represent the flashing and rainout dynamics. PHAST predicts a faster and complete release, whereas ALOHA and ADAM estimate longer durations and smaller total masses due to differences in their physical modelling approaches.

Table 8.10 summarizes the main results of the discharge phase obtained from the three software tools. These findings emphasize that the modelling of the discharge phase, and in particular the treatment of two-phase flow and flashing phenomena, strongly affects the predicted conditions at the source term and thus the subsequent toxic dispersion. After the discharge phase, the dispersion phase begins, during which the chlorine pool

Table 8.10: Summary of the main release-phase results obtained from the three software tools.

Result	**PHAST**	**ALOHA**	**ADAM**
Mass rate [kg/s]	58.69	39.3	55-52
Time of release [s]	722	1,500	1,700
Total amount release [kg]	42,000	39,258	28,798

rapidly evaporates, forming a dense gas cloud. The dispersion is strongly influenced by meteorological conditions, particularly wind speed and atmospheric stability class.

In PHAST, the maximum cloud extent occurs under 2F conditions (wind speed 2 m/s, stability class F), reaching a distance of approximately 13,000 m for the 10 ppm concentration (Figure 8.5). Under 5D conditions (wind 5 m/s, class D), the maximum distance is around 5,600 m (Figure 8.4). PHAST also provides a side view of the cloud at the end of the release phase: as shown in Figure 8.6 and Figure 8.7, for a concentration of 10 ppm the cloud reaches a maximum height of about 100 m and a downwind distance of 4,100 m.

In ALOHA, the maximum toxic cloud extent is also obtained under 2F conditions, where the 10 ppm concentration reaches a distance greater than 10 km. ALOHA truncates the graphical output at the 10 km limit (Figure 8.9). In addition, the software displays wind direction confidence lines, which represent the region where, about 95% of the time, the chemical cloud is expected to remain, considering typical variations in wind direction. At lower wind speeds, the wind direction fluctuates more, and these confidence lines widen, forming a circular pattern when the wind is very weak.

In ADAM, similar results are obtained: the maximum cloud extent occurs under 2F conditions, with the 10 ppm concentration reaching a distance exceeding 17 km (Figure 8.11). Like PHAST, ADAM provides a side view of the cloud (Figure 8.12 and Figure 8.13), which allows evaluation of its vertical development and shape. Figure 8.10 - Figure 8.13 present the results for the two meteorological scenarios considered.

Table 8.11 summarizes the results obtained with the three software tools. It should be noted that, in both PHAST and ADAM, the concentration was calculated at an elevation of 0 m, i.e. at ground level. Although dispersion simulations are often performed at a reference height of 1.7 m (the typical human breathing zone), this assumption would underestimate the affected area in the case of dense gases such as chlorine, which tend to remain close to the ground. Therefore, the reference height was set to 0 m to more accurately represent the actual behaviour and spread of the toxic cloud near the surface.

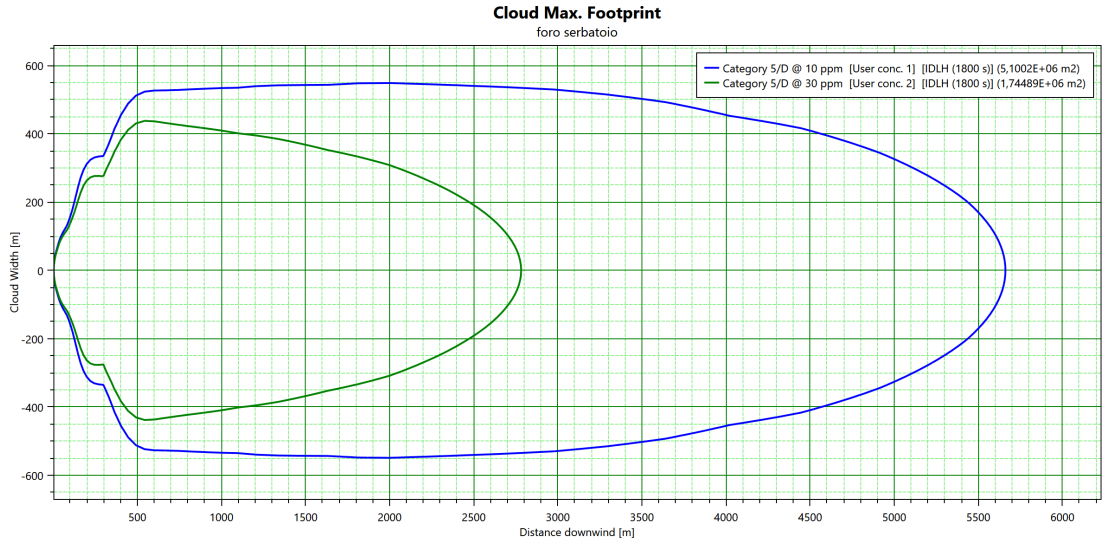

Figure 8.4: Cloud Max Footprint of chlorine dispersion with a wind speed of 5 m/s and stability class D, simulated with PHAST.

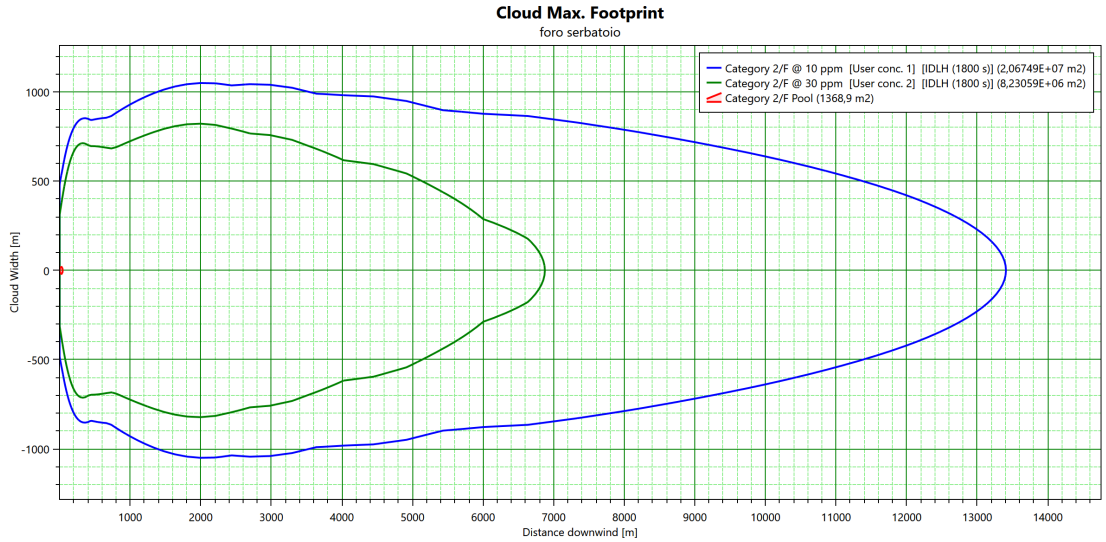

Figure 8.5: Cloud Max Footprint of chlorine dispersion with a wind speed of 2 m/s and stability class F, simulated with PHAST.

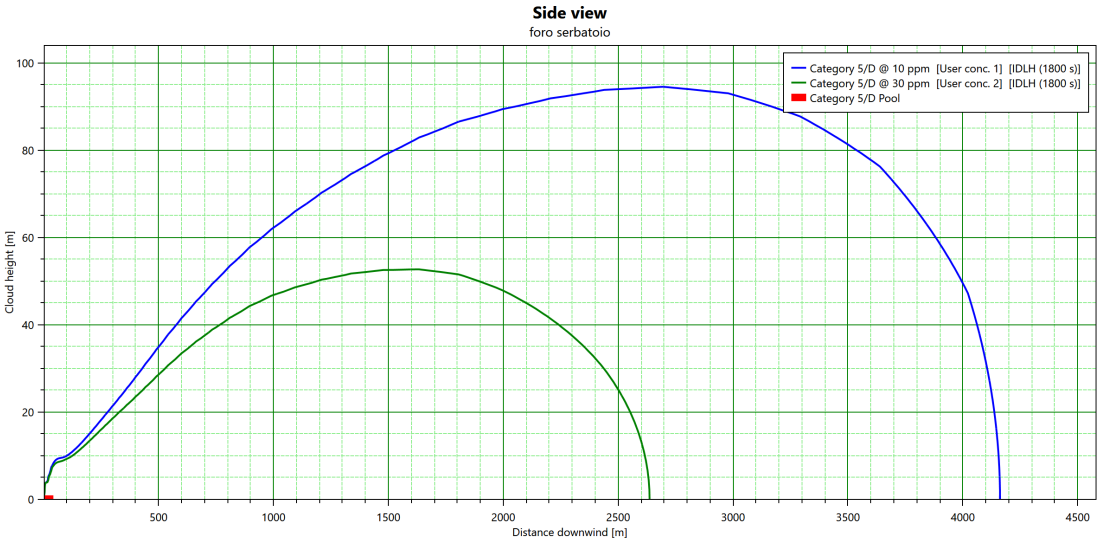

Figure 8.6: – Side view of the chlorine cloud for a wind speed of 5 m/s and class D at t=722s, simulated with PHAST.

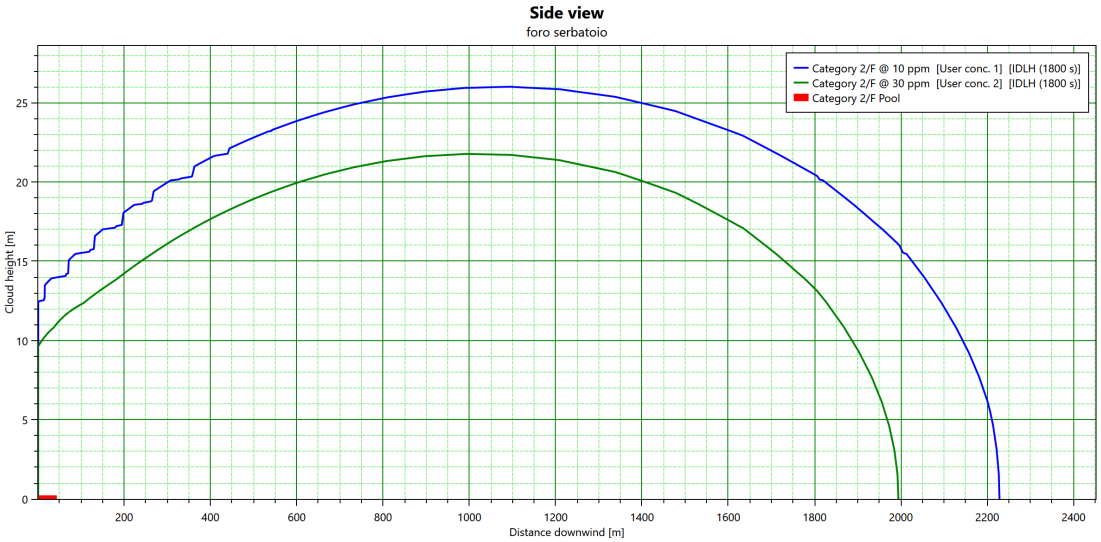

Figure 8.7: Side view of the chlorine cloud for a wind speed of 2 m/s and class F at t=722 s, simulated with PHAST.

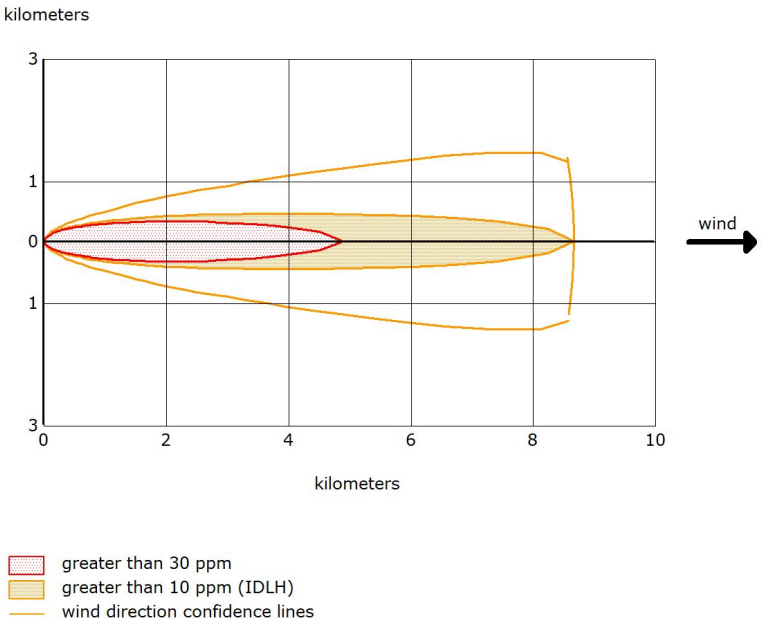

Figure 8.8: Chlorine dispersion with a wind speed of 5 m/s and stability class D, simulated with ALOHA.

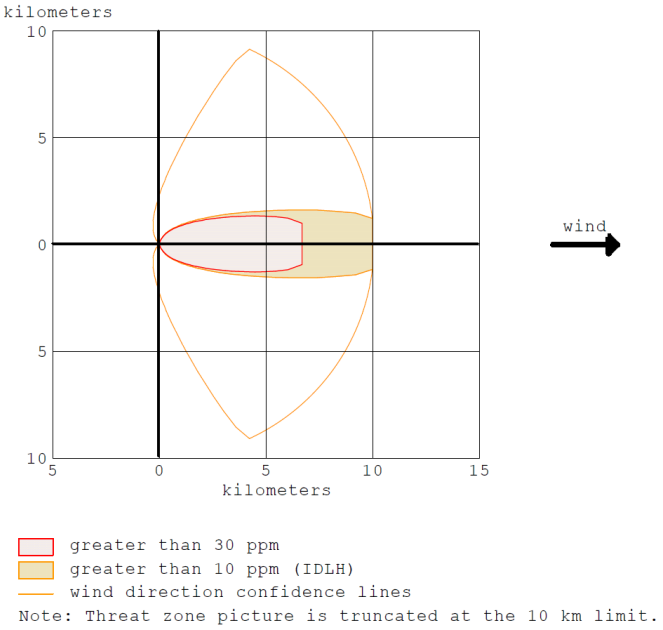

Figure 8.9: Chlorine dispersion with a wind speed of 2 m/s and stability class F, simulated with ALOHA.

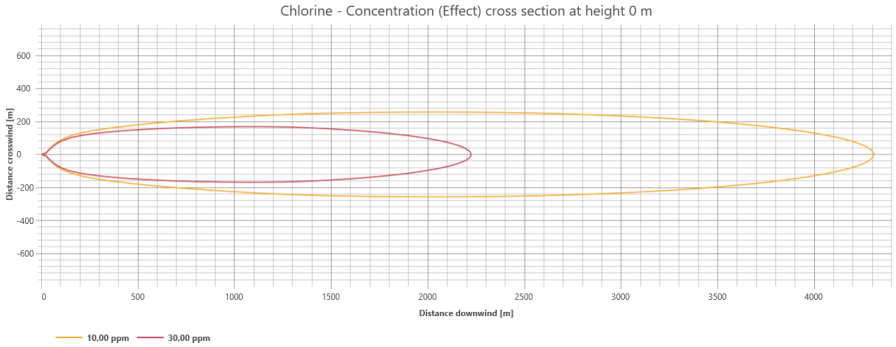

Figure 8.10: Chlorine dispersion with a wind speed of 5 m/s and stability class D, simulated with ADAM. The red contour represents the 30 ppm concentration and the yellow contour the 10 ppm concentration.

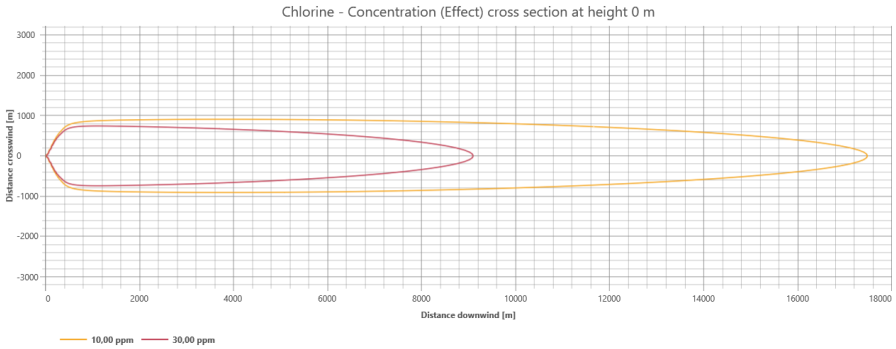

Figure 8.11: Chlorine dispersion with a wind speed of 2 m/s and stability class F, simulated with ADAM. The red contour represents the 30 ppm concentration and the yellow contour the 10 ppm concentration.

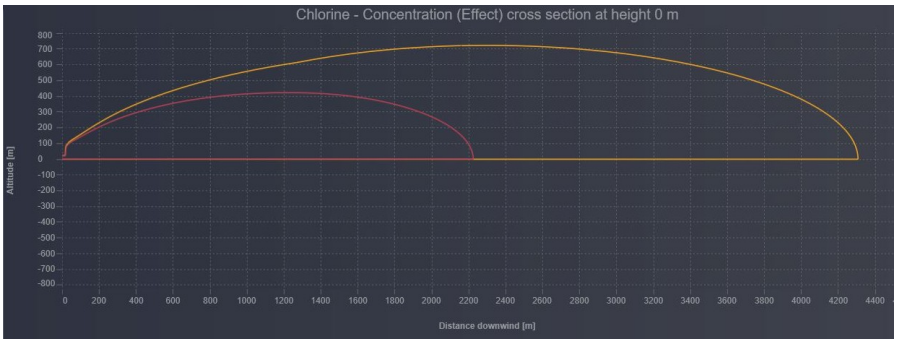

Figure 8.12: Side view of the chlorine dispersion (wind speed 5 m/s, stability class D) corresponding to Figure 8.10.

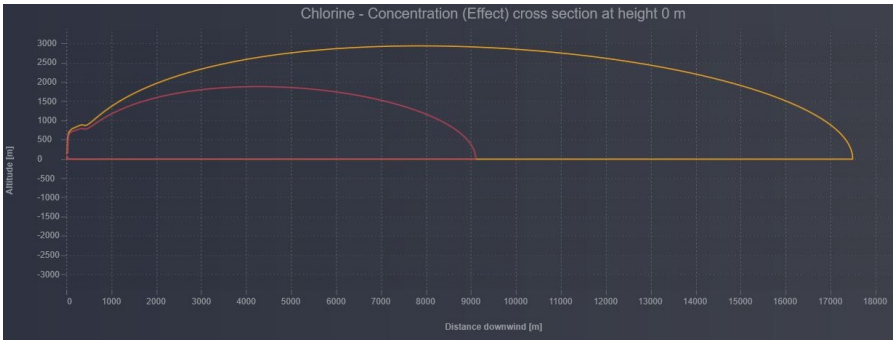

Figure 8.13: Side view of the chlorine dispersion (wind speed 2 m/s, stability class F) corresponding to Figure 8.11.

Overall, the results show that the atmospheric stability class and wind speed strongly affect the extent of the chlorine cloud. Under stable conditions (Class F), all models predict a wider and longer-lasting cloud due to reduced atmospheric mixing and lower turbulence. Quantitative differences among the models arise from their different treatments of two-phase flashing, rainout phenomena, and dense gas dispersion algorithms. In particular, ADAM predicts the largest downwind distances for the 10 ppm threshold, PHAST provides intermediate values, while ALOHA reaches its graphical limit of 10 km; therefore, the actual cloud extent may exceed this distance but cannot be fully represented within the model output.

Since the results of the damage area extent directly influence land-use planning and territorial compatibility assessments, the dispersion results for the 2F stability class, which produced the largest impact areas, were selected for mapping. The map illustrates the potential spread of the toxic cloud from the release point, showing how it could reach nearby residential zones or sensitive receptors such as schools, nurseries, hospitals, and other public facilities (Figure 8.14).

Table 8.11: Downwind distances [m] for 10 ppm and 30 ppm chlorine concentrations obtained with PHAST, ALOHA, and ADAM under different meteorological conditions.

Model	**Weather condition 5D**		**Weather condition 2F**	
	10 ppm	30 ppm	10 ppm	30 ppm
PHAST	5,661	2,781	13,407	6,875
ALOHA	8,800	4,900	$> 10,000$	6,700
ADAM	4,306	2,223	17,486	9,097

(a) Predicted impact area under stability class 2F calculated with PHAST.

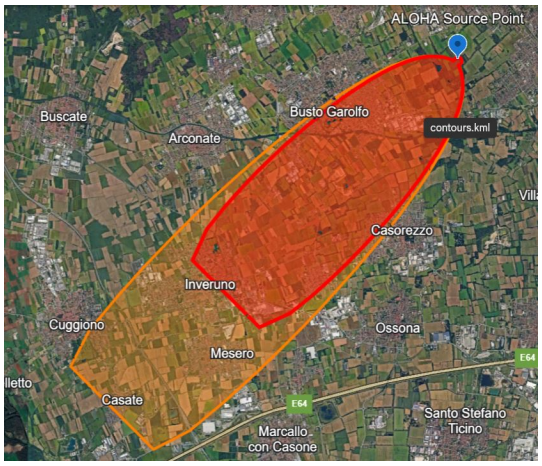

(b) Predicted impact area under stability class 2F calculated with ALOHA.

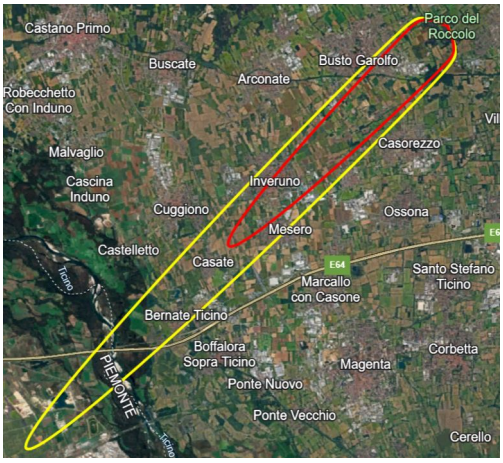

(c) Predicted impact area under stability class 2F calculated with ADAM.

Figure 8.14: Impact areas under stability class 2F, obtained from the three modelling tools (PHAST, ALOHA, and ADAM).

8.4.2 Results for the Pressurized Ammonia Release Scenario

The simulation of the ammonia release scenario aimed to evaluate the dispersion behavior of a toxic cloud generated by the sudden leak of pressurized anhydrous ammonia from a process pipeline connected to the storage tank. The results were expressed in terms of downwind distances corresponding to the reference toxic threshold (IDLH = 300 ppm) and are illustrated in the following figures and tables.

As for the chlorine case, the atmospheric stability class and wind speed significantly influence the extent of the ammonia cloud. Under stable conditions (Class F, 2 m/s), all models predict a larger and more persistent cloud due to reduced atmospheric mixing and lower turbulence. Conversely, under neutral conditions (Class D, 5 m/s), the predicted affected area is considerably smaller, as enhanced dispersion promotes faster dilution of the gas.

Although ammonia is lighter than air under ambient conditions, in this case the release occurs under pressure and involves rapid flashing of the liquid, producing a cold and temporarily dense vapor cloud. As a result, all models treat the dispersion as a dense gas behavior in the near field, with subsequent transition to a buoyant plume as the cloud warms and mixes with ambient air.

The boiling temperature of ammonia is $-33.3\,^{\circ}\mathrm{C}$, therefore, when released from a pressurized pipeline under the storage conditions considered, rapid flashing takes place. As a result, the cloud initially behaves as a dense, cold mixture consisting of ammonia vapor, liquid droplets and ambient air.

In PHAST, the release rate remains almost constant at approximately 8.68 kg/s, with a total release duration of 3,600 s (1 h), until the storage tank is fully depleted. The total released mass is about 31,200 kg, and the jet exit velocity is approximately 207 m/s (Figure 8.15).

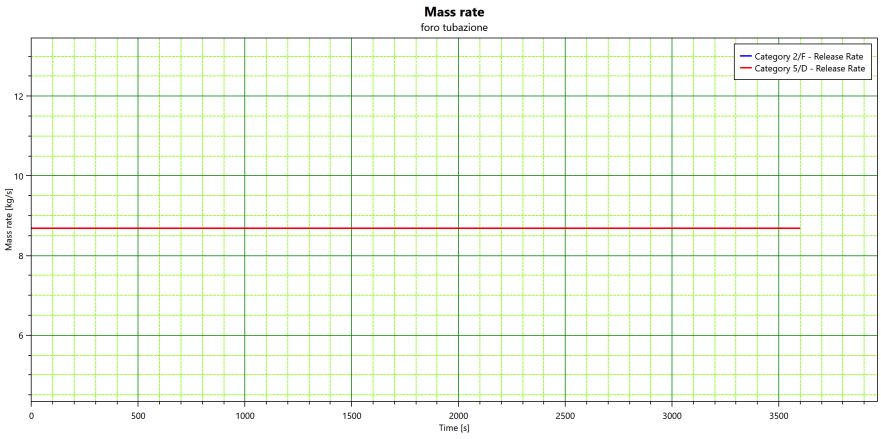

Figure 8.15: Time evolution of release rate simulated with PHAST for the pressurized ammonia release.

In ALOHA, the mass flow rate is 646 kg/min (equal to 10.77 kg/s). The release duration is also set to 1 hour, since the software does not allow simulating longer releases (Figure 8.16). The total mass discharged is approximately 38,800 kg.

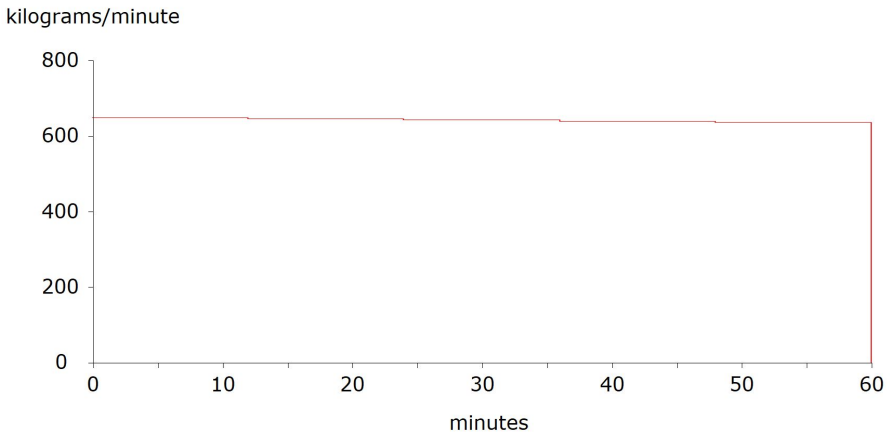

Figure 8.16: Release rate profile simulated with ALOHA for the pressurized ammonia release.

In ADAM, the release rate decreases gradually over time due to the pressure decay inside the equipment. The release lasts 1,800 s (30 min) and the total discharged mass is approximately 12,400 kg (Figure 8.17).

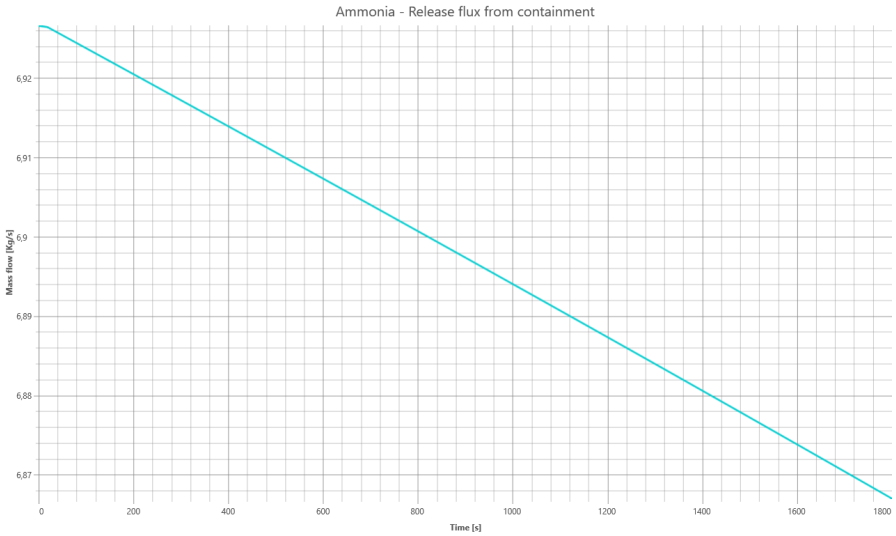

Figure 8.17: Time evolution of the release flux simulated with ADAM for the pressurized ammonia release.

In both PHAST and ADAM, ammonia remains in liquid phase at the release point due to rapid flashing. Table 8.12 summarizes the release-phase results obtained from the three software tools.

Table 8.12: Summary of the main release-phase results obtained from the three software tools.

Result	**PHAST**	**ALOHA**	**ADAM**
Mass rate [kg/s]	8.68	10.76	6.9 – 6.87
Time of release [s]	3,600	$> 3{,}600$	1,700
Total amount release [kg]	31,248	38,760	12,414

The dispersion phase results for the pressurized ammonia release scenario were evaluated using PHAST, ALOHA and ADAM. The analysis was performed for the toxic concentration threshold of 300 ppm (IDLH), under the two meteorological conditions considered: stability class D with 5 m/s wind speed and stability class F with 2 m/s wind speed.

PHAST predicts that the behavior of the ammonia cloud is initially governed by dense gas dynamics, due to the strong flashing of the liquid phase and the consequent cooling below ambient temperature. As reported in the PHAST documentation, the model has been validated by comparison with the experimental data reported by McQuaid. The results, shown in Figure 8.18, indicate that the toxic footprint extends up to approximately 620 m under D5 conditions and around 1,990 m under F2 conditions. Under stable atmospheric conditions, the reduced turbulence and stratification of the air limit the vertical mixing, resulting in a larger and more persistent ground-level cloud. The side view (Figure 8.19) confirms this behavior: the F2 plume remains close to the ground with a maximum height of about 10 m, while the D5 plume, affected by stronger turbulence, is shorter but more elevated (up to about 14 m). This behavior confirms that, although ammonia is lighter than air under ambient conditions, the initial release occurs as a cold and dense vapor cloud due to rapid depressurization and evaporation, leading to dense gas effects in the early dispersion phase before gradual dilution and lift-off.

In ALOHA, the dispersion pattern reflects the same influence of meteorological stability observed in PHAST. Under neutral conditions (D5), the model predicts a maximum downwind distance of about 1,600 m, while under stable conditions (F2) the toxic footprint extends up to 2,900 m (Figure 8.20 and Figure 8.21). In the F2 scenario, ALOHA automatically truncated the release at 1 hour, as the software does not simulate discharge durations beyond this time limit.

Unlike PHAST and ADAM, the model does not allow the definition of pipeline geometry (such as pipe length); therefore, the release is treated as an orifice directly at the source. This simplification may affect the initial jet behaviour and the early dispersion dynamics but still provides a consistent estimation of the downwind extent of the toxic cloud for the 300 ppm threshold.

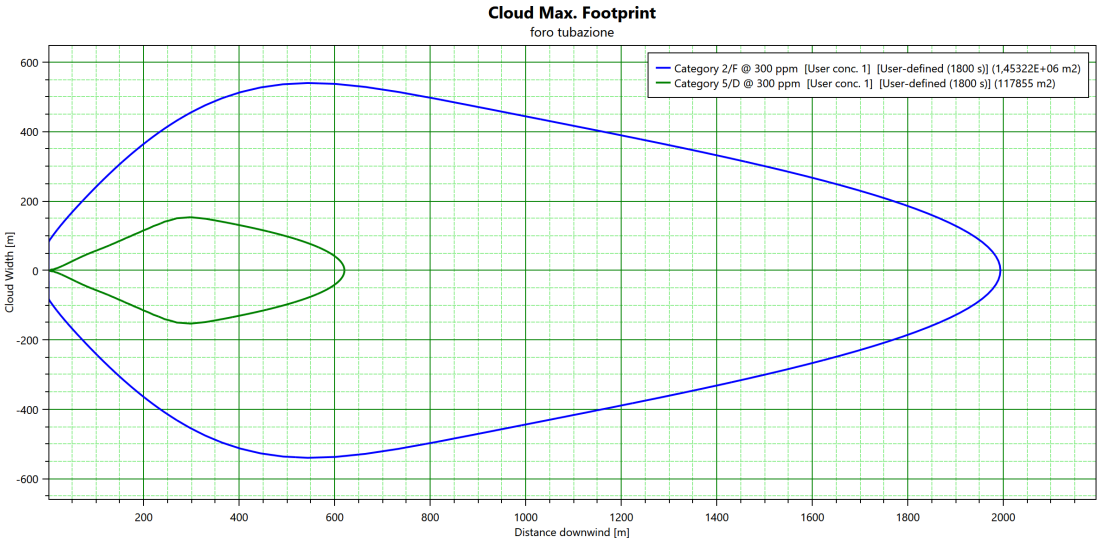

Figure 8.18: Cloud maximum footprint simulated with PHAST for stability classes D5 and F2 (toxic concentration = 300 ppm.

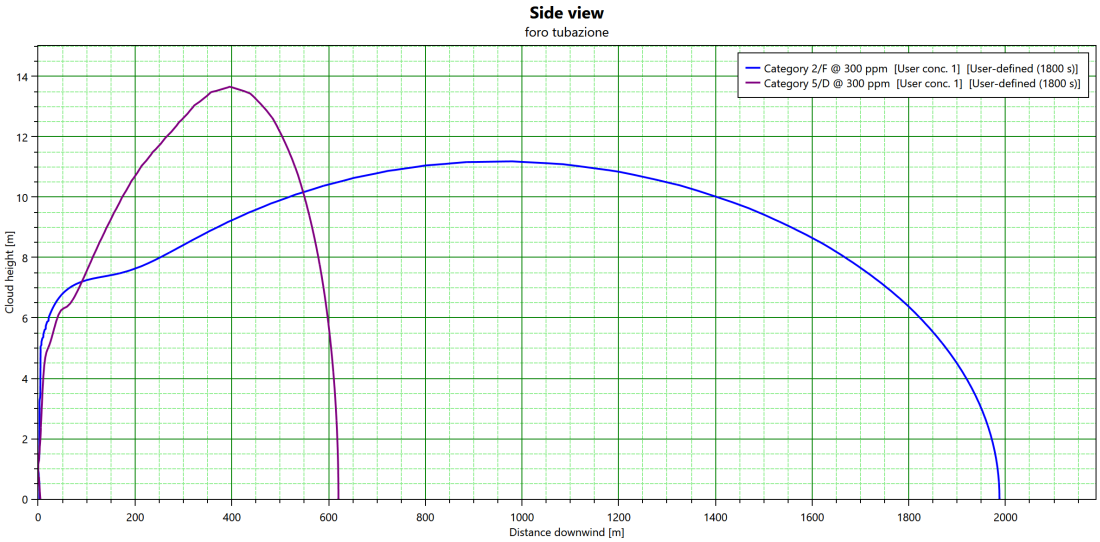

Figure 8.19: Side view of the ammonia cloud simulated with PHAST for stability classes D5 and F2 (toxic concentration = 300 ppm).

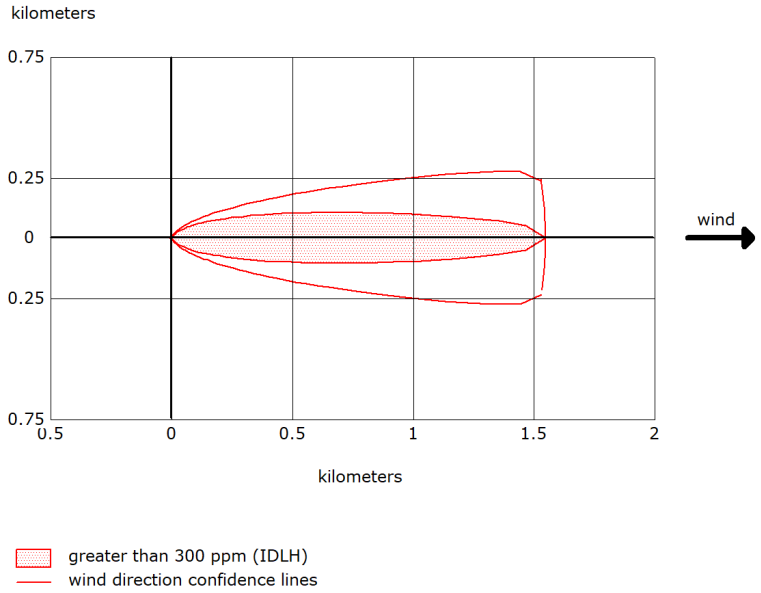

Figure 8.20: Dispersion footprint of ammonia simulated with ALOHA for stability class D5 (toxic concentration = 300 ppm).

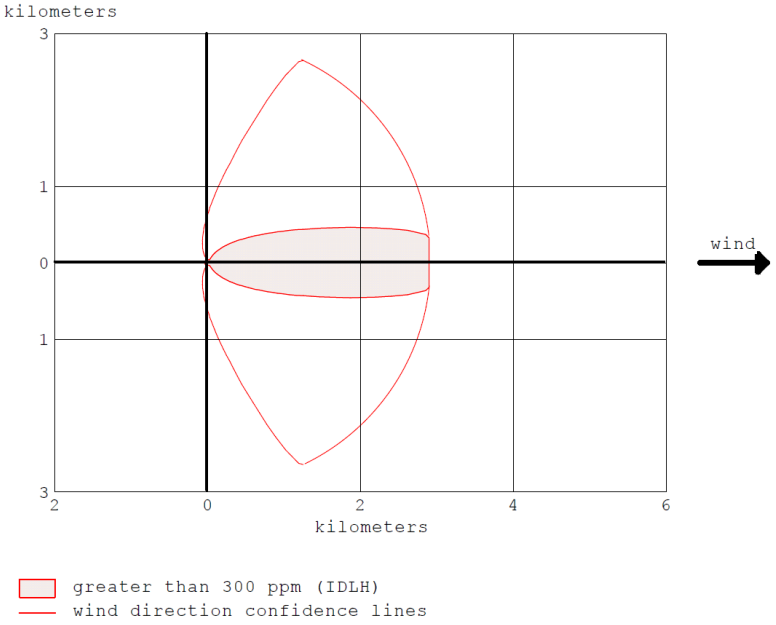

Figure 8.21: Dispersion footprint of ammonia simulated with ALOHA for stability class F2 (toxic concentration = 300 ppm).

The results obtained with ADAM (Figure 8.22 and Figure 8.23) are consistent with the general trends observed in PHAST and ALOHA. The model predicts downwind distances of approximately 775 m for D5 and 2,900 m for F2 conditions. However, in the vertical section, ADAM shows a more pronounced lifting of the plume as the dispersion progresses. Consequently, ADAM tends to simulate a more vertically dispersed cloud and slightly lower ground-level concentrations at longer distances compared to PHAST.

Figure 8.22: Dispersion footprint of ammonia simulated with ADAM for stability class D5 (toxic concentration = 300 ppm).

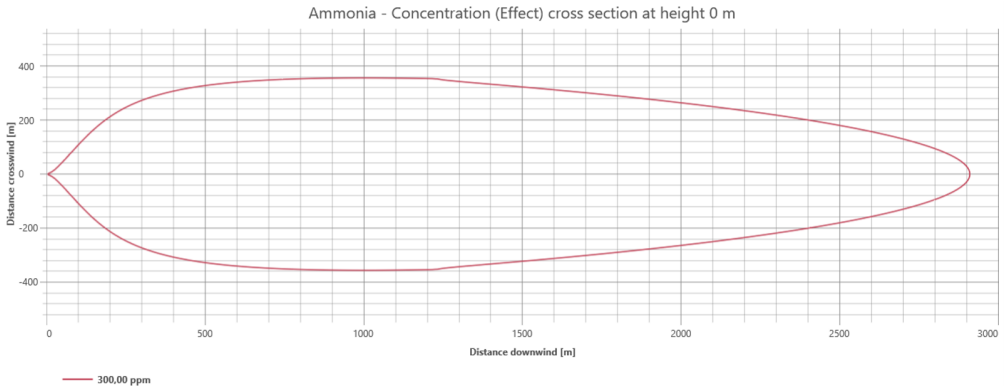

Figure 8.23: Dispersion footprint of ammonia simulated with ADAM for stability class F2 (toxic concentration = 300 ppm).

Table 8.13 summarizes the maximum downwind distances corresponding to the toxic threshold (300 ppm) predicted by the three models. For land-use planning purposes, only the most conservative meteorological condition (F, 2 m/s) was mapped (Figure 8.26). Under this scenario, the toxic cloud (300 ppm) may extend outside the industrial site and reach urban or sensitive areas located downwind of the release point.

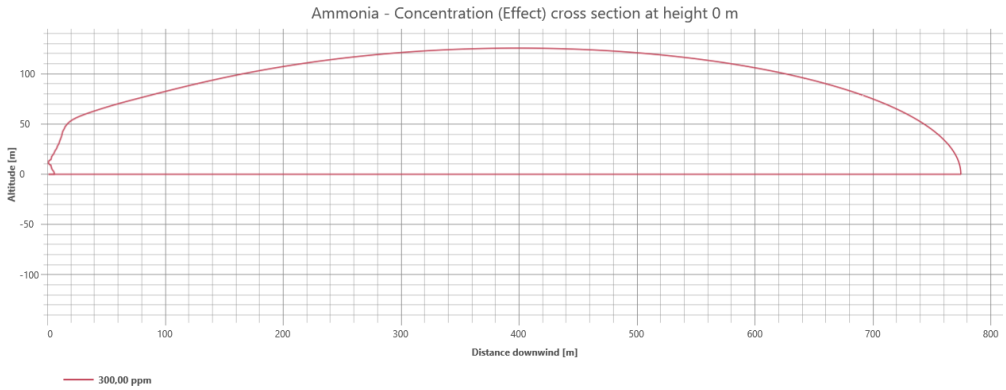

Figure 8.24: Side view of the ammonia dispersion (wind speed 5 m/s, stability class D) corresponding to Figure 8.22.

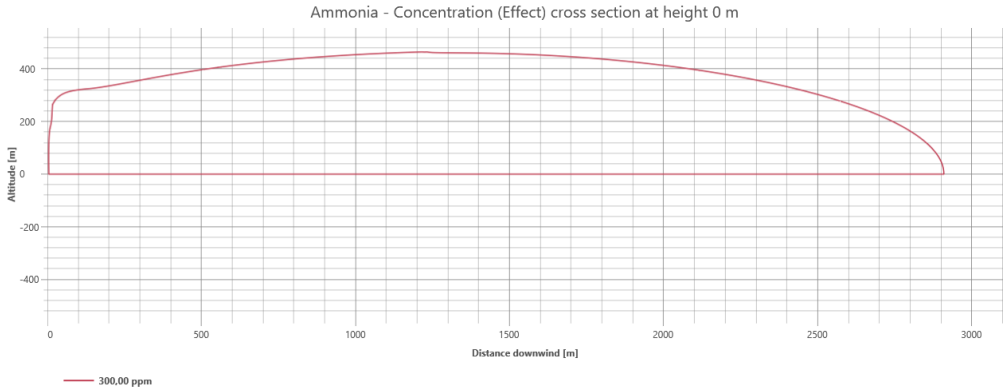

Figure 8.25: Side view of the ammonia dispersion (wind speed 2 m/s, stability class F) corresponding to Figure 8.23.

Table 8.13: Summary of downwind distances [m] corresponding to 300 ppm (IDLH) predicted by PHAST, ALOHA and ADAM.

Model	**Weather condition 5D**	**Weather condition 2F**
PHAST	620	1,994
ALOHA	1,600	2,900
ADAM	774.5	2,909

(a) Predicted impact area under stability class 2F calculated with PHAST.

(b) Predicted impact area under stability class 2F calculated with ALOHA.

(c) Predicted impact area under stability class 2F calculated with ADAM.

Figure 8.26: Impact areas under stability class 2F, obtained from the three modelling tools (PHAST, ALOHA, and ADAM).

8.4.3 Results for the Methanol Release

The outflow of methanol from the tank results in an initial liquid discharge driven by hydrostatic pressure, forming a pool at ground level and progressively generating flammable vapours. The three software tools display substantially different trends in terms of mass flowrate and release duration. In order to ensure comparability with ALOHA, which limits the simulation time to 1 hour, the dispersion simulations in PHAST were also constrained to a total duration of 3,600 s. PHAST assumes a steady liquid release with constant mass rate (≈ 4.37 kg/s) for the entire duration (3,600 s) (Figure 8.27).

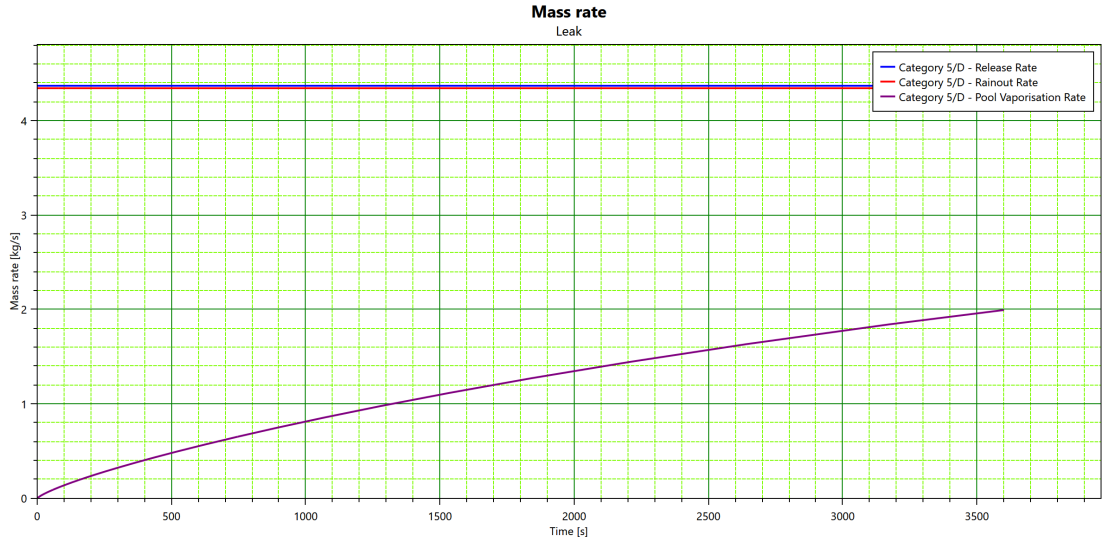

Figure 8.27: Methanol release rate, rainout and pool vaporization calculated by PHAST.

Unlike PHAST and ADAM, ALOHA does not calculate an instantaneous mass flow curve over time. Instead, it provides the maximum average sustained release rate, averaged over at least one minute. For this scenario, ALOHA estimated a sustained release rate of 27.8 kg/min (≈ 0.46 kg/s) and limited the release duration to 1 hour, reaching a total discharged mass of 1,051 kg. The methanol was released as a liquid, forming an evaporating pool on the ground with a maximum diameter of 33 m (Figure 8.28).

ADAM calculates a decreasing mass flow over time, starting from ≈ 3.5 kg/s and progressively reducing to ≈ 3.8 kg/s (Figure 8.29). In ADAM, the atmospheric storage tank was modelled in a similar way to PHAST. However, the software interrupts the liquid discharge before the liquid level reaches the leak elevation. This behaviour is due to the internal pressure drop that occurs inside the vessel during the release, which reduces the driving head at the leak point. As a consequence, the total released mass predicted by ADAM is lower than the one calculated by PHAST.

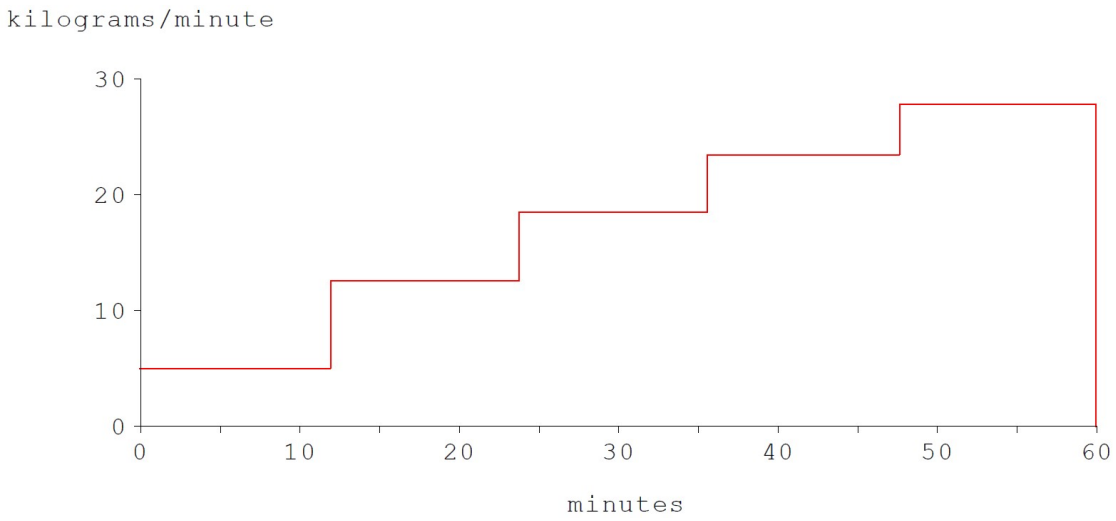

Figure 8.28: Release rate profile simulated with ALOHA for the methanol release.

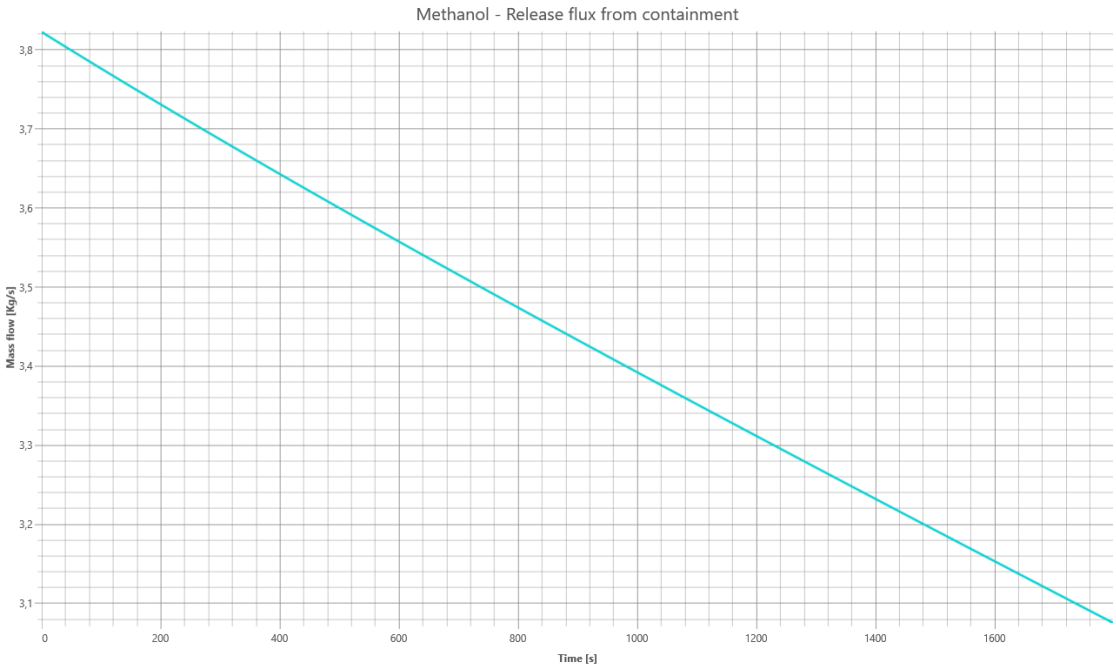

Figure 8.29: Time evolution of the release flux simulated with ADAM for the methanol release.

Table 8.14 summarizes the main results of the discharge phase obtained from the three software tools, allowing a direct comparison of the different trends described in this section.

Table 8.14: Comparison of release rate, release duration and total released mass of methanol modelled with PHAST, ALOHA and ADAM.

Result	**PHAST**	**ALOHA**	**ADAM**
Mass rate [kg/s]	4.37	0.46	3 – 3.8
Time of release [s]	3,600	> 3,600	1,797
Total amount release [kg]	15,732	1,051	6,177

As observed in the previous case studies (chlorine and ammonia), the most conservative condition for methanol dispersion is the one corresponding to stability class F and a wind speed of 2 m/s, where atmospheric turbulence is reduced and the cloud remains closer to the ground.

In all simulations, the methanol pool was assumed to spread freely over the ground, without physical obstructions. This assumption is reflected in the PHAST output, where the evaporating pool expands in all directions from the release point (Figure 8.30 and Figure 8.31). The side-view plots show that, under stability class D and 5 m/s wind speed, the vapour cloud gradually rises from ground level as it moves downwind, forming a single continuous plume (Figure 8.32). Under stability class F and 2 m/s, two distinct elevation peaks can be observed: the first occurring near the release point, and the second at a greater distance, where the cloud begins to rise and follow the wind direction (Figure 8.33).

For ALOHA, the largest toxic cloud extension is obtained under class 2F (Figure 8.35), reaching approximately 338 m for the 600 ppm concentration threshold. Under D5 conditions (Figure 8.34), the software reports very limited distances (16 m for 6,000 ppm and 52 m for 600 ppm) and does not generate the threat zone map. According to ALOHA, the footprint is not displayed because near-field dispersion is affected by patchiness and the Gaussian model provides a reduced level of confidence close to the release point. The extension obtained for the 2F condition is in the same order of magnitude as the one predicted by PHAST for the same scenario, although minor deviations are observed due to the different dispersion algorithms adopted.

In ADAM, for both meteorological classes (D5 and F2), only the 600 ppm concentration contour is detected (Figure 8.36 and Figure 8.37), while the 6000 ppm threshold is not reached within the simulated domain. When comparing the lateral concentration profiles with those generated in PHAST (Figure 8.38 and Figure 8.39), differences can be observed in the vertical evolution of the cloud, particularly in the height and shape of the plume as it moves downwind from the release point.

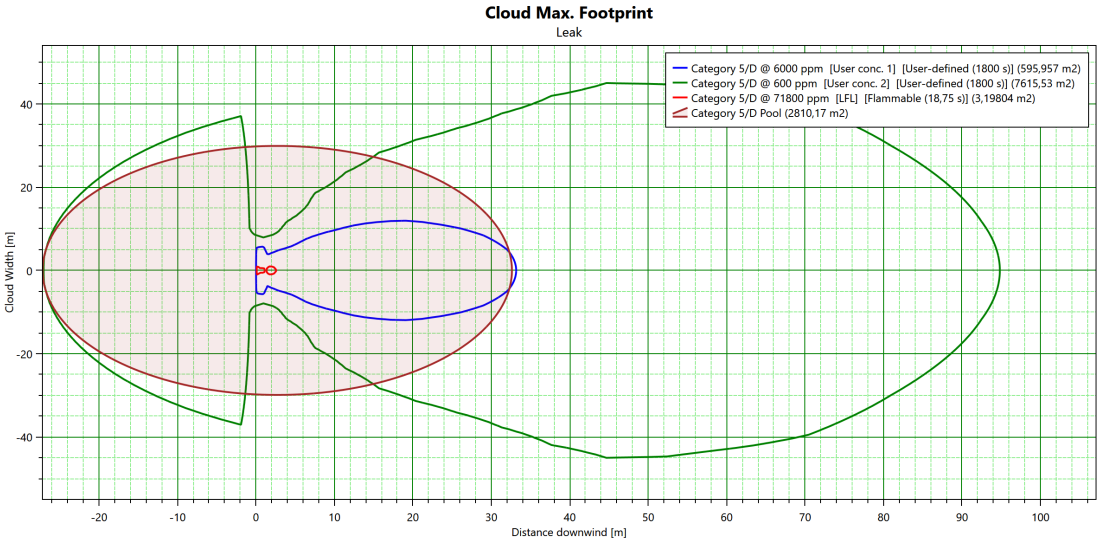

Figure 8.30: Cloud Max Footprint of methanol dispersion with a wind speed of 5 m/s and stability class D, simulated with PHAST.

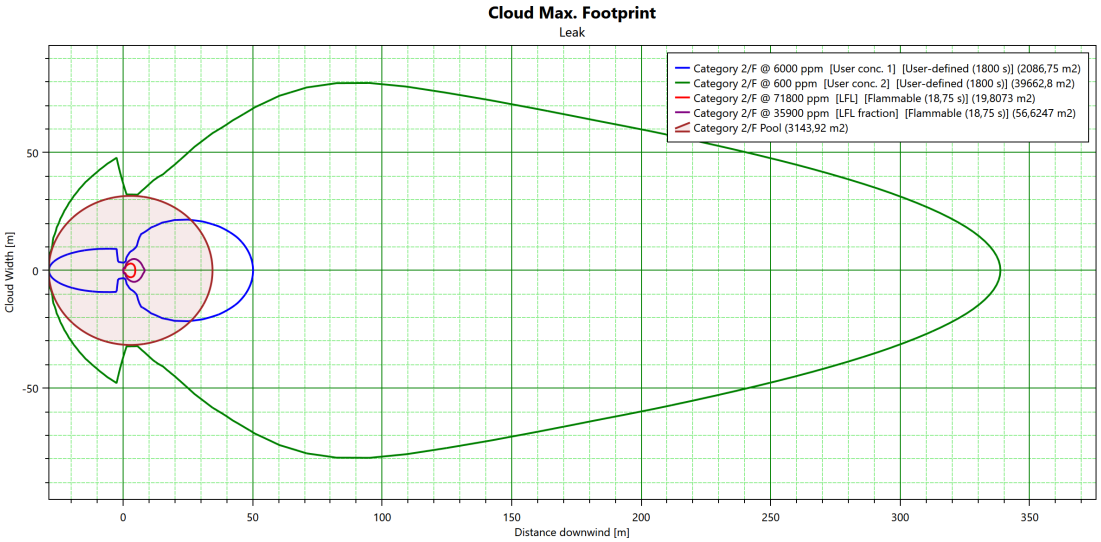

Figure 8.31: Cloud Max Footprint of methanol dispersion with a wind speed of 2 m/s and stability class F, simulated with PHAST.

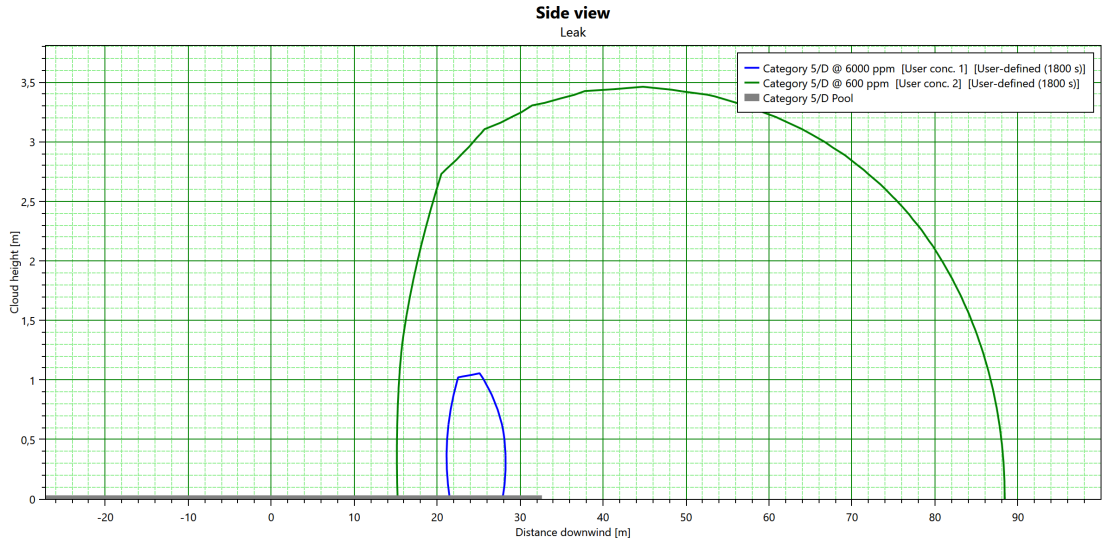

Figure 8.32: Side view of methanol cloud dispersion with a wind speed of 5 m/s and stability class D, simulated with PHAST.

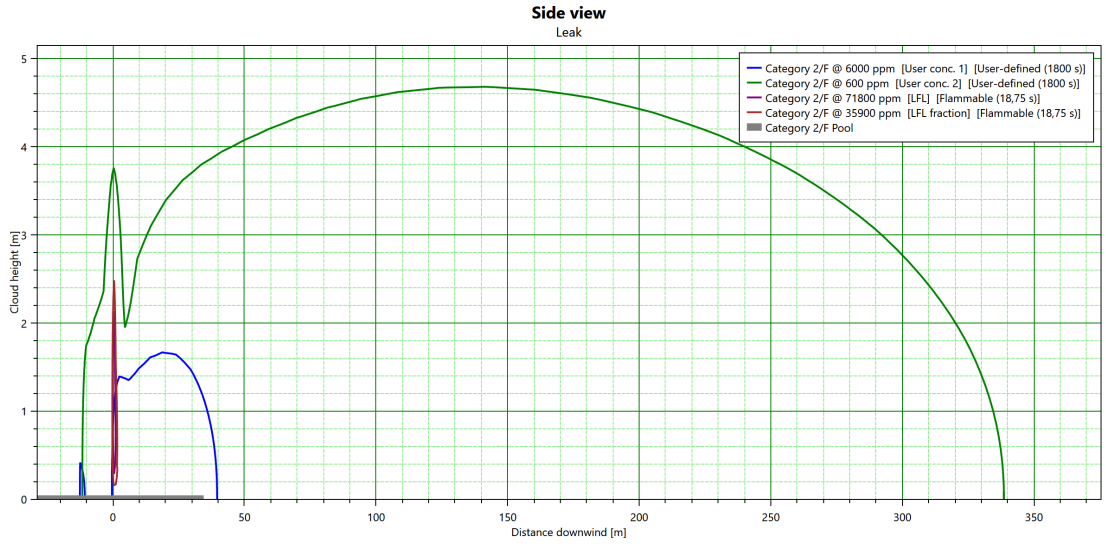

Figure 8.33: Side view of methanol cloud dispersion with a wind speed of 2 m/s and stability class F, simulated with PHAST.

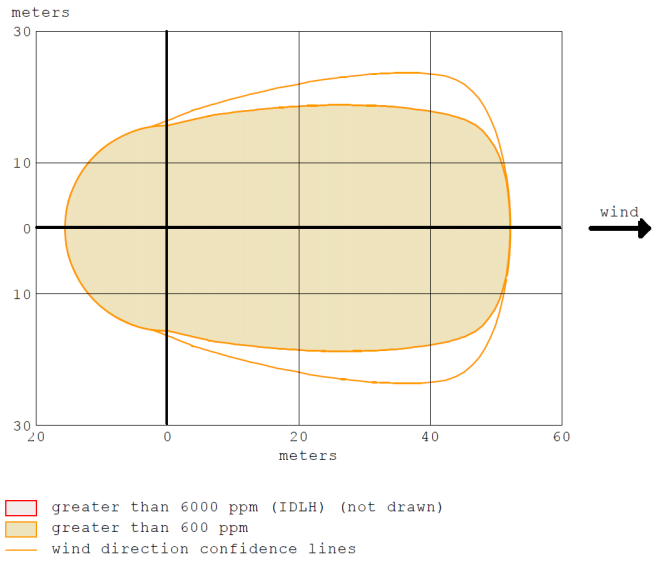

Figure 8.34: Toxic dispersion footprint of methanol at ground level with a wind speed of 5 m/s and stability class D, simulated with ALOHA.

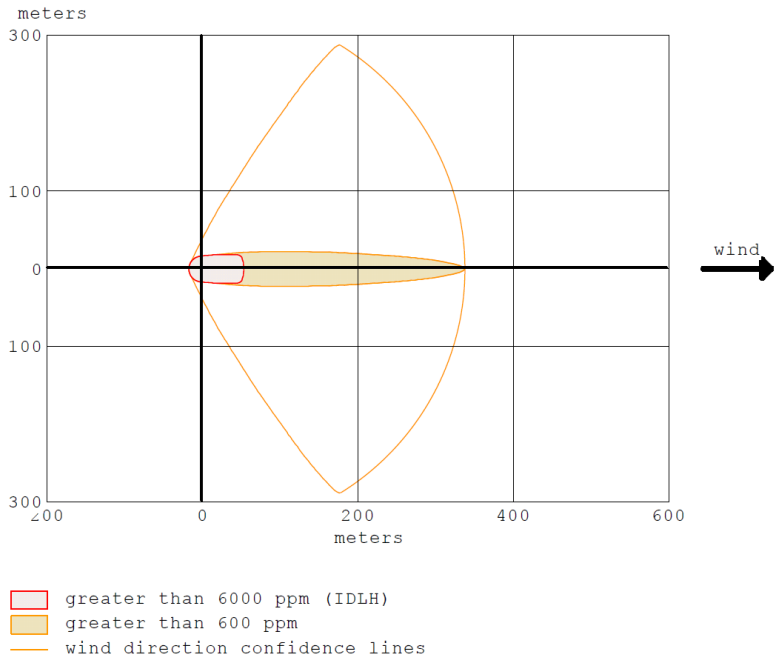

Figure 8.35: Toxic dispersion footprint of methanol at ground level with a wind speed of 2 m/s and stability class F, simulated with ALOHA.

Compared to PHAST and ALOHA, ADAM predicts shorter downwind distances for the toxic concentration thresholds in both stability classes. This results in a smaller cloud footprint, indicating a more limited spatial extent of the methanol vapor cloud under the same initial and boundary conditions.

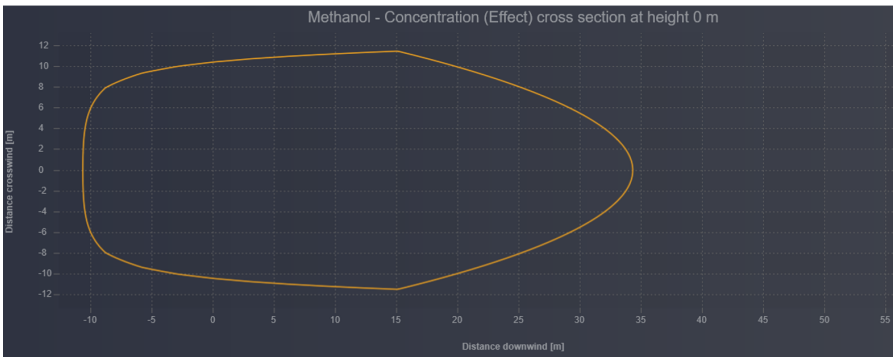

Figure 8.36: Cloud Max Footprint of methanol dispersion at 6000 ppm with a wind speed of 5 m/s and stability class D, simulated with ADAM.

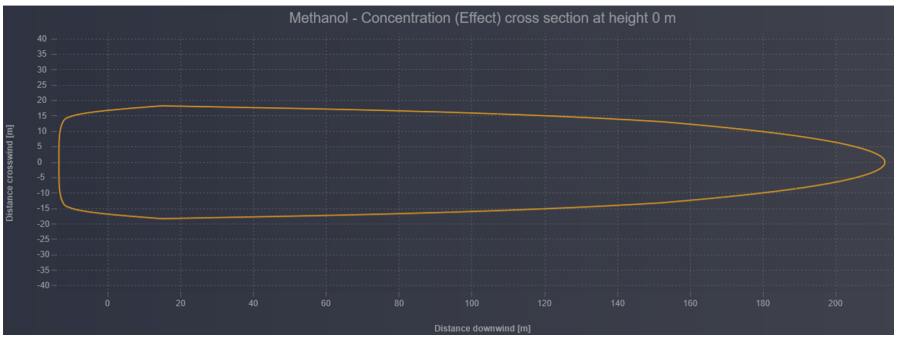

Figure 8.37: Cloud Max Footprint of methanol dispersion at 6000 ppm with a wind speed of 2 m/s and stability class F, simulated with ADAM.

Table 8.15 summarizes the maximum downwind distances of the toxic methanol cloud predicted by PHAST, ALOHA and ADAM for the two concentration thresholds (600 ppm and 6,000 ppm) and for both meteorological conditions. As expected, the largest cloud extensions occur under stability class F with a wind speed of 2 m/s, where atmospheric turbulence is minimal. Under these conditions, PHAST and ALOHA provide comparable distances for the 600 ppm threshold, whereas ADAM predicts shorter values. The differences observed among the software tools are attributable to the dispersion models implemented (dense gas integral model in PHAST, Gaussian approach in ALOHA, and hybrid dense gas behavior in ADAM) and to the different treatment of pool evaporation and cloud buoyancy.

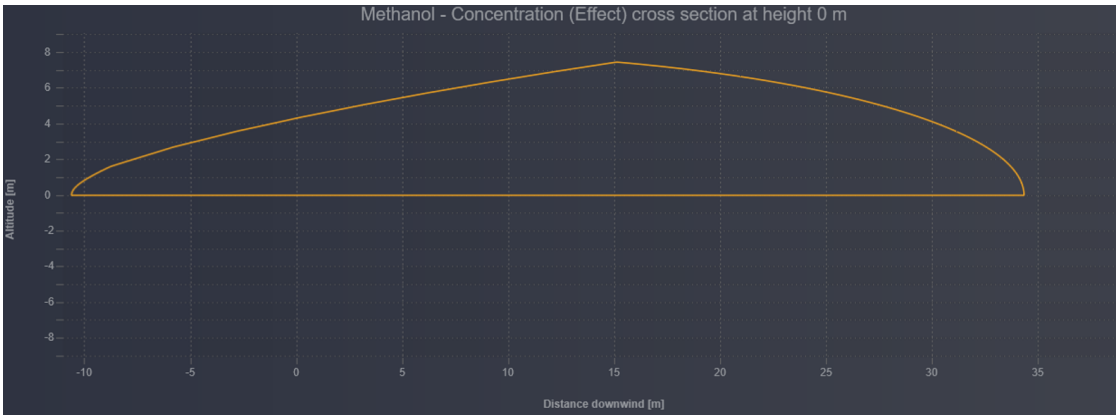

Figure 8.38: Side view of methanol cloud dispersion at 6000 ppm with a wind speed of 5 m/s and stability class D, simulated with ADAM.

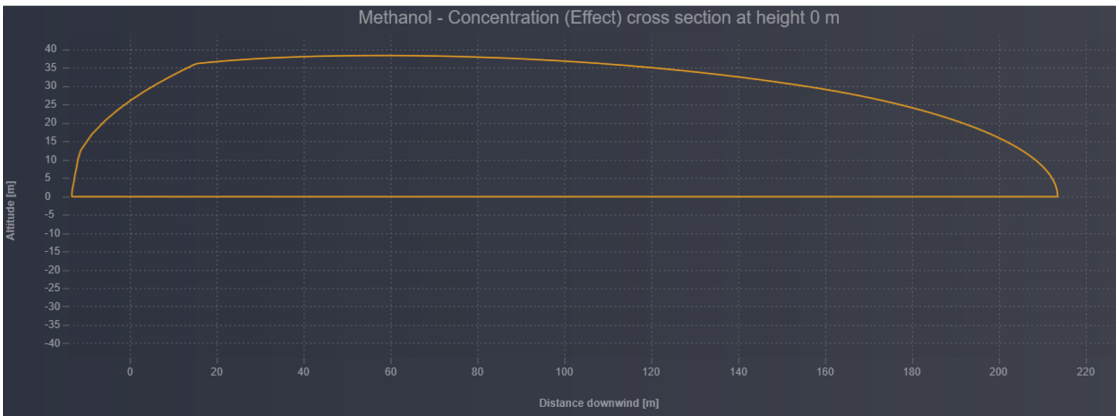

Figure 8.39: Side view of methanol cloud dispersion at 6000 ppm with a wind speed of 2 m/s and stability class F, simulated with ADAM.

Table 8.15: Downwind distances of methanol toxic dispersion at 600 ppm and 6,000 ppm for stability classes D (5 m/s) and F (2 m/s), simulated with PHAST, ALOHA and ADAM.

Model	**Weather condition 5D**		**Weather condition 2F**	
	600 ppm	6000 ppm	600 ppm	6000 ppm
PHAST	94.2	32.6	342	50.3
ALOHA	52	16	338	54
ADAM	34.3	–	213.4	–

Figure 8.40 show the toxic cloud footprint for stability class 2F, identified as the worst-case condition and the most relevant for land-use planning.

Methanol is not only toxic but also flammable, and its accidental release may lead to two main hazardous phenomena: pool fire and flash fire. A pool fire may occur after the release phase, when the liquid forms a spreading pool that can be ignited if an ignition source is present. The resulting thermal effects were assessed in terms of heat radiation. The threshold values adopted for damage evaluation are those specified by the Italian Decree of 9 May 2001 (see Section 6.5). The following paragraphs report and compare the results obtained with the three software tools.

In PHAST, pool fires can be simulated assuming either early or late ignition. According to the Technical Reference Manual, an early pool fire occurs when the liquid is ignited while the pool is still forming during the release, whereas a late pool fire is assumed when ignition takes place after the pool has reached its maximum spreading diameter. PHAST calculates the dynamic pool diameter over time and provides thermal radiation distances for both conditions (Figure 8.41 and Figure 8.42). For this reason, both early and late pool fire results are reported in Table 8.16.

ALOHA also includes a pool fire model. However, it assumes a circular pool of uniform thickness on a flat surface and does not explicitly distinguish between early and late ignition phases. ALOHA can simulate a pool fire coupled with a continuous liquid release, but it applies a steady-state pool diameter limited to 200 m and uses simplified solid-flame correlations for thermal radiation. ALOHA results for stability classes D (5 m/s) and F (2 m/s) are presented in Figure 8.43 and Figure 8.44.

ADAM allows the calculation of pool formation and the resulting pool fire. The software uses a solid flame model to estimate thermal radiation, assuming a cylindrical tilted flame above the liquid surface. The pool size may be calculated dynamically from the release or imposed by the user. However, ADAM does not distinguish between early and late pool fire ignition conditions. Furthermore, the predicted hazard radii are identical for both meteorological conditions (D5 and F2) (Figure 8.45).

Table 8.16: Thermal radiation damage distances (m) for methanol pool fire at 12.5, 5 and 3 kW/m^2.

	High lethality 12.5 kW/m²	**Irreversible injury 5 kW/m²**	**Reversible injury 3 kW/m²**
Weather condition 5D			
PHAST	(21.6) 57.7	(28.7) 76.5	(33.9) 90.9
ALOHA	< 10	13	15
ADAM	19.7	37.2	45.2
Weather condition 2F			
PHAST	(19.4) 56.2	(27.8) 78.7	(33.9) 94.3
ALOHA	< 10	10	13
ADAM	19.7	37.2	45.2

Distances in brackets refer to early pool fire.

(a) Predicted impact area under stability class 2F calculated with PHAST.

(b) Predicted impact area under stability class 2F calculated with ALOHA.

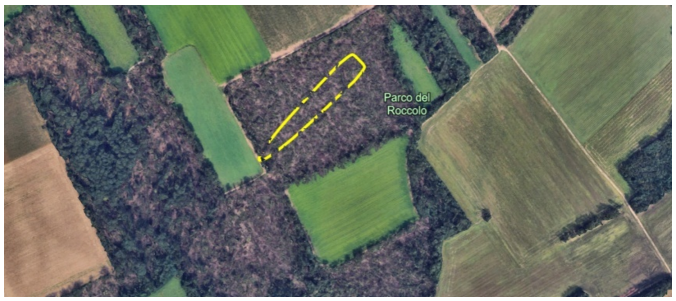

(c) Predicted impact area under stability class 2F calculated with ADAM.

Figure 8.40: Impact areas under stability class 2F, obtained from the three modelling tools (PHAST, ALOHA, and ADAM).

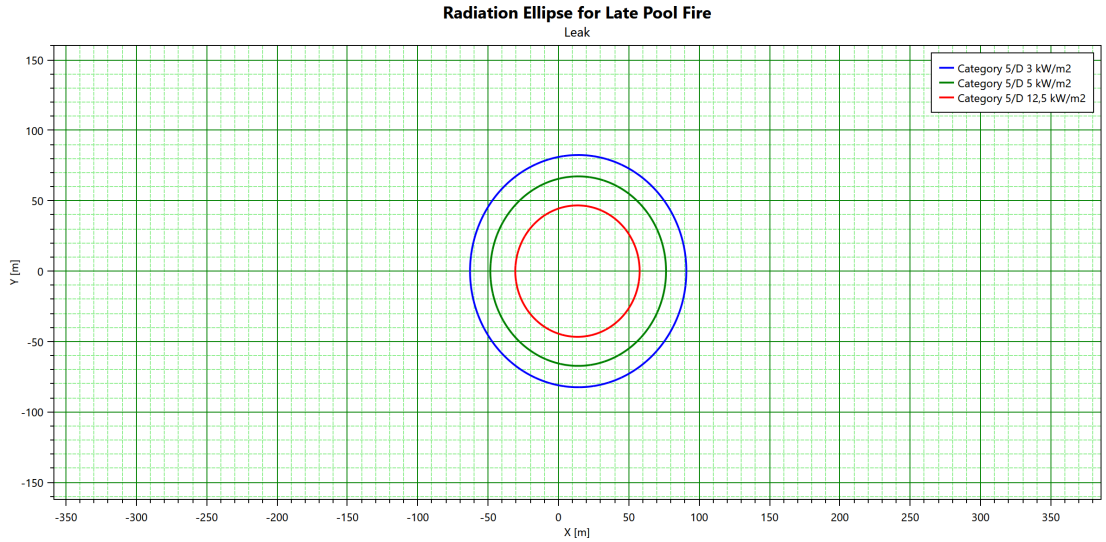

Figure 8.41: Methanol pool fire – thermal radiation footprint (3, 5 and 12.5 kW/m^2) under stability class D (5 m/s), simulated with PHAST (late pool fire).

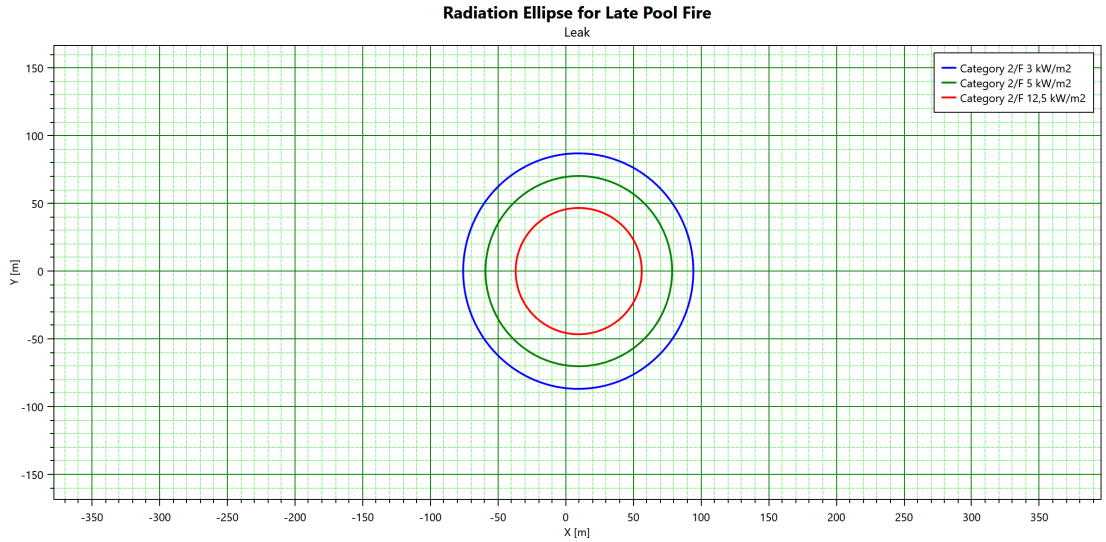

Figure 8.42: Methanol pool fire thermal radiation footprint (3, 5 and 12.5 kW/m^2) under stability class F (2 m/s), simulated with PHAST (late pool fire).

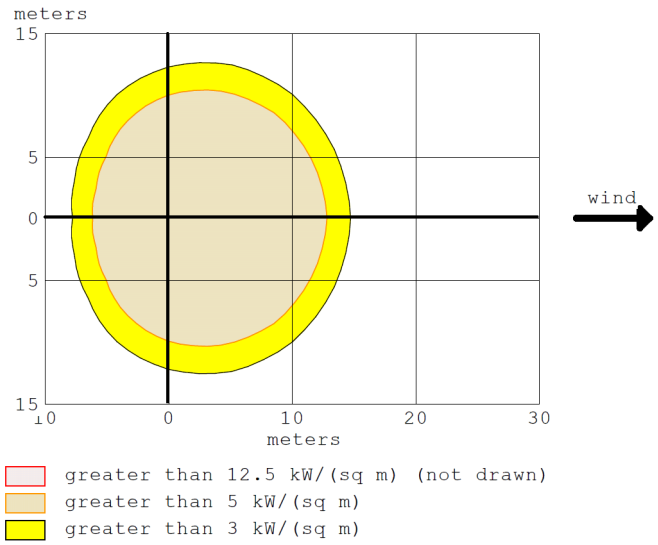

Figure 8.43: Methanol pool fire thermal radiation zones (ALOHA) under stability class D (5 m/s).

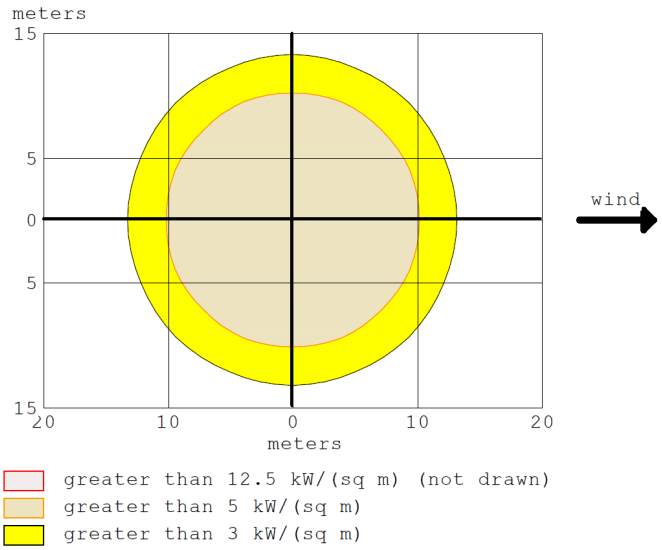

Figure 8.44: Methanol pool fire thermal radiation zones (ALOHA) under stability class F (2 m/s).

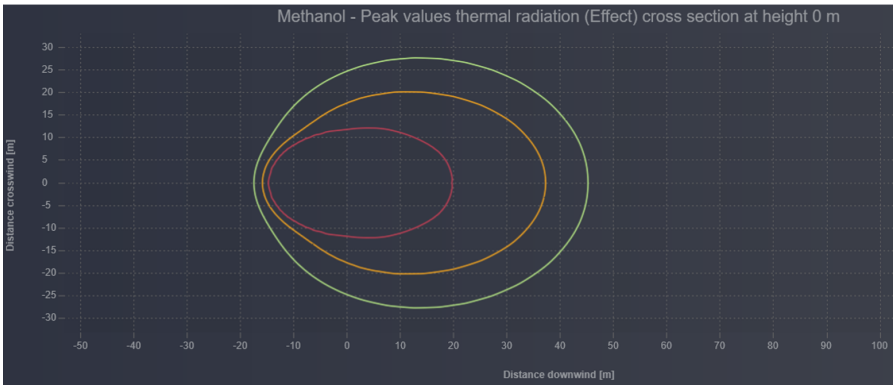

Figure 8.45: Methanol pool fire thermal radiation contours simulated with ADAM for both stability classes D (5 m/s) and F (2 m/s). The red line indicates the 12.5 kW/m^2 isoradiation, the yellow line the 5 kW/m^2 level, and the green line the 3 kW/m^2 level.

A flash fire can occur when a flammable vapor cloud is ignited, producing a combustion of the entire cloud volume without significant overpressure, as the flame is not accelerated by congestion or turbulence. Although the associated shock wave and flame duration are limited, the ignition of the flammable cloud may result in the involvement of personnel, equipment and structures within the flammable region.

The impact thresholds adopted for flash fire consequences are those defined in the Italian Ministerial Decree of 9 May 2001 (see Section 6.5).

Among the three software tools considered, PHAST is the only one able to calculate the extent of the cloud within the flammable range for both meteorological conditions. Figure 8.46 and Figure 8.47 show the extent of the zones corresponding to the Lower Flammability Limit (LFL = 71,800 ppm) and to half of the LFL (35,900 ppm), which are assumed to represent high lethality and start of lethality, respectively. As already observed in the previous scenarios, the largest extension of the flammable cloud is obtained under stability class 2F, whereas turbulent conditions (class 5D) lead to faster dilution below the flammability range.

With regard to flash fire, ALOHA identifies the region where the vapour cloud lies within the flammable range and could be ignited. However, for both meteorological conditions (D5 and 2F), no graphical flammable contour is generated. This is because, in the near-field region close to the leak source, the model issues a warning indicating that dispersion predictions may be unreliable; therefore, ALOHA does not display the threat zone on the map.

Nonetheless, the software still provides the corresponding downwind distances for the Lower Flammability Limit (LFL) and for 1/2 LFL. These values are reported in Table 8.17 and should be interpreted taking into account the warning on near-field uncertainty rather than as unavailable or invalid results.

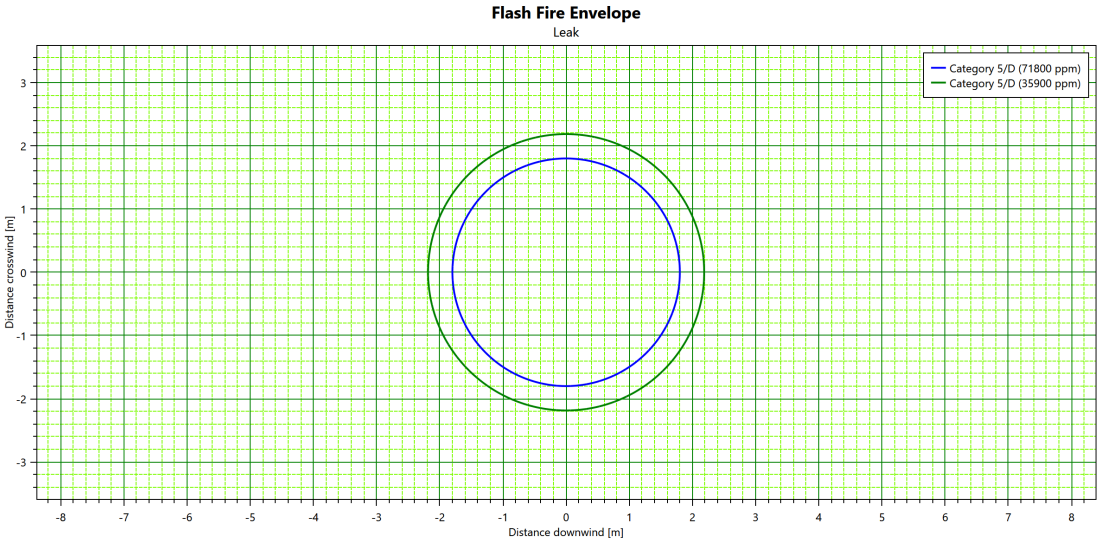

Figure 8.46: Flash fire envelope for methanol release (stability class 5D), PHAST simulation. Contours correspond to LFL (71,800 ppm) and to one-half of the LFL (35,900 ppm).

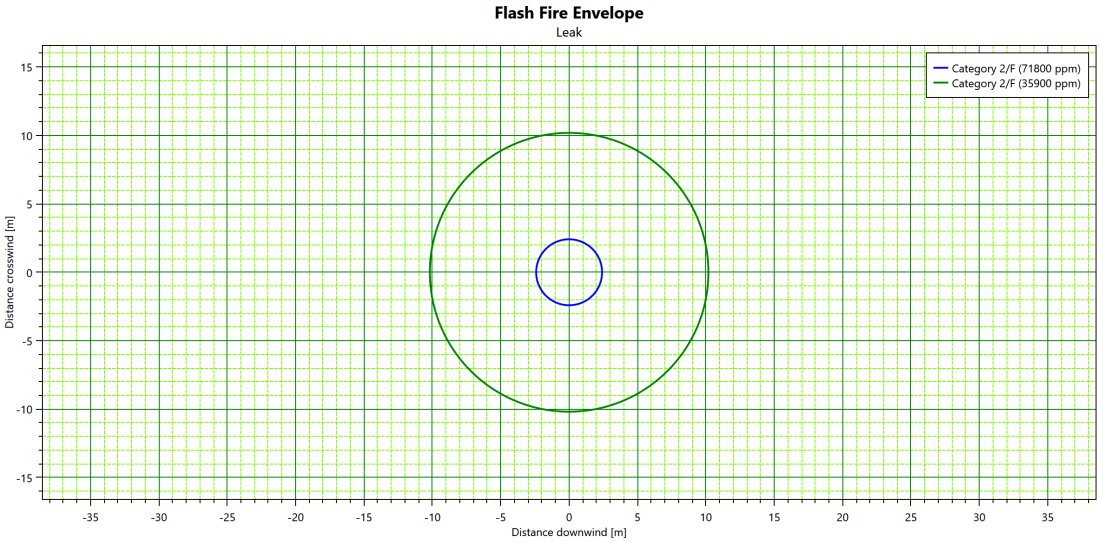

Figure 8.47: Flash fire envelope for methanol release (stability class 2F), PHAST simulation.

Table 8.17: Flammable cloud distances (LFL and 1/2 LFL) predicted by PHAST, ALOHA and ADAM under D5 and F2 conditions.

	High lethality LFL 71,800 ppm	**Start of lethality 1/2 LFL 35,900 ppm**
	Weather condition 5D	
PHAST	(1.8)	(2.2)
ALOHA	16*	16*
ADAM	–	–
	Weather condition 2F	
PHAST	2.4	10
ALOHA	22*	31*
ADAM	–	–

(*): indicate values provided by ALOHA without graphical representation, due to near-field patchiness affecting result reliability.

In ADAM, under the simulated conditions, the concentration of methanol vapours never reaches the flammable range; therefore, no flash fire envelope is generated and no quantitative distances are reported.

8.5 Conclusion

The simulations carried out allowed for a systematic comparison of the three dispersion modelling tools (PHAST, ALOHA and ADAM) and provided insight into the influence of meteorological conditions on toxic cloud behaviour and damage distances. All models consistently demonstrated the critical role of atmospheric stability class and wind speed. Stable conditions (class F, 2 m/s) generated wider and longer-lasting clouds compared to neutral conditions (class D, 5 m/s), due to reduced turbulence and limited vertical mixing.

For dense gases (chlorine and ammonia), the results showed that under neutral conditions (D/5) ALOHA predicted the longest downwind distances, whereas under stable conditions (2F) ADAM produced the most extensive impact ranges. In the case of chlorine, PHAST and ADAM provided nearly identical distances under class 2F.

For methane dispersion, greater variability among the models was observed in class D/5, while PHAST and ALOHA produced comparable distances under 2F conditions.

Regarding flammable scenarios, methane was used as reference. Pool fire behaviour was found to be almost independent of meteorological conditions, as the phenomenon is mainly controlled by pool formation and combustion dynamics. PHAST resulted in the largest damage areas, primarily due to the higher predicted liquid release and larger pool diameter. Under D/5 conditions, PHAST and ADAM provided similar early pool fire distances, whereas ALOHA consistently yielded the smallest impact areas.

For the flash fire scenario, only PHAST was able to calculate the flammable footprint. ALOHA issued a warning indicating that dispersion predictions might be unreliable, while ADAM did not consider the scenario applicable under the defined assumptions.

Differences observed among the three models are attributable to the different modelling approaches adopted (biphasic release, pool evaporation, dense gas dispersion algorithms), as well as to the different level of input detail required. Despite the effort to maintain equal boundary conditions, some tools employ simplified models while others require more detailed specifications.

All simulations were performed assuming a receptor height of 0 m above ground level. Although 1.7 m is often used as the typical human breathing height, this assumption can lead to an underestimation of damage distances when dealing with dense gases such as chlorine and ammonia, which tend to remain close to the ground, as also confirmed by the plume vertical cross-sections.

Overall, the results enabled the identification of areas potentially affected by lethal or critical effects on the exposed population, thus providing an objective basis for land-use planning and risk evaluation. The comparative analysis also helped to highlight strengths and limitations of the investigated models, supporting an informed selection of the most appropriate tool according to the required level of detail and the purpose of the assessment.

Chapter 9

Conclusion

This PhD thesis aimed to develop a structured and operational methodological tool to support the preparation and assessment of Safety Reports required under the Seveso III Directive, as implemented by Legislative Decree 105/2015. Particular attention was devoted to identifying the minimum technical contents that must always be explicitly stated, in order to ensure, on the one hand, greater transparency in the assumptions adopted by the analyst and, on the other hand, to support the competent authority during the review phase, facilitating the revision and verification of the analyses.

The systematic clarification of assumptions, input data, and selection criteria also ensures the reproducibility of the assessments carried out and the comparability among different establishments, reducing interpretative discretion and increasing the overall consistency of the submitted documentation.

From this perspective, the contribution developed does not merely provide a theoretical framework of the Quantitative Risk Analysis process, but proposes a structure organized along all the logical phases of risk analysis, system definition, hazard identification, frequency estimation, consequence analysis, risk calculation and evaluation, with a level of detail that makes it practically usable both by analysts and, above all, by the Competent Authorities during review and inspection activities.

Within the Seveso framework, the quality of risk analysis depends decisively on the completeness with which hazards are identified and characterized: an unidentified hazard is, by definition, an unmanaged risk.

This thesis systematically emphasizes that a restrictive interpretation of the concept of "dangerous substance," limited only to those substances formally determining the Seveso classification of an establishment, may lead to an underestimation of the actual risk, especially in the presence of mixtures, residues, by-products, and wastes capable of generating significant accident scenarios.

The correct selection of reference substances and the definition of actual operating conditions therefore constitute essential prerequisites for the entire QRA process.

The innovative aspect of this work lies in not having focused exclusively on a single phase of risk analysis, such as hazard identification techniques, but in having shifted attention to an earlier stage, namely when the analyst becomes familiar with the plant, un-

derstands its process units, operations performed, and, most importantly, the substances actually present and their properties.

A substantial part of the thesis was therefore devoted to the main calorimetric techniques, their advantages and limitations, and above all to the information that can be derived from them. Such information, often considered as a separate specialized field, should instead be integrated into risk analysis, as it allows the identification of possible deviations or scenarios not immediately evident through traditional hazard identification techniques.

For example, during a HAZOP study, a deviation such as the failure to open a cooling system valve may be generically assessed as "high temperature." However, the availability of calorimetric data makes it possible to determine whether such a temperature increase would merely result in heating of the mass or could trigger exothermic reactions or decomposition phenomena, and, crucially, at what temperature these phenomena may occur.

Having quantitative information, such as an onset temperature or a specific decomposition temperature, substantially changes the perception and evaluation of the deviation. A HAZOP explicitly stating that decomposition reactions are triggered above 130°C provides a level of awareness and alertness significantly different from a generic indication of "high temperature."

For this reason, calorimetric test results should not remain confined to the characterization phase, but should be systematically integrated into hazard analysis techniques, so that the link between intrinsic substance properties and potential process deviations remains explicitly visible.

The main methodological result consists in having brought together, within a single operational framework, phases that in practical applications are often treated as independent blocks: system definition and structured data collection, hazard identification through consolidated techniques, frequency formalization using probabilistic models such as FTA and ETA with contributions from HRA, consequence modeling with particular attention to source model assumptions and transmission phenomena, and risk evaluation using quantitative tools and standard representations such as risk matrices, F–N curves, and iso-risk contours.

This integration reduces the implicit discretion that may characterize individual phases and makes explicit the interdependencies between decisions taken at different stages of the analysis. For instance, the selection of the reference substance or meteorological conditions is not a neutral choice, but directly influences the extent of the damage area, the severity of consequences, and consequently the final calculated risk value.

Throughout the thesis, the importance of verifiability of assumptions has been repeatedly emphasized. For each phase of the analysis, the minimum required technical documentation is identified, and the need to rely on updated and consistent data is highlighted, including PFDs, P&IDs, operating and maintenance procedures, substance inventories, operating conditions, and descriptions of prevention and protection barriers.

This approach is particularly relevant within the context of Competent Authorities, as it allows not only the evaluation of the final outcome of the analysis, such as an

impact distance or a risk value, but also the robustness of the logical process followed, the traceability of decisions made, and the internal consistency of the overall assessment.

A central issue addressed in this thesis concerns the risk of incomplete or inconsistent classification, which arises particularly in the case of mixtures and wastes. In this context, the criticality is not merely formal, but directly affects the selection of accident scenarios and, ultimately, the design and verification of prevention and mitigation measures.

The thesis highlights the need for a rigorous interpretation of regulatory and toxicological data and shows how the classification of a substance or waste as "hazardous" may vary depending on the reference framework considered, such as CLP, Seveso, or waste legislation, leading to possible misalignments. A material classified as hazardous under one regulation may not automatically be considered hazardous under another, and vice versa.

In this context, it is essential to clarify that, for Seveso purposes, the classification of mixtures and wastes must be conducted according to transparent, justified, and reproducible criteria; that in practical assessments waste is generally assimilated to a mixture and therefore requires a classification approach consistent with CLP principles; and that the criteria for assigning hazardous properties HP to waste refer to the hazard statements H of CLP but involve different calculation methods and concentration thresholds compared to the classification of mixtures under CLP, so that the outcomes are not necessarily equivalent.

As a consequence, for the same waste stream, the assignment of a specific HP class does not automatically translate into an equivalent classification for Seveso purposes. It is therefore technically possible that two apparently similar wastes, belonging to the same HP hazard family, may lead to different conclusions in terms of Seveso applicability and identification of relevant scenarios, depending on actual concentrations and applied criteria.

The main implication is that classification cannot be reduced to a superficial documentary verification. When waste composition is variable, as frequently occurs in recovery and treatment plants, compositional uncertainty and the possible presence of contaminants or incompatibilities may introduce an additional risk of unforeseen reactivity.

In such contexts, the thesis supports the need to complement regulatory information with at least a screening-level experimental characterization aimed at identifying potential exothermic behavior, decomposition phenomena, or thermal instability. Even a standard calorimetric test, such as DSC used as a first-level investigation, can represent a fundamental tool to detect thermal behaviors incompatible with expected operating conditions and to prevent undesirable scenarios.

This aspect is particularly relevant in recovery plants, where the "raw material" is intrinsically variable and where incompatibilities between streams, accidental mixing, or reactions induced by unforeseen impurities may occur.

The second applied part of the thesis demonstrates that the determination of the damage area is not a mechanical output of the software, but the result of a chain of modeling choices. For the same initiating event, the definition of the scenario, including boundary conditions, source model, release geometry, duration, presence or absence of

containment, receptor height, and meteorological conditions, directly affects the extent of the impact areas.

For this reason, the thesis carried out a systematic comparison between PHAST, ALOHA, and ADAM on representative substances such as ammonia, chlorine, and methanol, highlighting differences attributable both to the implemented models and to the level of detail required as input.

A crucial methodological aspect, particularly for toxic scenarios, concerns the selection of toxicological values. Adopted thresholds, such as IDLH, cannot be modified for convenience or to obtain less onerous impact results, but must be selected rigorously, explicitly declared, and justified according to the purpose of the analysis and the relevant regulatory and technical framework.

In the case study, for example, ammonia dispersion was assessed by explicitly adopting the IDLH threshold of 300 ppm and comparing results under two representative meteorological conditions, showing significant differences in the impact distances estimated by the different tools.

The comparison between software tools is not an end in itself, but allows the development of awareness regarding levels of conservatism, intrinsic limitations, and fields of application of each model, supporting a justified selection of the most appropriate tool according to the objective of the analysis, whether screening, regulatory review, or design, and the available level of detail.

The thesis also shows that, even when maintaining consistent boundary conditions, differences between models, for example Gaussian approaches versus dense gas models, treatment of pool evaporation, or handling of buoyancy effects, may lead to different impact footprints. In the case of methanol, discrepancies are discussed that can be attributed to the different physical treatment of the phenomenon and to the dispersion models adopted.

From a continuous improvement perspective, a further development could involve the broader use of advanced CFD modeling, which is still underutilized in ordinary practice. In complex configurations characterized by obstacles, partial confinement, dense urban or industrial geometries, or logistics involving numerous substances and articulated layouts, computational fluid dynamics models could provide a more realistic representation of dispersion and fire phenomena, reducing uncertainties associated with simplified assumptions.

Another area of potential development concerns the strengthening of historical analysis and organizational learning. The creation of an anonymous, structured, and shareable database dedicated to the collection of accidents and near-miss events, including detailed technical descriptions of the event and root causes, could represent a highly valuable tool for both operators and Competent Authorities. Systematic analysis of such information would allow identification of recurring causes, common criticalities, and scenarios not immediately evident in traditional analyses, improving the quality of hazard identification and facilitating knowledge transfer among similar installations.

In conclusion, the thesis demonstrates that the robustness of a QRA within the Seveso framework does not depend solely on the adoption of quantitative models, but

primarily on the quality and completeness of the initial information, the regulatory and toxicological coherence of the choices made, and the ability to integrate experimental characterization, modeling, and critical evaluation.

Bibliography

[1] CCPS, *Guidelines for Developing Quantitative Safety Risk Criteria*, American Institute of Chemical Engineers, Center for Chemical Process Safety, New York, 2009.

[2] TNO, *Purple Book: Guidelines for Quantitative Risk Assessment (CPR 18E)*, Committee for the Prevention of Disasters, 2005.

[3] U.S. Chemical Safety and Hazard Investigation Board (CSB), *Improving Reactive Hazard Management: A Review of Selected Reactive Chemical Incidents (1980–2001)*, Reactive Incident Data Report, Washington D.C., 2002. Available at: https://www.csb.gov/assets/1/20/reactiveincidentdatareport.pdf

[4] P. Cardillo, *Incidenti in ambiente chimico: guida allo studio e alla valutazione delle reazioni fuggitive*, Stazione Sperimentale per i Combustibili, San Donato Milanese, 1998.

[5] D. A. Crowl and J. F. Louvar, *Chemical Process Safety: Fundamentals with Applications*, 4th ed., Boston, MA: Pearson Education, 2019.

[6] C. Pasturenzi, M. Dellavedova, L. Gigante, A. Lunghi, M. Canavese, C. Sala Cattaneo, and S. Copelli, "Thermochemical stability: A comparison between experimental and predicted data," *Journal of Loss Prevention in the Process Industries*, vol. 28, pp. 79–91, 2014. DOI: 10.1016/j.jlp.2013.03.011.

[7] *Guidelines for Chemical Reactivity Evaluation and Application to Process Design*, Center for Chemical Process Safety (CCPS) of the American Institute of Chemical Engineers (AIChE), Wiley, Hoboken, NJ, USA, 1995.

[8] ISPRA, *Stabilità dei reattori chimici*, Rapporto tecnico n. 4162, Roma, Italy, 2013.

[9] W. Tsang and E. S. Domalski, *An Appraisal of Methods for Estimating Self-Reaction Hazards*, NBSIR 74-551, Physical Chemistry Division, Institute for Materials Research, National Bureau of Standards, Washington, D.C., June 1974.

[10] Setaram (KEP Technologies Group), *Calvet – High Sensitivity Heat Flow Calorimeter*. Available at: https://setaramsolutions.com/product/calvet

[11] F. Stoessel, *Thermal Safety of Chemical Processes: Risk Assessment and Process Design*, 2nd completely revised and extended ed., Wiley-VCH Verlag GmbH & Co. KGaA, Weinheim, Germany, 2008.

[12] Innovhub – Stazioni Sperimentali per l'Industria, Internal technical documentation on the adiabatic calorimeter PHI-TEC II, Milan, Italy, 2023.

[13] J. Singh, "Reliable scale-up of thermal hazards data using the PHI-TEC II calorimeter," *Thermochimica Acta*, vol. 226, pp. 211–220, Elsevier Science Publishers B.V., Amsterdam, 1993.

[14] J. P. Burelbach, *Advanced Reactive System Screening Tool (ARSST)*, Fauske & Associates, Inc., Burr Ridge, Illinois, USA.

[15] Innovhub – Stazioni Sperimentali per l'Industria.

[16] Center for Chemical Process Safety (CCPS), *Process Safety for Engineers: An Introduction*, 2nd ed., American Institute of Chemical Engineers (AIChE), New York, 2022.

[17] J. D. DeHaan and D. J. Icove, *Kirk's Fire Investigation*, 7th ed., Pearson Education, Upper Saddle River, NJ, 2012.

[18] K. Satyanarayana and P. G. Rao, "Improved equation to estimate flash points of organic compounds," *Journal of Hazardous Materials*, vol. 32, pp. 81–85, Elsevier Science Publishers B.V., Amsterdam, 1992.

[19] M. Vidal, W. J. Rogers, J. C. Holste, and M. S. Mannan, "A review of estimation methods for flash points and flammability limits," *Process Safety Progress*, 2004. DOI: 10.1002/prs.10004.

[20] M. Hristova and S. Tchaoushev, "Calculation of flash points and flammability limits of substances and mixtures," *Journal of the University of Chemical Technology and Metallurgy*, vol. 41, no. 3, pp. 291–296, 2006.

[21] M. Hristova, "Measurement and prediction of binary mixture flash point," *Central European Journal of Chemistry*, vol. 11, no. 1, pp. 57–62, 2013. DOI: 10.2478/s11532-012-0131-1.

[22] P. R. Amyotte and F. I. Khan (Eds.), *Methods in Chemical Process Safety – Volume 3: Dust Explosions*, Elsevier, Academic Press, 2020.

[23] N. P. Cheremisinoff, *Dust Explosion and Fire Prevention Handbook: A Guide to Good Industry Practices*, CRC Press, Taylor & Francis Group, 2014.

[24] ISPESL, "Metodo per l'analisi e la valutazione delle conseguenze di eventi incidentali connessi a determinate attività industriali," *Fogli di informazione*, 1° supplemento monografico, anno VI, n. 1/93, 1993.

[25] K. S. N. Raju, *Chemical Process Industry Safety*, McGraw Hill Education (India) Private Limited, New Delhi.

[26] N. Hyatt, *Guidelines for Process Hazards Analysis: Hazards Identification & Risk Analysis*, CRC Press LLC, Dyadem Press, 2003.

[27] L. Fiorentini and R. Sicari, *Analisi valutazione e gestione operativa del rischio*, EPC, 2020.

[28] J. D. Andrews and T. R. Moss, *Reliability and Risk Assessment*, Professional Engineering Publishing Limited, London, 2002.

[29] J. C. H. Schüller et al., *Methods for Determining and Processing Probabilities (Red Book, CPR 12E)*, Committee for the Prevention of Disasters, The Hague, 2nd ed., 1997.

[30] Center for Chemical Process Safety (CCPS), *Guidelines for Hazard Evaluation Procedures*, 3rd ed., American Institute of Chemical Engineers (AIChE), John Wiley & Sons, Inc., New York, 2008.

[31] M. Madonna et al., "Il fattore umano nella valutazione dei rischi: confronto metodologico fra le tecniche per l'analisi dell'affidabilità umana," *Prevenzione Oggi*, 5(1–2), pp. 67–83, 2007.

[32] M. Rausand, *Risk Assessment: Theory, Methods, and Applications*, John Wiley & Sons, Inc., Hoboken, New Jersey, 2011.

[33] Health and Safety Executive (HSE), *Review of Human Reliability Assessment Methods*, Research Report RR679, 2009.

[34] S. Mannan (Ed.), *Lee's Loss Prevention in the Process Industries: Hazard Identification, Assessment and Control*, Vol. 1, 3rd ed., Elsevier, 2005.

[35] Presidenza del Consiglio dei Ministri – Dipartimento della Protezione Civile, D.P.C.M. 31 marzo 1989, Gazzetta Ufficiale della Repubblica Italiana, n. 93, 21 aprile 1989.

[36] International Association of Oil & Gas Producers (IOGP), *Risk Assessment Data Directory – Process Release Frequencies*, Report No. 434-01, 2010.

[37] Center for Chemical Process Safety (CCPS), *Process Safety for Engineers: An Introduction*, 2nd ed., AIChE, New York, 2018.

[38] Center for Chemical Process Safety (CCPS), *Guidelines for Chemical Process Quantitative Risk Analysis*, 2nd ed., AIChE, New York, 2000.